[American Journal of Science, Vol. 319, March, 2019, P. 159–254, DOI 10.2475/03.2019.01]

American Journal of Science

MARCH 2019

MESOZOIC–CENOZOIC GEOLOGICAL EVOLUTION OF THE HIMALAYAN-TIBETAN OROGEN AND WORKING TECTONIC HYPOTHESES

PAUL KAPP*,† and PETER G. DeCELLES*,†

ABSTRACT. The Himalayan-Tibetan orogen culminated during the Cenozoic India – Asia collision, but its geological framework and initial growth were fundamentally the result of multiple, previous ocean closure and intercontinental suturing events. As such, the Himalayan-Tibetan orogen provides an ideal laboratory to investigate geological signatures of the suturing process in general, and how the Earth's highest and largest orogenic feature formed in specific. This paper synthesizes the Triassic through Cenozoic geology of the central Himalayan-Tibetan orogen and presents our tectonic interpretations in a time series of schematic lithosphere-scale cross-sections and paleogeographic maps. We suggest that north-dipping subducting slabs beneath Asian continental terranes associated with closure of the Paleo-, Meso-, and Neo-Tethys oceans experienced phases of southward trench retreat prior to intercontinental suturing. These trench retreat events created ophiolites in forearc extensional settings and/or a backarc oceanic basins between rifted segments of upper-plate continental margin arcs. This process may have occurred at least three times along the southern Asian margin during northward subduction of Neo-Tethys oceanic lithosphere: from ~174 to 156 Ma; 132 to 120 Ma; and 90 to 70 Ma. At most other times, the Tibetan terranes underwent Cordilleran-style or collisional contractional deformation. Geological records indicate that most of northern and central Tibet (the Hoh-Xil and Qiangtang terranes, respectively) were uplifted above sea level by Jurassic time, and southern Tibet (the Lhasa terrane) north of its forearc region has been above sea level since ~100 Ma. Stratigraphic evidence indicates that the northern Himalayan margin of India collided with an Asian-affinity subduction complex – forearc – arc system beginning at ~60 Ma. Both the Himalaya (composed of Indian crust) and Tibet show continuous geological records of orogenesis since ~60 Ma. As no evidence exists in the rock record for a younger suture, the simplest interpretation of the geology is that India – Asia collision initiated at ~60 Ma. Plate circuit, paleomagnetic, and structural reconstructions, however, suggest that the southern margin of Asia was too far north of India to have collided with it at that time. Seismic tomographic images are also suggestive of a second, more southerly Neo-Tethyan oceanic slab in the lower mantle where the northernmost margin of India may have been located at ~60 Ma. The geology of Tibet and the India – Asia suture zone permits an alternative collision scenario in which the continental margin arc along southern Asia (the Gangdese arc) was split by extension beginning at ~90 Ma, and along with its forearc to the south (the Xigaze forearc), rifted southward and opened a backarc ocean basin. The rifted arc collided with India at ~60 Ma whereas the hypothetical backarc ocean basin may not have been consumed until ~45 Ma. A compilation of igneous age data from Tibet shows that the most recent phase of Gangdese arc magmatism in the southern Lhasa terrane initiated at ~70 Ma, peaked at ~51 Ma, and terminated at ~38 Ma. Cenozoic potassic-adakitic magmatism initiated at ~45 Ma within a ~200-km-wide elliptical area within the northern Qiangtang terrane, after

* Department of Geosciences, University of Arizona, Tucson, Arizona 85721 U.S.A.
† Coresponding authors: pkapp@email.arizona.edu, decelles@email.arizona.edu

which it swept westward and southward with time across central Tibet until ~26 Ma. At 26 to 23 Ma, potassic-adakitic magmatism swept southward across the Lhasa terrane, a narrow (~20 km width), orogen-parallel basin developed at low elevation along the axis of the India – Asia suture zone (the Kailas basin), and Greater Himalayan Sequence rocks began extruding southward between the South Tibetan Detachment and Main Central Thrust. The Kailas basin was then uplifted to >4 km elevation by ~20 Ma, after which parts of the India – Asia suture zone and Gangdese arc experienced >6 km of exhumation (between ~20 and 16 Ma). Between ~16 and 12 Ma, slip along the South Tibetan Detachment terminated and east-west extension initiated in the northern Himalaya and Tibet. Potassic-adakitic magmatism in the Lhasa terrane shows a northward younging trend in the age of its termination, beginning at 20 to 18 Ma until volcanism ended at 8 Ma. We interpret the post-45 Ma geological evolution in the context of the subduction dynamics of Indian continental lithosphere and its interplay with delamination of Asian mantle lithosphere.

Key words: Tibet, Himalaya, India – Asia Collision, suture

INTRODUCTION

The scientific motivation for this paper is to better understand the process of intercontinental suturing through synthesis of the geology of the archetype India – Asia suture zone, together with that of older, Mesozoic suture zones in Tibet (fig. 1). An intercontinental suture is the surface expression of the boundary between two continental lithospheric terranes joined by collision following the subduction of intervening oceanic lithosphere. Sutures are widespread, first-order tectonic elements within all of Earth's continents (Burke and others, 1977; Dewey, 1977; Moores, 1981). Despite structural reactivation, sutures are resilient features that may be recognized by regional structural, sedimentary, and petrologic patterns across thousands of kilometers; in central Asia, sutures commonly occupy prominent valleys. Intercontinental sutures separate a former continental-margin arc system from a former passive continental margin, or two former continental-margin arc systems. Forearc basins, subduction complex rocks, ophiolites, ocean plate stratigraphy, and intra-oceanic arc fragments are commonly exposed along intercontinental suture zones, but they may also be absent. Sutures may also be associated with high-pressure and/or ultra-high pressure rocks that were subducted into the mantle and then exhumed before, during, or after terminal suturing (for example, Hacker and Gerya, 2013). Post-suturing magmatism is commonly widespread and highly variable in composition. In addition, development of a suture zone is usually associated with marked changes in regional plate kinematics.

Our current conceptions of suturing raise a number of outstanding questions in tectonics. Sutures are sites of Earth's greatest mountain ranges, yet they begin as deep oceanic troughs. How do the paleogeography and paleoelevation of a suture zone evolve with time? What geodynamic processes may cause regional plate kinematics to change—breakoff/tearing of leading subducting slabs, buoyancy forces associated with continental subduction, increased gravitational potential energy of the upper plate in response to crustal thickening and/or lithospheric removal, and/or destruction of an intra-oceanic subduction zone via obduction? Is Mediterranean-style rollback of remnant oceanic lithosphere and opening of marginal oceanic basins a typical precursor of intercontinental collision? When and by what processes are suture-zone high-pressure and ultrahigh-pressure rocks subducted and exhumed? What happens when a continent collides with a mature, Andean-style margin? At which stage in the suturing process does arc-type magmatism shut off and why? What is the kinematic evolution of the subducted/underthrust lower-plate continental lithosphere and how is it similar to or different from that of oceanic subduction? Underthrusting of the lower plate may require removal of upper-plate lower lithosphere. Does lithospheric

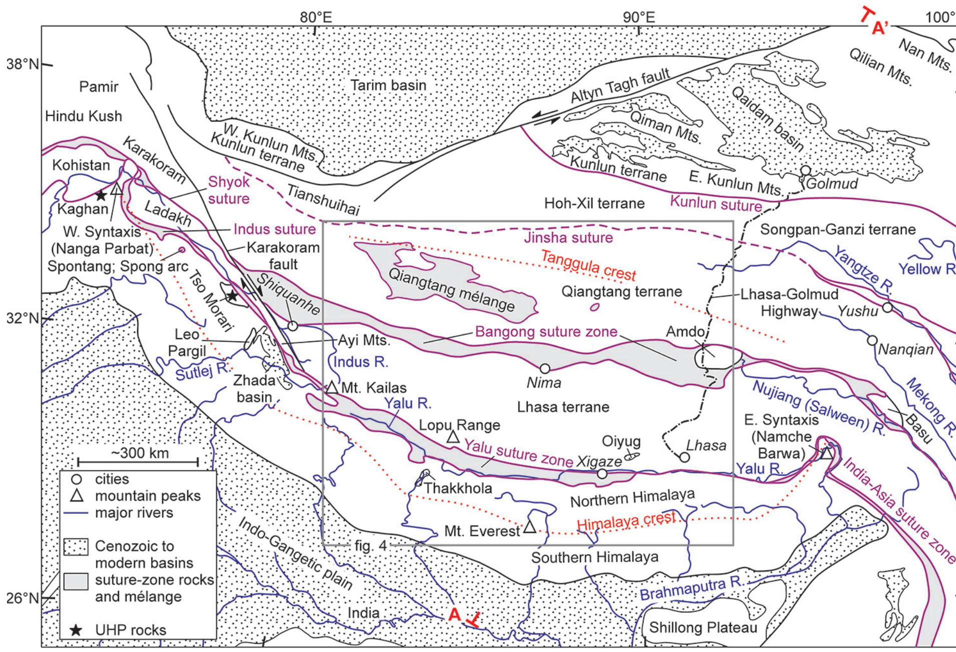

Fig. 1. Map of the Himalaya, Tibet, and adjacent regions showing the locations of major terranes and their bounding suture zones (purple lines with gray filled regions including subduction-complex rocks), basins (stippled pattern), rivers, cities, and geographic features and localities noted in the text. Abbreviations as follows: Mts., mountains; R., River. A and A' indicate ends of topographic and cross-section profiles in figure 2.

removal occur during distinct, large-volume events or in a more continuous piecemeal or dripping fashion? How much of the original crustal material is preserved within suture zones and where and when during the suturing process does the remainder go (subducted vs. underthrust vs. eroded)? Although we do not provide definitive answers to any of these questions, we hope that a synthesis of Himalayan-Tibetan geology will provide constraining parameters for tectonic interpretations and numerical simulations, as well as new insights.

The second motivation for this synthesis is that it is timely. During the past two decades, parts of the Himalaya and Tibetan Plateau have evolved from geological frontiers to some of the most intensely investigated natural laboratories on Earth. In places, the geological history has been resolved down to the one million-year time scale. Research on this orogenic system is published with such high frequency that it is impossible for a person with a casual interest in the region to stay current. Accompanying the flurry of new information is a multitude of contrasting, if not diverging, hypotheses. For example, perhaps the most scientifically important debate centers on the timing of the final disappearance of oceanic lithosphere between Indian and Asian continental lithospheres (the definition of intercontinental collision adopted here), with estimates ranging from ~65 Ma (Yin and Harrison, 2000; Ding and others, 2005, 2017a) to 25 to 20 Ma (van Hinsbergen and others, 2012). Knowledge of this timing is required to determine: (1) the geological, plate kinematic, paleogeographic, and climatic signatures of intercontinental suturing and subsequent orogenesis; (2) the finite strain budget of continental lithosphere—how many thousands of kilometers of north-south convergence by continental deformation and subduction have occurred;

and (3) the volume budget of continental lithosphere, with implications for its fate during collisional tectonics (for example, how much is recycled back into the mantle; Replumaz and others, 2010a; Ingalls and others, 2016). The timing of initial India-Asia collision is only one of many significant questions that are debated in the context of the longer term geological evolution of the Himalaya and Tibetan Plateau (fig. 1). Published summaries tend to focus on the Late Cretaceous to Cenozoic history of the region (Tapponnier and others, 1981, 2001; Burg and Chen, 1984; Harrison and others, 1992; Hodges, 2000; Royden and others, 2008; Searle and others, 2011; Wang and others, 2014a), even though much of the geology was produced by earlier events (Şengör, 1984; Chang and others, 1986; Dewey and others, 1988; Yin and Harrison, 2000).

The format of this paper is as follows. First, we provide an overview of the modern Himalayan-Tibetan orogen (figs. 1, 2, and 3). We then present the geological evolution from Triassic through late Cenozoic time, along with our working tectonic hypotheses in temporally sequential lithosphere-scale cross-sections. We focus on the central part of the orogen between 80°E and 92°E (figs. 3 and 4), in accord with our field research during the past ~20 years; this region is where the orogen is broadest in its north-south dimensions, has its highest mean elevations, and exhibits geological features that generally strike subperpendicular to plate convergence directions since at least Mesozoic time (fig. 1). A more holistic assessment of the Himalayan-Tibetan orogen would broaden its aperture to the Himalayan syntaxes, Pamir, and farther beyond in all directions, but is not attempted here. The synthesis starts during the Triassic to provide a regional geological framework, insight about tectonic processes that occurred during the consumption of older oceans (Paleo-Tethys and Meso-Tethys) and subsequent inter-terrane collisional events, and to provide initial conditions for the Late Cretaceous through Cenozoic tectonic history of the region. For example, the India – Asia suturing conundrum is based fundamentally on conflicting interpretations of the suture zone geology that extends back to at least Jurassic time (Aitchison and others, 2000, 2007 versus Ding and others, 2005 and Hu and others, 2016a). We acknowledge that the presented tectonic evolution is non-unique and under-constrained, and hence should be considered as a time series of working, testable hypotheses, along with those proposed by other researchers. One robust conclusion, however, is that the geological history of the Himalaya and Tibet does not conform to monotonic models of intercontinental collision and plateau growth in time and space; instead, a wide variety of tectonic modes have operated over the past ~220 Ma to produce this remarkable orographic feature.

THE MODERN HIMALAYAN-TIBETAN OROGEN

Topographic Expression

Terms employed to describe the Himalayan-Tibetan orogen consist of a mixture of geological, political, and physiographical names that are used variably in the literature. The problem is most acute in the transition from the Himalaya to the Tibetan Plateau where all three types of terms are applied. Our approach is to use as much as possible geologically defined terms to subdivide the orogen into its components. We refer to rocks and mountains south of the suture zone between India and Asia (the Indus-Yalu suture zone; see below; fig. 1) as the Himalayan thrust belt, including the so-called Tethyan (or Tibetan) part of the Himalaya. Rocks and physiographic elements north of the suture are referred to as parts of the Tibetan Plateau. This approach ignores the fact that the topography of some regions between the highest peaks of the Himalaya and the suture zone appears to be more plateau-like than the remainder of the steeply southward sloping Himalaya (fig. 2A). However, this northern part of the Himalaya is rugged and mostly externally drained, whereas the Tibetan Plateau thus defined is mostly internally drained and has relatively lower relief,

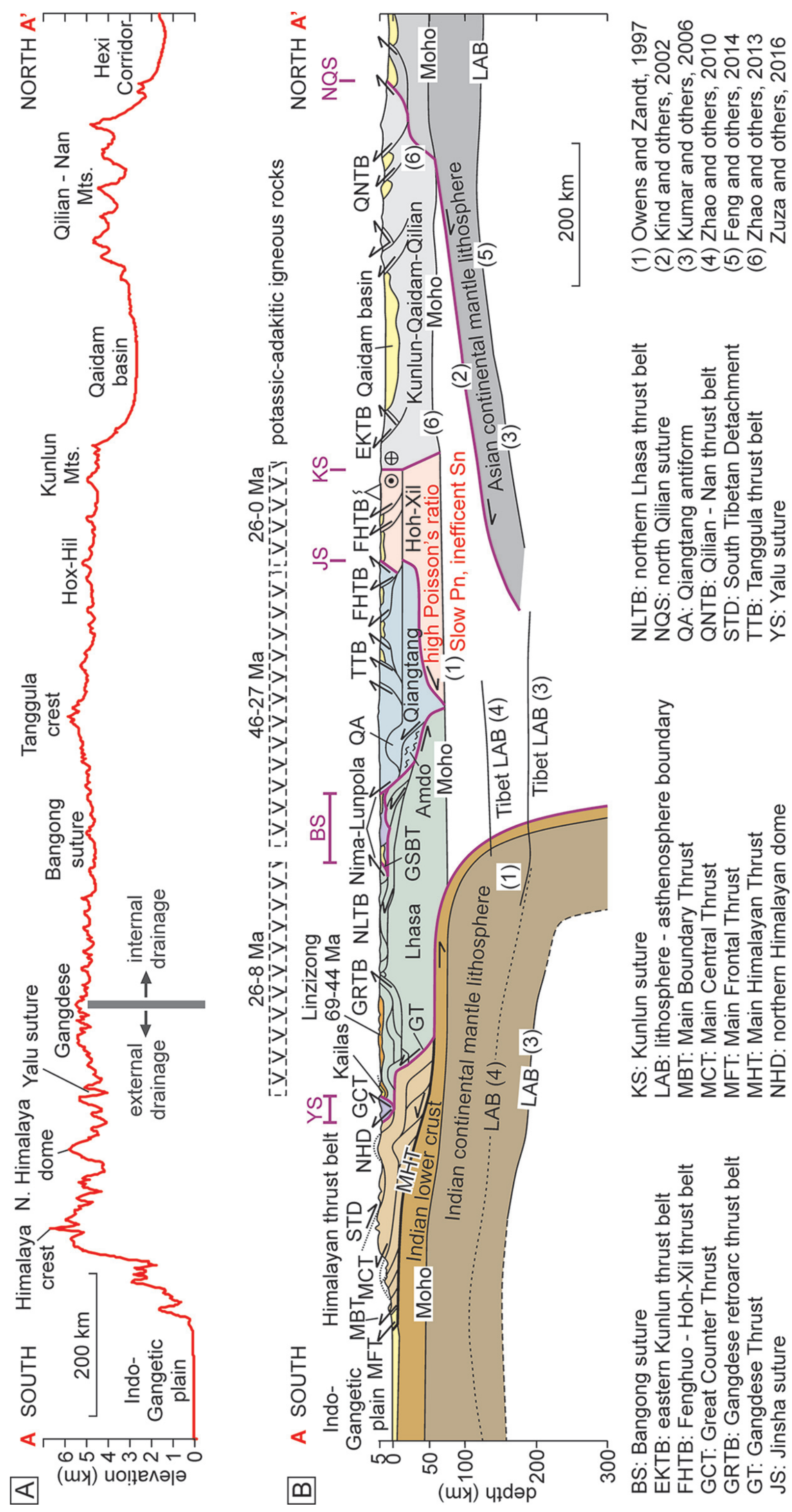

Fig. 2. (A) Topographic profile across the Himalayan-Tibetan orogen. Abbreviated is Mts., mountains. (B) Schematic lithosphere-scale cross-section of the Himalayan-Tibetan orogen.

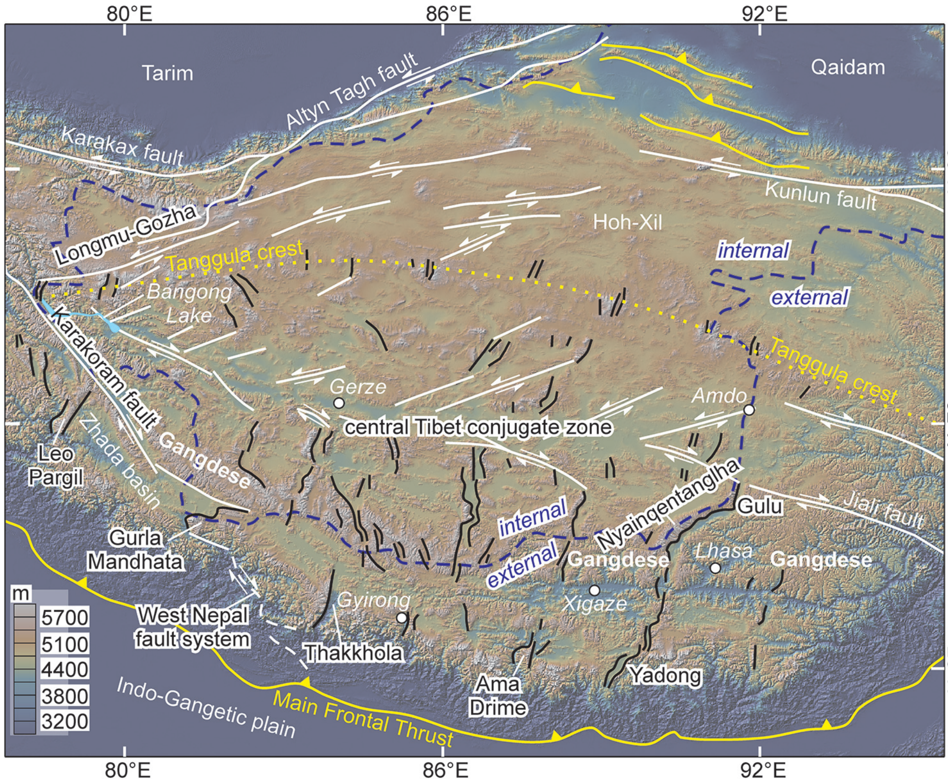

Fig. 3. Digital elevation map of the Himalaya and Tibetan Plateau from Geomapapp.org with major active faults superimposed (yellow = thrust; black = normal; white = strike-slip).

and the suture zone between Indian and Asian rocks is a conspicuous feature, both geologically and physiographically (figs. 1, 2, and 3).

The near-sea-level Indo-Gangetic plain rims the northern Indian subcontinent and laps up against the south flank of the Himalayan thrust belt (fig. 1). It is a peripheral or pro-foreland basin, flexed downward by the weight of the thrust belt (Lyon-Caen and Molnar, 1983), which forms a southward-convex salient extending for ~2400 km between the peaks of Nanga Parbat in the west and Namche Barwa in the east (fig. 1). The Indo-Gangetic plain is underlain by a wedge of foreland basin sediment that tapers southward from a maximum thickness of ~7 km to a feather-edge onlapping the northern Indian craton (Lyon-Caen and Molnar, 1983; Raiverman and others, 1983; Burbank and others, 1996). The foreland basin is fed by the Brahmaputra (Siang) and Indus Rivers, which bracket the Himalaya on the east and west, respectively, and numerous other rivers that drain the southern flank of the thrust belt (fig. 1) and the northern flank of the Indian craton.

Over a horizontal distance of only ~100 km, Himalayan topography rises in elevation from near sea level to the highest peaks at elevations of >8.5 km along the axial crest of the range (fig. 2A). The highland drainage basins of the Indus and Brahmaputra Rivers abut each other ~300 km west of the midpoint along the southern arcuate flank of the Tibetan Plateau at Mt. Kailas [the Brahmaputra River becomes the Yalu (or Yarlung) River in Tibet; fig. 1]. From Mt. Kailas, the Indus flows northwestward and the Yalu eastward within prominent (~2-km-scale relief), narrow valleys that

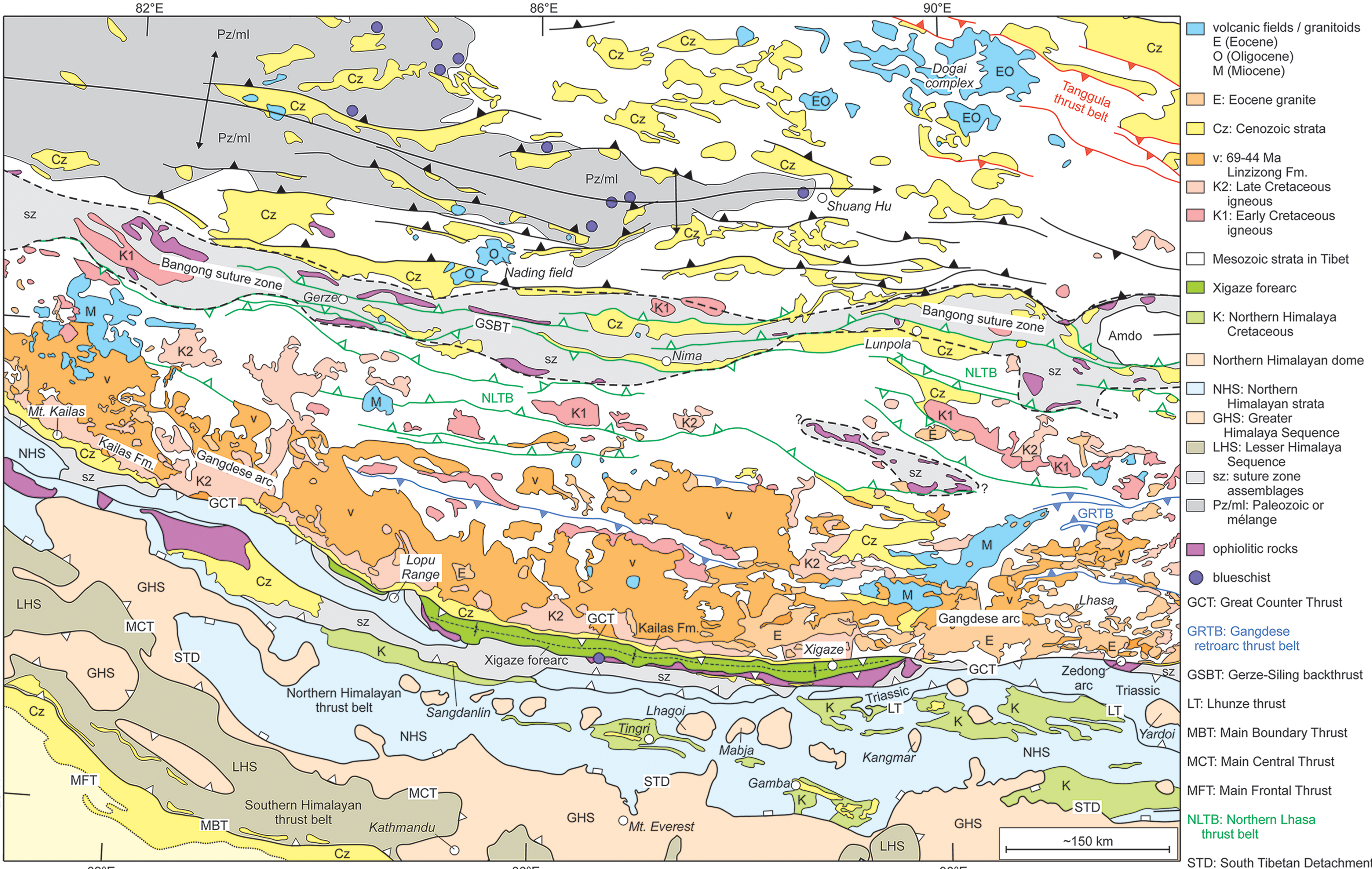

Fig. 4. Geological map of the central Himalayan-Tibetan orogen, compiled from Pan and others (2004), 1:500,000 geological map of the Gangdese-Himalaya (Wang and others, 2006), and our mapping. Late Cenozoic to recent normal and strike-slip faults are not shown for clarity (see fig. 3).

parallel the arcuate Himalaya to the south. These valleys roughly demarcate the suture zone between rocks of Indian affinity in the Himalayan thrust belt and the southern continental margin of Asia (Lhasa terrane) to the north. Hence, the Indus-Yalu suture zone, and its western (Indus) and eastern (Yalu) segments, are named after these rivers (Gansser, 1964). The Himalayan thrust belt is divided geographically into the northern Himalaya and southern Himalaya by the topographic crest of the range (Yin, 2006; fig. 1).

The Tibetan Plateau extends >1000 km north of the Yalu suture zone (YSZ), and >2000 km east to west. The plateau is divisible into relatively rugged, externally-drained flanking areas and a vast, internally drained core region dominated by hydrologically closed lake basins (figs. 1 and 3). The plateau's northern boundary is demarcated by the Altyn Tagh fault and the transition from the Nan Mountains (fig. 1) to the Hexi Corridor (fig. 2A). The eastern margin of the plateau is more diffuse, as elevation diminishes gradually toward northern Indo-China. To the west, the plateau is separated from the Karakoram, Hindu Kush, and Pamir Mountains by the Karakoram strike-slip fault (figs. 1 and 3).

Directly north of the YSZ, the southward-convex, ~100-km-wide Gangdese (or Transhimalaya) Mountains have relatively high relief (>1.5 km) on their southern flank (figs. 2A and 3). West of Xigaze city, the Gangdese Mountains generally taper northward, dropping ≥500 m in elevation into the southern part of the internally drained plateau-proper, and their crest roughly follows the divide between internal and external drainage (figs. 2A and 3). North of Lhasa city, the northeast-southwest-trending Nyainqentanglha Mountains form a prominent divide between internal and external drainage (fig. 3). Near and to the east of Xigaze, the Gangdese Mountains are deeply incised by tributaries of the Yalu River.

Roughly 300 km north of the YSZ is an east-west trending topographic depression that includes numerous closed basins from Bangong Lake in the west to near Amdo city in the east (fig. 3). This depression roughly marks the position of the Mesozoic Bangong (-Nujiang) suture zone between the Qiangtang and Lhasa terranes (figs. 1 and 2). Westernmost Tibet exhibits higher relief than central Tibet because of river incision during prior phases of external drainage (Gourbet and others, 2017).

Mean elevation increases northward from the Bangong suture to the crest of the northward-convex Tanggula Mountains (figs. 1 and 2A). The Tanggula Mountains define the southern boundary of a region of permafrost, which extends northward across the Hoh-Xil region to the eastern Kunlun Mountains (fig. 1). Permafrost partial melting during summer, extreme cold during winter and spring, and scarce freshwater (even stream water is salty in many places) make the Tanggula Mountains and Hoh-Xil region west of the Lhasa-Golmud Highway (fig. 1) the most inhospitable and least investigated part of Tibet.

Active Tectonics

Geodetic studies indicate that India is converging ~N20°E relative to Eurasia at a rate of ~36 mm/yr, and about half of this convergence (18–20 mm/yr) is accommodated in the Himalayan thrust belt by slip along the Main Himalayan Thrust and its updip southward imbricates including the Main Frontal Thrust (figs. 1, 2B, and 3; Bilham and others, 1997; Avouac, 2003; Jouanne and others, 2004; Bettinelli and others, 2006; Ader and others, 2012; Stevens and Avouac, 2015). Seismic reflection profiles image the Main Himalayan Thrust (or basal Himalayan décollement) dipping 10 to 20° northward beneath the northern Himalaya to depths of 45 to 55 km (fig. 2B); its down-dip extent has not been resolved north of the YSZ (Nelson and others, 1996; Hauck and others, 1998; Makovsky and others, 1999; Schulte-Pelkum and others, 2005; Nábělek and others, 2009; Gao and others, 2016). Combined geodetic and seismic reflection data demonstrate that the Indian lower continental crust and underlying lithospheric mantle are actively underthrusting northward. The remainder of the geodetic convergence is accommodated in a distributed manner across the Tibetan Plateau and tectonically active mountain ranges in central Asia (Shen and others, 2000; Zhang and others, 2004c).

From the Main Frontal Thrust to approximately the Himalayan crest, most active deformation is characterized by folding and thrust faulting (Nakata, 1989; Mugnier and others, 1994; Lavé and Avouac, 2001; Bettinelli and others, 2006; Ader and others, 2012; Bollinger and others, 2014; Avouac and others, 2015; Hossler and others, 2016; Whipple and others, 2016; Wesnousky and others, 2017). Seismic activity in the thrust belt is concentrated at depths of 10 to 15 km beneath the medial part of the southern Himalaya (Pandey and others, 1999; Cattin and Avouac, 2000). Most of this activity is in the form of microseisms, but the 2015 Gorkha, Nepal earthquakes involved two $Mw \geq 7.2$ events on low-angle segments of the Main Himalayan Thrust (Whipple and others, 2016; Elliott and others, 2016; Duputel and others, 2016; Jouanne and others, 2017). Large, surface-rupturing earthquakes seem to be confined to the Main Frontal Thrust system (for example, Sapkota and others, 2013; Bollinger and others, 2014). Between the Himalayan crest and the Kunlun Mountains, surficial and upper crustal deformation are dominated by strike-slip and normal faulting (fig. 3; Tapponnier and Molnar, 1976; Taylor and Yin, 2009). The northwestern Tibetan Plateau is bounded by the northeast-striking, left-lateral Altyn Tagh fault and its more easterly-striking splay within the Western Kunlun Mountains (Karakax fault, fig. 3). The Altyn Tagh fault also feeds slip southwestward into the Longmu-Gozha fault system, which extends to the trace of the northwest-striking right-lateral Karakoram fault (fig. 3; Raterman and others, 2007; Van Buer and others, 2015; Chevalier and others, 2017). The Karakoram fault feeds slip southeastward into the top-to-the west-northwest Gurla Mandhata detachment system (Murphy and others, 2002), which in turn links with the diffuse, northwest-striking, dextral Western Nepal fault system (fig. 3; Murphy and Copeland, 2005; Murphy and others, 2014).

Other active faults in the northern Himalaya are mostly orogen-perpendicular normal faults that localize late Miocene to active extensional basins (for a review see DeCelles and others, 2018), the most prominent of which include those bounding the Leo Pargil massif/horst (Thiede and others, 2006; Saylor and others, 2010), Thakkhola graben (Colchen, 1999; Hurtado Jr. and others, 2001; Garzione and others, 2003), Ama Drime massif/horst (Jessup and others, 2008b; Langille and others, 2010), and the Yadong graben (Burchfiel and others, 1991; Cogan and others, 1998) (fig. 3). The Zhada basin in the western northern Himalaya (figs. 1 and 3) may have been generated by orogen-parallel stretching and crustal thinning between Leo Pargil and Gurla Mandhata, along with incision by the Sutlej River (Murphy and others, 2009; Saylor and others, 2010). Collectively, active faulting within the northern Himalaya accommodates >30 mm/yr of orogen-parallel extension (Styron and others, 2011). This extension is balanced in part by orogen-perpendicular contraction across the western and eastern Himalayan syntaxes (Burg and others, 1997, 1998; Seeber and Pêcher, 1998); the remainder results in lengthening of the Himalayan arc (Klootwijk and others, 1985).

Most short-wavelength (<50 km) topographic relief in Tibet is related to rifting along northerly-striking normal faults (fig. 3; Armijo and others, 1986; Taylor and others, 2003). Within the Bangong suture depression, rifts are less prominent and kinematically linked with longer-strike-length conjugate strike-slip faults (northwest-striking and right-lateral in the south and northeast-striking and left-lateral in the north) that accommodate distributed north-south shortening and eastward extrusion (fig. 3, central Tibet conjugate zone, the right-lateral part of which is the Karakoram-Jiali fault zone; Armijo and others, 1989; Taylor and others, 2003; Yin and Taylor, 2011). The rate of east-west extension between 79°E and 93°E longitude is ~22 mm/yr (Zhang and others, 2004c). The northernmost rifts in Tibet cut orthogonally across the crest of the Tanggula Mountains (Kapp and Guynn, 2004). Farther north, the Hoh-Xil region exhibits distributed left-lateral strike-slip faults oriented sub-parallel to the Altyn Tagh fault; to the east, left-lateral displacement is localized along the Kunlun fault (Van der Woerd and others, 1998; Li and others, 2005; Fu and Awata, 2007; fig. 3).

Lithospheric Structure

The thickness of the Himalayan-Tibetan crust varies spatially, generally increasing northward across the Himalaya from ~40 km to 65 to 70 km near the YSZ (Hauck and others, 1998; Schulte-Pelkum and others, 2005; Nábělek and others, 2009; Gao and others, 2016). The thickest crust, up to 85 to 90 km, is present beneath western Tibet and the Lhasa terrane (Kind and others, 2002; Wittlinger and others, 2004). Crustal thickness decreases northward and eastward to 60 to 70 km beneath the Qiangtang and Hoh-Xil – Songpan-Ganzi terranes (fig. 2B; Vergne and others, 2002; Tseng and others, 2009; Karplus and others, 2011; Zhang and others, 2011c). Tibetan crust, at least locally beneath the rifts, contains layers of low-viscosity, partially-molten or brine-bearing mid-crust that may be flowing in response to regional topographic gradients (Bird, 1991; Fielding and others, 1994; Nelson and others, 1996; Royden and others, 1997; Makovsky and Klemperer, 1999; Clark and Royden, 2000; Beaumont and others, 2001; Klemperer, 2006; Hetényi and others, 2011).

The topography of Tibet is, at least partially, isostatically compensated by lateral variations in the density of the lower crust and upper mantle. The lower part of the thick crust of southern Tibet is interpreted to be eclogitized and underlain by thick, cold lithosphere of the Indian plate (fig. 2B; Schulte-Pelkum and others, 2005; Hetényi and others, 2007; Nábělek and others, 2009). In contrast, the lower part of the thinner northern Tibetan crust includes lower-density metasedimentary rocks and is underlain by an anomalously hot mantle lithosphere as indicated by inefficient *S*-wave propagation, low *P*-wave velocities, strong seismic anisotropy, and very high-temperature lower crustal xenoliths in ~3 Ma volcanic rocks (fig. 2B; Ni and Barazangi, 1983; Brandon and Romanowicz, 1986; Owens and Zandt, 1997; Hacker and others, 2000; Zhao and others, 2001; Pullen and Kapp, 2014). Most geophysical images show the Indian mantle lithosphere to be underthrust subhorizontally beneath most or all of western Tibet (Zhou and Murphy, 2005; Nábělek and others, 2009; Zhao and others, 2010). To the east, Indian mantle lithosphere either underthrusts most of the Lhasa terrane (fig. 2B; Owens and Zandt, 1997; DeCelles and others, 2002; Tilmann and others, 2003) or subducts more steeply northward beneath a wedge of Asian mantle (Kosarev and others, 1999; Li and others, 2008; Zhao and others, 2010). Potentially complicating seismic resolution is that the Indian plate itself may be complexly deformed or torn beneath southern Tibet (Yin, 2000; Liang and others, 2012, 2016; Razi and others, 2016). Despite the evidence for northward underthrusting or subduction of Indian lithosphere, there are no associated Benioff-like zones of intermediate-depth seismicity like those beneath the Pamir (Roecker, 1982; Sippl and others, 2013; Kufner and others, 2016, 2017). Rather, the deepest seismicity is restricted to scarce events at near-Moho depths beneath the southwestern Nyainqentanglha Mountains and to the southwest beneath the northern Himalaya (Chen and Molnar, 1983; Jackson, 2002; Chen and Yang, 2004). Given that fault plane solutions indicate ~east-west extension, Yin (2000) suggested that east-west extension may affect the entire composite lithosphere, including the subducting Indian plate.

Geological Framework

The Himalayan-Tibetan orogen is composed of a collage of continental crustal, oceanic island arc, ophiolitic, and subduction-complex rocks separated by, or encompassed within suture zones along which former oceanic basins and substantial tracts of continental lithosphere were subducted. The geological assemblages are lumped into four first-order terranes—the Kunlun, Hoh-Xil, Qiangtang, and Lhasa—which are bounded by the Kunlun, Jinsha, Bangong, and Indus-Yalu suture zones (fig. 1). The sutures are generally younger southward and record the overall accretionary expansion of the southern Asian continent during the Mesozoic – Cenozoic (Allègre and others, 1984; Şengör, 1984; Chang and others, 1986; Dewey and others, 1988; Şengör and Natal'in, 1996; Yin and Harrison, 2000). The most recent addition to the Asian landmass is the Indian subcontinent, the upper crustal parts of which were shortened and accreted within the Himalayan thrust belt as it drove into and beneath the Lhasa terrane during the Cenozoic.

The Kunlun terrane is exposed in the western and eastern Kunlun Mountains (fig. 1). It consists of Archean to Proterozoic basement and Cambrian to Devonian and Permian to Early Jurassic arc rocks (Şengör, 1984; Dewey and others, 1988; Matte and others, 1996; Mattern and others, 1996; Cowgill and others, 2003; Roger and others, 2003). To the south of the Kunlun suture, the Tianshuihai – Hoh-Xil – Songpan-Ganzi terrane (nomenclature from west to east) includes voluminous Triassic turbidite-bearing strata (fig. 1; Nie and others, 1994; Zhou and Graham, 1996; Weislogel and others, 2006; Enkelmann and others, 2007; Weislogel, 2008; Ding and others, 2013). These rocks are interpreted as submarine fan deposits, the distal parts of which accumulated on Paleo-Tethys oceanic lithosphere. The Triassic Paleo-Tethys ocean basin included one or more intra-oceanic subduction zones and associated island arcs, with the Yushu-Yidun arc in eastern Tibet being best documented (Reid and others, 2007; Yang and others, 2012; Wang and others, 2013). Triassic and older rocks in the Hoh-Xil terrane are locally overlain by Upper Cretaceous through Miocene nonmarine strata (Pan and others, 2004; Wu and others, 2008; Staisch and others, 2014). The Hoh-Xil terrane experienced major upper-crustal shortening during Late Triassic through Middle Jurassic and Eocene through Oligocene time (Coward and others, 1988; Roger and others, 2008, 2010; Ding and others, 2013; Staisch and others, 2014, 2016).

The Qiangtang terrane has been divided into a northern Qiangtang terrane of purported Cathaysian affinity, exposing mostly Triassic to Jurassic shallow marine and nonmarine strata, and a southern Qiangtang terrane of Gondwana affinity, exposing mostly upper Paleozoic to Jurassic marine strata (Metcalfe, 1988; Li and Zheng, 1993; Li and others, 1995). Exposures of blueschist- and eclogite-bearing mélange define a discontinuous, but enormous (up to 150-km-wide and >600-km-long) east-west trending belt of subduction complex rocks within the central part of the Qiangtang terrane (figs. 1 and 4; Hennig, 1915; Li and others, 1995; Kapp and others, 2000, 2003b; Zhang and others, 2006; Liang and others, 2017). Rare basement rocks in the southern Qiangtang terrane consist of 476 to 471 Ma gneisses (Pullen and others, 2011b; Zhao and others, 2014). The Qiangtang terrane has been above sea level since at least Early Cretaceous time and experienced moderate shortening and syncontractional basin development during Eocene – Oligocene time (fig. 5; for example, Kapp and others, 2003b, 2005).

Bangong suture-zone assemblages between the Qiangtang and Lhasa terranes include Upper Triassic to Lower Cretaceous deep marine (turbiditic) strata, ophiolites, and mélanges (Girardeau and others, 1984a, 1985a; Pearce and Deng, 1988; Kapp and others, 2003a, 2005, 2007a; Wang and others, 2008b; Baxter and others, 2009; Dong and others, 2016; Zeng and others, 2016; Zhang and others, 2016b). The

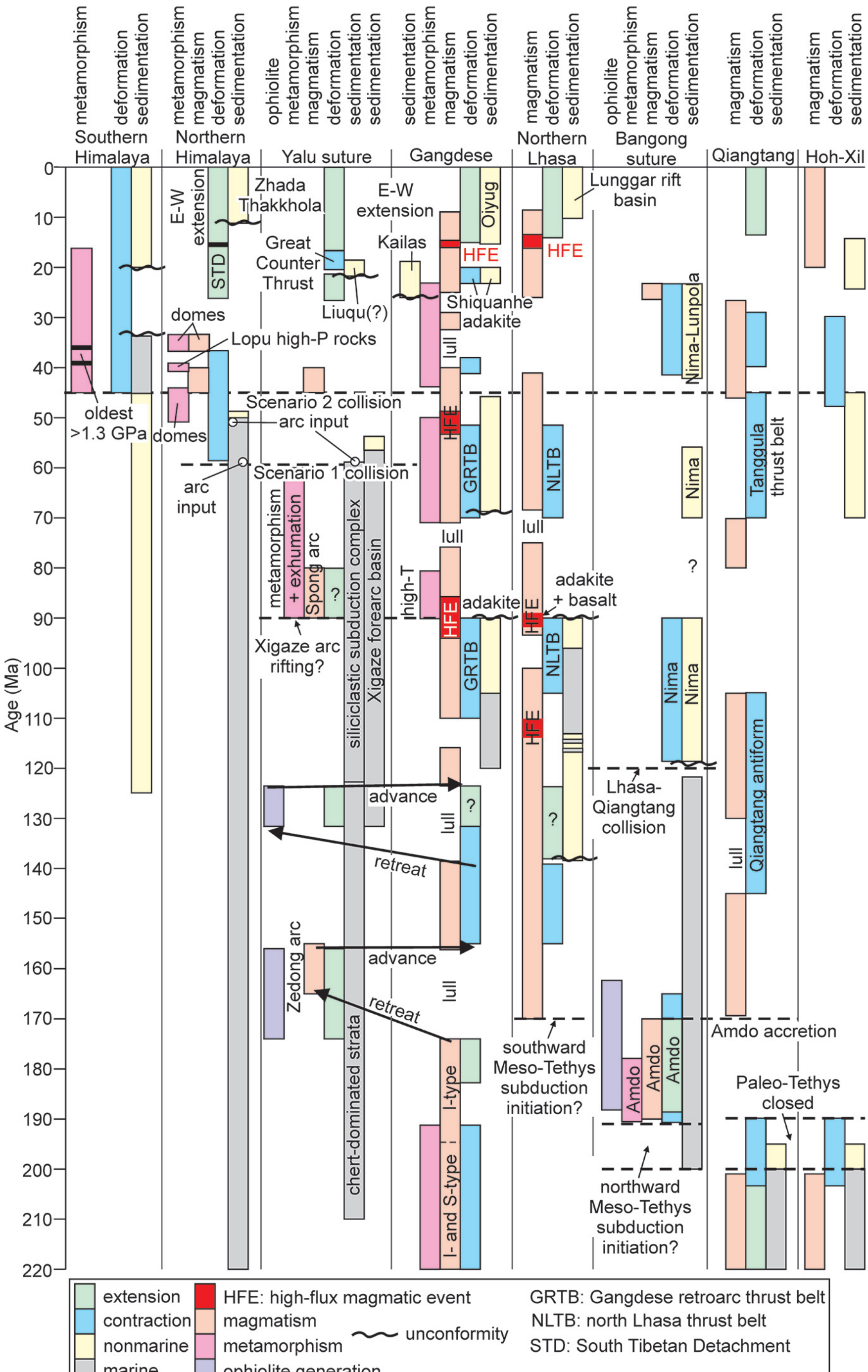

Fig. 5. Time-space-geology summary chart indicating timing of ophiolite generation, metamorphism, magmatism, deformation, and sedimentation in the Himalayan-Tibetan orogen. Arrows indicate time intervals of interpreted Neo-Tethyan trench advance and retreat.

assemblages are intruded by Early Cretaceous granitoids and locally unconformably overlain by marine or nonmarine Lower Cretaceous strata and uppermost Cretaceous to Miocene nonmarine strata (fig. 5; for example, Kapp and others, 2003a, 2005, 2007a; DeCelles and others, 2007a). Jurassic to Early Cretaceous igneous and Lower Cretaceous sedimentary rocks are widely exposed in the northern Lhasa terrane (Pan and others, 2004). The Bangong suture zone and northern Lhasa terrane were shortened and uplifted above sea level during Cretaceous development of the southward younging northern Lhasa thrust belt (NLTB; figs. 2B, 4, and 5; Kapp and others, 2007a; Volkmer and others, 2007, 2014; Rohrmann and others, 2012). The Bangong suture zone and parts of the northern Lhasa terrane experienced thrust reactivation and intermontane basin development during latest Cretaceous and Oligocene – early Miocene time (fig. 5; Kapp and others, 2003a, 2007b; DeCelles and others, 2007a; Volkmer and others, 2007, 2014).

The southern Lhasa terrane is dominated by the Gangdese (or Transhimalayan) magmatic arc, composed predominantly of Mesozoic to Eocene intrusive and extrusive igneous rocks (fig. 4; Maluski and others, 1982; Schärer and others, 1984; Coulon and others, 1986; Debon and others, 1986). The arc edifice is represented by widely exposed 69 to 44 Ma volcanic-bearing strata of the Linzizong Formation (figs. 2B and 4; Coulon and others, 1986; He and others, 2007; Xu and others, 2015a; Zhu and others, 2015). The southern Lhasa terrane was uplifted above sea level by ∼100 Ma and shortened by the Gangdese retroarc thrust belt (GRTB, figs. 2B, 4, and 5) that was active (although possibly intermittently) between mid-Cretaceous and Eocene time (Kapp and others, 2007b; Leier and others, 2007b; Pullen and others, 2008a).

Cenozoic "post-collisional" or "syn-collisional" (ultra)potassic and adakitic igneous rocks are broadly distributed across Tibet (for example, Turner and others, 1996; Ding and others, 2003; Chung and others, 2005; Chen and others, 2013; Ou and others, 2017; figs. 2B and 4). The potassic-adakitic rocks are Eocene – Oligocene in the Qiangtang terrane, late Oligocene – Miocene in the Lhasa terrane, and mostly Miocene – Quaternary in the Hoh-Xil terrane (figs. 2B and 4; Ding and others, 2003). All of the potassic-adakitic volcanic fields are flat-lying or gently tilted above angular unconformities, indicating minimal upper-crustal shortening and exhumation since their eruption.

The YSZ is marked by four belts of rocks that constitute, from north to south, the Gangdese magmatic arc, Kailas basin, Xigaze forearc basin, and Xigaze accretionary complex including ophiolites and mélanges (fig. 4). The Kailas basin is a narrow (<15 km) but extensive (>1300 km long) late Oligocene to early Miocene basin that onlaps northward onto the Gangdese arc and rests in the footwall of the Miocene south-dipping Great Counter thrust system to the south (figs. 2B and 4; Gansser, 1964; Yin and others, 1999; Aitchison and others, 2002, 2009; Murphy and Yin, 2003; DeCelles and others, 2011, 2016b; Leary and others, 2016a; Li and others, 2017c). In the central part of the YSZ, the Great Counter Thrust carries the Xigaze forearc basin in its hanging wall, whereas along strike to the west and east where the forearc basin is absent, it carries other YSZ assemblages or Himalayan rocks in its hanging wall (fig. 4). Miocene south-dipping thrust faults involve YSZ rocks to the south of, and locally branch from the main trace of the Great Counter Thrust (Burg and others, 1987; Ratschbacher and others, 1994; Yin and others, 1999). We refer to these faults collectively as the Great Counter thrust system, and note that it and associated north-vergent folds modified the primary structural architecture of the YSZ. South of the Great Counter Thrust lies the Aptian – Eocene Xigaze forearc basin, a >6 km thick upward-shoaling, mostly marine forearc basin that filled with detritus of mainly Lhasa terrane affinity (Einsele and others, 1994; Dürr, 1996; Ding and others, 2005; Wang and others, 2012; An and others, 2014; Orme and others, 2015; Hu and others, 2016b;

Orme and Laskowski, 2016). Along its southern outcrop limit, the forearc basin is in fault-, and locally depositional-, contact with the Xigaze accretionary belt, an assemblage of ophiolites, mélanges, and sedimentary rocks that represent the accretionary prism that formed during Cretaceous – Paleocene northward subduction of Neo-Tethyan oceanic lithosphere (Tapponnier and others, 1981; Burg and Chen, 1984; Burg and others, 1987; Cai and others, 2012; Orme and Laskowski, 2016; An and others, 2017).

The Himalayan thrust belt lies to the south of the Xigaze forearc basin and accretionary belt, and consists of a southward verging orogenic wedge composed of Paleo-Mesoproterozoic low-grade metasedimentary and metaigneous rocks (Lesser Himalayan Sequence), Neoproterozoic-early Cambrian amphibolite-facies metasedimentary rocks intruded by Cambrian-Ordovician plutons and Neogene leucogranites (Greater Himalayan Sequence), Ordovician-Mesozoic sedimentary rocks (Tethyan Himalayan Sequence), Cenozoic foreland basin deposits, and Neogene extensional basin deposits (see reviews by Hodges, 2000; Martin, 2017; and DeCelles and others, in review[1]). Although most Himalayan workers include Cambrian, or even upper Proterozoic, rocks in the Tethyan Himalayan Sequence, we restrict this term to rocks that are above a prominent late Cambrian-early Ordovician unconformity, which is a preferred allostratigraphic boundary (Wiesmayr and Grasemann, 2002; Gehrels and others, 2006a, 2006b; DeCelles and others, 2016a, in review[2]). Rocks below this unconformity are commonly intruded by Cambrian-Ordovician plutons and dikes, whereas the rocks above the unconformity are not, but typically contain detrital zircons derived from the plutons below the unconformity. Cambrian rocks are known to be part of the Greater Himalayan Sequence (for example, Parrish and Hodges, 1996; DeCelles and others, 2000; Steck, 2003), and a logical scheme would include all of the Cambrian rocks in the same tectonostratigraphic package. We do not subscribe to schemes of Himalayan tectonostratigraphy based on fault or shear zone locations (Searle and others, 2008) or metamorphic grade (Goscombe and others, 2006, 2018; Searle and others, 2008). With the exception of the Neogene extensional basins, all of the rocks in the Himalayan thrust belt have been scraped off of India as it has underthrust the southern flank of the Lhasa terrane. For purposes of brevity, in this paper we informally divide the Himalaya into northern and southern parts on either side of the Himalayan topographic crest (figs. 1 and 4). Although this does not conform to the standard geographical zonation used in many Himalayan studies (for examples, Hodges, 2000), it is simple, does not require a lengthy explanation (as more commonly used alternatives do), and yet sufficiently conveys critical geographic information. We are not advocating abandonment of more commonly employed geographic zonations.

In the central part of the Himalaya, the brittle, top-to-the-north Miocene South Tibetan Detachment fault is present more or less along the Himalayan topographic crest (fig. 4), and juxtaposes Tethyan Himalayan Sequence strata or Neoproterozoic to Cambrian Greater Himalayan Sequence rocks in the hanging wall against higher-grade Greater Himalayan Sequence rocks in the footwall (Burg and Chen, 1984; Burchfiel and others, 1992). We distinguish the brittle South Tibetan Detachment fault from the underlying latest Oligocene to mid-Miocene top-to-the-north South Tibetan ductile shear zone in footwall Greater Himalayan Sequence rocks (for example, Vannay and others, 2004; Kellett and Grujic, 2012; timing summarized in Webb and others, 2017 and Goscombe and others, 2018). This is because the ductile shear zone is not limited

[1] DeCelles, P. G., Carrapa, B., Ojha, T. P., Gehrels, G. E., and Collins, D., in review, Structural and thermal evolution of the Himalayan thrust belt in Midwestern Nepal: Geological Society of America Special Paper.

[2] Ibid.

to the Himalayan crest, but also crops out to the south within klippen in the southern Himalaya (Kellett and Grujic, 2012; He and others, 2015, 2016; Soucy La Roche and others, 2017; Kellett and others, 2019) and perhaps to the north in the northern Himalayan gneiss domes (Larson and others, 2010; Wagner and others, 2010) (fig. 2B). Structurally lower, and to the south, the Greater Himalayan Sequence is juxtaposed against the Lesser Himalayan Sequence by the top-to-the-south Main Central Thrust (figs. 2B and 4; Heim and Gansser, 1939). Recent studies have documented a number of mostly top-to-the-south "tectonometamorphic discontinuities" within the lower part of the Greater Himalayan Sequence (for example, Carosi and others, 2018; Goscombe and others, 2018). To simplify description, we henceforth refer to all top-to-the-south shear zones in Greater Himalayan Sequence rocks as parts of the Main Central Thrust system, and note that it was active at generally the same time as top-to-the-north motion on the South Tibetan Detachment and shear zone (Main Central Thrust system timing summarized in Goscombe and others, 2018). Surficial thrusting subsequently propagated southward into Lesser Himalayan rocks, first as the Ramgarh/Munsiari Thrust (~14–12 Ma) and then into a system of splay thrusts (~11–5 Ma) that form a large duplex in Lesser Himalayan rocks beneath the Ramgarh and Main Central Thrusts (DeCelles and others, 2001, 2016a; Mitra and others, 2010; Long and others, 2011; Robinson and McQuarrie, 2012; Webb, 2013; Robinson and Martin, 2014). Thrusting propagated southward to the Main Boundary Thrust system by latest Miocene time (Meigs and others, 1995; Burbank and others, 1996; DeCelles and others, 2001; Chirouze and others, 2013), juxtaposing the Lesser Himalayan Sequence in the hanging wall against Miocene-Pliocene foreland basin strata of the Siwalik Group in the footwall, and then to the Main Frontal Thrust since ~2 Ma (Powers and others, 1998; Chirouze and others, 2013; DeCelles and others, in review[3]) (figs. 2B and 4). Both the Main Boundary and Main Frontal Thrusts are active during the Holocene (Nakata, 1989; Mugnier and others, 1994; Lavé and Avouac, 2000; Burgess and others, 2012; Hossler and others, 2016).

TRIASSIC – EARLY CRETACEOUS TECTONIC EVOLUTION OF NORTHERN TIBET

In this section, we summarize the closure history of the Paleo-Tethys ocean between the Kunlun and Qiangtang terranes and tectonic events that may have occurred during the early stages of Meso-Tethys oceanic subduction between the Qiangtang and Lhasa terranes and Neo-Tethys oceanic subduction northward beneath the southern margin of the Lhasa terrane.

Paleo-Tethys Ocean Closure

Permian – Jurassic magmatism in the Kunlun terrane is attributed to northward subduction of Paleo-Tethys oceanic lithosphere beneath the southern Asian margin (Şengör, 1984; Dewey and others, 1988; Yin and Harrison, 2000; Roger and others, 2003). Tectonically, the closure style of the Paleo-Tethys may have been similar to that of the Cenozoic Mediterranean, with Triassic continental collision between the North and South China blocks to the east and coeval subduction zone retreat and opening of marginal backarc ocean basins to the west as Gondwana-affinity terranes drifted northward (fig. 6A; Pullen and others, 2008b). In addition to rapidly generating accommodation for the thick, mostly Upper Triassic turbiditic strata within the Hoh-Xil – Songpan-Ganzi basin, slab rollback may explain the broad distribution and geochemical compositions of syndepositional igneous rocks that intruded the Triassic strata (de Sigoyer and others, 2014; Zhang and others, 2014b).

[3] Ibid.

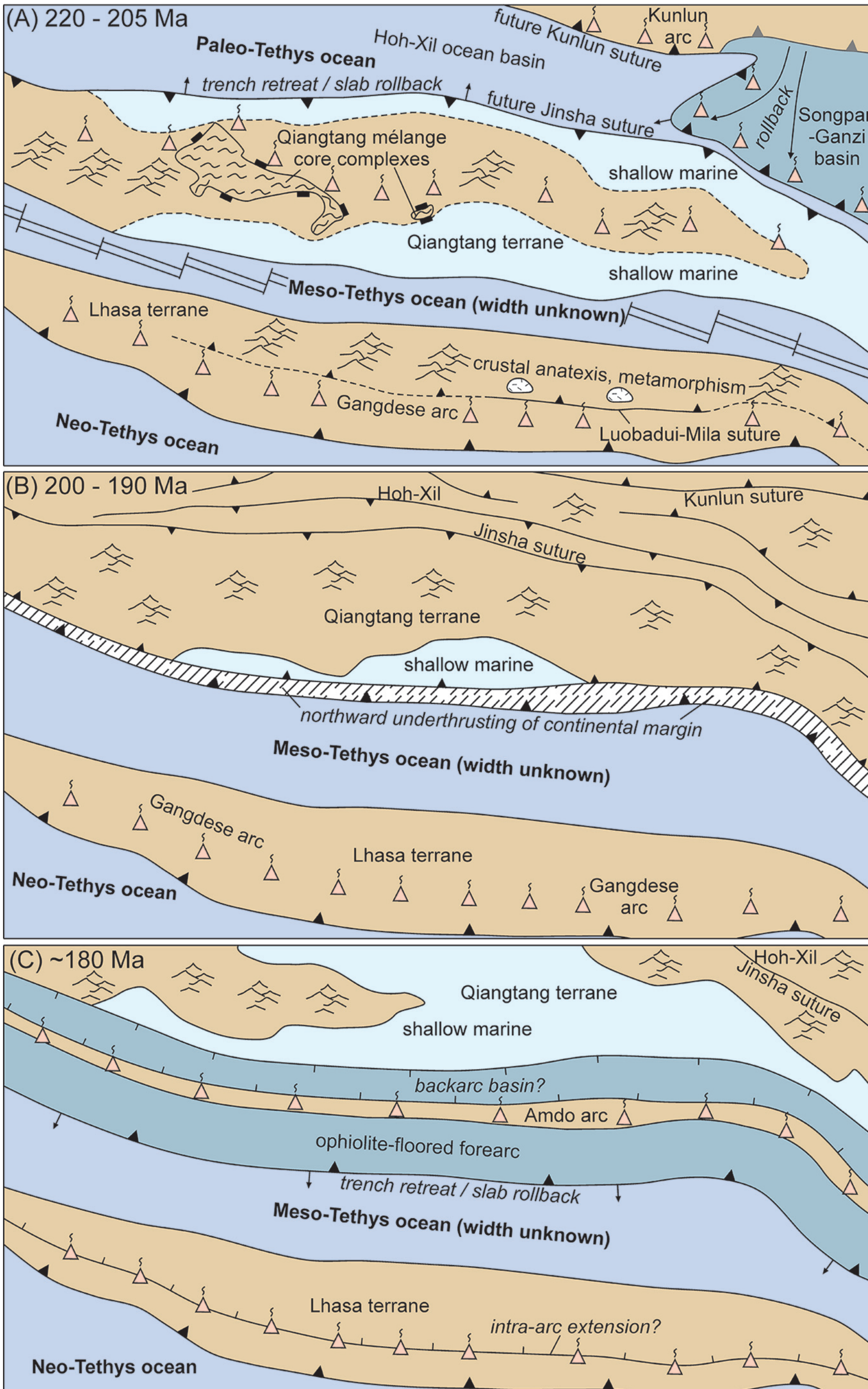

Fig. 6. Schematic paleogeographic and paleotectonic reconstructions from (A) 220 Ma to (H) 90 Ma. Arrow-tipped dotted lines show sediment dispersal patterns that are consistent with sedimentary paleocurrent and/or provenance data. Abbreviations are as follows: GRTB, Gangdese retroarc thrust belt; GSBT, Gerze-Siling backthrust; NLTB, north Lhasa thrust belt.

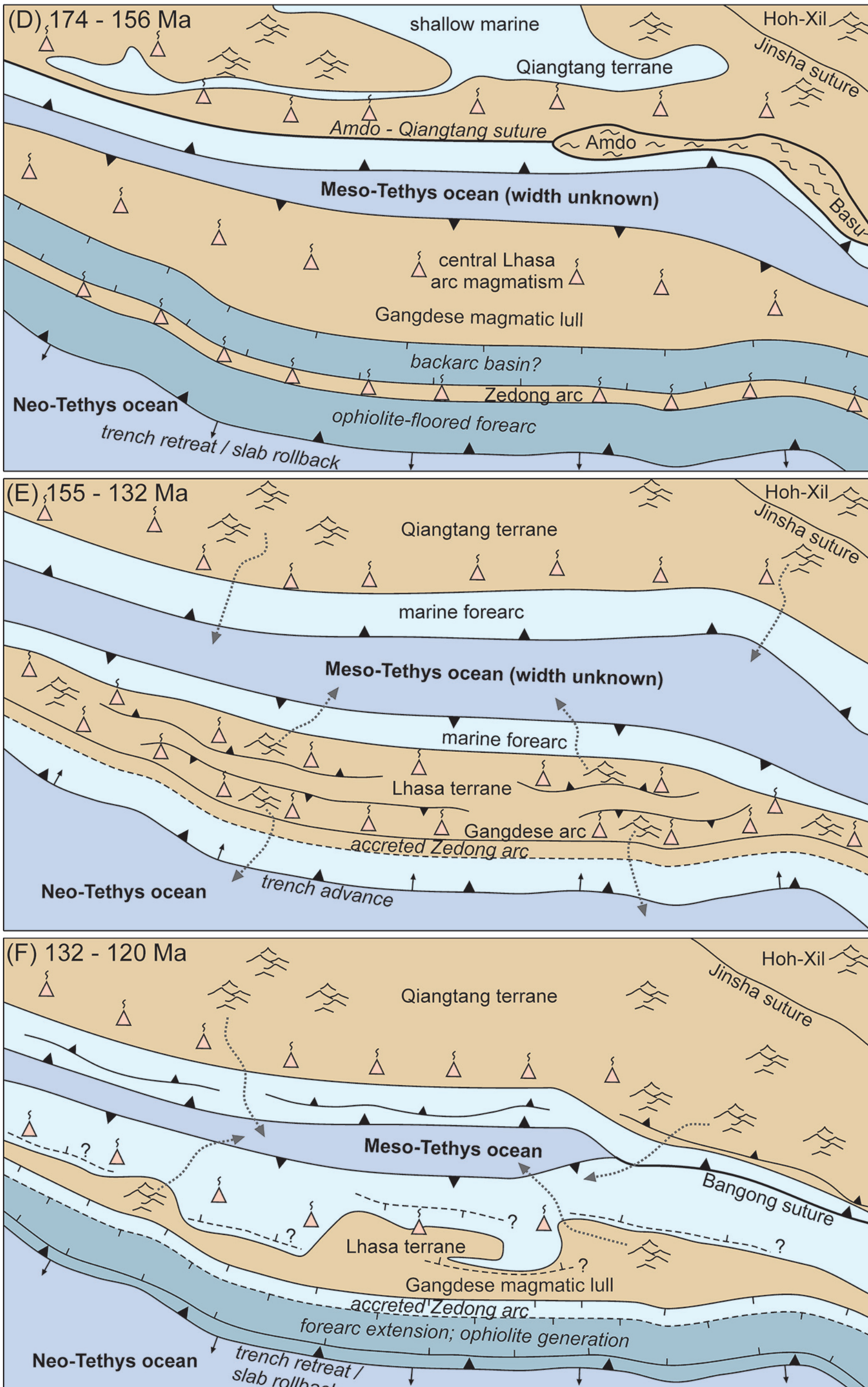

Fig. 6. (continued).

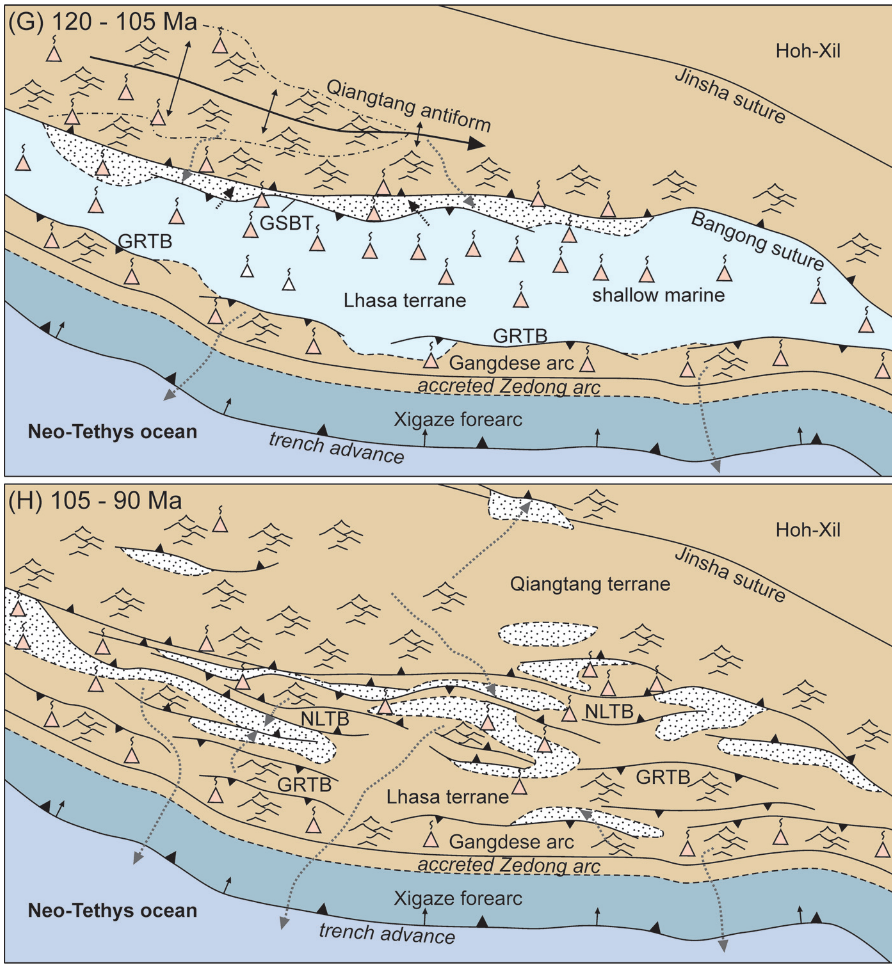

Fig. 6. (continued).

The southern part of the Paleo-Tethys was also subducting southward beneath the Qiangtang terrane during Triassic – Early Jurassic time along the Jinsha suture (figs. 6A and 7A). The Hoh-Xil – Songpan-Ganzi terrane was strongly shortened and uplifted above sea level during the Late Triassic (in the east) to Middle Jurassic (in the west) (Roger and others, 2008, 2010; Ding and others, 2013). Magmatic, sedimentary, and thermochronologic records suggest a 200 to 190 Ma age for the final consumption of oceanic lithosphere between the Kunlun and Jinsha sutures (figs. 5, 6B, and 7B; Dewey and others, 1988; Roger and others, 2010; Yang and others, 2012; Ding and others, 2013; Zhang and others, 2014b).

High-Pressure Mélange Within the Qiangtang Terrane

Central Qiangtang mélange is dominated by a siliciclastic matrix and includes blocks of Gondwanan-affinity Paleozoic – Triassic strata, Paleo-Tethys arc-affinity sandstone, marble, ophiolitic rock, and amphibolite-, blueschist- and eclogite-facies metabasite and schist (Hennig, 1915; Li and others, 1995; Kapp and others, 2000, 2003b; Zhang and others, 2006; Pullen and others, 2008b; Liang and others, 2017).

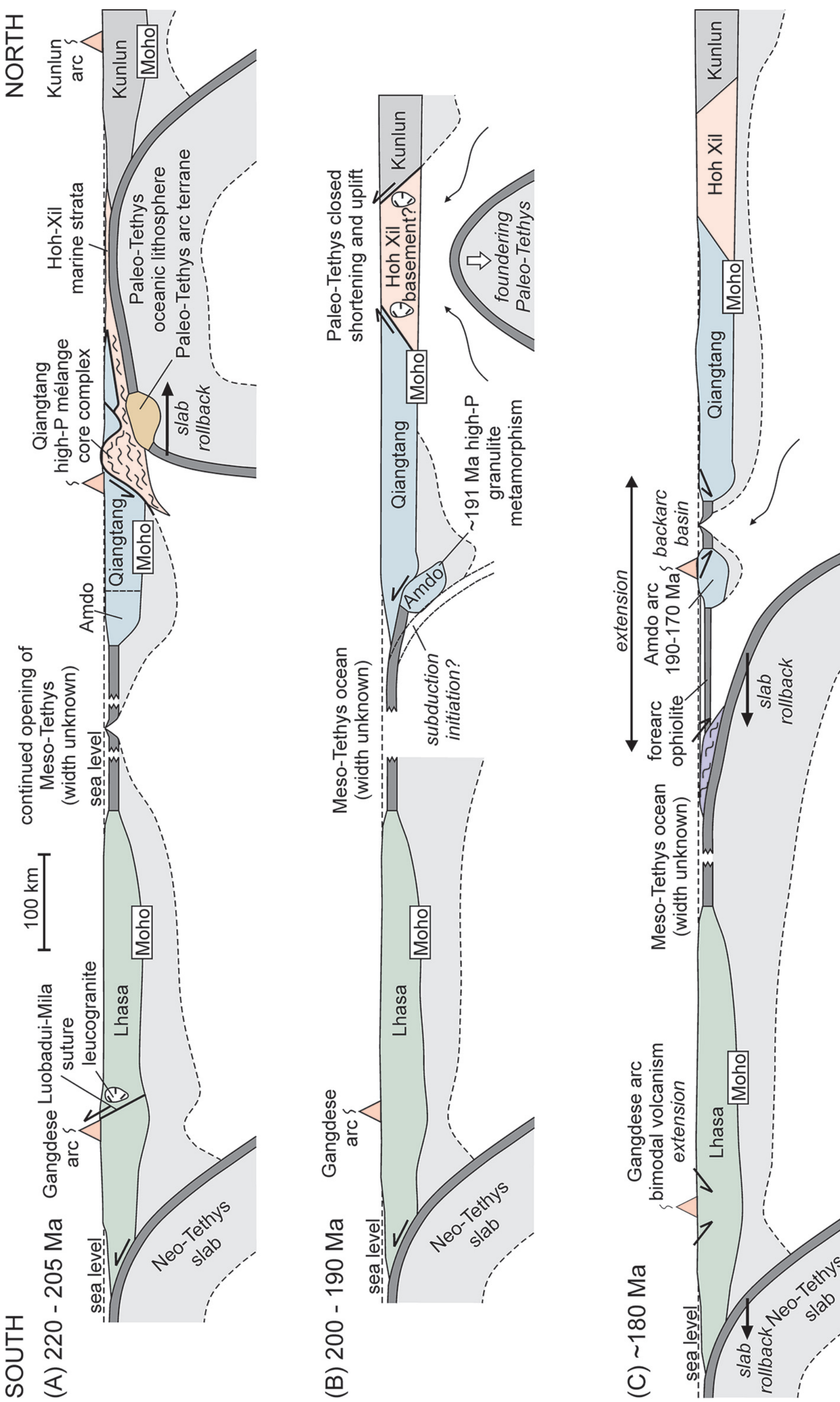

Fig. 7. Tectonic evolution illustrated in schematic lithosphere-scale cross-sections with no vertical exaggeration from (A) 220 Ma to (H) 90 Ma. Oceanic crust is shaded in gray. Dashed line indicates base of mantle lithosphere. Interpretations are italicized to distinguish them from observations.

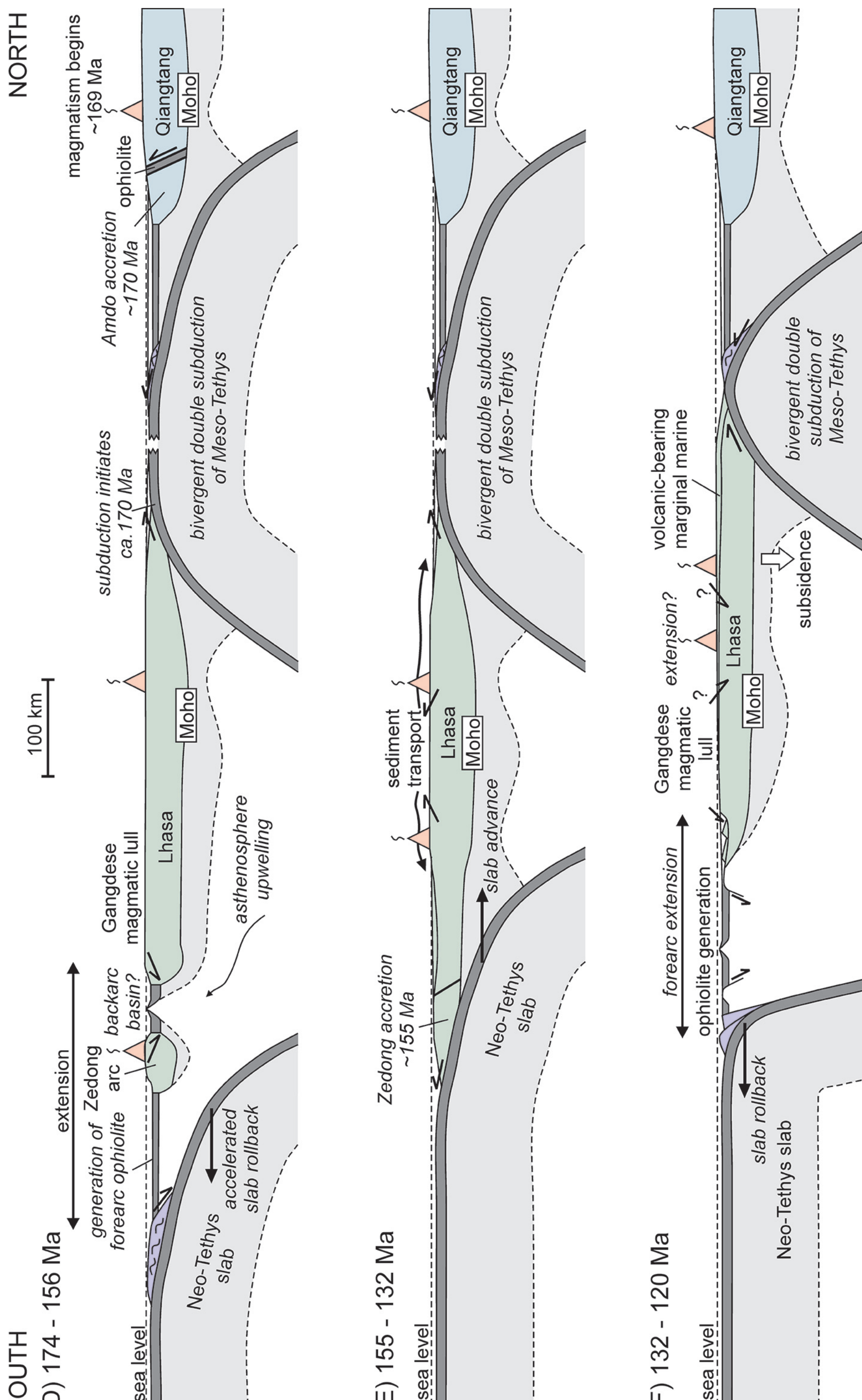

Fig. 7. (continued).

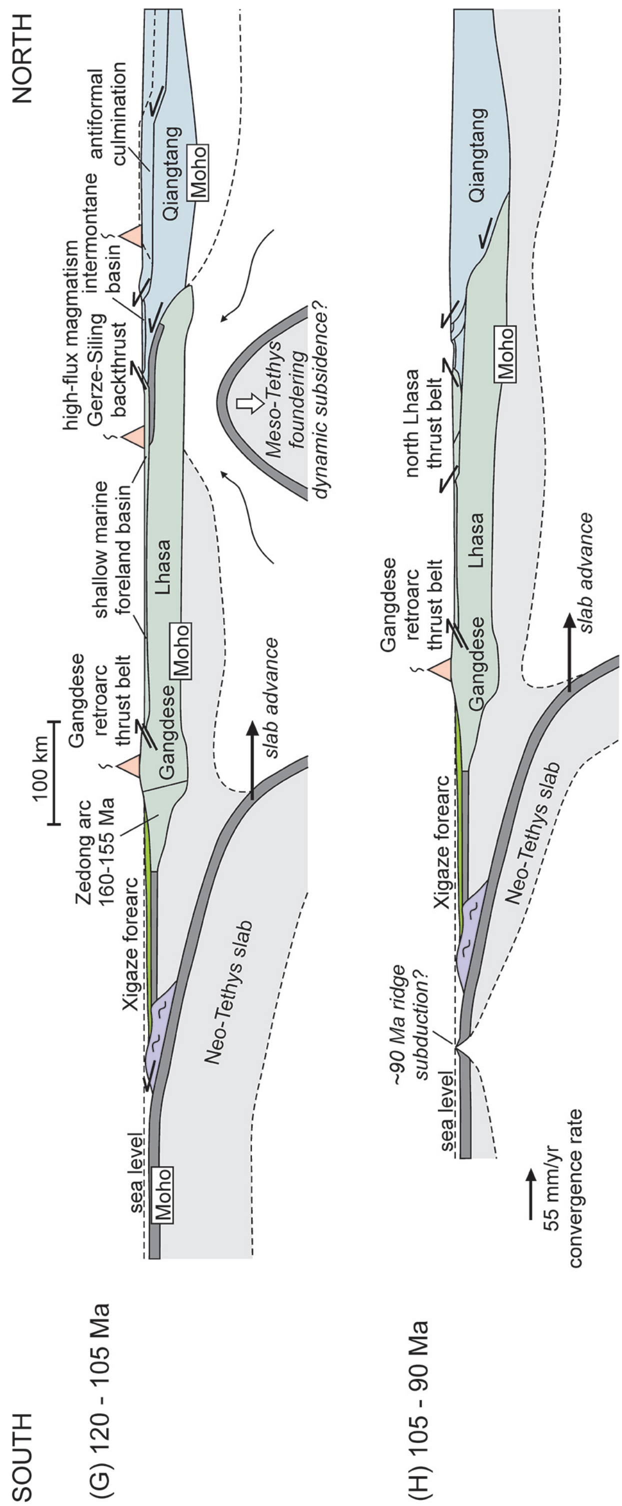

Fig. 7. (continued).

The mélange was metamorphosed at high pressure between 244 and 230 Ma (Pullen and others, 2008b; Zhai and others, 2011) and exhumed to upper-crustal levels between 225 and 204 Ma (Kapp and others, 2000, 2003b; Liang and others, 2017). The Qiangtang mélange has been interpreted to mark the trace of the Longmu Co – Shuang Hu suture, along which the southern Qiangtang terrane was subducted northward beneath the northern Qiangtang terrane (Li and others, 1995; Zhang and others, 2006; Wu and others, 2015). Where mapped in detail, however, the mélanges are structurally beneath Gondwanan-affinity continental margin strata in the footwalls of 225 to 204 Ma domal, low-angle normal faults (Kapp and others, 2003b; Gehrels and others, 2011; Pullen and others, 2011b). Given this structural setting, and the coeval timing of mélange formation and exhumation and southward subduction along the Jinsha suture, it was suggested that the rocks in the mélange were underthrust southward beneath the Qiangtang continental margin from the Jinsha suture during a phase of flat-slab subduction (Kapp and others, 2000). The mélange was subsequently exhumed by extension in an intracontinental setting during northward rollback of the Paleo-Tethys oceanic slab (figs. 6A and 7A; Kapp and others, 2000). Regardless of which, if either, interpretation is correct, one conclusion can be made—if there is an additional suture in the Qiangtang terrane, its trace must be located to the north of the northernmost exposures of mélange, which in the west are as close as ~25 km to the Jinsha suture (fig. 1; Tang and Zhang, 2014). Additionally, widespread Jurassic strata in the Qiangtang terrane probably obscure the full spatial extent of exhumed mélange.

Assembly of the Lhasa Terrane

The Lhasa terrane was located along the northern margin of Gondwana near Greater India (Şengör, 1984; Metcalfe, 1988) or northwestern Australia (Audley-Charles, 1983; Zhu and others, 2011a) during the late Paleozoic. The oldest rocks in the central Lhasa terrane include ~856 Ma orthogneisses that underwent amphibolite-facies metamorphism between 690 and 660 Ma (Dong and others, 2011b) and ~766 to 760 Ma gabbros (Hu and others, 2018). Cambrian to Devonian marine strata are locally exposed, whereas Carboniferous – Permian strata are more widespread (Pan and others, 2004). Permian volcanic-bearing sequences in the central Lhasa terrane and an east-west-trending belt of Permian – Triassic eclogite-facies metabasites ~120 km east-northeast of Lhasa city have been interpreted in the context of a south-facing ocean-continent convergent margin and an additional suture within the Lhasa terrane (the Luobadui-Mila suture; figs. 6A and 7A; Yang and others, 2009; Zhu and others, 2009c, 2010; Cheng and others, 2012; Zhang and others, 2014d; Weller and others, 2016). The central Lhasa terrane records high-grade metamorphism and S-type magmatism between 225 and 192 Ma, attributed to crustal thickening during collisional orogenesis following ocean closure along the Luobadui-Mila suture (figs. 5 and 6A, Pullen and others, 2008a; Dong and others, 2011a; Zhang and others, 2014d; Weller and others, 2015, 2016; Zhou and others, 2017).

Meso-Tethys Oceanic Subduction and the Amdo Arc Terrane

Opening of the Meso-Tethys ocean commenced by the Permian (Fan and others, 2015) and continued throughout Triassic – Early Jurassic time (figs. 6A and 7A; Schneider and others, 2003; Baxter and others, 2009). An unknown length of Meso-Tethys oceanic lithosphere was consumed along the Bangong suture zone between the Qiangtang and Lhasa terranes. Subduction of Meso-Tethyan oceanic lithosphere initiated at ~200 Ma along the central Bangong suture (Zhang and others, 2016b; Li and others, 2017b), coeval with final closure of the Paleo-Tethys ocean (fig. 5). Ophiolitic and boninitic (forearc-indicative) rocks within the Bangong suture zone generally yield crystallization ages between 188 and 162 Ma (fig. 5; Shi and others, 2004; Shi, 2007; Baxter and others, 2009; Liu and others, 2014b; Liu and others, 2016b; Wang and others, 2016a; Huang and others, 2017a).

The Amdo micro-terrane within the eastern Bangong suture zone (figs. 1 and 4) is bounded by belts of ophiolitic rocks and includes 920 to 820 Ma and 540 to 460 Ma orthogneisses (Xu and others, 1985; Coward and others, 1988; Guynn and others, 2006, 2012; Zhang and others, 2012c). Amdo gneisses experienced high-pressure (equivalent to ~50-km-depth) granulite-facies metamorphism at ~191 Ma, amphibolite-facies metamorphism between 181 and 178 Ma, granitoid intrusion between 190 and 170 Ma, and rapid exhumation to mid-crustal levels between 170 and 165 Ma (fig. 5; Guynn and others, 2006, 2012; Zhang and others, 2014d; Yan and others, 2016; Liu and others, 2017).

We suggest that suturing of the Qiangtang – Hoh-Xil – Kunlun terranes at 200 to 190 Ma may have induced northward subduction of Meso-Tethys oceanic lithosphere, along with underthrusting of the Amdo terrane beneath the Qiangtang terrane (figs. 6B and 7B). Subsequent rollback of the Meso-Tethys slab may have led to ophiolite generation in the upper plate (between ~188 and 162 Ma) and rifting of the Amdo terrane from the Qiangtang terrane (figs. 6C and 7C). The Amdo terrane is interpreted to have accreted back to the Qiangtang terrane at 170 to 165 Ma, synchronous with the beginning of arc magmatism and southward retreat of marine facies within the southern Qiangtang terrane (figs. 6D, 7D, and 8A; Kapp and others, 2005; Guynn and others, 2006; Pullen and others, 2011b; Liu and others, 2014a, 2017; Fan and others, 2016; Li and others, 2016a, 2016b; Wu and others, 2016; Ma and others, 2018). A Jurassic igneous-metamorphic complex similar to the Amdo terrane is exposed within the Bangong suture zone ~500 km to the southeast near Basu (fig. 1; 500–492 Ma protolith, 186–174 Ma granitoid intrusions, ~173 Ma metamorphism, ~165 Ma exhumation; Li and others, 2017a). Given this, together with the along-strike consistency in the timing of ophiolite generation and magmatism in central Tibet, it is likely that the Amdo terrane extended farther along strike of the orogen, but has in most other places either been buried by sediment or underthrust beneath the Qiangtang terrane (Guynn and others, 2006). No documented Cenozoic analogs exist for the proposed history of induced subduction, coeval underthrusting, and subsequent rifting and ophiolite generation along a continental margin (Stern, 2004). As such, the model described here is highly speculative and alternatives should be considered.

Magmatism also initiated in the northern Lhasa terrane at ~170 Ma (fig. 8A), coeval with amalgamation of the Amdo and Qiangtang terranes. This may indicate initiation of bivergent double subduction (northward and southward) of Meso-Tethys oceanic lithosphere (figs. 6D and 7D; Zhu and others, 2011b, 2016). This interpretation contrasts with the widely held previous view that Jurassic (and Early Cretaceous) magmatism in the northern Lhasa terrane was related to northward low-angle subduction of Neo-Tethys oceanic lithosphere on the southern side of the Lhasa terrane (Coulon and others, 1986; Matte and others, 1996; Yin and Harrison, 2000; Kapp and others, 2005, 2007a), which has been shown to be incompatible with the Jurassic – Cretaceous Gangdese magmatic arc record (Zhu and others, 2009d).

Neo-Tethys Oceanic Subduction and the Zedong Arc Terrane

The oldest, Mesozoic Gangdese arc magmatic rocks interpreted to be related to northward subduction of Neo-Tethys oceanic lithosphere are Middle to Late Triassic in age (Ji and others, 2009; Wang and others, 2016b). Additional studies are needed to determine the timing relations and potential geodynamic linkages between Triassic collisional orogenesis along the Luobadui-Mila suture and initiation of Neo-Tethys oceanic subduction. The Gangdese arc experienced bimodal volcanism between 195 and 174 Ma, possibly in an extensional setting, and a magmatic lull between 174 and

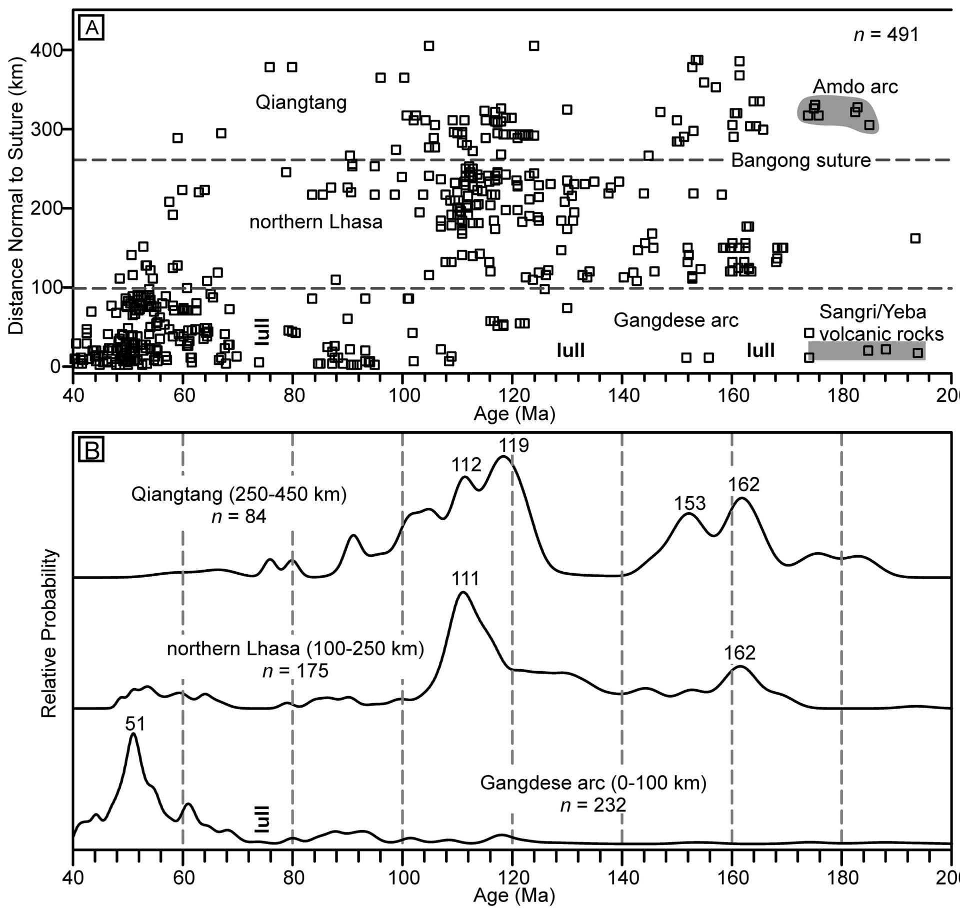

Fig. 8. Temporal and spatial distribution of igneous rocks in Tibet between the longitudes of 81°E and 91.8°E. (A) Arc-normal distance of 200–40 Ma igneous rocks from the Yalu suture versus age. (B) Relative probability curves of igneous rock ages in the Gangdese arc (0–100 km from suture), northern Lhasa terrane (100–250 km from suture), and Qiangtang terrane (250–400 km from suture). The compiled data and their sources are available online in the Tibetan magmatism database of Chapman and Kapp (2017). The vast majority of the ages are weighted mean U-Pb zircon ages. Some $^{40}Ar/^{39}Ar$ ages are included, but only for volcanic rocks, and they were filtered by removing analyses with complex age spectra and those potentially compromised by argon loss due to burial or magmatic reheating. Igneous rocks of all types and compositions were included; specific compositions are noted in text when relevant to tectonic interpretations. The age distributions of intrusive and extrusive rocks are broadly similar and were combined to maximize resolution of temporal-spatial patterns. The compilation is incomplete given the rapidly growing abundance of published data, and biased toward Cretaceous and Cenozoic rocks. Age range of Sangri/Yeba volcanic rocks is from Zhu and others (2008) and Kang and others (2014).

156 Ma (figs. 5, 6C and 6D, 7C and 7D, and 8A; Zhu and others, 2008, 2011b; Ji and others, 2009; Kang and others, 2014; Wei and others, 2017). The 174 to 156 Ma Gangdese magmatic lull was coeval with the first of two major episodes of ophiolite generation within the YSZ (for example, the Spontang, Kiogar, and Luobusa ophiolites; Pedersen and others, 2001; Hébert and others, 2012) and magmatism in the Zedong arc (Aitchison and others, 2000; McDermid and others, 2002; Zhang and others, 2014a) (fig. 5), which is restricted to a small (~25 km by ~2 km) exposure within the eastern part of the YSZ (fig. 4). It is debated whether the Zedong arc developed in an intra-oceanic setting (Aitchison and others, 2000;

McDermid and others, 2002) or represents a part of the Gangdese arc (Zhang and others, 2014a).

We suggest that southward rollback of the Neo-Tethys oceanic slab accelerated at ~174 Ma and may have led to ophiolite generation in a forearc setting and rifting of the Zedong arc from the Lhasa terrane margin (figs. 6D and 7D). The Zedong arc may have accreted back to the Asian margin at ~155 Ma, during which magmatism ceased in the Zedong arc and reinitiated in the Gangdese arc (figs. 5, 6E, and 7E). Between 155 and 132 Ma, the central Lhasa terrane shortened across east-west striking thrust faults (Murphy and others, 1997; Ding and Lai, 2003) and shed sediment northward into the Meso-Tethys ocean (Zhang and others, 2011a) and southward into the near-sea-level southern Lhasa terrane (Leeder and others, 1988; Leier and others, 2007b) (figs. 6E and 7E).

EARLY CRETACEOUS TECTONICS IN THE YALU SUTURE ZONE AND LHASA TERRANE (132-120 MA)

The Lhasa terrane was fully consolidated by Early Cretaceous time, setting the stage for the onset of subduction-related events along its southern margin that would establish the geological foundation of what would eventually evolve into the India – Asia collision zone. Key elements of this part of the story include the Gangdese magmatic arc, Xigaze forearc basin, and ophiolitic rocks and structurally underlying mélanges. The northern Lhasa terrane also experienced Early Cretaceous magmatic and tectonic activity leading up to terminal Lhasa – Qiangtang collision.

The Gangdese-Xigaze Arc-Trench System

The Gangdese magmatic arc, which was already well developed by Jurassic time, experienced a lull in activity during the Early Cretaceous until ~120 Ma (figs. 5 and 8). An explanation for this lull that is compatible with coeval events documented farther south (see below) is that the Neo-Tethys oceanic slab rolled back southward relative to Asia while ophiolitic rocks were created in a forearc extensional setting (figs. 6F and 7F; Dai and others, 2013b; An and others, 2014; Maffione and others, 2015; Griffin and others, 2016; Xiong and others, 2016; Butler and Beaumont, 2017).

The Xigaze forearc basin is preserved in an east-west trending synclinorium (fig. 4; Burg and Chen, 1984; Einsele and others, 1994; Orme and others, 2015). Despite the fact that a depositional contact with the Gangdese arc rocks has never been documented, the Xigaze forearc basin is widely interpreted to have developed proximal to the Gangdese continental margin arc (Tapponnier and others, 1981; Burg and Chen, 1984; Einsele and others, 1994; Dürr, 1996). The only allochthonous interpretation for the Xigaze forearc is that of Aitchison and others (2011), who proposed that it was translated to its current position in the YSZ from near Myanmar by dextral strike-slip faulting during the Late Cretaceous. However, this is not supported by U-Pb detrital zircon data from >85 Ma Xigaze forearc strata, which are consistent with a Lhasa terrane provenance (fig. 9, to be discussed in a subsequent section).

The contact between the Xigaze forearc basin and suture-zone assemblages to the south is in most places a south-dipping fault associated with the early Miocene Great Counter thrust system (Burg and Chen, 1984; Ratschbacher and others, 1994; Ding and others, 2005; Sanchez and others, 2013; Laskowski and others, 2017). There are several localities along the length of the Xigaze forearc basin, however, where its basal strata have been interpreted to sit depositionally on ophiolitic rocks (Nicolas and others, 1981; Girardeau and others, 1984b, 1985b, 1985c; Einsele and others, 1994; Wang and others, 2012; An and others, 2014; Huang and others, 2015; Maffione and others, 2015; Orme and Laskowski, 2016; Laskowski and others, 2017). These depositional contacts would be impossible if the ophiolites formed above an intra-oceanic subduction zone as suggested by Aitchison and others (2000, 2007) at sub-equatorial

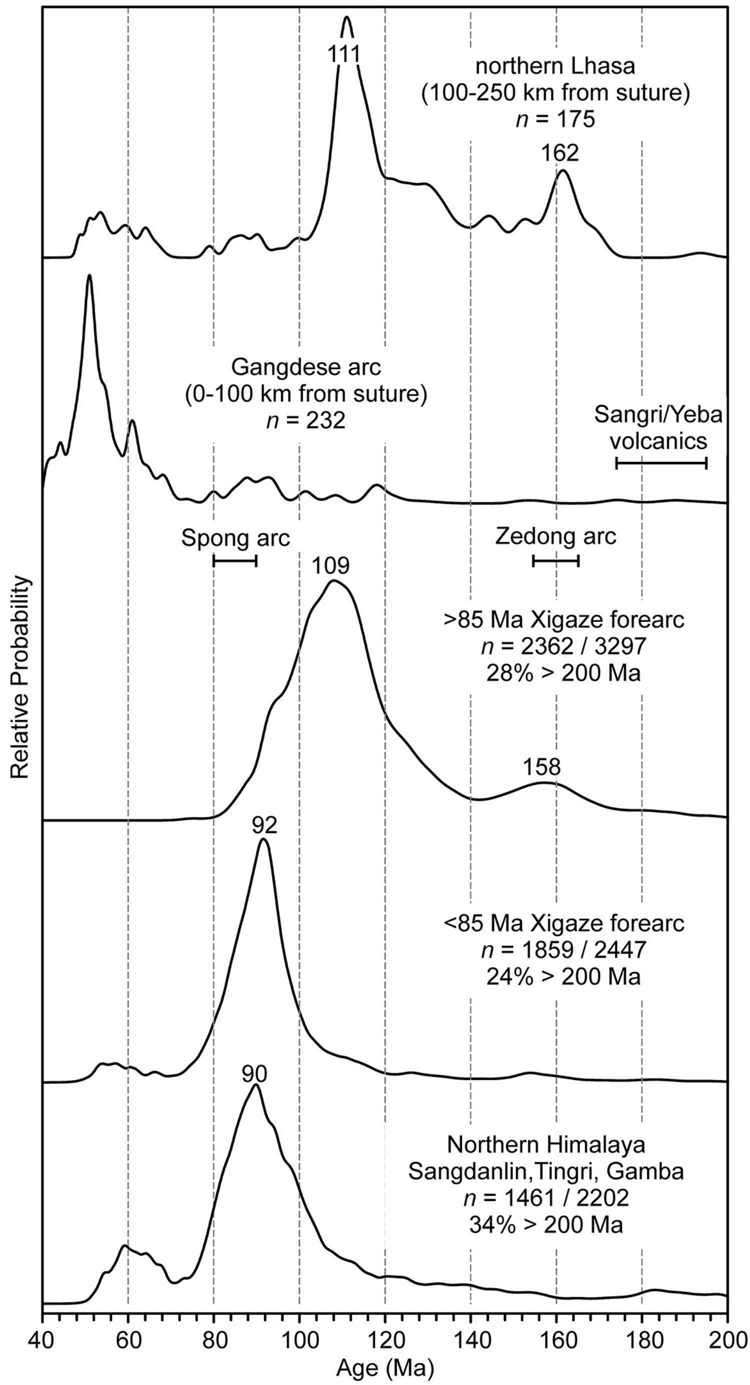

Fig. 9. Relative probability curves of igneous rock ages in the northern Lhasa terrane and Gangdese arc between the longitudes of 81°E and 91.8°E (Chapman and Kapp, 2017) compared to those of U-Pb detrital zircon ages in Xigaze forearc strata (Wu and others, 2010; Aitchison and others, 2011; An and others, 2014; Orme and others, 2015; Hu and others, 2016b; Orme and Laskowski, 2016) and Paleocene – Eocene northern Himalayan strata (Najman and others, 2010; Hu and others, 2012, 2015; DeCelles and others, 2014; Wu and others, 2014; Li and others, 2015b).

latitudes (based on a paleomagnetic study be Abrajevitch and others, 2005). With respect to the Abrajevitch and others (2005) work, a more recent paleomagnetic study yielded a paleolatitude of 16.5 ± 4°N after correction for compaction-induced inclination shallowing, indistinguishable from that of the Lhasa terrane during the Early Cretaceous (Huang and others, 2015).

Ophiolites to the south of the Xigaze forearc basin (fig. 4) crystallized between 132 and 125 Ma (Malpas and others, 2003; Dai and others, 2012a, 2013b; Hébert and others, 2012; Chan and others 2015; Zhang and others, 2016a), are locally overlapped by 132 to 112 Ma chert-bearing strata (Ziabrev and others, 2003), and are underlain by ophiolitic mélanges that include blocks of 132 to 123 Ma amphibolites interpreted as remnants of a dismembered metamorphic sole (Guilmette and others, 2009, 2012). Ophiolites of similar age are present along the Indus suture in Ladakh (fig. 1; for example, the Nidar ophiolite; Zyabrev and others, 2008) and as far southeast as Myanmar (Liu and others, 2016a). The contact at the base of the ophiolitic rocks is assumed to have originally been the top of a north-dipping subduction channel, referred to as the Yalu/Yarlung Zangbo (or Main) Mantle thrust (Tapponnier and others, 1981; Burg and Chen, 1984; Burg and others, 1987; Ratschbacher and others, 1994; Ding and others, 2005).

The Early Cretaceous YSZ ophiolites likely formed in a forearc extensional setting during slab rollback or subduction (re)initiation along the Asian margin (figs. 6F and 7F, Dai and others, 2013b; An and others, 2014; Maffione and others, 2015; Griffin and others, 2016; Xiong and others, 2016; Butler and Beaumont, 2017). This tectonic model explains: (1) the coeval generation of ophiolites and initial deposition of Xigaze forearc strata; (2) anomalously thin or locally absent sections of oceanic crust (Pozzi and others, 1984; Girardeau and others, 1985b, 1985c), with forearc strata sitting in depositional contact on mantle rocks and ophiolitic mélanges in places (Huang and others, 2015; Maffione and others, 2015; Orme and Laskowski, 2016; Laskowski and others, 2017); (3) the sub-continental mantle signature of ultrahigh-pressure minerals found in some YSZ ophiolites (Griffin and others, 2016); and (4) the coeval magmatic lull in the Gangdese arc (Xiong and others, 2016; figs. 5 and 8). Furthermore, the two episodes of forearc ophiolite generation along the southern margin of Asia (figs. 6D through 6F and 7D through 7F) explain why some YSZ ophiolitic massifs exhibit both Jurassic and Early Cretaceous crystallization ages (Griffin and others, 2016; Xiong and others, 2017a, 2017b).

YSZ subduction-complex rocks are diverse in age and lithology. The most widespread unit is a siliciclastic-matrix mélange that has been referred to as 'wildflysch with exotic blocks', the Yamdrok mélange, or Bainang terrane, among other local names (Gansser, 1964; Shackelton, 1981; Tapponnier and others, 1981; Burg and others, 1987; Searle and others, 1987, Liu and Einsele, 1996; Aitchison and others, 2000; Liu and Aitchison, 2002; Cai and others, 2012; Metcalf and Kapp, 2017). Blocks in the mélange are dominated by Neo-Tethys ocean plate stratigraphy, but also include northern Himalayan strata as young as late Paleocene in age (Burg and others, 1987; An and others, 2017; Metcalf and Kapp, 2017) and Deccan Trap-like intra-plate volcanic rocks (Dupuis and others, 2005). The mélange is interpreted to have formed before and during initial entry of the northern Indian continental margin into the Asian trench (Burg and others, 1987) or an intra-oceanic trench (Aitchison and others, 2000). Ophiolitic rocks are in places structurally interlayered with and underlain by imbricated thrust sheets of Triassic to Aptian chert-dominant strata, interpreted as accreted Neo-Tethys ocean plate stratigraphy (Tapponnier and others, 1981; Ziabrev and others, 2003, 2004; Cai and others, 2012). A southward-younging Aptian to Paleocene accretionary complex is locally exposed south of the ophiolites (Cai and others, 2012; Li and others, 2015a). YSZ accretionary complex rocks include sandstones with zircon U-Pb ages and εHf values that are similar to those of the Xigaze forearc basin and igneous rocks in the Lhasa terrane, providing further evidence that the ophiolites to the north formed adjacent to the Asian margin (figs. 6F and 6G and 7F and 7G; Cai and others, 2012; Li and others, 2015a; An and others, 2017; Metcalf and Kapp, 2017).

Considered in totality, the age of the Xigaze ophiolites, the age and provenance of the basal Xigaze forearc basin fill, the locally exposed depositional contact between them, and the age and provenance of subduction complex rocks to the south of the ophiolites are all consistent with the Xigaze forearc-trench system having formed along the southern margin of the Lhasa terrane (Tapponnier and others, 1981; Burg and Chen, 1984), rather than far offshore in the Neo-Tethys ocean (Aitchison and others, 2000, 2007; Hébert and others, 2012; Gibbons and others, 2015; Jagoutz and others, 2015).

Lhasa Terrane Events (132–120 Ma)

In the northern Lhasa terrane, deposition of volcanic-bearing clastic marginal-marine strata commenced at 138 to 131 Ma above a regional angular unconformity and transitioned into shallow-marine limestones between 120 and 110 Ma (figs. 6F and 6G and 7F and 7G; Zhang and others, 2004b; Volkmer and others, 2007; Ma and others, 2014). This subsidence has been attributed to initial Lhasa – Qiangtang collision (Leeder and others, 1998; Leier and others, 2007b; Volkmer and others, 2007), development of the Gangdese retroarc thrust belt (Zhang and others, 2011a), and backarc extension (Zhang and others, 2004b, 2012a). The regional onset of deposition may also signal termination of the prior phase of Lhasa terrane shortening. Geological data are at present insufficient to distinguish among these and other possibilities.

LHASA – QIANGTANG COLLISION AND CORDILLERAN-STYLE ASIAN MARGIN (120-90 MA)

Lhasa – Qiangtang Collision and Lhasa Terrane Tectonics

Deep-marine sedimentation continued along the central Bangong suture zone until at least 125 to 121 Ma (Kapp and others, 2007a; Baxter and others, 2009). Lhasa – Qiangtang continental collision occurred by ~118 Ma at the longitude of Nima (figs. 1 and 4), when nonmarine strata began to accumulate on an angular unconformity above transposed, marine turbiditic strata (fig. 5; Kapp and others, 2005, 2007a). Suturing was diachronous along strike (Yin and Harrison, 2000), occurring earlier in the east near Amdo at ~130 Ma (fig. 6F; Guynn and others, 2006) and later in westernmost Tibet at ~100 Ma (Matte and others, 1996; Liu and others, 2014a). Early Cretaceous calc-alkaline and high-K calc-alkaline magmatism spanned the northern Lhasa terrane, Bangong suture zone, and southern Qiangtang terrane (figs. 6G and 8A). The 120 to 105 Ma (peaking at ~111 Ma) high-flux magmatism in the northern Lhasa terrane (fig. 8B) has been attributed to foundering of Meso-Tethys oceanic lithosphere following initiation of Lhasa – Qiangtang collision (fig. 7G; Zhu and others, 2016).

In the northern Lhasa terrane, ~120 to 96 Ma shallow-marine limestone was deposited in a foreland basin peripheral to the Lhasa – Qiangtang collision zone (figs. 6G and 7G; Leier and others, 2007b; BouDagher-Fadel and others, 2017 and references therein). Within the Bangong suture zone, the northernmost exposures of mid-Cretaceous limestone terminate against the south-dipping, north-vergent Gerze – Siling backthrust (GSBT, figs. 2B, 4, 6G, and 7G). Footwall rocks include nonmarine conglomerates of overlapping age (118–90 Ma; Kapp and others, 2007a; DeCelles and others, 2007a). Similar-aged conglomerates are present in the footwall of a north-dipping, south-vergent thrust system to the north, which defines the boundary between the Qiangtang terrane and Bangong suture zone (figs. 6G and 7G). The

Cretaceous nonmarine intermontane basin rocks in the Bangong suture zone experienced ≥50 percent shortening, approximately two-thirds of which occurred prior to the Cenozoic. Thrusting was demonstrably active between 120 and 90 Ma (Kapp and others, 2007a).

North-dipping thrust faults propagated southward into the northern Lhasa thrust belt by ~105 Ma (Volkmer and others, 2007, 2014) and involve 96 to 91 Ma nonmarine strata (Sun and others 2015b) (figs. 4, 5, 6H, and 7H). The absence of marine strata younger than ~96 Ma in Tibet, north of the Gangdese forearc, suggests that it has been above sea level since this time. The southern Lhasa terrane was shortened by the north-vergent Gangdese retroarc thrust belt (figs. 2B, 4, 6H, and 7H; Kapp and others, 2007b; Pullen and others, 2008a). Near Lhasa, nonmarine upward-coarsening clastic red beds between 105 and 90 Ma with generally northward paleocurrent indicators have been interpreted as retroarc flexural foredeep deposits (Leier and others, 2007a). Both the northern Lhasa and Gangdese retroarc thrust belts accommodated ≥50 percent north-south shortening between ~105 and 50 Ma (Kapp and others, 2003a, 2007b; Volkmer and others, 2007, 2014); whether shortening was continuous or episodic during this time interval is unknown.

Cordilleran-Type Margin in the Southern Lhasa Terrane

Between 120 and 100 Ma, a Cordilleran-style orogen developed in southern Tibet (Burg and others, 1983; Chang and others, 1986; England and Searle, 1986; Coward and others, 1988; Ratschbacher and others, 1992; Kapp and others, 2007b; figs. 6G and 7G). Magmatism resumed within the Gangdese arc (fig. 8) and turbidites accumulated in the Xigaze forearc basin. Detrital zircons in >85 Ma Xigaze forearc strata yield U-Pb age populations with peaks at ~158 Ma and 109 Ma (fig. 9; Wu and others, 2010; Aitchison and others, 2011; An and others, 2014; Orme and others, 2015; Hu and others, 2016b; Orme and Laskowski, 2016). The ~158 Ma forearc population overlaps with the age of the Zedong arc (fig. 9; McDermid and others, 2002; Zhang and others, 2014a), and may suggest that this arc was more extensive along strike in an inner forearc setting (figs. 6G and 7G). Alternatively, or in addition, Jurassic igneous rocks in the northern Lhasa terrane (figs. 8 and 9) could have provided detritus into the forearc either directly or indirectly via sediment recycling (figs. 6G and 6H). The ~109 Ma forearc age peak coincides with the ~111 Ma high-flux magmatic event in the northern Lhasa terrane (figs. 8 and 9; Zhu and others, 2009b, 2016). These data reinforce the notion that the Xigaze forearc basin developed along the Lhasa terrane margin before 85 Ma.

Cretaceous Deformation in the Qiangtang Terrane

The largest structure in the Qiangtang terrane is a >600 km long and up to 240-km-wide, east-plunging antiformal culmination, defined by Paleozoic strata and mélange in its core (fig. 4; Yin and Harrison, 2000). Most of the growth and erosional exhumation of the antiform occurred during the Cretaceous, as indicated by thermochronologic studies and exposures of gently dipping Cretaceous volcanic rocks sitting above angular unconformities (Kapp and others, 2003b, 2005; Li and others, 2010; Rohrmann and others, 2012; Song and others, 2013). The youngest marine strata in the Qiangtang terrane are ~125 Ma near the eastern termination of the antiform (Li and Batten, 2004). The Qiangtang culmination is interpreted as an anticline that formed above a north-dipping mid-crustal thrust ramp-to-flat transition (figs. 6G and 7G); accordingly, its north-south width (up to 240 km in the west and tapering to the east) may provide an estimate for the magnitude of shortening required to produce it.

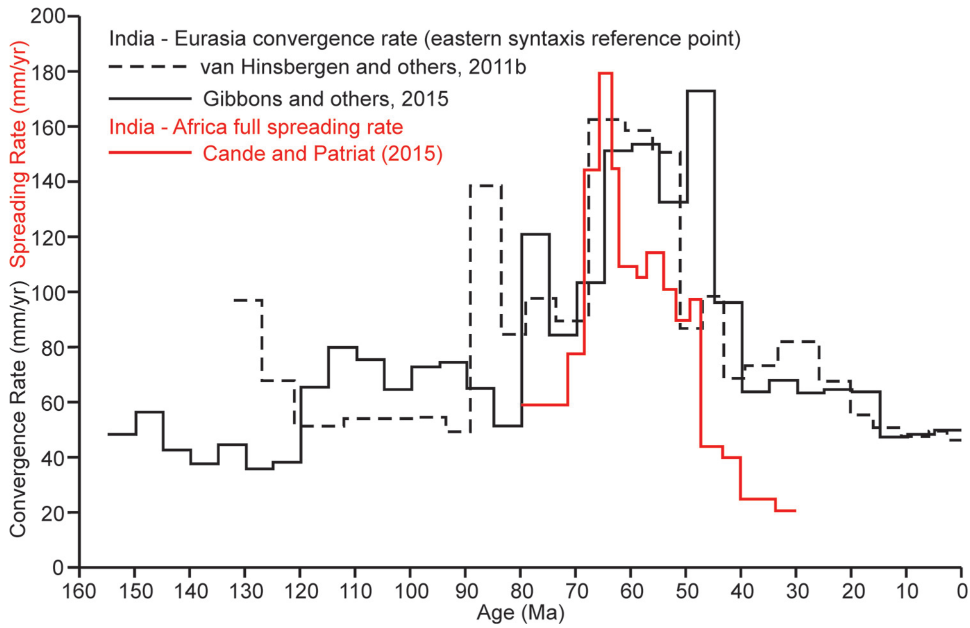

Fig. 10. Reconstructions of India – Eurasia convergence (black dashed and solid lines; van Hinsbergen and others, 2011b; Gibbons and others, 2015) and the rate of oceanic spreading between India and Africa (red line; Cande and Patriat, 2015).

The Putative "Greater India Basin"

The relative motion between India and stable Asia is constrained by plate circuit reconstructions (fig. 10; Molnar and Tapponnier, 1975; Patriat and Achache, 1984; Besse and Courtillot, 1988; Dewey and others, 1989; Molnar and Stock, 2009; Copley and others, 2010; van Hinsbergen and others, 2011b; White and Lister, 2012; Zahirovic and others, 2012; Gibbons and others, 2015). Although differences exist among the reconstructions because of the different rotation models, time scales, and interpolation methods used, all reconstructions show ~3000 km of convergence since 50 Ma and >4000 km since 60 Ma. If no oceanic lithosphere remained to be subducted at these times, then all of this convergence must have been accommodated by deformation and subduction of continental lithosphere. A similar convergence history is also suggested by the paleomagnetically-determined apparent polar wander paths for Eurasia and India (Klootwijk, 1984; Torsvik and others, 2012; Hu and others, 2016a). Present estimates of total shortening in the Himalaya (DeCelles and others, 2002; Long and others, 2011; Webb, 2013) plus total Cenozoic shortening in Asia (van Hinsbergen and others, 2011a, 2019) are ~2000 km, which leaves a roughly equal amount of convergence that is not accounted for by upper crustal shortening if collision between Indian and Asian continental lithosphere was underway by ~60 Ma (Yin and Harrison, 2000; Ding and others, 2005; DeCelles and others, 2014; Hu and others, 2016a).

Based on analysis of paleomagnetic data, van Hinsbergen and others (2012) suggested the mismatch between convergence and shortening can be explained with a model in which the northern Himalaya rifted >2000 km northward from India as a microcontinent during the mid-Cretaceous, accompanied by opening of an intervening oceanic "Greater India basin." In this model, the northern Himalayan microcontinent collided with Asia during Paleocene-Eocene time (fig. 11A), after which the Greater India basin subducted northward beneath Asia until continental India collided at

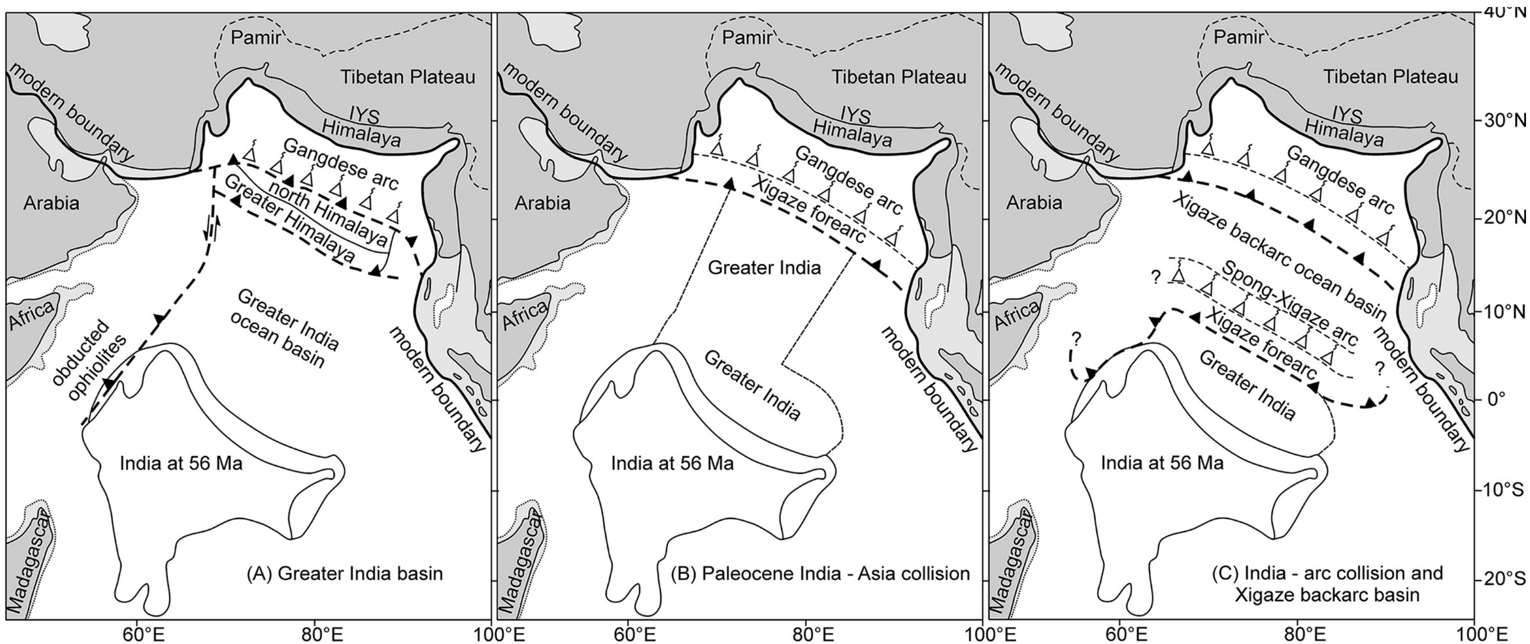

Fig. 11. Competing hypotheses for the Cenozoic history of India – Asia suturing. The maps show the reconstructed position of India at 56 Ma (Molnar and Stock, 2009; van Hinsbergen and others, 2011b) relative to modern positions of other continents (gray) and the southern Eurasian plate boundary. The restored position of the Gangdese arc (southern Tibetan margin) at ~56 Ma is consistent with paleomagnetic records (Lippert and others, 2014; Hu and others, 2016a), seismic tomography (van der Voo and others, 1999; Hafkenscheid and others, 2006), and kinematic restorations of Cenozoic deformation in Asia (van Hinsbergen and others, 2011a, 2019). (A) The Greater India basin hypothesis suggests that northern Himalayan and Greater Himalayan Sequence rocks rifted from India during the Cretaceous and opened an intervening Greater India ocean basin, which may not have closed by northward subduction beneath Asia until as recently as ~30–25 Ma (van Hinsbergen and others, 2012, 2019). (B) A ~60 Ma collision between India and Asia requires a >2000 km north-south length of continental Greater India to have subducted northward beneath Tibet. (C) A third possibility is that the Xigaze forearc basin, along with the hypothetical Spong-Xigaze arc, rifted southward from Tibet during the Late Cretaceous and collided with India at ~60 Ma, prior to closure of a backarc ocean basin to the north.

25 to 20 Ma along a cryptic subduction zone located within the Greater Himalayan Sequence or along the Main Central Thrust (figs. 2B and 4). Subsequent research has shown that the investigated northern Himalayan rocks experienced post-depositional remagnetization, and thus cannot be used to provide robust paleolatitude estimates (Huang and others, 2017b); this removes the evidence for, but does not disprove the hypothesis of a Greater India basin (van Hinsbergen and others, 2019). In any case, significant paleolatitudinal separation between India and the northern Himalaya during the Cretaceous is expected—it should have been roughly equivalent to the total subsequent shortening within the Himalayan thrust belt, which could reasonably be on the order of ~1000 km (DeCelles and others, 2002; Long and others, 2011; Webb, 2013).

A number of geological observations and plate-kinematic problems challenge the validity of the Greater India basin hypothesis. For example, uppermost Cretaceous to lower Paleocene sandstones in the northern Himalaya have detrital zircon U-Pb ages that are either (1) similar to those of Lower Cretaceous and older northern Tethyan Himalayan Sequence strata, with prominent Cambrian and 0.8 to 1.2 Ga age populations (Hu and others, 2010; Gehrels and others, 2011; DeCelles and others, 2014) or (2) a mix of those characteristic of the Tethyan Himalayan Sequence and Indian-affinity Lesser Himalaya Sequence (with a dominant age population between 1.7 and 2.0 Ga) (Garzanti and Hu, 2015). The former suggests no major change in provenance before and after the proposed Cretaceous opening of the Greater India basin whereas the latter is at direct odds with its existence. Northern Himalayan strata also record an increase in siliciclastic supply and accumulation rates during the latest Cretaceous, followed by progradation of coastal quartzarenites during the early Paleocene (Garzanti and Hu, 2015). Garzanti and Hu (2015) interpreted these observations, together with detrital spinel in latest Cretaceous through Paleocene northern Himalayan strata with compositions similar to those of the Deccan Traps, in the context of dynamic uplift and erosion of cratonic India and its inner passive continental margin during the Deccan flood basalt event. It is furthermore unclear how Eocene – Oligocene high-grade metamorphism and anatexis of the Greater Himalayan Sequence metasedimentary rocks (see Kohn, 2014 and Goscombe and others, 2018 for recent reviews) could have occurred in the hanging wall of the purported suture megathrust, proximal to the hypothesized northward subducting Greater India basin oceanic lithosphere where depressed thermal gradients would be expected. In contrast, this metamorphic record is in accord with detrital records of Himalayan orogenesis within Eocene – lower Miocene central Himalayan foreland basin strata in the Lesser Himalaya (on continental India, which would have been on the opposite side of the Greater India basin, if present) (DeCelles and others, 1998, 2004, 2014; Najman and others, 2005; Jain and others, 2009; Ravikant and others, 2011), which van Hinsbergen and others (2019) instead attribute to ophiolite emplacement along the western margin of India (fig. 11A). Finally, the Greater India basin model also requires that the Indian plate was largely surrounded by oceanic spreading centers, which is not compatible with its rapid northward migration during Cretaceous time (fig. 10). In our view, until geological evidence for an actual suture zone of mid-Cenozoic age is found within the central part of the Himalayan thrust belt, the Greater India basin should be regarded with skepticism. As discussed later in this paper, however, the India – Asia convergence problem remains a significant issue for all models explaining the Cenozoic collision event(s).

90 TO 70 MA: NEO-TETHYS FLAT SLAB SUBDUCTION OR OPENING AND CLOSING OF A XIGAZE BACKARC BASIN?

The Lhasa terrane experienced major tectono-thermal activity between ~94 and 80 Ma (fig. 5). Adakitic igneous rocks of this age are present in the eastern Gangdese magmatic arc, along with 90 to 81 Ma granulite-facies (moderate pressure to near-ultrahigh temperature) metaigneous and metasedimentary rocks (Zhang and others, 2010a; Jiang and others, 2012; Guo and others, 2013; Zheng and others, 2014). Late Cretaceous (94–80 Ma) adakitic rocks, along with tholeiitic basalts, are also present within the northern Gangdese arc and Lhasa terrane (Meng and others, 2014; Wang and others, 2014b; Chen and others, 2015; Ma and others, 2015; Sun and others, 2015c). There are no well-documented 90 to 70 Ma sedimentary basins in the Lhasa terrane, nor is there demonstrable evidence of upper-crustal shortening or extension between ~90 and 70 Ma (fig. 5). The Xigaze forearc basin experienced a decrease in accumulation rate between 88 and 78 Ma (Wang and others, 2012; Orme and Laskowski, 2016). Some amphibolite blocks within YSZ ophiolitic mélanges record a phase of exhumation between 90 and 80 Ma (Malpas and others, 2003; Bao and others, 2013). The Gangdese arc exhibits a magmatic lull between 78 and 72 Ma (figs. 5 and 8).

The relatively sparse geological information available for the 90 to 70 Ma time interval permits two end-member tectonic scenarios that place profoundly different constraints on the latest Cretaceous paleogeography of the southern Asian margin and interpretations of subsequent geological events. 90 to 70 Ma Scenario 1 follows most previously published interpretations, which call upon continued Cordilleran-style orogenesis along the southern Asian margin (fig. 12A). 90 to 70 Ma Scenario 2 raises the possibility for a phase of rifting along the southern Asian margin and the opening of a backarc ocean basin (fig. 13B).

90 to 70 Ma Scenario 1: Continued Cordilleran Style Orogeny in Southern Asia?

One interpretation attributes the ~94 to 80 Ma tectono-thermal event in the Lhasa terrane to the subduction of a Neo-Tethys oceanic ridge (figs. 7H and 12A; Zhang and others, 2010a; Guo and others, 2013). Oceanic ridge subduction could potentially explain uplift of the Xigaze forearc basin and exhumation of subduction complex rocks between 88 and 78 Ma. The 78 to 72 Ma magmatic lull within the Gangdese arc has been widely attributed to northward flat-slab subduction of Neo-Tethys oceanic lithosphere beneath the Lhasa terrane (Ding and others, 2003; Chung and others, 2005; Wen and others, 2008; Guo and others, 2013), which in turn may have been caused by subduction of relatively younger and more buoyant oceanic lithosphere that formed adjacent to the ridge (fig. 12A).

90 to 70 Ma Scenario 2: Rifting of the Xigaze Terrane From Asia?

The geology of the broader Neo-Tethyan realm motivates an alternative, Neo-Tethys oceanic slab rollback scenario to explain the 90 to 70 Ma geological evolution of the southern Asian margin. The ~95 to 90 Ma Oman/Semail ophiolite was rotated clockwise and translated southward above a retreating subduction zone prior to its obduction onto the Arabian margin at ~75 Ma (Searle and others, 2015; Morris and others, 2016). Ophiolites within the suture zone between India and the Helmand/Afghan block in Pakistan were generated between ~80 and 65 Ma (Beck and others, 1995, 1996; Gnos and others, 1997; Kakar and others, 2012). Southward rollback of a northward subducting slab beneath the Kohistan arc (fig. 1), beginning at 90 to 80 Ma, was proposed to explain intra-arc rifting, high-flux magmatism, arc crustal thinning, exhumation of amphibolite- and granulite-facies arc rocks, and blueschist exhumation within the Indus suture zone to the south (Khan and others, 1993; Treloar and others, 1996; Burg and others, 2006; Bouilhol and others, 2010; Burg, 2011). The intra-oceanic Spong arc in the northwestern Himalaya (fig. 1) was active between ~90 and 80 Ma (Corfield and others, 2001; Pedersen and others, 2001). These Late Cretaceous, retreating oceanic subduction zones within the western Neo-Tethys may have extended eastward and transitioned into the north-dipping subduction zone beneath the continental margin Gangdese arc. A second interpretation of the ~94 to 80 Ma tectono-thermal event in the Lhasa terrane attributes it to asthenospheric upwelling

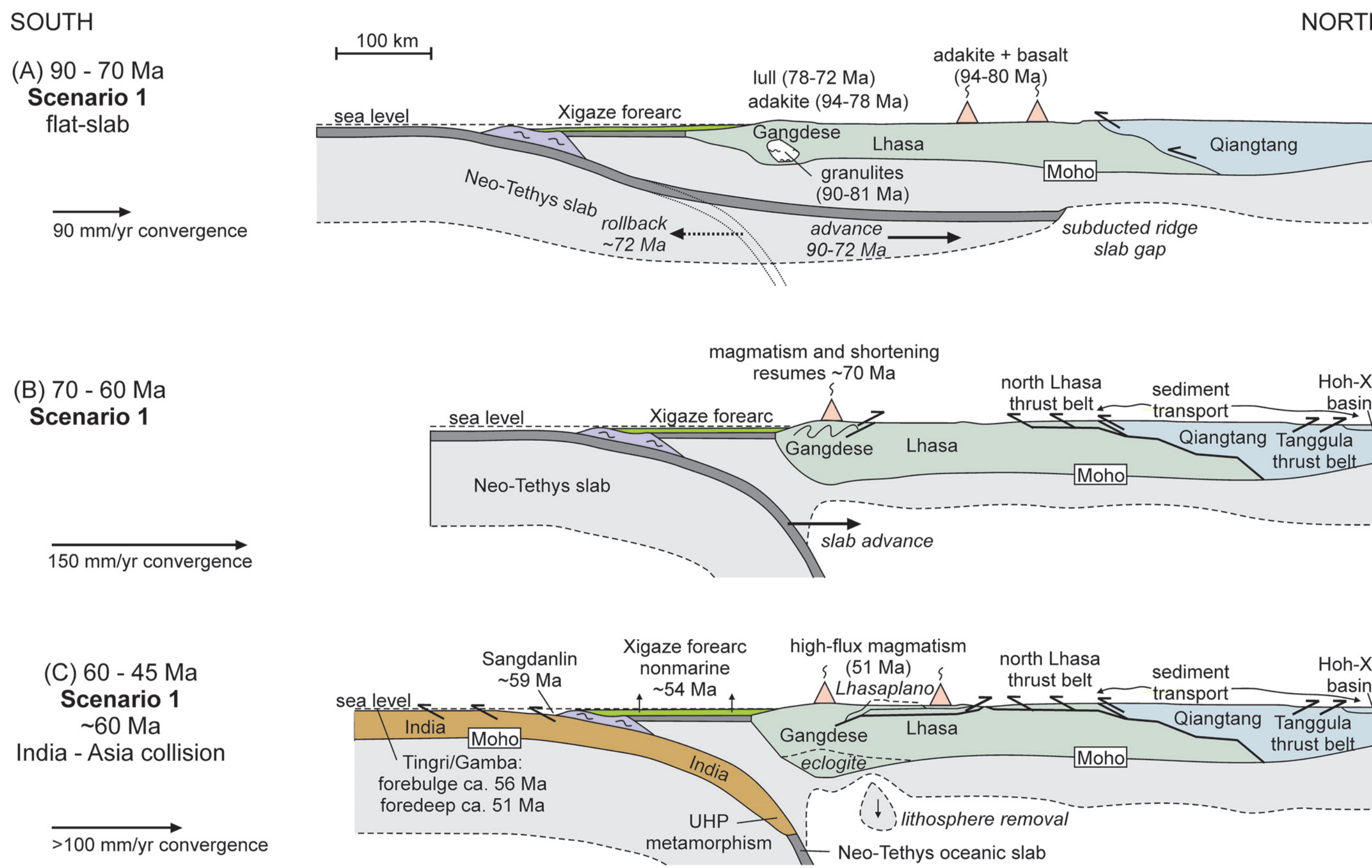

Fig. 12. Tectonic Scenario 1 illustrated in schematic lithosphere-scale cross-sections with no vertical exaggeration from (A) 90 Ma to (C) 45 Ma. It attributes the Late Cretaceous magmatic lull in the Gangdese arc to Neo-Tethyan flat-slab subduction and the appearance of arc detritus in northern Himalayan strata at ~60 Ma to initial India – Asia collision. Oceanic crust is shaded in gray. Dashed line indicates base of mantle lithosphere. Interpretations are italicized to distinguish them from observations.

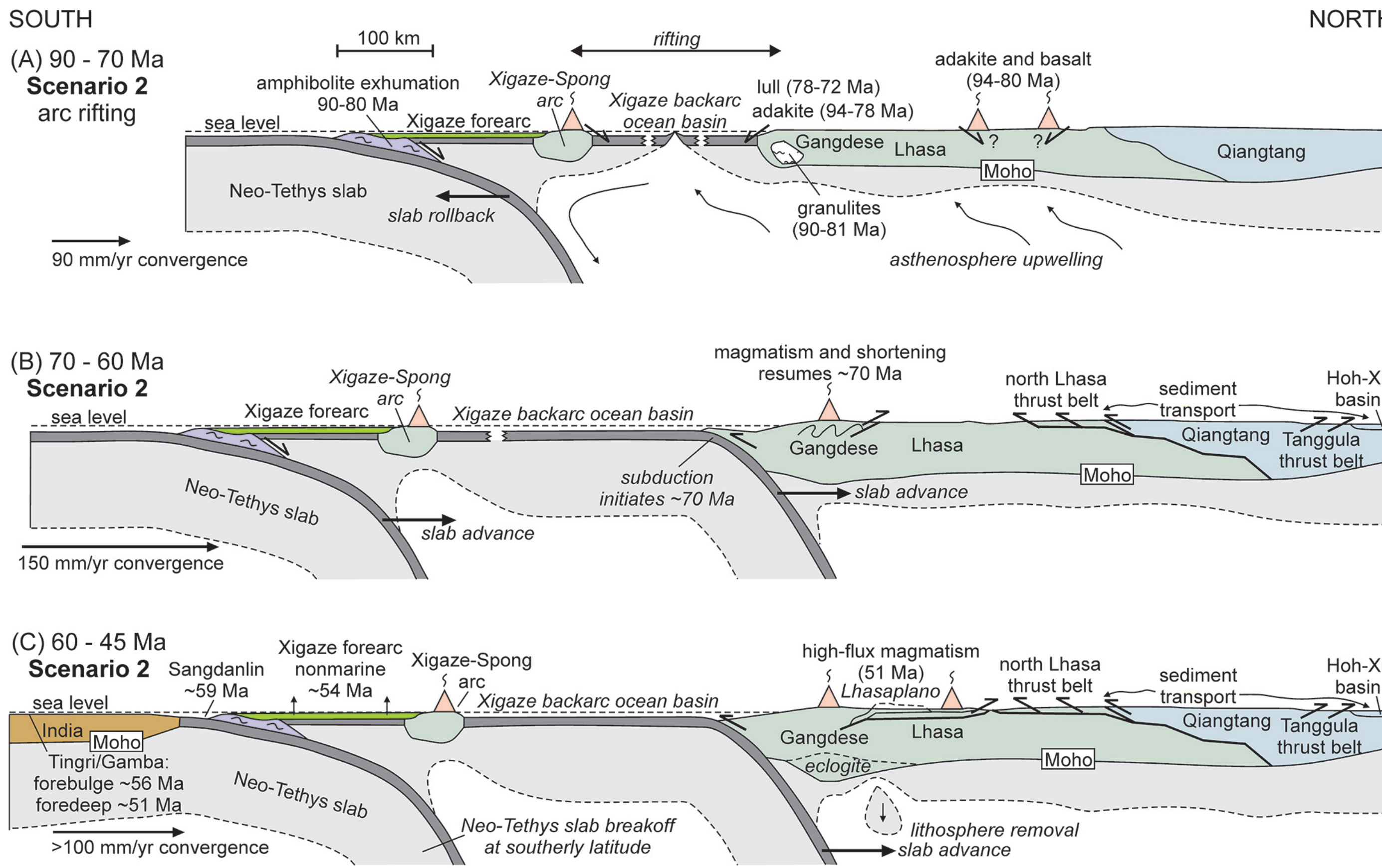

Fig. 13. Tectonic Scenario 2 illustrated in schematic lithosphere-scale cross-sections with no vertical exaggeration from (A) 90 Ma to (C) 45 Ma. It raises the possibility that the Xigaze terrane (including the Xigaze forearc and the Xigaze-Spong arc) rifted southward from Asia during the Late Cretaceous and collided with India at ~60 Ma, prior to final closure of the Xigaze backarc ocean basin. Oceanic crust is shaded in gray. Dashed line indicates base of mantle lithosphere. Interpretations are italicized to distinguish them from observations.

induced by rollback of the Neo-Tethys oceanic slab (fig. 13A; Ma and others, 2013, 2015; Xu and others, 2015b). Decreased coupling along the subduction interface during slab rollback could also potentially explain Xigaze forearc basin uplift and exhumation of YSZ subduction complex rocks between 88 and 78 Ma.

We raise the possibility that the northward subducting Neo-Tethys slab beneath Tibet began to rollback at ~90 Ma, thereby inducing upper-plate extension (fig. 13A). This may have led to rifting of a composite terrane consisting of the Xigaze subduction complex, Xigaze forearc basin, and the southern part of the pre-existing Gangdese magmatic arc (henceforth referred to as the Xigaze arc) from the Asian margin and opening of a backarc ocean basin (henceforth referred to as the Xigaze backarc basin) to the north of the Xigaze arc (fig. 13A). Our use of the term "backarc basin" follows Ingersoll (2012), who also reiterates that many extensional backarc ocean basins originate from intra-arc rifting. The newly formed backarc oceanic plate may be equivalent to the Kshiroda plate of Jagoutz and others (2015). The 90 to 80 Ma intra-oceanic Spong arc (fig. 1; Corfield and others, 2001; Pedersen and others, 2001) may be a vestige of the broader Xigaze arc, which developed in an intra-oceanic setting after rifting (figs. 11C and 13A). The Xigaze forearc basin was inundated by detrital zircons with an age population peaking at ~92 Ma (and overlapping with the age of the Spong arc) from ~85 Ma until the end of deposition at ~54 Ma (fig. 9). The Lhasa terrane Gangdese arc also includes ~92 Ma igneous rocks, but these rocks were being buried by the 69-44 Ma volcanic-bearing Linzizong Formation (figs. 2B and 4; He and others, 2007; Zhu and others, 2017) during Paleocene – Eocene Xigaze forearc deposition.

Northward Acceleration of India and Renewed Orogenesis in Tibet (~ 70 Ma)

The northward motion of the Indian plate accelerated at ~70 Ma, resulting in India – Asia convergence rates of >120 mm/yr (fig. 10). Magmatism resumed in the Gangdese arc at ~70 Ma, along with shortening and rapid exhumation in the Gangdese retroarc and northern Lhasa terrane thrust belts (figs. 5 and 8; Matte and others, 1996; Kapp and others, 2003a, 2007b; Volkmer and others, 2007; Hetzel and others, 2011; Rohrmann and others, 2012; Haider and others, 2013). Along the Lhasa-Golmud Highway, ~45 km northwest of Lhasa, folded Cretaceous strata are unconformably overlain by the weakly deformed 69 to 44 Ma Linzizong Formation (Burg and others, 1987; Kidd and others, 1988; Pan, ms, 1993). Timing of deformation at this locality is bracketed by ~72 Ma volcanic flows within the youngest folded Cretaceous strata (Sun and others, 2012) and a ~69 Ma andesite at the base of the Linzizong Formation above the unconformity (Zhu and others, 2017). The forces that caused rapid motion of the Indian plate may have accelerated the rate of Neo-Tethys subduction and trench advance in the case of 90 to 70 Ma Scenario 1 (fig. 12B) and/or induced northward subduction of the Xigaze backarc ocean basin beneath the Lhasa terrane in the case of 90 to 70 Ma Scenario 2 (fig. 13B); either scenario could explain the ~70 Ma rejuvenation of Gangdese arc magmatism and Asian upper-crustal shortening.

70 TO 45 MA: DEVELOPMENT OF THE LHASAPLANO, INITIATION OF HIMALAYAN OROGENESIS, AND ALTERNATIVE COLLISION SCENARIOS

70 to 45 Ma: The Tibetan Record

The Gangdese arc experienced high-K, calc-alkaline intrusive and extrusive magmatism between ~70 and 40 Ma (fig. 8; Maluski and others, 1982; Xu and others, 1985, 2015a; Coulon and others, 1986; Pearce and Mei, 1988; Harris and others, 1988; Chung and others, 2005; He and others, 2007; Zhu and others, 2015). The arc experienced a high-flux magmatic episode centered at ~51 Ma (fig. 8B) with broad compositional (basaltic to rhyolitic) and isotopic variations (moderately evolved to juvenile) (Mo and others, 2007, 2008; Lee and others, 2009; Ma and others, 2014; Zhu and others, 2015). Temporal shifts to more isotopically evolved magmatism have been used to infer the age of India – Asia suturing, but the timing of the shifts varies from study to study (Ji and others, 2009, 2012; Lee and others, 2009; Chu and others, 2011; Bouilhol and others, 2013; Jiang and others, 2014) and there is nothing observed isotopically in the Gangdese arc that has not been documented in other continental margin arcs which formed above oceanic subduction zones (Ducea and others 2001, Haschke and others, 2006; DeCelles and others, 2009; Cecil and others, 2011; Pepper and others, 2016). There is also a spatial trend toward more evolved isotopic values northward across the Gangdese arc and into the central Lhasa terrane (for example, a decrease of ~30 zircon εHf units over a north-south distance of only ~75 km, or ~0.4 εHf/km; Chapman and others, 2017). This spatial isotopic trend was established prior to Cenozoic time and thus any study attempting to attribute igneous isotopic variations to tectonic processes must focus on suites of igneous rocks at a single locality.

The Gangdese retroarc thrust belt was reactivated from at least 70 to 52 Ma (fig. 5; Kapp and others, 2007b; Pullen and others, 2008a). Angular unconformities within the Linzizong Formation indicate synkinematic deposition (Pan and others, 2004; Kapp and others, 2007b; Zhu and others, 2015, 2017). Lhasa terrane metasedimentary rocks along the northwestern flank of the eastern Himalayan syntaxis (fig. 1) experienced amphibolite- to granulite-facies metamorphism and migmatization between 71 and 50 Ma (Guo and others, 2012; Zhang and others, 2013; Palin and others, 2014). Paleoaltimetric studies of the Linzizong Formation suggest that the axis of the Gangdese arc may have been at elevations of >4 km by 60 to 54 Ma (fig. 14; Ding and others, 2014; Ingalls and others, 2018), while its northern part was at moderate elevation (~2.6 km at ~46 Ma; fig. 14; Xu and others, 2015a). The geological evidence points to the development of an elevated "Lhasaplano" in the Gangdese arc region during Paleocene – Eocene time (figs. 12B and 12C and 13B and 13C; Kapp and others, 2005, 2007b).

Large parts of the northern Lhasa and Qiangtang terranes experienced rapid exhumation between ~70 and 45 Ma, followed by minimal erosion (less than a few kilometers; Matte and others, 1996; Kapp and others, 2003a; Wang and others, 2008a, 2014a; Hetzel and others, 2011; Rohrmann and others, 2012; Haider and others, 2013; Song and others, 2013). The transition to slow erosion rates may indicate the establishment of low-relief, plateau-like conditions by ~45 Ma (Rohrmann and others, 2012). Conversely, the 70 to 45 Ma phase of rapid exhumation has been attributed to the planation of a low-elevation peneplain by rivers that transported sediment southward across the Gangdese arc, beveling the angular unconformity at the base of the Linzizong Formation (Hetzel and others, 2011; Haider and others, 2013). Apart from the difficulty of explaining rapid erosion by peneplanation at low elevation, the main problem with this interpretation is that Linzizong Formation deposition was coeval with, not younger than the timing of rapid exhumation in the plateau interior. Additionally, no deeply incised paleo-river channels that dissect the Gangdese arc have been documented.

The Qiangtang terrane was a relative topographic high between 70 and 45 Ma, shedding detritus northward into the nonmarine Hoh-Xil basin and southward into intermontane basins along the Bangong suture zone (figs. 12B and 12C and 13B and 13C; DeCelles and others, 2007a; Dai and others, 2012b; Staisch and others, 2014). Latest Cretaceous to Eocene basins along the Bangong suture, and ~800 km to the east near Nanqian (fig. 1), consisted of narrow, topographically partitioned fluvio-lacustrine depocenters (Luo and others, 1996; Ai and others, 1998; Horton and others, 2002; DeCelles and others, 2007a). The Tanggula thrust belt (figs. 2B and 4; >89 km

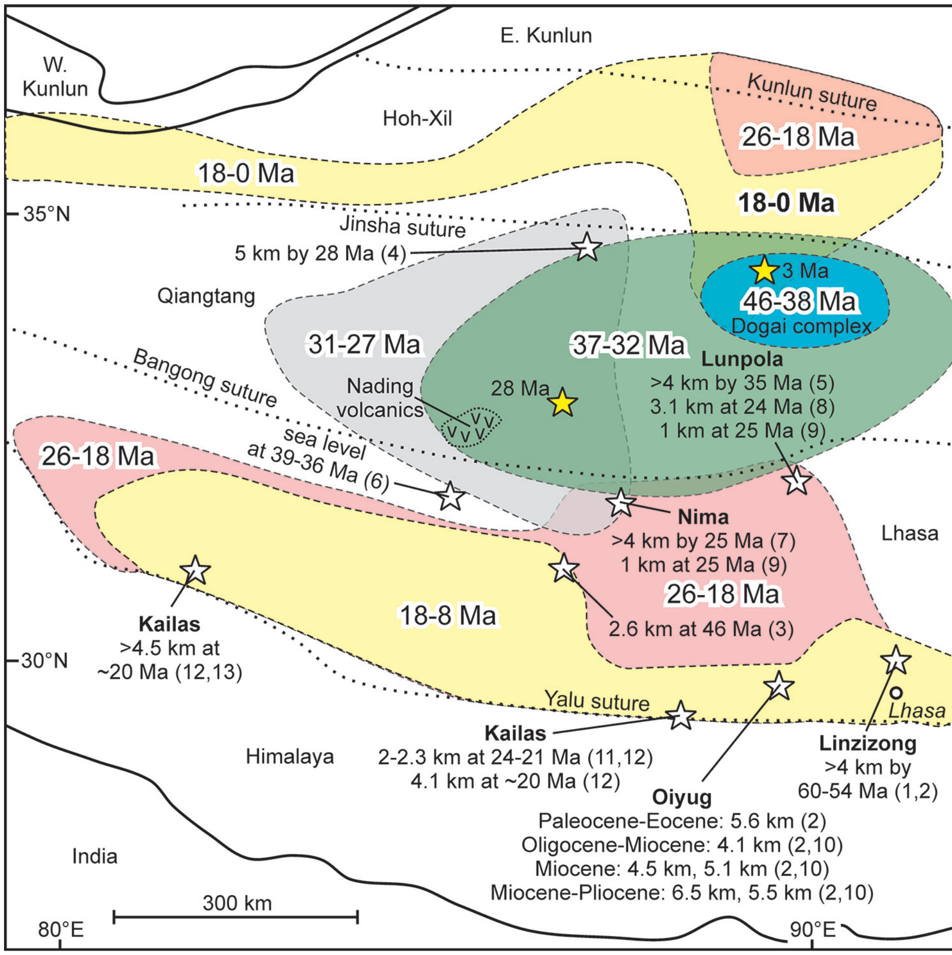

Fig. 14. Temporal-spatial distribution of (ultra)potassic, adakitic, and leucogranitic igneous rocks in Tibet with ages indicated by shaded regions: 46–38 Ma (blue); 37–32 Ma (green); 31–27 Ma (gray); 26–18 Ma (pink); <18 Ma (yellow). Compiled data and their sources from database of Chapman and Kapp (2017). Paleoaltimetric results are indicated at the white starred localities: (1) Ding and others, 2014; (2) Ingalls and others, 2018; (3) Xu and others, 2015a; (4) Xu and others, 2013a; (5) Rowley and Currie, 2006; (6) Wei and others, 2016; (7) DeCelles and others, 2007b; (8) Jia and others, 2015; (9) Wu and others, 2017; (10) Currie and others, 2016; (11) Ding and others, 2017b; (12) DeCelles and others, 2011; (13) Xu and others, 2018. Yellow stars indicate xenolith localities and ages of the volcanic host rocks (Hacker and others, 2000; Ding and others, 2007).

shortening over 59 km; >60%) and Nanqian-Yushu thrust belt (>61 km shortening over 83 km; >43%) to the east were both north-vergent and active by at least 51 Ma and until ~38 Ma (fig. 5; Spurlin and others, 2005; Wang and others, 2008a; Li and others, 2012). The upper-crustal shortening history, paleogeographic constraints, basin architecture and facies, and minimal regional post-45 Ma exhumation in central Tibet are consistent with net elevation gain and a decrease in topographic relief (with material eroded from topographic highs filling adjacent fluvio-lacustrine depocenters)—perhaps reflecting the establishment of a proto-plateau (fig. 15A).

Shortening also initiated farther north within mountain ranges bounding the Qaidam basin at 50 to 45 Ma (Jolivet and others, 2001; Yin and others, 2002; 2008;

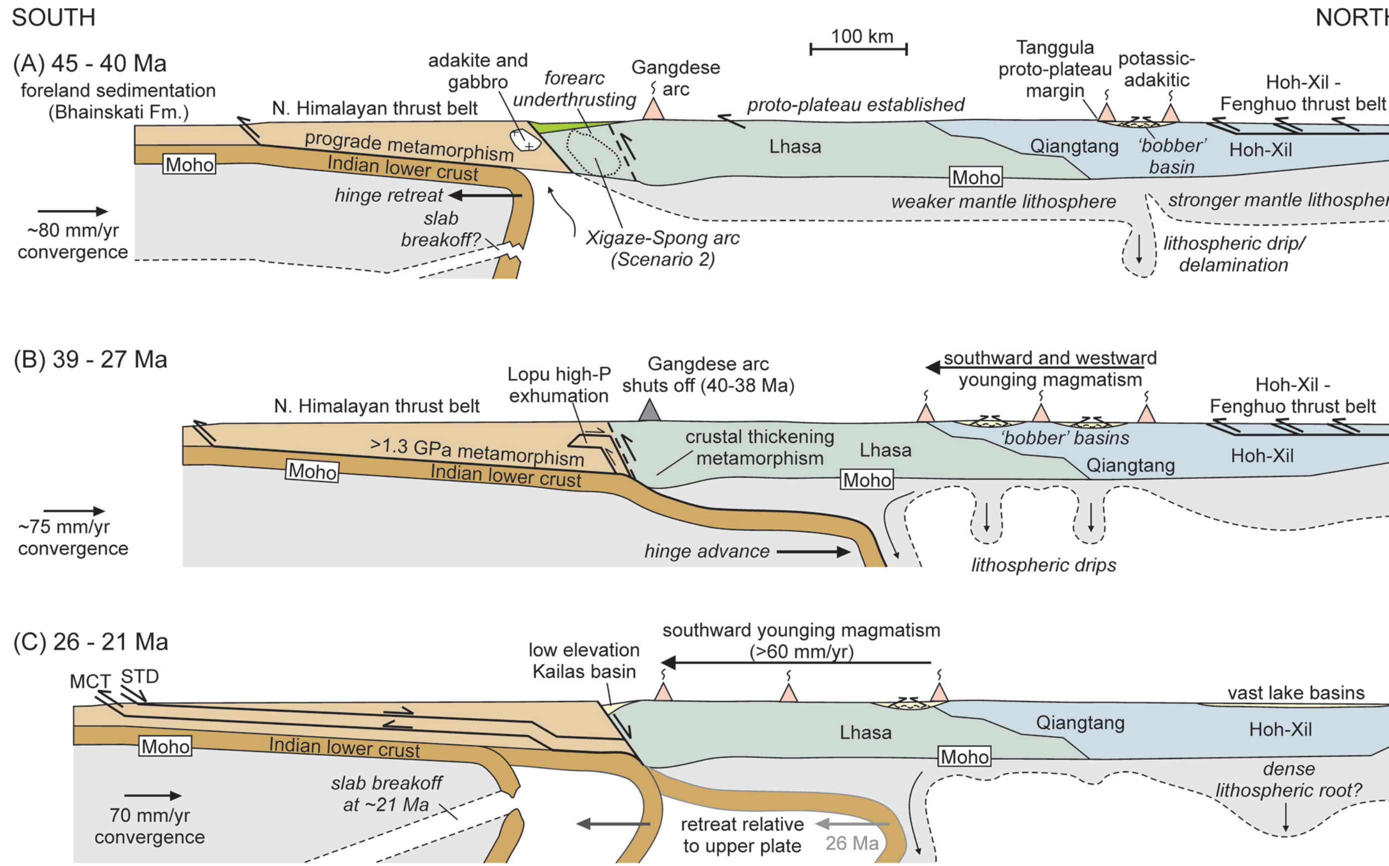

Fig. 15. Tectonic evolution illustrated in schematic lithosphere-scale cross-sections with no vertical exaggeration from (A) 45–40 Ma to (E) 16–0 Ma. Oceanic crust is shaded in gray. Dashed line indicates base of mantle lithosphere. Interpretations are italicized to distinguish them from observations.

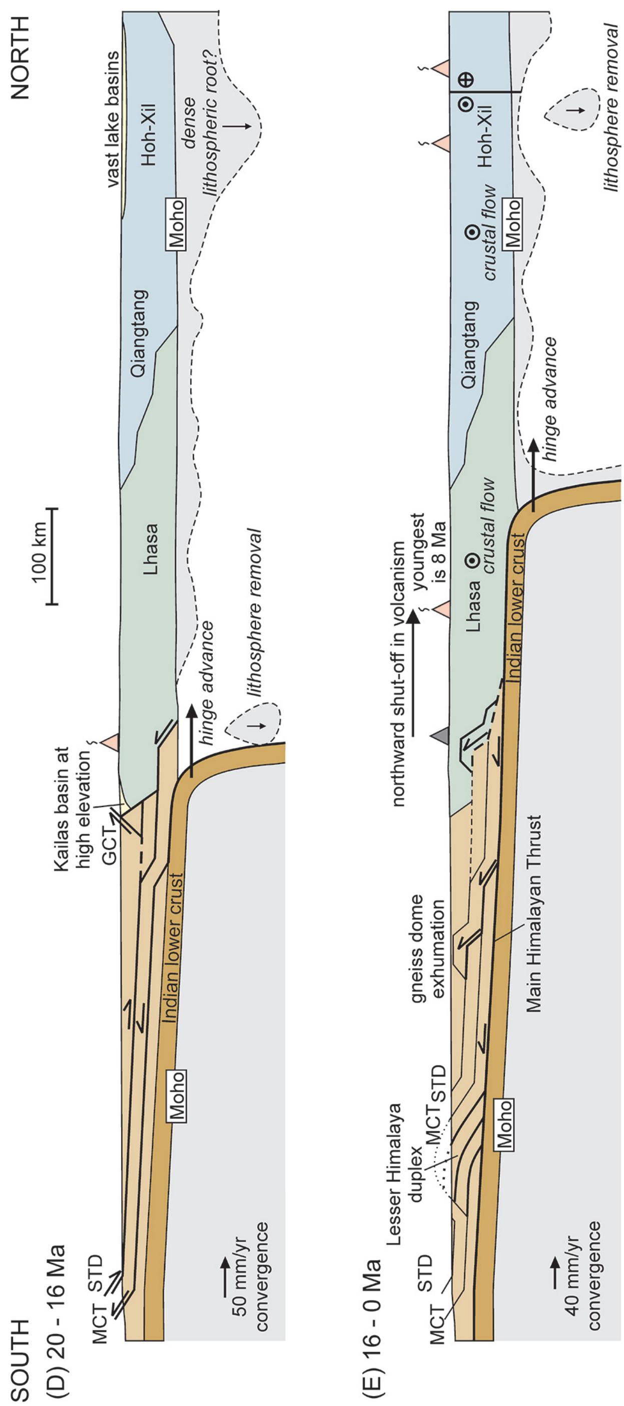

Fig. 15. (continued).

Clark and others, 2010; Duvall and others, 2011; Wang and others, 2015c). Even the Longmen Mountains along the eastern margin of the Tibetan Plateau record ~65 Ma high-grade metamorphism and Late Cretaceous to Eocene exhumation (Wallis and others, 2003; Yan and others, 2011; Tian and others, 2016). This far-field deformation in Asia may reflect a combination of: a highly compressional southern Asian plate boundary; the establishment of thick crust and substantial surface elevation (high gravitational potential energy) in the Lhasa and Qiangtang terranes; and the presence of a vast region of tectonically preconditioned, weak Asian continental lithosphere.

The Himalayan Record

Appearance of arc-derived detritus in the northern Himalaya.—The northern Indian passive margin (preserved in strata of the northern Himalaya) experienced an increase in accumulation rates and siliciclastic supply beginning at ~72 Ma and was characterized by deposition of southerly-derived, hyper-quartzose sandstones during the latest Cretaceous (Ding and others, 2005; DeCelles and others, 2014; Garzanti and Hu, 2015; Hu and others, 2016a). The increased sediment accumulation rates and northward progradation of quartzose sandstone have been attributed to surface uplift above the Deccan plume and post-plume thermal subsidence of the northern Himalaya (Garzanti and Hu, 2015). Uppermost Cretaceous to Paleocene northern Himalayan passive margin quartzose sandstones are disconformably overlain by northerly-derived arkosic sandstones containing Cretaceous to Paleocene arc-derived detritus (fig. 9). The age of this stark compositional change provides a minimum age constraint on the collision between India and either the Gangdese continental margin arc (90 to 70 Ma Scenario 1; fig. 12C) or an intra-oceanic Xigaze arc (90–70 Ma Scenario 2; fig. 13C). This provenance change occurred at ~60 Ma in a deep-water section (Sangdanlin section) directly south of the YSZ, and farther south in shelfal deposits at ~51 Ma (Tingri and Gamba sections) (figs. 4, 5, 12C, and 13C; Ding and others, 2005; Zhu and others, 2005; Najman and others, 2010; Wang and others, 2011; Hu and others, 2012, 2015, 2016a; DeCelles and others, 2014; Li and others, 2015b). Additionally, southward younging disconformities in northern Himalayan sections between ~68 Ma and 56 Ma have been attributed to the development of a collisional flexural forebulge, signaling the initial downflexure of the north Indian passive margin as it entered the trench along the south flank of Asia (Garzanti and others, 1987; Beck and others, 1995, 1996; Ding and others, 2005, 2016b; Zhang and others, 2012b; Hu and others, 2012, 2016a; DeCelles and others, 2014). In this context, the southward younging in appearance of arc detritus across the northern Himalaya (from ~60–51 Ma) records the southward propagation of the nascent northern Himalayan thrust belt and its associated foredeep depozone (Ding and others, 2005, 2016b; Zhang and others, 2012b; DeCelles and others, 2014). Arc detritus appeared in the lower Indus basin on the Indian plate at ~50 Ma (Zhuang and others, 2015).

Still up for debate is whether the appearance of arc detritus within northern Himalayan strata marks collision with an intra-oceanic arc that was isolated within the Neo-Tethys throughout its evolution (Aitchison and others, 2000, 2007; Hébert and others, 2012; Bouilhol and others, 2013; Chatterjee and others, 2013; Baxter and others, 2016) or with the continental margin forearc of southern Asia (Hu and others, 2016a and references therein). The compiled U-Pb detrital zircon age spectrum for the arc-derived Paleocene – Eocene northern Himalayan strata exhibits a dominant population with a peak at ~90 Ma and a trough between 75 and 70 Ma, similar to that of <85 Ma Xigaze forearc strata (fig. 9). Ages >200 Ma (not shown on fig. 9) compose a significant percentage of the total ages determined for both the Xigaze forearc (28–24%) and northern Himalayan (34%) strata. Both assemblages also exhibit an age population at ~215 Ma, overlapping with the ages of igneous rocks in the central Lhasa terrane (Chu and others, 2006; Wang and others, 2016b), and Precambrian age distributions characteristic of peri-Gondwanan terranes (Gehrels and others, 2011). Furthermore, the northern Himalayan sandstones include ~160 to 110 Ma zircons with relatively evolved εHf values similar to those within the Xigaze forearc and coeval igneous rocks in the northern Lhasa terrane (Zhu and others, 2009b, 2011b; Wu and others, 2010, 2014; Hu and others, 2012, 2016b).

Together with previously discussed evidence linking the Xigaze forearc basin and ophiolites to the southern flank of Asia during Early Cretaceous time, the abundance of >200 Ma zircons (including Precambrian zircons) and presence of Mesozoic zircons with negative εHf values in northern Himalayan strata exclude the possibility that the collided arc developed throughout its entire history in an isolated, intra-oceanic setting. Instead, all evidence supports collision of the northern Himalaya with the Xigaze forearc and an arc of Lhasa terrane affinity beginning at ~60 Ma. The western Xigaze forearc basin transitioned from marine to nonmarine deposition between 58 and 54 Ma, and the youngest strata are ~51 Ma (fig. 5; Orme and others, 2015; Hu and others, 2016b), providing additional evidence for its Paleocene collision with the northern Himalaya. Dispersal of large mammals and insects between India and Asia was also underway by ~54 Ma, requiring a semi-continuous land bridge between the two continents during that time (Gingerich and others, 1997; Clyde and others, 2003; Rust and others, 2010; Clementz and others, 2011).

60 to 45 Ma Himalayan record of deformation and metamorphism.—The northern Himalayan thrust belt is exposed between the YSZ and the South Tibetan Detachment (Burg and Chen, 1984; Burg and others, 1984; Burchfiel and others, 1992; Ratschbacher and others, 1994; Murphy and Yin, 2003) (fig. 4). The northernmost, oldest record of the thrust belt consists of ~59 Ma siliciclastic-matrix mélange with blocks of northern Himalayan strata that formed during initial subduction of the Indian continental margin (Burg and others, 1987; Metcalf and Kapp, 2017). In the northern Himalaya east of Xigaze, the north-dipping Lunzhe thrust (LT; fig. 4) carries in its hanging wall Triassic strata that were penetratively shortened and variably metamorphosed between 51 and 44 Ma (Ratschbacher and others, 1994; Dunkl and others, 2011); undeformed ~44 Ma granitoids cross-cut the deformation fabric (Aikman and others, 2008). The structurally underlying Yardoi (or Yala-Xiangbo) gneiss dome (fig. 4) experienced metamorphic zircon growth between 48 and 45 Ma (Ding and others, 2016a). The Kangmar and Mabja domes to the west (fig. 4) yielded Lu-Hf garnet dates between 54 and 49 Ma (Smit and others, 2014).

Eocene northern Himalayan shortening and metamorphism were contemporaneous with ultrahigh-pressure (UHP) metamorphism of Indian continental margin rocks adjacent to the Indus suture in the northwestern Himalaya (Khagan and Tso Morari, fig. 1). Khagan UHP metamorphism occurred between 47 and 45 Ma (Kaneko and others, 2003; Parrish and others, 2006; Wilke and others, 2010; Rehman and others, 2013). Tso Morari UHP metamorphism may be as old as 55 to 51 Ma (de Sigoyer and others, 2000; Leech and others, 2005; St-Onge and others, 2013) or as young as ~47 Ma (Donaldson and others, 2013). Metamorphism of Greater Himalayan Sequence rocks (figs. 2B and 4) initiated at ~45 Ma (oldest population of Cenozoic monazite dates; Catlos and others, 2002; Martin and others, 2007; Carosi and others, 2010; Iaccarino and others, 2015; Larson and Cottle, 2015; Gibson and others, 2016; Braden and others, 2017) and continued through Miocene time (Vannay and Hodges, 1996; Guillot, 1999; Guillot and others, 1999; Godin and others, 2001; Harris and others, 2004; Martin and others, 2007; Cottle and others, 2009; Kellett and others, 2014; Kohn, 2014; Goscombe and others, 2018).

Working Tectonic Hypotheses for India – Asia Collision

Consistent with our analysis of the period 90 to 70 Ma, we present two collision scenarios to explain the geological records of continuous orogenesis in Tibet and the

Himalaya between 60 and 45 Ma. Collision Scenario 1 invokes collision of India with the southern margin of Asia at ~60 Ma (figs. 11B and 12C). Collision Scenario 1 is compatible with a large body of geological data, but is challenged by plate circuit (fig. 10) and apparent polar wander path reconstructions that place India >4000 km south of the Lhasa terrane during Paleocene time (fig. 11). Collision Scenario 2 invokes collision of the hypothetical rifted Xigaze ophiolite-forearc-arc terrane with India at ~60 Ma followed by closure of the Xigaze backarc ocean basin and terminal India – Asia suturing at ~45 Ma (figs. 11C and 13C). Collision Scenario 2 is similar to other Asian arc-rifting models that are more consistent with the high-velocity seismic tomographic anomalies in the lower mantle south of the continental portion of the Indian plate and the India – Asia convergence history (Hafkenscheid and others, 2006; Zahirovic and others, 2012, 2016; Gibbons and others, 2015), except arc rifting occurred at ~90 Ma instead of during Jurassic – Early Cretaceous time. The largest shortcoming of Collision Scenario 2 is a lack of demonstrable geological evidence for the former existence of the Xigaze backarc ocean basin. We suggest, however, that if a post-60 Ma suture is required to explain other non-geological datasets (plate circuits, paleomagnetic data, mantle tomography), then its most geologically plausible location would be within or structurally buried at depth beneath the Gangdese arc (by the Great Counter Thrust and/or an older Cenozoic north-dipping thrust to the north; figs. 2B, 4, and 15A). Both scenarios are discussed at more length in the following text.

Collision Scenario 1: 60 Ma India – Asia collision.—Advocates of a >50 Ma India – Asia collision interpret Gangdese arc magmatism in the context of subduction of Indian continental lithosphere followed by breakoff of the leading Neo-Tethyan oceanic slab (ranging from 55–45 Ma) (Chemenda and others, 2000; Yin and Harrison, 2000; DeCelles and others, 2002, 2011; Negredo and others, 2007; Lee and others, 2009; Jiang and others, 2014; Zhu and others, 2015, 2017). There is a perception among some that 'arc-type' magmatism should cease following the initiation of intercontinental collision (for example, Aitchison and others, 2007). Yet some young intercontinental collisional orogens are associated with significant calc-alkaline 'arc' rocks that were emplaced tens of millions of years after the consumption of intervening oceanic lithosphere (for example, the Lesser Caucasus and Turkish-Iranian Plateau, Carpathians, and Alps; Tiepolo and others, 2002, 2014; Seghedi and others, 2004; Dilek and others, 2010). The observation that hydrous supracrustal assemblages have experienced UHP conditions (Hacker and Gerya, 2013) demonstrates that continental subduction can provide volatiles to the mantle wedge. However, volatile-fluxed melting may not be the most important factor for generating voluminous arc magmas as high-flux events in Cordilleran-style arcs may be fueled primarily by underthrusting melt-fertile foreland crust beneath the arc (Ducea and others 2001, 2015; DeCelles and others, 2009). Finally, there are simply no well-documented examples of other intercontinental collisions involving long-lived, large-magnitude, continental subduction against which the Cenozoic Gangdese arc may be compared. Here, we provide more specific interpretations about the timing and diversity of tectonic processes that may have acted during the 60 to 45 Ma stage of intercontinental collision.

Collision Scenario 1 (figs. 11B and 12C) posits that India – Asia intercontinental collision led to subduction and UHP metamorphism of Himalayan supracrustal rocks beneath Asia (Tso Morari and Kaghan; Guillot and others, 1997; O'Brien and others, 2001) and continued upper-crustal shortening within the Gangdese retroarc and northern Lhasa terrane thrust belts (Kapp and others, 2007a, 2007b; Volkmer and others, 2007; Pullen and others, 2008a). Rapid retroarc thrusting may have fed melt-fertile crust beneath, and rejuvenated magmatism within the Gangdese arc at ~70 to 60 Ma (fig. 8B). Magmatic differentiation, combined with sub-arc lithospheric thickening, may have generated a dense eclogitic root (fig. 12C; DeCelles and others, 2007a). Foundering of the lithospheric root is interpreted to have ignited the ~51 Ma Gangdese arc high-flux magmatic event (fig. 8B) and increased gravitational potential energy that terminated shortening within the Gangdese retroarc thrust belt (at ~51 Ma) and accelerated farther-field shortening within the Tanggula-Nanqian-Yushu thrust belt and along the northeastern margin of Tibet (Kapp and others, 2007b).

The Himalayan foreland basin record youngs southward (fig. 12C), from ~60 Ma continental trench (proximal foredeep) strata in the northernmost Himalaya, a ~56 Ma forebulge disconformity and overlying ~51 Ma distal foredeep strata in the southern northern Himalaya, to the appearance of northern Himalayan detritus on top of the Lesser Himalayan Sequence in a back-bulge to distal forebulge depozone at ~45 Ma (DeCelles and others, 1998, 2004, 2014; Ding and others, 2005, 2017a; Najman and others, 2005; Jain and others, 2009; Ravikant and others, 2011; Hu and others, 2016a). The timing of Himalayan crustal shortening and prograde metamorphism also youngs southward from ~59 Ma along the YSZ (Burg and others, 1987; Metcalf and Kapp, 2017), between 54 and 45 Ma within the northern Himalaya (Ratschbacher and others, 1994; Aikman and others, 2008; Smit and others, 2014; Ding and others, 2016a), and beginning at ~45 Ma within the Greater Himalayan Sequence (Catlos and others, 2002; Martin and others, 2007; Cottle and others, 2009; Carosi and others, 2010; Iaccarino and others, 2015; Gibson and others, 2016).

Collision Scenario 2: 60 Ma India – Xigaze arc collision and 45 Ma closure of the Xigaze backarc basin.—In this scenario, the Xigaze backarc basin continued to open above the southward retreating Neo-Tethyan oceanic trench until ~70 Ma (fig. 13A). Continuous arc magmatism would be expected during slab retreat, but the Xigaze forearc and Paleocene – Eocene northern Himalayan foreland basin strata show a paucity of 75 to 70 Ma detrital zircons (fig. 9). Many retreating oceanic subduction zones, however, are characterized by volcanic centers within the physiographic backarc basin and are topographically or bathymetrically isolated from the outer forearc basin and subduction complex (for example, the Hellenic, Calabrian, eastern Banda, Marianas, Okinawa, and Tonga subduction zones). The renewed influx of ~70 Ma and younger zircons into the Xigaze forearc basin (fig. 9) may signal a transition to Neo-Tethyan slab advance in response to the northward acceleration of Indian plate motion at that time (figs. 10 and 13B).

The southern flank of the composite Xigaze ophiolite belt – forearc basin – arc began colliding with the northern Himalayan margin of India at ~60 Ma (fig. 13C). Collision occurred at 10-5°N paleolatitude, corresponding to the latitude of seismic high velocity anomalies in the lower mantle (anomaly III of Van der Voo and others, 1999) whereas the southern margin of Asia was located at 19° ± 4°N at 52 ± 4 Ma (fig. 11C; Lippert and others, 2014; Hu and others, 2016a). The Xigaze arc terrane may have had a southward convex geometry, with a more northerly westernmost extent that served as a land bridge from India to Asia to facilitate early Eocene faunal exchange (Gingerich and others, 1997; Clyde and others, 2003, Rust and others, 2010; Clementz and others, 2011). A modern analogue is the eastward convex Japan arc, which has nearly continuous land bridges with the Korean Peninsula in the south, and eastern Russia in the north.

The pre-45 Ma history of Himalayan foreland basin sedimentation, deformation, and metamorphism can be explained in the context of Collision Scenario 2. Arc-continent collisional orogenesis commonly persists for >10 Myr and can result in UHP continental margin metamorphism, several hundreds of kilometers of crustal shortening, and crustal thickening and anatexis within the continental lower plate (Cloos and others, 2005; Searle and Treloar, 2010; Tate and others, 2015). Early Cretaceous and older detrital zircons of "Lhasa terrane affinity" in Paleocene – Eocene Himalayan strata could have been reworked from >85 Ma Xigaze forearc basin strata (fig. 8) during collision of the Xigaze terrane. The interpretation of 70 to 45 Ma tectonism in Tibet is similar in both Scenarios, with Tibetan shortening driven by rapid convergence of Xigaze backarc basin lithosphere in Scenario 2 (figs. 13B and 13C) and intercontinental collision in Scenario 1 (figs. 12B and 12C). Given that India – Xigaze terrane collision (if it occurred) continued until the Xigaze backarc basin was consumed, there are no resolvable temporal gaps in the geological records of Himalayan and Tibetan orogenesis.

In Collision Scenario 2, the vast majority of the Xigaze – Spong arc was subducted or underthrusted beneath the Gangdese arc following closure of the Xigaze backarc ocean basin (fig. 15A). The location of the ~45 Ma suture between the northern Himalaya and the Xigaze – Spong arc would be approximately along the northernmost strand of the Great Counter thrust system (figs. 2B and 4). Tectonic slivers of ophiolitic rock and paragneiss are present within the Great Counter thrust zone bounding the northern margin of the Xigaze forearc basin (Laskowski and others, 2017). Future investigations of these and other 'exotic' rocks along the Great Counter Thrust, along with metasedimentary rocks within the southernmost Gangdese arc (some of which have Eocene maximum depositional ages; Xu and others, 2013b), have potential to test this hypothesis.

45 to 26 Ma: Advance of Greater India and Asian Mantle Delamination

45 to 38 Ma Slab Breakoff Followed by Low-Angle Subduction of Greater Indian Lithosphere

A number of researchers have proposed ~45 Ma breakoff of the leading part of the northward subducting Indian slab to explain Eocene metamorphism and UHP rock exhumation in the Himalaya, magmatism in Asia and the northern Himalaya, deceleration of India – Asia convergence (fig. 10), and the latitudinal positions and depths of interpreted slabs in seismic tomographic images (for example, Guillot and others, 1997, 2003; Van der Voo and others, 1999; Chemenda and others, 2000; DeCelles and others, 2002, 2011; Kohn and Parkinson, 2002; Replumaz and others, 2010b; Ji and others, 2016). In the ~60 Ma Collision Scenario 1, the leading Indian slab was attached to Neo-Tethyan oceanic lithosphere (fig. 12C), whereas in ~45 Ma Collision Scenario 2, it consisted of Xigaze backarc basin lithosphere (fig. 13C).

As slab breakoff is widely invoked but challenging to demonstrate (see Garzanti and others, 2018 for a recent discussion), we explore the extent to which the Eocene geology in the central sector of the Himalayan-Tibetan orogen may be consistent with it. Assemblages within the YSZ and northern Himalaya are intruded by 45 to 40 Ma igneous rocks, some of which are adakitic leucogranites and asthenosphere-derived gabbros (Ding and others, 2005, 2016a; Aikman and others, 2008, 2012; Pullen and others, 2011a; Zeng and others, 2011, 2014; Hou and others, 2012; Liu and others, 2014c; Ji and others, 2016). To permit this magmagenesis, we interpret the hinge in the subducting Indian slab to have retreated to the south relative to the surface trace of the YSZ at ~45 Ma (fig. 15A), perhaps owing to anchoring of the deeper part of the slab in the lower mantle.

Within the Lopu Range, ~700 km southeast of Tso Morari and ~600 km west of Lhasa (figs. 1 and 4), a dome of meta-Himalayan (probably upper Greater Himalayan Sequence) rocks is exposed structurally beneath YSZ rocks (Ding and others, 2005; Sanchez and others, 2013; Laskowski and others, 2016, 2017). The rocks experienced pressures of ≥1.5 GPa at temperatures of ≤ 600 °C (relatively high pressure/temperature conditions consistent with subduction), prograde metamorphism at 40.4 ± 1.4 Ma (Lu-Hf garnet date), and exhumation to mid-crustal levels between 39 and 27 Ma in the footwall of a domal, top-to-the-north shear zone (Laskowski and others, 2016). Gangdese arc granites to the north of the meta-Himalayan rocks (and locally elsewhere along strike) are as young as ~38 Ma (Sanchez and others, 2013;

Laskowski and others, 2017). Termination of Gangdese arc magmatism at ~38 Ma is interpreted to mark a transition to northward, low-angle subduction of Indian continental lithosphere beneath Tibet (fig. 15B). Whatever caused the hinge in the subducting Indian plate to first retreat southward relative to the surface position of the YSZ, and then advance back northward (slab breakoff?), is tentatively constrained to have occurred between ~45 and 38 Ma.

Northern Himalayan Thrust Belt and Greater Himalayan Sequence Metamorphism

The structural style of the northern Himalayan fold-thrust belt is different from that of the Miocene and younger southern Himalayan thrust belt that involves Greater Himalaya and Lesser Himalayan sequence rocks. In most places away from the northern Himalayan gneiss domes and the South Tibetan Detachment fault where Paleozoic (meta)sedimentary rocks are exposed, the northern Himalayan thrust belt involves low-grade to unmetamorphosed Mesozoic strata. These strata are deformed by south-vergent upright to recumbent folds at scales from tens of meters to several tens of kilometers (synclinoria and anticlinoria), where not overprinted by north-vergent structures associated with the Great Counter Thrust and South Tibetan Detachment fault (Fuchs, 1975, 1987; Burg and Chen, 1984; Ratschbacher and others, 1994; Wiesmayr and Grasemann, 2002; Godin, 2003; Murphy and Yin, 2003; Carosi and others, 2007; Aikman and others, 2008; Kellett and Godin, 2009; Antolín and others, 2011). No major thrust sheets at the >10-km-scale have been documented in the northern Himalaya south of the Lunzhe thrust (labeled 'LT' on fig. 4, south of Lhasa). Continuous Paleozoic through Cretaceous stratigraphic sections compose the carapaces of northern Himalayan gneiss domes (Lee and others, 2000, 2006). Although these rocks are internally deformed by folding and thrusting, there is no structural repetition at regional scale. Rather, the thrust faults generally terminate within tens of kilometers along strike into folds. This contrasts with other major Miocene and younger Himalayan faults like the northernmost Great Counter Thrust, South Tibetan Detachment, Main Central Thrust, Ramgarh Thrust, and Main Boundary Thrust, which can be traced continuously for 2000 km along strike of the orogen. A north-dipping Gyirong-Kangmar thrust was previously interpreted to be present to the south of the northern Himalayan domes and kinematically linked with dome formation (Burg and others, 1984; Ratschbacher and others, 1994; Hauck and others, 1998). More recent Chinese 1:200,000 scale geological maps (unpublished) do not show this fault, however; nor were we able to identify it in the vicinity of Tingri or south of the Lhagoi dome (fig. 4).

The timing of shortening in the northern Himalaya is poorly constrained south of the Lunzhe thrust (fig. 4). Locally within the southern part of the northern Himalaya, synkinematic illite analyses were interpreted to indicate metamorphic recrystallization between 46 and 42 Ma (Wiesmayr and Grasemann, 2002) and there is detrital thermochronologic evidence for a phase of rapid cooling between 41 and 37 Ma (Shen and others, 2016). The timing of northern Himalayan shortening also can be inferred from the history of prograde metamorphism in structurally underlying Greater Himalayan Sequence rocks (Hodges, 2000; Kohn, 2014). The Greater Himalayan Sequence includes Neoproterozoic – Cambrian medium- to high-grade metasedimentary rocks and Cambrian-Ordovician intrusive granites/orthogneisses that were unconformably overlapped by Tethyan Himalayan strata after Early Ordovician time (DeCelles and others, 2000, 2016a; Wiesmayr and Grasemann, 2002; Gehrels and others, 2006a, 2006b; Myrow and others, 2010). The structurally upper part of Greater Himalayan Sequence rocks in general record an early phase of kyanite-zone peak-pressure (~1–1.4 GPa) metamorphism followed by higher-temperature sillimanite-zone metamorphism and near-isothermal decompression (Pêcher, 1989; Vannay and Hodges, 1996; Godin and others, 2006; Jessup and others, 2008a; Kohn, 2014; Chakraborty and others, 2016). The oldest high-pressure (>1.3 GPa) metamorphism is recorded in the structurally highest part of the Greater Himalayan Sequence and dated at 39 to 36 Ma (fig. 5; Hodges and others, 1996; Godin and others, 2001; Cottle and others, 2009; Corrie and Kohn, 2011; Kellett and others, 2014; Regis and others, 2014; Goscombe and others, 2018). Major Eocene Himalayan orogenesis is consistent with (1) the appearance of Himalayan detrital zircons and a ~45 Ma population of detrital zircon fission track ages in ~45 to 40 Ma distal foreland basin strata (DeCelles and others, 2004; Najman and others, 2005), and (2) an increased flux of sand with short detrital thermochronologic lag times into the Bengal Basin at ~38 Ma (Najman and others, 2008).

Attempts to quantify the magnitude of shortening in the northern Himalaya through construction of structural cross sections have yielded minimum values of 85 to 180 km in the northwestern Himalaya (Searle, 1986; Searle and others, 1988; Steck and others, 1993; Corfield and Searle, 2000; Murphy and Yin, 2003). In the central northern Himalaya, Ratschbacher and others' (1994) "first and speculative" cross sections yielded minimum shortening values of 130 to 140 km. These are probably bare minimum values because the cross sections do not capture smaller-scale penetrative deformation or the portion of the thrust belt that has been eroded up-dip of the modern trace of the South Tibetan Detachment. It is noteworthy that southerly klippen of Greater Himalayan Sequence rocks in Nepal and northern India were metamorphosed at depths of ~25 to 20 km (Johnson and others, 2001; Soucy La Roche and others, 2017), yet almost all of the tectonically thickened Tethyan Himalayan Sequence overburden has been eroded. The important consideration of erosion level is underscored at the Eastern Himalayan Syntaxis, where Greater Himalayan Sequence rocks are juxtaposed against the deepest exposed roots of the Gangdese arc with minimal intervening Tethyan Himalayan Sequence rocks (fig. 1). Shortening must have been sufficient to generate a >45 km thick orogenic wedge within the Himalaya by 39 to 36 Ma (as suggested by the Greater Himalayan Sequence metamorphic record) from an initially ≤20-km-thick sequence of Cambrian and younger sedimentary rocks. Thus, existing estimates of total shortening in the northern Himalaya (and that which involves Tethyan Himalayan Sequence strata more broadly) should be considered as bare minima.

Ductile shear, metamorphism, and partial melting within Greater Himalayan Sequence rocks continued during Oligocene through Miocene time, and generally youngs toward the south, although some out-of-sequence shear zones have been documented locally (Hodges and others, 1996; Vannay and Hodges, 1996; Godin and others, 2001, 2006; Grujic and others, 2002; Daniel and others, 2003; Kohn, 2008, 2014; Carosi and others, 2010, 2016; Warren and others, 2014; Larson and others, 2015; Iaccarino and others, 2015; Goscombe and others, 2018). Several northern Himalayan gneiss domes also record metamorphism and leucogranite emplacement between ~37 and 33 Ma (fig. 5; Lee and Whitehouse, 2007; Larson and others, 2010; Pullen and others, 2011a; Liu and others, 2014c; Horton and others, 2015). We suggest that while the Indian upper crust thickened and accreted in front of and structurally beneath the YSZ, the Indian lower crust and underlying mantle lithosphere subducted northward beneath the Gangdese arc, initially steeply and then at a lower angle by ~38 Ma based on the termination of Gangdese arc magmatism (figs. 15A and 15B).

Tibetan Record

Cenozoic (ultra)potassic and adakitic igneous rocks are widely distributed across the Tibetan Plateau (figs. 4 and 14). The oldest potassic-adakitic volcano-plutonic complex (46–38 Ma; referred to here as 'Dogai') is also the largest, exposed over an area of >6500 km^2 in the northeastern Qiangtang terrane along the northern crest of the Tanggula Mountains (figs. 1, 4, and 14; Wang and others, 2008a; Chen and others, 2013; Ou and others, 2017). The Dogai igneous complex covers an elliptical area, with a long axis of ~200 km (figs. 4 and 14), similar in geometry and scale to proposed Rayleigh-Taylor-type 'drips' of lithosphere beneath the Sierra Nevada and central Andes, among other orogens (Houseman and others, 1981; Zandt and others, 2004; Göğüs and Pysklywec, 2008; Beck and others, 2015; DeCelles and others, 2015; Wang and others, 2015a; Smith and others, 2017). Smaller exposures of similar age and younger (as young as 27 Ma) potassic-adakitic volcanic rocks and north-striking dikes, are also present over a distance of >300 km along strike to the west of the Dogai field (figs. 4 and 14; Liu and others, 2008; Wang and others, 2010; Chen and others, 2013).

Volcanic rocks of the Dogai complex lie flat and unconformably on top of strongly shortened Mesozoic strata at modern elevations of 5000 to 5200 m. This demonstrates that shortening ceased, and that low-relief topographic conditions were achieved in this region by 46 Ma. Paleogene alluvial fan and fluviolacustrine strata are locally exposed proximal to the western margin of the Dogai complex over an approximately 150 km by 150 km area (fig. 4; Xu and others, 2013a). The Paleogene strata are constrained to be younger than ~51 Ma and older than ~28 Ma and include interbeds of gypsum; the lower parts of the successions are tightly folded while their upper parts are gently folded, suggesting syncontractional deposition (Xu and others, 2013a). Stable isotope studies suggest that the strata may have been deposited at ~5 km elevation under arid conditions (fig. 14; Xu and others, 2013a). The flat-lying nature of the Eocene – Oligocene volcanic rocks versus the adjacent, shortened and syncontractional Paleogene strata presents an apparent enigma about the temporal-spatial distribution of crustal shortening in the region. Rocks in the Tanggula thrust belt to the southeast (fig. 4) experienced rapid cooling between 60 and 40 Ma (Wang and others, 2008a; Song and others, 2013). Within the Hoh-Xil basin, shortening commenced after 51 Ma but probably no later than ~47 Ma, continued until at least 34 Ma, and largely ceased by 27 Ma (fig. 5; Staisch and others, 2014, 2016). The magnitude of Hoh-Xil shortening is estimated at ~50 percent (Coward and others, 1988) or ~26 percent (Staisch and others, 2016). Paleoaltimetric studies suggest that the Hoh-Xil region underwent 1700 to 2600 m of surface uplift during the Paleogene, but the estimates of absolute paleoelevation are highly uncertain (Polissar and others, 2009; Quade and others, 2011).

The ages of potassic-adakitic volcanic rocks decrease across the Qiangtang terrane from the northeast (46–38 Ma) to the west and south (37–27 Ma) (fig. 14; Ding and others, 2003, 2007). Studies of xenoliths in Qiangtang volcanic rocks (yellow stars on fig. 14) indicate temperatures of 980 to 1260 °C at near-Moho depths by ~28 Ma (Ding and others, 2007) and until at least ~3 Ma (Hacker and others, 2000). Cenozoic shortening in the Qiangtang terrane, south of the Tanggula Mountains, is characterized by mostly north-dipping thrust faults with Paleogene (dominantly Eocene – Oligocene?) fluviolacustrine strata in their footwalls (Kapp and others, 2003b, 2005). Hanging-wall and footwall cut-offs limit displacement on individual thrust faults to a few kilometers. Folds in Paleogene strata are generally kilometer-scale in wavelength and amplitude and have moderate inter-limb angles, except in the proximal footwalls of thrust faults where overturned synclines are ubiquitous. The magnitude of Cenozoic shortening across the central Qiangtang terrane is ~25 percent (Kapp and others, 2003b, 2005), but it may have been localized to the modern outcrop extents of the Paleogene basins. For example, the Nading volcanic fields in the southern Qiangtang terrane (figs. 4 and 14) are ~36 to 28 Ma and sit flat at relatively high modern elevations (generally >5 km) atop a basement of shortened Paleozoic – Mesozoic rocks (Ding and others, 2007). In contrast, approximately 50 km along strike to the east, coeval fluviolacustrine strata (with a ~35 Ma interbedded tuff) are folded and repeated by thrust faults (Kapp and others, 2005).

Paleoaltimetric studies suggest that the Lunpola basin along the Bangong suture was at an elevation of >4 km by 35 Ma (fig. 14; Rowley and Currie, 2006), although the age assignments of the investigated strata remain in question. In contrast, a stable isotope study of 39 to 36 Ma lacustrine carbonate strata within the Bangong suture zone ~400 km to the west yielded near-sea-level paleoelevations (fig. 14), along with the presence of putative warm-water marine foraminifera (interpreted to be transported inland during storm surges although they could also be eolian) (Wei and others, 2016). Marine water had withdrawn from central Asia via the Tarim and Tajik basins by ~39 Ma (Sun and Jiang, 2013; Bosboom and others, 2014; Carrapa and others, 2015), so the plausibility of this occurrence of marine foraminifera is in question.

It can be concluded that Eocene – Oligocene magmatism in central Tibet was: (1) transient within a given ~100 km by 100 km region, lasting over a time interval of ~10 Myr; (2) spatially diachronous, initiating in the northeast Qiangtang terrane and decreasing in age toward the west and south across central Tibet (figs. 14 and 16); (3) coeval with nearby but localized and moderate-magnitude upper-crustal shortening; the bulk of regional shortening predated magmatism; (4) coeval with or shortly pre-dated establishment of >4 km elevation within a given region; and (5) contemporaneous with very high temperatures at near-Moho depths (Ding and others, 2007). Collectively, these observations are consistent with potassic and adakitic magmatism being associated with removal of negatively buoyant Asian mantle lithosphere (Molnar and others, 1993; Turner and others, 1993, 1996) rather than intracontinental subduction (Deng, 1991; Arnaud and others, 1992; Tapponnier and others, 2001; Ding and others, 2003; Lai and Qin, 2013). Furthermore, most Paleogene volcanic fields in central Tibet sit outside of, at higher modern elevations, and are much less shortened than adjacent sedimentary basins of coeval age. This suggests that Paleogene shortening and subsidence were spatially localized, proximal to the modern outcrop extents of the basins.

We propose that individual Paleogene basins in central Tibet may have developed initially as ~100-km-wide ovaloid depocenters above negatively buoyant lithospheric drips (figs. 15A and 15B), and experienced accelerated subsidence and intrabasin shortening during progressive growth of the drips. The larger volcanic fields were emplaced atop basin-bounding topographic bulges above areas of maximum lithospheric thinning. Similar "bobber" basins have been interpreted in the high elevation hinterlands of the central Andes (DeCelles and others, 2015; Wang and others, 2015a) and North American Cordilleran thrust belt (Smith and others, 2017). Initial dripping and progressive southward removal of Asian lithosphere is predicted in numerical models of India – Asia collision that include a weak, metasomatized lithosphere in the upper plate (retro-plate) between India and stronger Asian lithosphere to the north (see fig. 4 of Kelly and others, 2016 and fig. 9 of Li and others, 2016c). Within the rheologic context, it makes sense that mantle removal initiated beneath the axis of the Tanggula Mountains, as they mark the northernmost extent of major Jurassic to ~45 Ma magmatism and upper-crustal deformation in Tibet (figs. 5 and 8). The modern Tanggula Mountains may be a topographic relict of the northern topographic margin of the ~45 Ma proto-Tibetan Plateau (fig. 15A).

The magnitude of 45 to 26 Ma upper-crustal shortening in the southern Lhasa terrane is minimal based on the widespread preservation of the angular unconformity beneath the Linzizong Formation (figs. 2B and 4). Deeper crustal levels of the Gangdese arc, however, record Eocene – Oligocene metamorphism due to tectonic thickening and/or magmatic underplating. The easternmost Gangdese arc experienced upper-amphibolite-facies metamorphism, metamorphic zircon growth, and crustal anatexis between 44 and 26 Ma (Dong and others, 2010; Zhang and others,

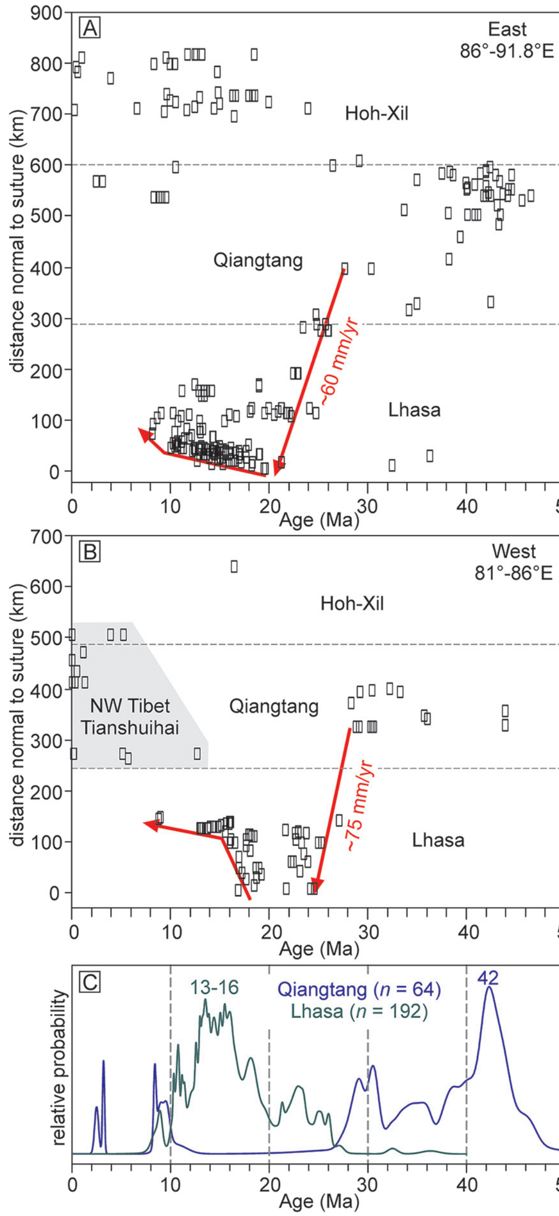

Fig. 16. Temporal-spatial distribution of 50–0 Ma (ultra)potassic, adakitic, and leucogranitic igneous rocks in Tibet between the longitudes of 81°E and 91.8°E (references in online Tibetan magmatism database of Chapman and Kapp, 2017). Down-pointing arrows indicate possible southward sweeps in magmatism and their rates. Left-pointing arrows highlight the post-20 Ma northward younging in the age of magmatic termination. These trends are apparent at narrower longitudinal windows (for example, where igneous rocks have been dated along and adjacent to individual north-south trending rifts), albeit defined by fewer data. The cut-off at 91.8°E was determined by iteratively including or excluding data near that longitude and assessing whether they served to blur or better resolve the temporal-spatial trends. To the east (between 91.8°E and the longitude of the eastern Himalayan syntaxis), Cenozoic potassic volcanic fields are rare, including in central Tibet, and the ages of adakitic rocks in the Gandgese arc increase eastward from ~20 Ma to ~30 Ma as noted by Zhang and others (2014c).

2010b; Palin and others, 2014; Zhang and others, 2015). Some metasedimentary rocks include Gangdese-arc-aged detrital zircons as young as 46 to 41 Ma with 38 to 23 Ma metamorphic rims, interpreted to represent Gangdese forearc basin strata that were underthrust beneath the arc shortly after deposition (Xu and others, 2013b). The north-south width of Gangdese forearc lithosphere (~300 km for most continental margin forearcs) was likely intact until ~38 Ma, when arc magmatism ceased. The Gangdese forearc (which may have included the hypothetical, accreted Xigaze-Spong arc) may have underthrust beneath the Gangdese arc as Indian lithosphere subducted at a lower angle beneath the Lhasa terrane (figs. 15A and 15B). In the Ayi Mountains of far western Tibet (fig. 1), Gangdese arc orthogneisses in the footwall of a domal normal fault experienced metamorphic zircon growth between 40 and 32 Ma (Zhang and others, 2011b).

OLIGOCENE-MIOCENE LITHOSPHERIC DELAMINATION AND INDIAN SLAB ANCHORING (26-21 MA)

After 26 Ma, the locus of potassic-adakitic magmatism swept southward across the Lhasa terrane (Nomade and others, 2004; Chung and others, 2009), reaching the position of the YSZ first in the west at ~24 Ma and then east of 86°E at ~20 Ma (figs. 15C and 16). Delamination of Asian mantle lithosphere is predicted to have increased surface elevation on the order of 1 to 2 km (Molnar and Stock, 2009; Kelly and others, 2016; Li and others, 2016c). Initial stable isotopic studies suggested that the Lunpola and Nima basins were arid and at near-modern elevations by ~35 Ma (?) and 26 Ma, respectively (fig. 14, Rowley and Currie, 2006; DeCelles and others, 2007a, 2007b; Polissar and others, 2009). Subsequent palynological and isotopic studies place the Lunpola basin at ~3 km elevation between 26 and 22 Ma (Sun and others, 2014; Jia and others, 2015). Late Oligocene subtropical fossil plants and fish from the Nima and Lunpola basins have also been used to argue for low (~1 km) surface elevation (Wu and others, 2017), but a reassessment of paleoelevation based on stable isotopes suggests that at least the Nima basin was at modern elevations by 26 Ma (Huntington and others, 2015). Regardless of uncertainties about absolute elevation, it is intriguing that Lunpola basin leaf-wax records suggest a ~900 m elevation reduction between 25.5 and 21.6 Ma, followed by 500 to 1000 m of surface uplift between 21.6 and 20.4 Ma (Jia and others, 2015). These results could be interpreted within the context of subsidence above delaminating/dripping lithosphere followed by its detachment and surface uplift (Wang and others, 2015a), or they could be an artifact of climate change. Paleoaltimetric studies of the Oiyug basin in the southern Lhasa terrane suggest that it was at near-modern elevation throughout Oligocene – Miocene time (fig. 14; Currie and others, 2016; Ingalls and others, 2018).

To the south, the YSZ was warm, wet, and at relatively low elevation during Late Oligocene – early Miocene time (DeCelles and others, 2011, 2016b; Leary and others, 2017; Ding and others, 2017b). Along its entire ~1300 km outcrop extent in southern Tibet, the Kailas Formation is (1) depositional in buttress unconformity atop Gangdese arc rocks to the north, (2) regionally south-dipping, (3) in the footwall of the northernmost strand of the Great Counter Thrust, and (4) characterized by a Gangdese arc provenance and an overall upward-fining succession in its lower part and the appearance of suture-zone and/or northern Himalayan detritus in its coarser-grained upper part. The Kailas Formation is in most places exposed over a north-south distance of <10 km and filled a basin that was also narrow (<20 km), based on lithofacies along both the southern and northern flanks of the Kailas basin that require close proximity to sediment sources (DeCelles and others, 2011, 2016b). The initiation of basal Kailas deposition may decrease in age eastward from ~26 Ma near Mt. Kailas to ~23 Ma near Lhasa, mirroring the eastward younging trend in the initiation of potassic-adakitic magmatism across the Lhasa terrane (Leary and others, 2016a). A middle member of the Kailas Formation includes turbiditic strata that were deposited in deep (>100 m), warm (>25 °C), and probably meromictic lakes, as well as lake-marginal coal beds and deltaic facies (Wang and others, 2013; DeCelles and others, 2016b). Near Xigaze, paleoaltimetric studies of the Kailas Formation (locally referred to as the Qiabulin Formation) suggest a basin elevation of 2 to 2.3 km between 24 and 21 Ma (fig. 14; Ding and others, 2017b; Xu and others, 2018).

Some workers attribute Kailas basin development to slip on the bounding Great Counter Thrust (Yin and others, 1999; Aitchison and others, 2002; Wang and others, 2015b). This interpretation, however, cannot explain: (1) the dominance of a northerly/footwall Gangdese arc provenance for most of the Kailas basin fill; (2) the rapid generation of sediment accommodation over a narrow north-south distance; (3) the absence of contractional growth structures associated with the Great Counter Thrust; (4) the rapid, brief, and nearly linear subsidence history of the basin; (5) the classic "lacustrine sandwich" pattern of extensional basin stratigraphy in which fine-grained lacustrine deposits are underlain and overlain by coarse-grained intervals (Lambiase, 1990; Schlische, 1992); and (6) why the suture zone region was at relatively low elevation tens of millions of years after initial intercontinental collision (DeCelles and others, 2011, 2016b). An alternative is that the Kailas basin developed initially as a narrow, low-elevation half-graben basin, bounded on the south by a north-dipping normal fault and onlapping onto the Gangdese arc in the north (fig. 15C; DeCelles and others, 2011). The hypothesized normal fault has not been documented, and would not be expected to be exposed because of its structural burial in the footwall of the younger Great Counter Thrust. A possible exception is where late Cenozoic ~north-striking rifts cut across the YSZ and expose deeper structural levels beneath the Great Counter Thrust; detailed future mapping in these regions has potential to test for the existence of the inferred Kailas basin-bounding normal fault. Putative growth strata within the Kailas Formation exhibit southward fanning bedding attitudes to shallower angles, consistent with the extensional interpretation (documented and suggested to be syncontractional by Wang and others, 2015b, but reinterpreted by Leary and others, 2016a). Also noteworthy is recognition of an Oligocene – Miocene phase of top-to-the-north reactivation of the Indus suture zone in Pakistan (Treloar and others, 1991; Burg and others, 1996; Vince and Treloar, 1996; Anczkiewicz and others, 2001).

The 26 to 23 Ma time interval marks a number of other kinematic transitions within the southern Tibetan – Himalayan orogen. Roughly orogen-parallel extension and vertical crustal thinning initiated at ~23 Ma within deeper levels of the southwestern Gangdese arc in the Ayi Mountains (Zhang and others, 2011b) and in Himalayan rocks within the Leo Pargil Range (fig. 1; Langille and others, 2012; Jessup and others, 2016). We attribute the orogen-parallel extension in westernmost Tibet to initial development of the adjacent right-lateral Karakoram fault system (fig. 1), and thus distinguish it from the younger onset of ~E-W extension in the northern Himalaya and Tibet to the east (to be presented in a subsequent section). The northern Himalayan domes experienced vertical crustal thinning and north-south stretching between 26 and 23 Ma (Lee and others, 2004, 2006; Lee and Whitehouse, 2007; Larson and others, 2010; Wagner and others, 2010; King and others, 2011). Ductile shearing and thinning in the northern Himalaya were likely kinematically linked with the top-to-the-north South Tibetan Detachment shear zone to the south, which also initiated between 26 and 23 Ma (Hodges and others, 1992, 1996; Searle and others, 1997; Godin and others, 2006; Chambers and others, 2011; Carosi and others, 2013; Kellett and others, 2013; Stübner and others, 2014; Leloup and others, 2015; Webb and others, 2017), coeval with top-to-the-south shear zones within the Greater Himalayan Sequence (Hodges and others, 1996; Godin and others, 2006; Carosi and others, 2010; Imayama and others, 2012; Montomoli and others, 2013; Wang and others, 2016c).

Our working hypothesis is motivated by the observation that Oligocene – Miocene magmatism swept southward across the Lhasa terrane at a rate of ~60 to 75 mm/yr (~60 mm/yr in the east where the trend is better defined; fig. 16A), comparable to the rate of India – Asia convergence during this time (fig. 10). This may be explained by anchoring of the leading portion of the subducting Indian slab in the mantle transition zone at ~26 Ma, which in turn slowed or stopped northward migration of the up-dip slab hinge (Replumaz and others, 2010b; Leary and others, 2016a; Webb and others, 2017). The trailing Indian plate and Himalayan-Tibetan orogen continued to translate northward relative to the anchored portion of the slab, such that the position of the suture at the surface moved northward with respect to the hinge in the subducting Indian slab (fig. 15C). In other words, the Indian mantle lithosphere and lower crust may have peeled or delaminated from beneath the orogen (Bird, 1978).

The kinematic response to Indian slab anchoring as presented does not require extension in the upper plate. However, simulations of oceanic subduction zones show transient changes in plate kinematics in response to interactions with the mantle transition zone (for example, alternating trench advance and retreat; Di Giuseppe and others, 2008; Schellart, 2008; Capitanio and others, 2010; Stegman and others, 2010; Magni and others, 2012). We speculate that the Indian slab hinge may have experienced a transient deceleration or tug back toward the overridden portion of the slab upon anchoring. An associated decrease in the ~north-south horizontal collisional stress, together with replacement of Indian lithosphere by asthenosphere, may have resulted in a vertical greatest compressive stress ($\sigma 1$) direction and an approximately north-south least compressive stress ($\sigma 3$) direction. This, in turn, may have reactivated the YSZ as a north-dipping normal fault, above which the relatively low-elevation and short-lived (<5 Myr at a given locality) Kailas basin developed, and initiated the South Tibetan Detachment shear zone within the Himalaya (fig. 15C).

UNDERTHRUSTING OF INDIAN LITHOSPHERE (21 – 0 MA)

North-south upper-crustal shortening resumed along the YSZ in the early Miocene, first in westernmost Tibet at 23 to 20 Ma near Shiquanhe (fig. 1; Kapp and others, 2003a; Gourbet and others, 2017). Great Counter Thrust motion occurred by ~21 Ma near Mt. Kailas (DeCelles and others, 2011, 2016b), ~20 Ma near Xigaze (Leary and others, 2016b), and ~19 to 18 Ma east of Xigaze (Ratschbacher and others, 1994; Yin and others, 1994; Quidelleur and others, 1997). Paleoaltimetric studies suggest that the Kailas basin was rapidly uplifted to high elevation (4–5 km) by 21 to 19 Ma (fig. 14; DeCelles and others, 2011; Xu and others, 2018). We attribute early Miocene shortening and surface uplift of the YSZ to a return to northward advancement of the hinge in the subducting Indian lithosphere after it tore free of the deeper, anchored portion of the Indian slab (figs. 15C and 15D). Top-to-the-north shearing and vertical thinning within the South Tibetan Detachment shear zone continued in the central Himalaya between 23 and 18 Ma (and later in places; Webb and others, 2017; Kellett and others, 2018). This may suggest that $\sigma 1$ remained vertical in the High Himalaya and continued to drive southward ductile flow of melt-weakened Greater Himalayan Sequence rocks above structurally lower underthrusting crust.

The northward younging trend in the age of magmatic termination in the Lhasa terrane, beginning at ~20 to 18 Ma (figs. 16A and 16B), is interpreted to record underthrusting of Indian lithosphere to the north of the YSZ at sufficiently shallow depths to extinguish partial melting of Asian mantle (figs. 15D and 15E). All of the Kailas basin, and much of the Gangdese arc and YSZ experienced >6 km of exhumation between 20 and 16 Ma (Copeland and others, 1987, 1995; Harrison and others, 1992, 1993; Dai and others, 2013a; Carrapa and others, 2014, 2017). Potassic-adakitic magmatism peaked in the Lhasa terrane between 16 and 13 Ma (fig. 16C), and may mark accelerated removal of Asian lithosphere induced by the impinging Indian lithosphere. The timing of cessation of significant slip on the South Tibetan Detachment varies from 16 to 12 Ma in the central Himalaya (Hodges and others, 1996; Edwards and Harrison, 1997; Godin and others, 2006; Cottle and others, 2009, 2011; Kellett and others, 2013; Nagy and others, 2015; Wang and others, 2016c) and occurred at least locally at elevations of ≥ 5000 m (Gébelin and others, 2013, 2017). Minor slip may have occurred as recently as Pliocene-Pleistocene time (Hodges and others, 2001; McDermott and others, 2013; Cooper and others, 2015). Orogen-parallel extension within the northern Himalaya (for example, at Gurla Mandhata, Thakkhola, Gyirong, and Ama Drime; fig. 3) and Lhasa and Qiangtang terranes initiated at 13 ± 3 Ma in most places (Garzione and others, 2000; Blisniuk and others, 2001; Murphy and others, 2002; Murphy and Copeland, 2005; Kali and others, 2010; Langille and others, 2010; Lee and others, 2011; Sundell and others, 2013; Woodruff Jr. and others, 2013; McCallister and others, 2014; Styron and others, 2015; Laskowski and others, 2017), along with southeastward propagation of the right-lateral Karakoram fault (Murphy and others, 2000, 2009; Phillips and others, 2004; van Hinsbergen and others, 2011a). The rift basins that have been investigated using paleoaltimetry (Zhada, Thakkhola, Oiyug; fig. 1) developed at elevations similar to, or perhaps even higher than their modern elevations (Garzione and others, 2000, 2003; Rowley and others, 2001; Spicer and others, 2003; Currie and others, 2005, 2016; Saylor and others, 2009; Khan and others, 2014; Huntington and others, 2015). The northern Himalayan domes were exhumed coeval with east-west extension, mostly at 12 ± 4 Ma (Lee and others, 2000, 2006; Zhang and others, 2004a; Quigley and others, 2006; Kawakami and others, 2007; Lee and Whitehouse, 2007; King and others, 2011; Aikman and others, 2012), likely by vertical ductile thinning or extrusion of melt-weakened crust above a ductile thrust ramp or duplex at depth (Hauck and others, 1998; Yin and others, 1999; Beaumont and others, 2004; Lee and others, 2006; King and others, 2011; Gao and others, 2016).

Several hypotheses have been raised to explain the initiation of ~east-west extension. These include gravitational spreading of weak crust (Molnar and Tapponnier, 1978; Dewey, 1988), an increase in gravitational potential energy as a result of removal of Asian lithosphere (England and Houseman, 1989; Molnar and others, 1993; Molnar and Stock, 2009), growth/expansion of the Himalayan arc (Seeber and Armbruster, 1984; Klootwijk and others, 1985; Molnar and Lyon-Caen, 1989; Murphy and others, 2009; Styron and others, 2011), northward insertion or underthrusting of Indian lithosphere which simultaneously maintained high gravitational potential energy and forced weak Asian crust and mantle lithosphere out of the way (Zhao and Morgan, 1985, 1987; DeCelles and others, 2002; Kapp and Guynn, 2004; Bendick and others, 2008; Sundell and others, 2013; Styron and others, 2015), basal shear stress related to underthrusting Indian lithosphere (McCaffrey and Nabelek, 1998; Liu and Yang, 2003; Copley and others, 2011), the onset of rapid (>70 mm/yr) eastward flow of deep crust from central Tibet into eastern Tibet (Clark and others, 2005; Royden and others, 2008), and/or a change in plate boundary conditions in East Asia (Yin, 2000). In our view, the observation of coeval northward younging magmatic termination in the Lhasa terrane (figs. 16A and 16B) and east-west upper-crustal extension, together with a northward younging pattern in the timing of subsequent rift acceleration (Styron and others, 2015), emphasizes the importance of Indian underthrusting as a driver for extension, northward and eastward crustal flow, and removal of Asian lithosphere (fig. 15E).

Extensive lake basins developed in the Hoh-Xil region between 24 and 14 Ma (Wu and others, 2008). The lacustrine strata are flat-lying to gently folded above a regional angular unconformity and exposed at modern elevations of ~4.6 km near the

Lhasa-Golmud Highway. Stable isotope studies suggest that these Miocene lakes were at minimum elevations of 3.4 km (Polissar and others, 2009) while paleobotanical studies place them at 1.4 to 2.9 km (Sun and others, 2015a). To the west of the Lhasa-Golmud Highway, ~19 Ma to Quaternary potassic-adakitic volcanic rocks are distributed within the higher (generally >5000 m elevation) and internally-drained part of the Hoh-Xil region (fig. 9; Wang and others, 2005). They may be attributed to lithospheric removal or decompression melting associated with lithospheric-scale transtensional faults in this region (fig. 15E; Cooper and others, 2002).

Beginning at ~11 Ma, the southern part of the Himalayan thrust belt transitioned from emplacement of large, long-distance-slip, low-taper thrust sheets to internal duplexing within the Lesser Himalaya, as well as to slower rates of shortening and forward propagation (Long and others, 2012; McQuarrie and others, 2014; DeCelles and others, 2016a). If duplexing is a signal of a thrust belt trying to build taper by internal shortening (Mitra and Boyer, 1986; DeCelles and Mitra, 1995; Malavieille, 2010), the 11 Ma transition may represent a period of increased erosion in the thrust belt and/or a general decrease in rock strength within the orogenic wedge. The latter is consistent with kinematic reconstructions showing that rocks involved in active thrusting since 11 Ma were predominantly Lesser Himalayan fine-grained sedimentary rocks, in contrast to the high-grade gneissic rocks that dominated the volume of the orogenic wedge during Main Central Thrust activity (Schelling, 1992; Long and others, 2011; DeCelles and others, 2016a). Slip on the Main Boundary Thrust occurred largely between ~9 and 3 Ma (Meigs and others, 1995; Burbank and others, 1996; DeCelles and others, 1998; Powers and others, 1998). The Main Frontal Thrust is presently active and has experienced slip events that generated large-magnitude earthquakes (Avouac, 2003; Bollinger and others, 2014). Recent (2015) major earthquakes in north-central Nepal took place along the basal Himalayan décollement, but did not propagate to the surface (Elliott and others, 2016; Bollinger and others, 2016).

DISCUSSION

Tibet was amalgamated by the successive Mesozoic – Cenozoic northward drift of continental crustal fragments away from Gondwanaland in the Southern Hemisphere and their subsequent collision with the southern margin of Asia in the Northern Hemisphere (Şengör, 1984; Dewey and others, 1988). This first-order tectonic history provides a number of repeated continental breakup and suturing experiments with broadly similar boundary conditions to investigate for potential common behaviors. These include Asian continental margin rifting events, punctuated by episodes of contraction/collision, and tectonically-induced plate kinematic reorganizations. Recent advances in our understanding of the geological and paleoenvironmental evolution of the Himalayan-Tibetan system, and in some cases with very high temporal resolution down to the one million-year timescale, also permit a fresh assessment of the history of Tibetan Plateau development.

Rifted Asian Arcs and Their Demise

Our interpretations of the post-220 Ma tectonic history call upon episodic southward trench retreat events that led to Asian margin forearc extension and ophiolite generation and/or rifting of a continental margin arc and opening of a backarc ocean basin prior to terminal intercontinental suturing. The proposed rifted arcs included the Paleo-Tethyan Triassic Yidun arc, the Meso-Tethyan Jurassic Amdo-Basu arc, and the Neo-Tethyan Jurassic Zedong and Late Cretaceous Spong (and hypothetical Xigaze) arcs. The Amdo and Zedong arcs accreted back to the Asian margin prior to terminal suturing, whereas the Yidun arc collided first with the northward-drifting Gondwanan Qiangtang terrane prior to final closure of the Paleo-Tethys ocean. It remains to be tested whether the hypothetical Xigaze arc rifted from

Asia to open a backarc ocean basin during the Late Cretaceous and collided with the northern margin of India at ~60 Ma prior to terminal India – Asia suturing (figs. 11C and 13).

The history of arc rifting along the southern margin of Asia is expected considering the comparatively stationary paleolatitude of Asia since the Mesozoic (Torsvik and others, 2012; Van der Voo and others, 2015) and the tendency of oceanic trenches to retreat because of the negative buoyancy of subducting lithosphere (Isacks and Molnar, 1971; Karig, 1974; Hamilton, 1988; Billen, 2010; Stegman and others, 2010). Trench advance is favored in scenarios where slab pull forces associated with two simultaneously active and similarly facing subduction zones combine (Čížková and Bina, 2015; Jagoutz and others, 2015). In our interpretations, trench advance and Asian margin contraction occurred, although not exclusively, when two north-dipping oceanic subduction zones were active, such as the 155 to 132 Ma (fig. 7E) and 70 to 45 Ma (Scenario 2, fig. 13) time intervals, and during intercontinental collision events such as the Lhasa – Qiangtang (120 –90 Ma) and India – Asia collisions.

The geology is consistent with all of the rifted Asian arcs having originally been laterally extensive along strike (for example, the regional along-strike age similarities exhibited by ophiolites and detrital and igneous records of magmatism), yet their modern exposures are geographically limited (figs. 1 and 4). We thus infer that rifted arc terranes are inherently subductable, at least to lower crustal levels, such that locally exposed remnants are fortuitous exceptions. Candidate locations where oceanic lithosphere may be consumed during convergence without leaving a geological trace—'cryptic' sutures—are most likely to be found within already recognized suture zones, or within arc complexes because of the tendency of rifting and oceanic spreading to localize along the weakest, central axis of an arc (for example, Molnar and Atwater, 1978).

Causes of Plate Kinematic Reorganizations

In an overall convergent tectonic setting, terrane accretion results in the demise of subduction and may induce initiation of oceanic subduction elsewhere to accommodate continued convergence (for example, induced subduction by transference of Stern, 2004). The final consumption of Paleo-Tethys oceanic lithosphere at 200 to 190 Ma may have induced initiation of northward Meso-Tethys subduction, forearc spreading, and rifting of the Amdo arc along the southern Qiangtang continental margin (figs. 7B and 7C). Accretion of the Amdo arc back to the Qiangtang terrane at ~170 Ma may have induced southward subduction of the Meso-Tethys beneath the northern Lhasa terrane (fig. 7D). The Indus-Yalu suture zone records ophiolite generation at 174 to 156 Ma, 132 to 123 Ma, and ~90 Ma. At least the latter two episodes were coeval with emplacement of global large igneous provinces (Zhu and others, 2009a; van Hinsbergen and others, 2011b; Bryan and Ferrari, 2013; Chatterjee and others, 2013). The renewal of Gangdese arc magmatism at ~70 Ma was contemporaneous with emplacement of the Deccan Traps and India's northward acceleration and rifting from the Seychelles (Cande and Stegman, 2011; van Hinsbergen and others, 2011b; Cande and Patriat, 2015). Hence, the geodynamic evolution of the Neo-Tethyan realm may have been modulated by mantle upwelling and plume-push that drove the breakup of Gondwanaland. Establishment of this whole-mantle convection engine provides an explanation for India's continued northward motion, and more broadly, for supercontinent assembly (Gurnis, 1988; Zhong and others, 2007; Becker and Faccenna, 2011; Yoshida and Santosh, 2011; Faccenna and others, 2013).

Most plate circuit reconstructions of India – Eurasia convergence show a deceleration (from >100 mm/yr – <80 mm/yr) over a time-scale of ~10 Myr during the Eocene (fig. 10). India's velocity relative to Africa shows a similar pattern, with gradual slowing from 63 to 47 Ma, followed by a rapid slowdown at ~47 Ma and a marked change in azimuth at ~43 Ma (fig. 10; Cande and Patriat, 2015). The period of gradual slowing is consistent with the geological records of continuous orogenesis in both the Himalaya and Tibet during this time interval while the more abrupt changes during the Middle Eocene may be related to slab breakoff (fig. 15A). A younger, less profound but resolvable deceleration of India – Asia convergence occurred between 20 and 11 Ma (Molnar and Stock, 2009). This is potentially attributable to ~21 to 20 Ma Indian slab breakoff and the subsequent rise in elevation and gravitational potential energy of the southern Himalayan-Tibetan orogen as a combined result of dynamic rebound (Husson and others, 2014; Webb and others, 2017), Indian underthrusting, and removal of Asian lithosphere (figs. 15C and 15D).

History of Plateau Growth and Surface Elevation Change

The central Qiangtang terrane was a relative topographic high throughout the Cretaceous (figs. 6E through 6H). The central axis of the Gangdese arc may have been at high elevation (>4 km) by Paleocene – Eocene time, consistent with paleoaltimetric studies of the Linzizong Formation at one locality near Lhasa (fig. 14; Ding and others, 2014; Ingalls and others, 2018) and >50 percent upper-crustal shortening within the Gangdese retroarc thrust belt (Kapp and others, 2007b). A relatively high-elevation proto-plateau may have been established in parts of central Tibet by ~45 Ma as a result of Late Cretaceous to Eocene shortening in the northern Lhasa terrane and Tanggula thrust belts (fig. 2B; Kapp and others, 2005; Wang and others, 2008a, 2014a; Rohrmann and others, 2012). The Himalayan metamorphic record requires a thickened crust (>50 km), and by inference substantial surface elevation in the Himalaya, by ~40 Ma. Collision-induced dripping/delamination of Asian lithosphere, together with moderate crustal shortening, likely further uplifted the Qiangtang terrane and Bangong suture zone during Eocene to Oligocene time (figs. 15A and 15B). Some paleoaltimetric studies on Eocene – lower Miocene basins in central Tibet yield elevations of 3 to 5 km, consistent with the geological history, while others place the Bangong suture region within ~1 km of sea level (Rowley and Currie, 2006; DeCelles and others, 2007b; Xu and others, 2013a, Jia and others, 2015; Wei and others, 2016; Wu and others, 2017; fig. 14). More paleoaltimetric studies are needed here and elsewhere within the Himalayan-Tibetan orogen to better understand why there are conflicting results, as well as to better resolve temporal-spatial variations in paleoelevation. The ~50 to 26 Ma paleoelevation history of the YSZ is unknown. Based on the Eocene to Oligocene history of deep burial and subsequent exhumation of Himalayan rocks in the Lopu Range (figs. 1 and 4; Laskowski and others, 2016, 2017), we infer significant surface uplift during this time. The most abrupt and drastic changes in surface elevation are recorded in the Kailas basin along the YSZ, which paleoaltimetric studies suggest was at 2 to 2.3 km elevation, or perhaps even lower (DeCelles and others, 2016b) between 26 and 21 Ma and was subsequently uplifted to 4 to 6 km elevation between 21 and 19 Ma (DeCelles and others, 2011; Ding and others, 2017b; Xu and others, 2018; fig. 14). Again, paleoaltimetric studies are still in their infancy, but the preliminary results are consistent with the sedimentary facies and paleoclimatic indicators in the Kailas basin (DeCelles and others, 2011, 2016b). Unlike the central and southern parts of Tibet, the Hoh-Xil region did not experience any significant upper-crustal shortening or magmatism during the Cretaceous. Eocene – Oligocene crustal shortening was insufficient to generate the modern crustal thickness (Staisch and others, 2016) and paleoaltimetric studies suggest that only moderate elevation was achieved by mid-Miocene time (Polissar and others, 2009; Sun and others, 2015a). This implicates lithospheric removal and/or crustal flow to generate surface uplift in northern Tibet since mid-Miocene time (Staisch and others, 2016).

Some conceptual and numerical models predict that the past elevation of the Tibetan Plateau was higher than its modern elevation. One general concept invokes initial crustal thickening and surface elevation gain, followed by radiogenic heating, melt-weakening of the mid-crust, and crustal flow driven by topographic gradients. Crustal flow leads to net crustal thinning and elevation loss in regions at higher elevation and crustal thickening and elevation gain in adjacent regions (Beaumont and others, 2004; Royden and others, 2008). Mid-Miocene to Recent east-west extension in the northern Himalaya and Tibet can also be viewed in the context of contributing to net crustal thinning and thereby elevation loss, with estimates on the order of ~1 km (Ge and others, 2015). Previously cited paleoaltimetric studies on Himalayan-Tibetan rift basins are permissive, if not supportive, of this. The continued influx of Indian crust beneath the Main Himalayan Thrust, however, should not be neglected. This serves to balance crustal thinning as a result of extension, crustal flow, and erosional loss in externally drained parts of the orogen. We argue that the current, mean elevation state (rising, falling, or steady) of the northern Himalaya and Tibetan Plateau has yet to be demonstrated.

Implications for Paleoclimate and Climate-Tectonic Linkages

A combination of paleogeographic, climatic, and tectonic factors can help explain why the Tibetan Plateau has grown to such extreme heights. Inasmuch as erosion competes against tectonically-induced surface uplift, the latter is more efficient in regions of drier climate and lower relief (Montgomery and others, 2001; Montgomery and Brandon, 2002). Most of Tibet has been located at northern, subtropical latitudes since the Cretaceous (Lippert and others, 2014), where aridity is enhanced because of the dry, descending Hadley cell. Late Cretaceous to Paleocene growth of the Gangdese Mountains likely generated an orographic barrier to Tethyan ocean moisture sources to the south, further contributing to arid conditions in Tibet to the north. Evidence of aridity includes the presence of eolianites in strata as old as latest Cretaceous to Paleocene within the Nima basin (DeCelles and others, 2007a) and evaporative lacustrine facies in all documented Paleocene – Miocene basins in central Tibet (for example, Horton and others, 2002; Kapp and others, 2005; DeCelles and others, 2007a; Xu and others, 2013a). Widely distributed outcrops of flat-lying to gently-tilted Eocene through Miocene volcanic rocks at similar modern elevations in central Tibet, together with the abundance of Eocene and older low-temperature thermochronologic dates and absence of exhumed Cenozoic metamorphic rocks away from late Cenozoic rifts, are consistent with relatively low erosion rates and topographic relief since Paleogene time.

The competing hypotheses for terminal India – Asia suturing (fig. 11) make markedly different predictions for land-sea distribution and oceanic circulation during the Paleogene, with uncertain but likely significant implications for paleoclimate (Lippert and others, 2014). Until these hypotheses are fully vetted, it will be challenging to confidently assess potential linkages among the Paleogene history of India – Asia suturing, associated chemical weathering, and changes in regional and global climate (for example, Raymo and Ruddiman, 1992; Zachos and others, 2001; Kent and Muttoni, 2008; Jagoutz and others, 2016). On the other hand, there is compelling evidence for India-Asia suturing and establishment of high elevations in the Himalaya (as inferred from its metamorphic record) and Tibetan Plateau by ~45 to 40 Ma. Inasmuch as the modern Asian monsoon is largely driven by the presence of an orographic barrier that insulates warm, moist air over low-land India by blocking southward flow of cool, dry air from the north (Boos and Kuang, 2010; Molnar and others, 2010), it is not surprising that the Asian monsoon may have been established by Eocene time (Licht and others, 2014).

An outstanding question is how the post-Eocene waxing and waning of the Asian monsoon and associated precipitation-driven erosion were caused by, or exerted a control on, the kinematic evolution of the Himalayan thrust belt. Intense monsoon rainfall may not have initiated until ~24 Ma (Clift and Webb, 2018). This was roughly coeval with the onset of slip along the South Tibetan Detachment and Main Central Thrust shear zones in the central Himalaya, and at first glance appears to support the idea that southward extrusion of Greater Himalayan Sequence rocks was triggered by focused monsoon precipitation and erosion along the southern Himalayan front (for example, Beaumont and others, 2001). However, it is not clear how monsoon intensification alone can explain along-strike variations in the timing of South Tibetan Detachment activity (Webb and others, 2017; Kellett and others, 2018) or why significant slip along the South Tibetan Detachment terminated roughly at the same time as monsoon precipitation peaked at ~15 Ma (Clift and Webb, 2018). Furthermore, a geodynamic mechanism seems necessary to link Oligocene – Miocene Himalayan and Tibetan (Kailas basin development and potassic-adakitic magmatism) tectonics more broadly, and their along-strike and across-strike temporal variations, such as changes in the dynamics of the subducting Indian slab (figs. 15C through 15E; DeCelles and others, 2011; Leary and others, 2016a; Webb and others, 2017). Indian slab anchoring followed by its breakoff, and associated dynamic subsidence and uplift, may have significantly altered the elevation and taper of the Himalayan orogenic wedge, which in turn may have modulated the strength of the Asian monsoon (Webb and others, 2017; Clift and Webb, 2018). It is difficult to advance beyond mere speculation, however, until major uncertainties about the Cenozoic kinematic and paleoelevation history of the Himalayan thrust belt and YSZ are resolved; some specific examples are provided in the concluding section.

The Question of Cenozoic Strike-Slip Shear Zones Along the Bangong and Yalu Suture Zones

This synthesis does not mention any Cenozoic strike-slip shear zones with displacements of more than a few tens of kilometers within the central parts of the Bangong and Yalu suture zones (as earlier proposed by Tapponnier and others, 1982) because none has been documented. Despite this fact, there have been rekindled suggestions of large-scale eastward extrusion of Asian lithosphere from in front of the Indian plate along the Bangong suture (Royden and others, 2008) or YSZ (Replumaz and Tapponnier, 2003; Replumaz and others, 2010a). Cenozoic extrusion of upper crustal material along the Bangong suture is precluded by the preservation of intact thrust belts of demonstrable Cretaceous age across the Bangong suture and northern Lhasa terrane. The YSZ was modified by the Miocene Great Counter Thrust such that older shear zones have been structurally buried in its footwall. Yet, there is no evidence of subvertical shear zones within the Gangdese arc, nor evidence of major strike-slip shearing within or between any of the YSZ assemblages. Rather, ductile north-dipping shear zones have been documented within and structurally beneath Gangdese arc rocks (for example, the Gangdese Thrust of Yin and others, 1994, which is locally exposed in the footwall of the Great Counter Thrust). Furthermore, no lithotectonic assemblages are 'missing' in the central part of the orogen. Instead, this is where the YSZ assemblages are most completely preserved and where the Lhasa terrane exhibits its largest north-south width (figs. 1 and 4). Additionally, paleomagnetic studies are inconsistent with significant vertical-axis rotations in southern and central Tibet required by some kinematic models of extrusion (Lippert and others, 2014).

CONCLUSIONS AND FUTURE DIRECTIONS

1. The Qiangtang terrane includes a large volume of block-in-sedimentary-matrix mélange (over large lateral distances and likely depths) that formed during Permian – Triassic time. This mélange does not demarcate a discrete suture, but rather a broad subduction complex (or multiple subduction complexes) that underplated Gondwanan-affinity continental margin rocks in many places. The structural setting of Qiangtang mélanges is analogous to

that of the Pelona-Orocopia-Rand subduction-complex schists in the southwestern United States, which underplated the North American continental margin over trench-normal distances of >300 km during latest Cretaceous to Paleogene northeastward flat-slab subduction of the oceanic Farallon plate (Jacobson and others, 1988, 2017). Future studies should aim to better document the location and petrogenesis of assemblages that comprise the Jinsha suture within the remote Hoh-Xil region to the north, along with the geology exposed between it and the northernmost exposures of Qiangtang mélange to the south.

2. Final closure of the Paleo-Tethys ocean at 200 to 190 Ma may have been synchronous with, and thus may have induced, initial northward subduction of the Meso-Tethys (Bangong) oceanic lithosphere beneath the Qiangtang terrane (fig. 7B). Future studies of the Jurassic Bangong suture zone ophiolitic rocks, Amdo terrane, and geology of the southern Qiangtang terrane may provide a rare opportunity to assess the viability and geological manifestations of induced subduction by transference. The Amdo arc terrane is inferred to have rifted southward from and then accreted back to the Qiangtang terrane during the Jurassic, prior to Lhasa – Qiangtang continental collision (figs. 7C and 7D).
3. Jurassic ophiolites along the YSZ are interpreted to have formed proximal to the southern Asian (Lhasa terrane) margin in a forearc (fig. 7D) or intra-oceanic arc extensional setting. The Jurassic Zedong arc may have rifted from, and subsequently rejoined, the southern Asian margin (figs. 7D and 7E).
4. Late Jurassic – Early Cretaceous magmatism in the southern Qiangtang terrane and northern Lhasa terrane is tentatively attributed to bivergent double subduction of Meso-Tethyan oceanic lithosphere, similar to the modern tectonic setting of the Molucca Sea (figs. 7D through 7F; Zhu and others, 2016). Bangong suture assemblages are exposed over a broad north-south distance (~100 km in many places; figs. 1 and 4) and have recently become a target of intensive study. A northwest-southeast trending belt of Mesozoic ophiolites is also exposed to the south within the Lhasa terrane, approximately midway between the cities of Lhasa and Nima (fig. 4), but has received relatively little attention since the early Chinese-British expeditions (Girardeau and others, 1985a; Pearce and Deng, 1988). The ophiolite belt has been proposed to represent a klippe that was thrust southward from the Bangong suture zone (Girardeau and others, 1985a, 1985b, 1985c; Coward and others, 1988) or an additional suture within the Lhasa terrane (for example, Hsü and others, 1995). Future investigations of ophiolites and their adjacent rocks within the Bangong suture and Lhasa terrane have strong potential to reshape our understanding of the history of Lhasa – Qiangtang suturing.
5. The preponderance of geological data suggests that Early Cretaceous ophiolites along the YSZ were generated proximal to the Lhasa terrane in a forearc extensional setting (and locally within the Jurassic ophiolites) during subduction (re)initiation or Neo-Tethyan slab rollback (fig. 7F). The Xigaze forearc basin developed on top of ophiolitic basement and was filled with sediment derived from the Lhasa terrane. This conclusion aligns with that of the Chinese-French team during the 1980's but conflicts with subsequent arguments that the YSZ ophiolites formed in an intra-oceanic setting thousands of kilometers away from the southern Asian margin.
6. A 120 to 105 Ma high-flux magmatic belt spans the northern Lhasa terrane, Bangong suture zone, and southern Qiangtang terrane (fig. 8). Peak

magmatism post-dates initial Lhasa – Qiangtang collision, at least locally, and was coeval with shallow marine limestone deposition across the Lhasa terrane. A correlative 120 to 100 Ma belt of igneous rocks is exposed west of the Karakoram fault, where it also spans terrane boundaries in the Karakoram and South and Central Pamir (Schwab and others 2004; Robinson, 2015; Chapman and others, 2018). Foundering of Meso-Tethys oceanic lithosphere is called upon as a tentative explanation (Zhu and others, 2016; fig. 7G).

7. The Lhasa terrane experienced granulite-facies metamorphism, adakitic and basaltic magmatism, and an apparent cessation of sedimentation between ~90 and 80 Ma, coeval with exhumation of amphibolites along the YSZ, development of the intra-oceanic Spong arc in the northwestern Himalaya, and rifting of the Kohistan arc. This was followed by a magmatic lull within the Gangdese arc between 78 and 72 Ma (fig. 8). We raise the possibility that a portion of the Gangdese arc, along with the entire Xigaze forearc, may have rifted from the southern margin of Asia at ~90 to 80 Ma in response to southward rollback of the Neo-Tethyan oceanic slab (fig. 13A). This in turn may have led to the opening of a backarc ocean basin between the Xigaze forearc in the south and the Asian margin to the north (fig. 13B). Nothing in the known geology, however, requires the former existence of the hypothetical backarc ocean basin. An alternative interpretation attributes the 90 to 80 Ma tectonothermal event in the Lhasa terrane to subduction of a Neo-Tethyan oceanic ridge, and the subsequent magmatic lull to northward flat-slab subduction of Neo-Tethyan oceanic lithosphere (figs. 12A and 12B). Distinguishing between these two alternatives is of fundamental importance given the very different constraints they would place on the subsequent history of India – Asia suturing (figs. 11A and 11B versus 11C).
8. The Gangdese magmatic arc experienced intra-arc to retro-arc shortening, high-grade metamorphism, and a high-flux magmatic event peaking at ~51 Ma during the 70 to 45 Ma time interval. At the same time, the northern Lhasa terrane and parts of the Qiangtang terrane experienced major upper-crustal shortening and accelerated exhumation. The 70 to 45 Ma tectonism may have led to the development of a high-elevation Lhasaplano along the axis of the Gangdese arc, and a proto-plateau within large parts of central Tibet. It remains to be tested whether this tectonism was driven in part by initial India – Asia collision (fig. 12C) or was exclusively Cordilleran in style during northward subduction of a hypothetical Xigaze backarc ocean basin (fig. 13C) or a hypothetical Greater India ocean basin (fig. 11A).
9. The northern Himalaya began colliding with the Xigaze forearc at ~60 Ma. Both the Himalaya and Tibet record a continuous history of orogenesis since 60 Ma. As there is no direct evidence in the rock record for a post-60 Ma suture anywhere within the central Himalayan-Tibetan orogen, the simplest interpretation of the geology is that India – Asia collision initiated at ~60 Ma (Collision Scenario 1; figs. 11B and 12C). Alternatively, a rifted portion of the Gangdese arc (the Xigaze terrane) collided with India at ~60 Ma prior to final closure of the hypothetical Xigaze backarc ocean basin at ~45 Ma (Collision Scenario 2; figs. 11C and 13C).Collision Scenario 2 is not as well supported by the geology, but is in better agreement with plate motion reconstructions and seismic tomographic anomalies in the lower mantle.
10. Yalu suture zone and northern Himalayan rocks were intruded by 45 to 40 Ma granitoids, prior to termination of magmatism within the Gangdese arc (and the initiation of >1.3 Ga metamorphism in Greater Himalayan Sequence rocks) between 40 and 38 Ma. We attribute this history to ~45 Ma southward

retreat of the hinge of the subducting Indian plate (relative to the surface YSZ) and a return to northward hinge advance beneath the Gangdese arc by ~38 Ma (figs. 15A and 15B).

11. Potassic-adakitic magmatism initiated at ~45 Ma within an ~200 km by ~100 km elliptical area in the northern Qiangtang terrane and then expanded westward and southward across the Qiangtang terrane and Bangong suture zone during Eocene – Oligocene time (fig. 14). We attribute Paleogene magmatism and basin subsidence and intrabasin shortening in central Tibet to dripping/delamination of Asian lithosphere (figs. 15A and 15B).
12. Between 26 and 20 Ma, potassic-adakitic magmatism swept southward across the Lhasa terrane at a rate comparable to that of India – Asia convergence (figs. 16A and 16B). This magmatic sweep was coeval with development of the narrow, orogen-parallel, warm, wet, and probably low-elevation Kailas basin along the southern flank of the Gangdese arc and the initiation of vertical ductile crustal thinning and north-south stretching in the northern Himalaya and the South Tibetan Detachment shear zone. At ~21 to 19 Ma, the Great Counter Thrust system became active along the YSZ and the Kailas basin was uplifted to elevations of >4 km. Parts of the YSZ and Gangdese arc experienced >6 km of exhumation between 20 and 16 Ma, coeval with the beginning of a northward younging termination in Lhasa terrane magmatism. Potassic-adakitic magmatism peaked in the Lhasa terrane between 16 and 13 Ma, roughly coeval with termination of the South Tibetan Detachment and initiation of east-west extension in the northern Himalaya and Tibet. Initial ~26 Ma retreat, and subsequent advance of the hinge in the subducting Indian plate relative to the surface YSZ, perhaps as a consequence of Indian slab anchoring and subsequent breakoff, might link Himalayan and Tibetan Miocene tectonism (figs. 15C through 15E). Interpretations could be refined by addressing the following questions and issues: (i) Did the Kailas basin in fact develop initially in the hanging wall of a north-dipping normal fault? If the normal fault interpretation proves valid, then this would suggest that at least parts of the orogen were thrown into north-south extension, even if locally short lived (~3 Myr) and of small magnitude. The Pamir gneiss domes were exhumed by north-south extension during net Miocene convergence between India and Asia (Stübner and others, 2013a, 2013b; Rutte and others, 2017a, 2017b), suggesting that the possibility of local north-south extension in the Himalayan-Tibetan orogen should not be dismissed. Furthermore, a normal fault interpretation for early Kailas basin development suggests that the Great Counter Thrust was not active until after ~21 Ma, and thus could not have been kinematically linked to the South Tibetan Detachment shear zone until this time. This in turn would preclude kinematic models of the Himalaya which balance top-to-the-north slip within the South Tibetan Detachment shear zone with shortening in the Great Counter Thrust system (Yin, 2006; Webb and others, 2007, 2017), at least until ~21 Ma. (ii) What was the kinematic and P-T history of northern Himalayan middle to lower crust? Granulitized eclogites have been documented in the High Himalaya near Ama Drime and in Bhutan, with proposed ages of eclogite-facies metamorphism ranging from ~38 Ma to 14 Ma (for example, Lombardo and Rolfo, 2000; Guillot and others, 2008; Corrie and others, 2010; Grujic and others, 2011; Kellett and others, 2014; Wang and others, 2017). Additional studies on these rocks may further constrain lithosphere-scale tectonic interpretations. (iii) Why did slip on the South Tibet Detachment terminate, and how diachronous was it along strike (see Webb and others, 2017, for their

interpretation)? (iv) East-west extension initiated roughly synchronously across most of the northern Himalaya and Tibet at 13 ± 3 Ma. Did a change in far-field plate boundary conditions contribute to this (Yin, 2000), or was the extension related to northward underthrusting of India and removal of Asian lithosphere?

13. Spatial variations in the age and strength of the Asian lithosphere predetermined the modern spatial extent of the Tibetan Plateau (Molnar and Tapponnier, 1981). Tibet exposes basement rocks that are Neoproterozoic or younger and experienced a protracted history of orogenesis and magmatism throughout Phanerozoic time. The northern Himalayan margin of India is also composed of relatively juvenile crust that experienced Cambrian – Ordovician tectonism (DeCelles and others, 2000; Gehrels and others, 2003; Cawood and others, 2007) and Early Cretaceous intra-plate magmatism (Jadoul and others, 1998; Zhu and others, 2009a; Hu and others, 2010). The relatively young age and tectonic preconditioning of the Himalayan-Tibetan lithosphere made it more susceptible to strain localization during the India – Asia collision than the cratonic blocks that bound the plateau margins. The vast expanse of extremely high ground in the Tibetan Plateau interior, on the other hand, may in part be attributed to its relatively dry climate since the Cretaceous. It is exciting to speculate about the future fate of the Tibetan Plateau physiography. Major rivers have incised headward into formerly internally-drained parts of the eastern Tibetan plateau since mid-Miocene time (Wu and others, 2008; Craddock and others, 2010; Rohrmann and others, 2012; Nie and others, 2018). Conversely, the area of internal drainage in parts of more arid western Tibet appears to have increased since the Miocene due to tectonic damming by the Karakoram fault (Murphy and Burgess, 2006; Gourbet and others, 2017). Which of these processes—rock uplift or river incision—will win in the future, and where?

BROADER FUTURE ISSUES

1. Major gains in our understanding of subduction zone initiation, ophiolite generation, and intercontinental suturing in general, along with the amalgamation history of Tibet in specific, would be gained if all Paleozoic – Mesozoic suture zones and associated orogenic belts in Tibet were scrutinized at a level of detail that the India – Asia suture zone has experienced in recent years.
2. Large parts of Tibet and the northern Himalaya remain poorly investigated in terms of rigorous geological mapping, structural-stratigraphic analysis, and construction of structural cross-sections and kinematic restorations. In a sense, a regional geological infrastructure has yet to be established; instead, it is extrapolated or inferred from a handful of relatively well-studied localities.
3. The history of India – Asia suturing and the timing of terminal intercontinental collision remain outstanding issues. All existing interpretations present challenges—we are missing evidence for either a large amount of Cenozoic shortening in the Himalaya and Asia or one or more Cenozoic suture zones. The search and the debate will continue until this issue is resolved.
4. The concept of slab breakoff (and its associated dynamic topographic effects) is increasingly called upon in tectonic interpretations of geological data from orogenic systems globally (for example, Garzanti and others, 2018). Although the process is consistent with numerical modeling results, a challenge remains in testing the concept through generation and synthesis of multi-disciplinary data sets, while simultaneously disproving or developing alternatives.
5. Paleoaltimetry in the Himalaya and Tibet is still in its infancy in both temporal and spatial coverage, along with an understanding of the uncertainties and limitations

in the various proxies used. The unparalleled high elevation and protracted growth history of the Himalayan-Tibetan orogen make it ideal for continued application and advancement of paleoaltimetric techniques. The possibility that parts of Tibet have undergone one or more phases of elevation loss during Cenozoic collisional orogenesis also warrants further consideration.

6. The Cenozoic paleodrainage evolution of the Himalaya and Tibet remains poorly understood. When were the Yalu and Indus rivers established and did parts of them formerly flow in opposite directions and/or merge with southward flowing Trans-Himalayan rivers? Were large parts of eastern Tibet internally drained prior to Miocene river incision? What parts of the internally drained Tibetan interior were previously externally drained and when? Which regions may have been episodically internally and externally drained? Studies that integrate basin analysis, low-temperature thermochronologic, cosmogenic nuclide erosion rate, and geomorphologic approaches may help to advance progress on this issue.
7. There is a need to synthesize and interpret geological data in the context of three-dimensional, internally consistent kinematic reconstructions of the entire Himalayan-Tibetan-Pamir orogenic system and beyond. GPlates may provide a platform for doing this, but the plethora and variety of data involved will require a broader community effort. Such kinematic reconstructions would permit assessment of along-strike variations, help identify inconsistencies in interpretations, and provide kinematic constraints for geodynamic models and bathymetric/topographic boundary conditions for oceanic circulation and climate models.
8. Previous deep seismic reflection profiling studies were successful at imaging the Main Himalayan Thrust, the middle to upper crustal structure of the northern Himalaya, melt or fluids at depths of 15 to 20 km, dipping lower-crustal reflections in southern Tibet, and the Moho (for examples, Nelson and others, 1996; Alsdorf and others, 1998; Gao and others, 2016). This knowledge about the structure of the deeper crust provided strong constraints on, and raised novel hypotheses about Himalayan-Tibetan orogenesis. Future seismic reflection profiling, and its expansion northward across Tibet, will likely lead to additional leap advances.

ACKNOWLEDGMENTS

This material is based upon work supported by the EAR Division of the National Science Foundation under grant numbers 0309844, 1008527, 1140068, 1419748, and 1763432. The manuscript was strengthened by detailed reviews from Christopher Beaumont, Jean-Pierre Burg, Rebecca Jamieson, Catherine Mottram, and Alex Webb, and suggestions from Associate Editor, Peter Cawood. We thank Lin Ding, Liyun Zhang, Fulong Cai, and Houqi Wang at the Institute of Tibetan Plateau Research, Chinese Academy of Sciences, for many years of collaboration and for introducing us to India – Asia suture zone geology. This work benefited from discussions with numerous other scientists involved in the National Science Foundation Continental Dynamics Project entitled "The suturing process: Insight from the India – Asia collision zone," and previous NSF-funded projects to work in Tibet, including: Christopher Beaumont, Nathaniel Borneman, Jared Butler, Barbara Carrapa, Clay Campbell, Eric Cowgill, Mihai Ducea, Guillaume Dupont-Nivet, George Gehrels, Carl Guilmette, Jerome Guynn, Bradley Hacker, T. Mark Harrison, Shundong He, Kip Hodges, Brian Horton, Wentao Huang, Rebecca Jamieson, Jessica Kapp, Andrew Laskowski, Ryan Leary, Andrew Leier, Peter Lippert, Marco Maffione, Kathryn Metcalf, Michael Murphy, Devon Orme, Jay Quade, Alexander Robinson, Peter Reiners, Joel Saylor, Matthijs Smit, Matthew Spurlin, Daniel Stockli, Richard Styron, Kurt Sundell, Michael Taylor, Douwe van Hinsbergen, John Volkmer, Ross Waldrip, An Yin, and George Zandt. Our field research over the past ~20 years would not have been possible without logistical assistance from Zhou Ma, Wang Zhou, and Rene Schrama in Lhasa. We also thank Duo Jie and Deng Jiu for their skilled driving and companionship during many expeditions.

REFERENCES

Abrajevitch, A. V., Ali, J. R., Aitchison, J. C., Badengzhu, Davis, A. M., Liu, J., and Ziabrev, S. V., 2005, Neotethys and the India-Asia collision: Insights from a palaeomagnetic study of the Dazhuqu ophiolite, southern Tibet: Earth and Planetary Science Letters, v. 233, n. 1–2, p. 87–102, https://doi.org/10.1016/j.epsl.2005.02.003

Ader, T., Avouac, J.-P., Liu-Zeng, J., Lyon-Caen, H., Bollinger, L., Galetzka, J., Genrich, J., Thomas, M., Chanard, K., Sapkota, S. N., Rajaure, S., Shrestha, P., Ding, L., and Flouzat, M., 2012, Convergence rate across the Nepal Himalaya and interseismic coupling on the Main Himalayan Thrust: Implications for seismic hazard: Journal of Geophysical Research-Solid Earth, v. 117, B04403, https://doi.org/10.1029/2011JB009071

Ai, H., Lan, L., Zhu, H., Zhang, K., and Zhen, T., 1998, The forming mechanism and petroleum geology of Tertiary Lunpola basin, southwest China: Acta Petrolei Sinica, v. 19, p. 21–27.

Aikman, A. B., Harrison, T. M., and Ding, L., 2008, Evidence for Early (>44 Ma) Himalayan crustal thickening, Tethyan Himalaya, southeastern Tibet: Earth and Planetary Science Letters, v. 274, n. 1–2, p. 14–23, https://doi.org/10.1016/j.epsl.2008.06.038

Aikman, A. B., Harrison, T. M., and Hermann, J., 2012, The origin of Eo- and Neo-himalayan granitoids, Eastern Tibet: Journal of Asian Earth Sciences, v. 58, p. 143–157, https://doi.org/10.1016/j.jseaes.2012.05.018

Aitchison, J. C., Badengzhu, Davis, A. M., Liu, J., Luo, H., Malpas, J. G., McDermid, I. R. C., Wu, H., Ziabrev, S. V., and Zhou, M., 2000, Remnants of a Cretaceous intra-oceanic subduction system within the Yarlung-Zangbo suture (southern Tibet): Earth and Planetary Science Letters, v. 183, n. 1–2, p. 231–244, https://doi.org/10.1016/S0012-821X(00)00287-9

Aitchison, J. C., Davis, A. M., Badengzhu, and Luo, H., 2002, New constraints on the India-Asia collision: The Lower Miocene Gangrinboche conglomerates, Yarlung Tsangpo suture zone, SE Tibet: Journal of Asian Earth Sciences, v. 21, n. 3, p. 251–263, https://doi.org/10.1016/S1367-9120(02)00037-8

Aitchison, J. C., Ali, J. R., and Davis, A. M., 2007, When and where did India and Asia collide?: Journal of Geophysical Research-Solid Earth, v. 112, B05423, https://doi.org/10.1029/2006JB004706

Aitchison, J. C., Ali, J. R., Chan, A., Davis, A. M., and Lo, C.-H., 2009, Tectonic implications of felsic tuffs within the Lower Miocene Gangrinboche conglomerates, southern Tibet: Journal of Asian Earth Sciences, v. 34, n. 3, p. 287–297, https://doi.org/10.1016/j.jseaes.2008.05.008

Aitchison, J. C., Xia, X., Baxter, A. T., and Ali, J. R., 2011, Detrital zircon U-Pb ages along the Yarlung-Tsangpo suture zone, Tibet: Implications for oblique convergence and collision between India and Asia: Gondwana Research, v. 20, n. 4, p. 691–709, https://doi.org/10.1016/j.gr.2011.04.002

Allègre, C. J., Courtillot, V., Tapponnier, P., Hirn, A., Mattauer, M., Coulon, C., Jaeger, J. J., Achache, J., Schärer, U., Marcoux, J., Burg, J. P., Girardeau, J., Armijo, R., Gariépy, C., Gopel, C., Li, T., Xiao, X., Chang, C., Li, G., Lin, B., Teng, J., Wang, N., Chen, G., Han, T., Wang, X., Den, W., Sheng, H., Cao, Y., Zhou, J., Qiu, H., Bao, P., Wang, S., Wang, B., Zhou, Y., and Xu, R., 1984, Structure and evolution of the Himalaya-Tibet orogenic belt: Nature, v. 307, p. 17–22, https://doi.org/10.1038/307017a0

Alsdorf, D., Brown, L., Nelson, K. D., Makovsky, Y., Klemperer, S., and Zhao, W., 1998, Crustal deformation of the Lhasa terrane, Tibet plateau from Project INDEPTH deep seismic reflection profiles: Tectonics, v. 17, n. 4, p. 501–519, https://doi.org/10.1029/98TC01315

An, W., Hu, X., Garzanti, E., BouDagher-Fadel, M. K., Wang, J., and Sun, G., 2014, Xigaze forearc basin revisited (South Tibet): Provenance changes and origin of the Xigaze Ophiolite: Geological Society of America Bulletin, v. 126, n. 11–12, p. 1595–1613, https://doi.org/10.1130/B31020.1

An, W., Hu, X., and Garzanti, E., 2017, Sandstone provenance and tectonic evolution of the Xiukang Mélange from Neotethyan subduction to India-Asia collision (Yarlung-Zangbo suture, south Tibet): Gondwana Research, v. 41, p. 222–234, https://doi.org/10.1016/j.gr.2015.08.010

Anczkiewicz, R., Oberli, F., Burg, J. P., Villa, I. M., Günther, D., and Meier, M., 2001, Timing of normal faulting along the Indus Suture in Pakistan Himalaya and a case of major $^{231}Pa/^{235}U$ initial disequilibrium in zircon: Earth and Planetary Science Letters, v. 191, n. 1–2, p. 101–114, https://doi.org/10.1016/S0012-821X(01)00406-X

Antolín, B., Appel, E., Montomoli, C., Dunkl, I., Ding, L., Gloaguen, R., and El Bay, R., 2011, Kinematic evolution of the eastern Tethyan Himalaya: Constraints from magnetic fabric and structural properties of the Triassic flysch in SE Tibet, *in* Poblet, J., and Lisle, R. J., editors, Kinematic Evolution and Structural Styles of Fold-and-Thrust Belts: London, Geological Society of London Special Publications, v. 349, p. 99–121, https://doi.org/10.1144/SP349.6

Armijo, R., Tapponnier, P., Mercier, J. L., and Han, T.-L., 1986, Quaternary extension in southern Tibet: Field observations and tectonic implications: Journal of Geophysical Research-Solid Earth, v. 91, n. B14, p. 13803–13872, https://doi.org/10.1029/JB091iB14p13803

Armijo, R., Tapponnier, P., and Tonglin, H., 1989, Late Cenozoic right-lateral strike-slip faulting in southern Tibet: Journal of Geophysical Research-Solid Earth, v. 94, n. B3, p. 2787–2838, https://doi.org/10.1029/JB094iB03p02787

Arnaud, N. O., Vidal, P., Tapponnier, P., Matte, P., and Deng, W. M., 1992, The high K_20 volcanism of

northwestern Tibet: Geochemistry and tectonic implications: Earth and Planetary Science Letters, v. 111, n. 2–4, p. 351–367, https://doi.org/10.1016/0012-821X(92)90189-3
Audley-Charles, M. G., 1983, Reconstruction of eastern Gondwanaland: Nature, v. 306, p. 48–50, https://doi.org/10.1038/306048a0
Avouac, J.-P., 2003, Mountain building, erosion, and the seismic cycle in the Nepal Himalaya: Advances in Geophysics, v. 46, p. 1–80, https://doi.org/10.1016/S0065-2687(03)46001-9
Avouac, J.-P., Meng, L., Wei, S., Wang, T., and Ampuero, J.-P., 2015, Lower edge of locked Main Himalayan Thrust unzipped by the 2015 Gorkha earthquake: Nature Geoscience, v. 8, p. 708–713, https://doi.org/10.1038/NGEO2518
Bao, P., Su, L., Wang, J., and Zhai, Q., 2013, Study on the tectonic setting for the ophiolites in Xigaze, Tibet: Acta Geologica Sinica (English Edition), v. 87, n. 2, p. 395–425, https://doi.org/10.1111/1755-6724.12058
Baxter, A. T., Aitchison, J. C., and Zyabrev, S. V., 2009, Radiolarian age constraints on Mesotethyan ocean evolution, and their implications for development of the Bangong-Nujiang suture, Tibet: Journal of the Geological Society, London, v. 166, n. 4, p. 689–694, https://doi.org/10.1144/0016-76492008-128
Baxter, A. T., Aitchison, J. C., Ali, J. R., Chan, J. S.-L., and Chan, G. H. N., 2016, Detrital chrome spinel evidence for a Neotethyan intra-oceanic island arc collision with India in the Paleocene: Journal of Asian Earth Sciences, v. 128, p. 90–104, https://doi.org/10.1016/j.jseaes.2016.06.023
Beaumont, C., Jamieson, R. A., Nguyen, M. H., and Lee, B., 2001, Himalayan tectonics explained by extrusion of a low-viscosity crustal channel coupled to focused surface denudation: Nature, v. 414, p. 738–742, https://doi.org/10.1038/414738a
Beaumont, C., Jamieson, R. A., Nguyen, M. H., and Medvedev, S., 2004, Crustal channel flows: 1. Numerical models with applications to the tectonics of the Himalayan-Tibetan orogen: Journal of Geophysical Research-Solid Earth, v. 109, B06406, https://doi.org/10.1029/2003JB002809
Beck, R. A., Burbank, D. W., Sercombe, W. J., Riley, G. W., Barndt, J. K., Berry, J. R., Afzal, J., Khan, A. M., Jurgen, H., Metje, J., Cheema, A., Shafique, N. A., Lawrence, R. D., and Khan, M. A., 1995, Stratigraphic evidence for an early collision between northwest India and Asia: Nature, v. 373, p. 55–58, https://doi.org/10.1038/373055a0
Beck, R. A., Burbank, D. W., Sercombe, W. J., Khan, A. M., and Lawrence, R. D., 1996, Late Cretaceous ophiolite obduction and Paleocene India-Asia collision in the westernmost Himalaya: Geodinamica Acta, v. 9, n. 2–3, p. 114–144, https://doi.org/10.1080/09853111.1996.11105281
Beck, S. L., Zandt, G., Ward, K. M., and Scire, A., 2015, Multiple styles and scales of lithospheric foundering beneath the Puna Plateau, central Andes, *in* DeCelles, P. G., Ducea, M. N., Carrapa, B., and Kapp, P. A., editors, Geodynamics of a Cordilleran Orogenic System: The Central Andes of Argentina and Northern Chile: Geological Society of America Memoir 212, p. 43–60, https://doi.org/10.1130/2015.1212(03)
Becker, T. W., and Faccenna, C., 2011, Mantle conveyor beneath the Tethyan collisional belt: Earth and Planetary Science Letters, v. 310, n. 3–4, p. 453–461, https://doi.org/10.1016/j.epsl.2011.08.021
Bendick, R., McKenzie, D., and Etienne, J., 2008, Topography associated with crustal flow in continental collisions, with application to Tibet: Geophysical Journal International, v. 175, n. 1, p. 375–385, https://doi.org/10.1111/j.1365-246X.2008.03890.x
Besse, J., and Courtillot, V., 1988, Paleogeographic maps of the continents bordering the Indian Ocean since the Early Jurassic: Journal of Geophysical Research-Solid Earth, v. 93, n. B10, p. 11791–11808, https://doi.org/10.1029/JB093iB10p11791
Bettinelli, P., Avouac, J.-P., Flouzat, M., Jouanne, F., Bollinger, L., Willis, P., and Chitrakar, G. R., 2006, Plate motion of India and interseismic strain in the Nepal Himalaya from GPS and DORIS measurements: Journal of Geodesy, n. 80, n. 8–11, https://doi.org/10.1007/s00190-006-0030-3
Bilham, R., Larson, K., Freymuller, J., and Project Idylhim members, 1997, GPS measurements of present-day convergence across the Nepal Himalaya: Nature, v. 386, p. 61–64, https://doi.org/10.1038/386061a0
Billen, M. I., 2010, Slab dynamics in the transition zone: Physics of the Earth and Planetary Interiors, v. 183, n. 1–2, p. 296–308, https://doi.org/10.1016/j.pepi.2010.05.005
Bird, P., 1978, Initiation of intracontinental subduction in the Himalaya: Journal of Geophysical Research-Solid Earth, v. 83, n. B10, p. 4975–4987, https://doi.org/10.1029/JB083iB10p04975
——— 1991, Lateral extrusion of lower crust from under high topography, in the isostatic limit: Journal of Geophysical Research, v. 96, n. B6, p. 10275–10286, https://doi.org/10.1029/91JB00370
Blisniuk, P. M., Hacker, B. R., Glodny, J., Ratschbacher, L., Bi, S., Wu, Z., McWilliams, M. O., and Calvert, A., 2001, Normal faulting in central Tibet since at least 13.5 Myr ago: Nature, v. 412, p. 628–632, https://doi.org/10.1038/35088045
Bollinger, L., Sapkota, S. N., Tapponnier, P., Klinger, Y., Rizza, M., Van der Woerd, J., Tiwari, D. R., Pandey, R., Bitri, A., and Bes de Berc, S., 2014, Estimating the return times of great Himalayan earthquakes in eastern Nepal: Evidence from the Patu and Bardibas strands of the Main Frontal Thrust: Journal of Geophysical Research- Solid Earth, v. 119, n. 9, p. 7123–7163, https://doi.org/10.1002/2014JB010970
Bollinger, L., Tapponnier, P., Sapkota, S. N., and Klinger, Y., 2016, Slip deficit in central Nepal: Omen for a repeat of the 1344 AD earthquake?: Earth, Planets and Space, v. 68, https://doi.org/10.1186/s40623-016-0389-1
Boos, W. R., and Kuang, Z., 2010, Dominant control of the South Asian monsoon by orographic insulation versus plateau heating: Nature, v. 463, p. 218–222, https://doi.org/10.1038/nature08707
Bosboom, R. E., Dupont-Nivet, G., Grothe, A., Brinkhuis, H., Villa, G., Mandic, O., Stoica, M., Kouwenhoven, T., Huang, W., Yang, W., and Guo, Z., 2014, Timing, cause and impact of the late Eocene stepwise sea retreat from the Tarim Basin (west China): Palaeogeography, Palaeoclimatology, Palaeoecology, v. 403, p. 101–118, https://doi.org/10.1016/j.palaeo.2014.03.035
BouDagher-Fadel, M. K., Hu, X., Price, G. D., Sun, G., Wang, J.-G., and An, W., 2017, Foraminiferal

biostratigraphy and palaeoenvironmental analysis of the mid-Cretaceous limestones in the southern Tibetan Plateau: Journal of Foraminiferal Research, v. 47, p. 188–207.
Bouilhol, P., Schaltegger, U., Chiaradia, M., Ovtcharova, M., Stracke, A., Burg, J.-P., and Dawood, H., 2010, Timing of juvenile arc crust formation and evolution in the Sapat Complex (Kohistan-Pakistan): Chemical Geology, v. 280, n. 3–4, p. 243–256, https://doi.org/10.1016/j.chemgeo.2010.11.013
Bouilhol, P., Jagoutz, O., Hanchar, J. M., and Dudas, F. O., 2013, Dating the India-Eurasia collision through arc magmatic records: Earth and Planetary Science Letters, v. 366, p. 163–175, https://doi.org/10.1016/j.epsl.2013.01.023
Braden, Z., Godin, L., and Cottle, J. M., 2017, Segmentation and rejuvenation of the Greater Himalayan sequence in western Nepal revealed by *in situ* U-Th/Pb monazite petrochronology: Lithos, v. 284–285, p.751–765, https://doi.org/10.1016/j.lithos.2017.04.023
Brandon, C., and Romanowicz, B., 1986, A "no-lid" zone in the Chang-Thang platform of Tibet: Evidence from pure path phase velocity measurements of long period Rayleigh waves: Journal of Geophysical Research-Solid Earth, v. 91, n. B6, p. 6547–6564, https://doi.org/10.1029/JB091iB06p06547
Bryan, S. E., and Ferrari, L., 2013, Large igneous provinces and silicic large igneous provinces: Progress in our understanding over the last 25 years: Geological Society of America Bulletin, v. 125, n. 7–8, p. 1053–1078, https://doi.org/10.1130/B30820.1
Burbank, D. W., Beck, R. A., and Mulder, T., 1996, The Himalayan foreland basin, *in* Yin, A., and Harrison, T. M., editors, The Tectonic Evolution of Asia: New York, Cambridge University Press, p. 149–188.
Burchfiel, B. C., Chen, Z., Royden, L. H., Liu, Y., and Deng, C., 1991, Extensional development of Gabo Valley, southern Tibet: Tectonophysics, v. 194, n. 1–2, p. 187–193, https://doi.org/10.1016/0040-1951(91)90283-X
Burchfiel, B. C., Zhiliang, C., Hodges, K. V., Yuping, L., Royden, L. H., Changrong, D., and Jiene, X., 1992, The South Tibetan Detachment System, Himalayan Orogen: Extension contemporaneous with and parallel to shortening in a collisional mountain belt: Geological Society of America Special Paper 269, p. 41, https://doi.org/10.1130/SPE269-p1
Burg, J.-P., 2011, The Asia-Kohistan-India collision: Review and Discussion, *in* Brown, D., and Ryan, P. D., editors, Arc-Continent Collision: Berlin, Springer-Verlag, p. 279–309, https://doi.org/10.1007/978-3-540-88558-0_10
Burg, J. P., and Chen, G. M., 1984, Tectonics and structural zonation of southern Tibet, China: Nature, v. 311, p. 219–223, https://doi.org/10.1038/311219a0
Burg, J.-P., Proust, F., Tapponnier, P., and Chen, G. M., 1983, Deformation phases and tectonic evolution of the Lhasa block (southern Tibet, China): Eclogae Geologicae Helvetiae, v. 76, n. 3, p. 643–665.
Burg, J. P., Guiraud, M., Chen, G. M., and Li, G. C., 1984, Himalayan metamorphism and deformations in the North Himalayan Belt (southern Tibet, China): Earth and Planetary Science Letters, v. 69, n. 2, p. 391–400, https://doi.org/10.1016/0012-821X(84)90197-3
Burg, J.-P., Leyreloup, A., Girardeau, J., and Chen, G.-M., 1987, Structure and metamorphism of a tectonically thickened continental crust: The Yalu Tsangpo suture zone (Tibet): Philosophical Transactions of the Royal Society of London, Series A, v. 321, n. 1557, p. 67–86, https://doi.org/10.1098/rsta.1987.0005
Burg, J.-P., Chaudhry, M. N., Ghazanfar, M., Anczkiewicz, R., and Spencer, D., 1996, Structural evidence for back sliding of the Kohistan arc in the collisional system of northwest Pakistan: Geology, v. 24, n. 8, p. 739–742, https://doi.org/10.1130/0091-7613(1996)024<0739:SEFBSO>2.3.CO;2
Burg, J.-P., Davy, P., Nievergelt, P., Oberli, F., Seward, D., Diao, Z., and Meier, M., 1997, Exhumation during crustal folding in the Namche-Barwa syntaxis: Terra Nova, v. 9, n. 2, p. 53–56, https://doi.org/10.1111/j.1365-3121.1997.tb00001.x
Burg, J.-P., Nievergelt, P., Oberli, F., Seward, D., Davy, P., Maurin, J.-C., Diao, Z., and Meier, M., 1998, The Namche Barwa syntaxis: Evidence for exhumation related to compressional crustal folding: Journal of Asian Earth Sciences, v. 16, p. 239–252.
Burg, J.-P., Jagoutz, O., Dawood, H., and Hussain, S. S., 2006, Precollision tilt of crustal blocks in rifted island arcs: Structure evidence from the Kohistan Arc: Tectonics, v. 25, n. 5, TC5005, https://doi.org/10.1029/2005TC001835
Burgess, W. P., Yin, A., Dubey, C. S., Shen, Z.-K., and Kelty, T. K., 2012, Holocene shortening across the Main Frontal Thrust zone in the eastern Himalaya: Earth and Planetary Science Letters, v. 357–358, p. 152–167, https://doi.org/10.1016/j.epsl.2012.09.040
Burke, K., Dewey, J. F., and Kidd, W. S. F., 1977, World distribution of sutures – the sites of former oceans: Tectonophysics, v. 40, n. 1–2, p. 69–99, https://doi.org/10.1016/0040-1951(77)90030-0
Butler, J. P., and Beaumont, C., 2017, Subduction zone decoupling/retreat modeling explains south Tibet (Xigaze) and other supra-subduction zone ophiolites and their UHP mineral phases: Earth and Planetary Science Letters, v. 463, p. 101–117, https://doi.org/10.1016/j.epsl.2017.01.025
Cai, F., Ding, L., Leary, R. J., Wang, H., Xu, Q., Zhang, L., and Yue, Y., 2012, Tectonostratigraphy and provenance of an accretionary complex within the Yarlung-Zangpo suture zone, southern Tibet: Insights into subduction-accretion processes in the Neo-Tethys: Tectonophysics, v. 574–575, p. 181–192, https://doi.org/10.1016/j.tecto.2012.08.016
Cande, S. C., and Patriat, P., 2015, The anticorrelated velocities of Africa and India in the Late Cretaceous and early Cenozoic: Geophysical Journal International, v. 200, n. 1, p. 227–243, https://doi.org/10.1093/gji/ggu392
Cande, S. C., and Stegman, D. R., 2011, Indian and African plate motions driven by the push force of the Réunion plume head: Nature, v. 475, p. 47–52, https://doi.org/10.1038/nature10174
Capitanio, F. A., Stegman, D. R., Moresi, L. N., and Sharples, W., 2010, Upper plate controls on deep subduction, trench migrations and deformations at convergent margins: Tectonophysics, v. 483, n. 1–2, p. 80–92, https://doi.org/10.1016/j.tecto.2009.08.020

Carosi, R., Montomoli, C., and Visonà, D., 2007, A structural transect in the Lower Dolpo: Insights on the tectonic evolution of Western Nepal: Journal of Asian Earth Sciences, v. 29, n. 2–3, p. 407–423, https://doi.org/10.1016/j.jseaes.2006.05.001

Carosi, R., Montomoli, C., Rubatto, D., and Visona, D., 2010, Late Oligocene high-temperature shear zones in the core of the Higher Himalayan Crystallines (Lower Dolpo, western Nepal): Tectonics, v. 29, n. 4, TC4029, https://doi.org/10.1029/2008TC002400

Carosi, R., Montomoli, C., Rubatto, D., and Visonà, D., 2013, Leucogranite intruding the South Tibetan Detachment in western Nepal: Implications for exhumation models in the Himalayas: Terra Nova, v. 25, n. 6, p. 478–489, https://doi.org/10.1111/ter.12062

Carosi, R., Montomoli, C., Iaccarino, S., Massonne, H.-J., Rubatto, D., Langone, A., Gemignani, L., and Visonà, D., 2016, Middle to late Eocene exhumation of the Greater Himalayan Sequence in the Central Himalayas: Progressive accretion from the Indian plate: Geological Society of America Bulletin, v. 128, n. 11–12, p. 1571–1592, https://doi.org/10.1130/B31471.1

Carosi, R., Montomoli, C., and Iaccarino, S., 2018, 20 years of geological mapping of the metamorphic core across Central and Eastern Himalayas: Earth-Science Reviews, v. 177, p. 124–138, https://doi.org/10.1016/j.earscirev.2017.11.006

Carrapa, B., Orme, D. A., DeCelles, P. G., Kapp, P., Cosca, M. A., and Waldrip, R., 2014, Miocene burial and exhumation of the India-Asia collision zone in southern Tibet: Response to slab dynamics and erosion: Geology, v. 42, n. 5, p. 443–446, https://doi.org/10.1130/G35350.1

Carrapa, B., DeCelles, P. G., Wang, X., Clementz, M. T., Mancin, N., Stoica, M., Kraatz, B., Meng, J., Abdulov, S., and Chen, F., 2015, Tectono-climatic implications of Eocene Paratethys regression in the Tajik basin of central Asia: Earth and Planetary Science Letters, v. 424, p. 168–178, https://doi.org/10.1016/j.epsl.2015.05.034

Carrapa, B., bin Hassim, M. F., Kapp, P. A., DeCelles, P. G., and Gehrels, G., 2017, Tectonic and erosional history of southern Tibet recorded by detrital chronological signatures along the Yarlung River drainage: Geological Society of America Bulletin, v. 129, n. 5–6, p. 570–581, https://doi.org/10.1130/B31587.1

Catlos, E. J., Harrison, T. M., Manning, C. E., Grove, M., Rai, S. M., Hubbard, M. S., and Upreti, B. N., 2002, Records of the evolution of the Himalayan orogen from *in situ* Th-Pb ion microprobe dating of monazite: Eastern Nepal and western Garhwal: Journal of Asian Earth Sciences, v. 20, n. 5, p. 459–479, https://doi.org/10.1016/S1367-9120(01)00039-6

Cattin, R., and Avouac, J. P., 2000, Modeling mountain building and the seismic cycle in the Himalaya of Nepal: Journal of Geophysical Research-Solid Earth, v. 105, n. B6, p. 13389–13407, https://doi.org/10.1029/2000JB900032

Cawood, P. A., Johnson, M. R. W., and Nemchin, A. A., 2007, Early Paleozoic orogenesis along the Indian margin of Gondwana: Tectonic response to Gondwana assembly: Earth and Planetary Science Letters, v. 255, n. 1–2, p. 70–84, https://doi.org/10.1016/j.epsl.2006.12.006

Cecil, M. R., Gehrels, G., Ducea, M. N., and Patchett, P. J., 2011, U-Pb-Hf characterization of the central Coast Mountains batholith: Implications for petrogenesis and crustal architecture: Lithosphere, v. 3, n. 4, p. 247–260, https://doi.org/10.1130/L134.1

Chakraborty, S., Anczkiewicz, R., Gaidies, F., Rubatto, D., Sorcar, N., Faak, K., Mukhopadhyay, D. K., and Dasgupta, S., 2016, A review of thermal history and timescales of tectonometamorphic processes in Sikkim Himalaya (NE India) and implications for rates of metamorphic processes: Journal of Metamorphic Geology, v. 34, n. 8, p. 785–803, https://doi.org/10.1111/jmg.12200

Chambers, J., Parrish, R., Argles, T., Harris, N., and Horstwood, M., 2011, A short-duration pulse of ductile normal shear on the outer South Tibetan detachment in Bhutan: Alternating channel flow and critical taper mechanics of the eastern Himalaya: Tectonics, v. 30, n. 2, TC2005, https://doi.org/10.1029/2010TC002784

Chan, G. H. N., Aitchison, J. C., Crowley, Q. G., Horstwood, M. S. A., Searle, M. P., Parrish, R. R., and Chan, J. S.-L., 2015, U-Pb zircon ages for Yarlung Tsangpo suture zone ophiolites, southwestern Tibet and their tectonic implications: Gondwana Research, v. 27, n. 2, p. 719–732, https://doi.org/10.1016/j.gr.2013.06.016

Chang, C., Chen, N., Coward, M. P., Deng, W., Dewey, J. F., Gansser, A., Harris, N. B. W., Jin, C., Kidd, W. S. F., Leeder, M. R., Li, H., Lin, J., Liu, C., Mei, H., Molnar, P., Pan, Y., Pan, Y., Pearce, J. A., Shackleton, R. M., Smith, A. B., Sun, Y., Ward, M., Watts, D. R., Xu, J., Xu, R., Yin, J., and Zhang, Y., 1986, Preliminary conclusions of the Royal Society and Academia Sinica 1985 geotraverse of Tibet: Nature, v. 323, p. 501–507, https://doi.org/10.1038/323501a0

Chapman, J. B., and Kapp, P., 2017, Tibetan magmatism database: Geochemistry, Geophysics, Geosystems, v. 18, n. 11, p. 4229–4234, https://doi.org/10.1002/2017GC007217

Chapman, J. B., Ducea, M. N., Kapp, P., Gehrels, G. E., and DeCelles, P. G., 2017, Spatial and temporal radiogenic isotopic trends of magmatism in Cordilleran orogens: Gondwana Research, v. 48, p. 189–204, https://doi.org/10.1016/j.gr.2017.04.019

Chapman, J. B., Scoggin, S. H., Kapp, P., Carrapa, B., Ducea, M. N., Worthington, J., Oimahmadov, I., and Gadoev, M., 2018, Mesozoic to Cenozoic magmatic history of the Pamir: Earth and Planetary Science Letters, v. 482, p. 181–192, https://doi.org/10.1016/j.epsl.2017.10.041

Chatterjee, S., Goswami, A., and Scotese, C. R., 2013, The longest voyage: Tectonic, magmatic, and paleoclimatic evolution of the Indian plate during its northward flight from Gondwana to Asia: Gondwana Research, v. 23, n. 1, p. 238–267, https://doi.org/10.1016/j.gr.2012.07.001

Chemenda, A. I., Burg, J.-P., and Mattauer, M., 2000, Evolutionary model of the Himalaya-Tibet system: Geopoem based on new modelling, geological and geophysical data: Earth and Planetary Science Letters, v. 174, n. 3–4, p. 397–409, https://doi.org/10.1016/S0012-821X(99)00277-0

Chen, J. L., Wu, J. B., Xu, J. F., Dong, Y. H., Wang, B. D., and Kang, Z. Q., 2013, Geochemistry of Eocene high-Mg# adakitic rocks in the northern Qiangtang terrane, central Tibet: Implications for early uplift of the plateau: Geological Society of America Bulletin, v. 125, n. 11–12, p. 1800–1819, https://doi.org/10.1130/B30755.1

Chen, J.-L., Xu, J.-F., Yu, H.-X., Wang, B.-D., Wu, J.-B., and Feng, Y.-X., 2015, Late Cretaceous high-Mg# granitoids in southern Tibet: Implications for the early crustal thickening and tectonic evolution of the Tibetan Plateau?: Lithos, v. 232, p. 12–22, https://doi.org/10.1016/j.lithos.2015.06.020

Chen, W.-P., and Molnar, P., 1983, Focal depths of intracontinental and intraplate earthquakes and their implications for the thermal and mechanical properties of the lithosphere: Journal of Geophysical Research-Solid Earth, v. 88, n. B5, p. 4183–4214, https://doi.org/10.1029/JB088iB05p04183

Chen, W.-P., and Yang, Z., 2004, Earthquakes beneath the Himalayas and Tibet: Evidence for strong lithospheric mantle: Science, v. 304, n. 5679, p. 1949–1952, https://doi.org/10.1126/science.1097324

Cheng, H., Zhang, C., Vervoort, J. D., Lu, H., Wang, C., and Cao, D., 2012, Zircon U-Pb and garnet Lu-Hf geochronology of eclogites from the Lhasa Block, Tibet: Lithos, v. 155, p. 341–359, https://doi.org/10.1016/j.lithos.2012.09.011

Chevalier, M.-L., Pan, J., Li, H., Sun, Z., Liu, D., Pei, J., Xu, W., and Wu, C., 2017, First tectonic-geomorphology study along the Longmu-Gozha Co fault system, Western Tibet: Gondwana Research, v. 41, p. 411–424, https://doi.org/10.1016/j.gr.2015.03.008

Chirouze, F., Huyghe, P., van der Beek, P., Chauvel, C., Chakraborty, T., Dupont-Nivet, G., and Bernet, M., 2013, Tectonics, exhumation, and drainage evolution of the eastern Himalaya since 13 Ma from detrital geochemistry and thermochronology, Kameng River Section, Arunachal Pradesh: Geological Society of America Bulletin, v. 125, n. 3–4, p. 523–538, https://doi.org/10.1130/B30697.1

Chu, M.-F., Chung, S.-L., Song, B., Liu, D., O-Reilly, S. Y., Pearson, N. J., Ji, J., and Wen, D.-J., 2006, Zircon U-Pb and Hf isotope constraints on the Mesozoic tectonics and crustal evolution of southern Tibet: Geology, v. 34, n. 9, p. 745–748, https://doi.org/10.1130/G22725.1

Chu, M.-F., Chung, S.-L., O-Reilley, S. Y., Pearson, N. J., Wu, F.-Y., Li, X.-H., Liu, D., Ji, J., Chu, C.-H., and Lee, H.-Y., 2011, India's hidden inputs to Tibetan orogeny revealed by Hf isotopes of Transhimalayan zircons and host rocks: Earth and Planetary Science Letters, v. 307, n. 3–4, p. 479–486, https://doi.org/10.1016/j.epsl.2011.05.020

Chung, S.-L., Chu, M.-F., Zhang, Y., Xie, Y., Lo, C.-H., Lee, T.-Y., Lan, C.-Y., Li, X., Zhang, Q., and Wang, Y., 2005, Tibetan tectonic evolution inferred from spatial and temporal variations in post-collisional magmatism: Earth-Science Reviews, v. 68, n. 3–4, p. 173–196, https://doi.org/10.1016/j.earscirev.2004.05.001

Chung, S.-L., Chu, M.-F., Ji, J., O'Reilly, S. Y., Pearson, N. J., Liu, D., Lee, T.-Y., and Lo, C.-H., 2009, The nature and timing of crustal thickening in Southern Tibet: Geochemical and zircon Hf isotopic constraints from postcollisional adakites: Tectonophysics, v. 477, n. 1–2, p. 36–48, https://doi.org/10.1016/j.tecto.2009.08.008

Čížková, H., and Bina, C. R., 2015, Geodynamics of trench advance: Insights from a Philippine-Sea-style geometry: Earth and Planetary Science Letters, v. 430, p. 408–415, https://doi.org/10.1016/j.epsl.2015.07.004

Clark, M. K., and Royden, L. H., 2000, Topographic ooze: Building the eastern margin of Tibet by lower crustal flow: Geology, v. 28, n. 8, p. 703–706, https://doi.org/10.1130/0091-7613(2000)28<703:TOBTEM>2.0.CO;2

Clark, M. K., House, M. A., Royden, L. H., Whipple, K. X., Burchfiel, B. C., Zhang, X., and Tang, W., 2005, Late Cenozoic uplift of southeastern Tibet: Geology, v. 33, n. 6, p. 525–528, https://doi.org/10.1130/G21265.1

Clark, M. K., Farley, K. A., Zheng, D., Wang, Z., and Duvall, A. R., 2010, Early Cenozoic faulting of the northern Tibetan Plateau margin from apatite (U-Th)/He ages: Earth and Planetary Science Letters, v. 296, n. 1–2, p. 78–88, https://doi.org/10.1016/j.epsl.2010.04.051

Clementz, M., Bajpai, S., Ravikant, V., Thewissen, J. G. M., Saravanan, N., Singh, I. B., and Prasad, V., 2011, Early Eocene warming events and the timing of terrestrial faunal exchange between India and Asia: Geology, v. 39, n. 1, p. 15–18, https://doi.org/10.1130/G31585.1

Clift, P. D., and Webb, A. A. G., 2018, A history of the Asian monsoon and its interactions with solid Earth tectonics in Cenozoic South Asia, *in* Treloar, P. J., and Searle, M. P., editors, Himalayan Tectonics: A Modern Synthesis: Geological Society, London, Special Publications, v. 483, https://doi.org/10.1144/SP483.1

Cloos, M., Sapiie, B., van Ufford, A. Q., Weiland, R. J., Warren, P. Q., and McMahon, T. P., 2005, Collisional Delamination in New Guinea: The Geotectonics of Subducting Slab Breakoff: Geological Society of America Special Papers, v. 400, 51 p., https://doi.org/10.1130/2005.2400

Clyde, W. C., Khan, I. H., and Gingerich, P. D., 2003, Stratigraphic response and mammalian dispersal during initial India-Asia collision: Evidence from the Ghazij Formation, Balochistan, Pakistan: Geology, v. 31, n. 12, p. 1097–1100, https://doi.org/10.1130/G19956.1

Cogan, M. J., Nelson, K. D., Kidd, W. S. F., Wu, C., and Project INDEPTH Team, 1998, Shallow structure of the Yadong-Gulu rift, southern Tibet, from refraction analysis of Project INDEPTH common midpoint data: Tectonics, v. 17, n. 1, p. 46–61, https://doi.org/10.1029/97TC03025

Colchen, M., 1999, The Thakkhola-Mustang graben in Nepal and the late Cenozoic extension in the Higher Himalayas: Journal of Asian Earth Sciences, v. 17, n. 5–6, p. 683–702, https://doi.org/10.1016/S1367-9120(99)00037-1

Cooper, F. J., Hodges, K. V., Parrish, R. R., Roberts, N. M. W., and Horstwood, M. S. A., 2015, Synchronous N-S and E-W extension at the Tibet-to–Himalaya transition in NW Bhutan: Tectonics, v. 34, n. 7, p. 1375–1395, https://doi.org/10.1002/2014TC003712

Cooper, K. M., Reid, M. R., Dunbar, N. W., and McIntosh, W. C., 2002, Origin of mafic magmas beneath northwestern Tibet: Constraints from ^{230}Th-^{238}U disequilibria: Geochemistry, Geophysics, Geosystems, v. 3, n. 11, 1065, https://doi.org/10.1029/2002GC000332

Copeland, P., Harrison, T. M., Kidd, W. S. F., Xu, R., and Zhang, Y., 1987, Rapid early Miocene acceleration of uplift in the Gangdese Belt, Xizang (southern Tibet), and its bearing on accommodation mechanisms of the India-Asia collision: Earth and Planetary Science Letters, v. 86, n. 24, p. 240–252, https://doi.org/10.1016/0012-821X(87)90224-X

Copeland, P., Harrison, T. M., Pan, Y., Kidd, W. S. F., Roden, M., and Zhang, Y., 1995, Thermal evolution of the Gangdese batholith, southern Tibet: A history of episodic unroofing: Tectonics, v. 14, n. 2, p. 223–226, https://doi.org/10.1029/94TC01676

Copley, A., Avouac, J.-P., and Royer, J.-Y., 2010, India-Asia collision and the Cenozoic slowdown of the Indian plate: Implications for the forces driving plate motions: Journal of Geophysical Research-Solid Earth, v. 115, n. B3, B03410, https://doi.org/10.1029/2009JB006634

Copley, A., Avouac, J.-P., and Wernicke, B. P., 2011, Evidence for mechanical coupling and strong Indian lower crust beneath southern Tibet: Nature, v. 472, p. 79–81, https://doi.org/10.1038/nature09926

Corfield, R. I., and Searle, M. P., 2000, Crustal shortening estimates across the north Indian continental margin, Ladakh, NW India, *in* Khan, M. A., Treloar, P. J., Searle, M. P., and Jan, M. Q., editors, Tectonics of the Nanga Parbat Syntaxis and the Western Himalaya: Geological Society, London, Special Publications, v. 170, p. 395–410, https://doi.org/10.1144/GSL.SP.2000.170.01.21

Corfield, R. I., Searle, M. P., and Pedersen, R. B., 2001, Tectonic setting, origin, and obduction history of the Spontang ophiolite, Ladakh Himalaya, NW India: The Journal of Geology, v. 109, n. 6, p. 715–736, https://doi.org/10.1086/323191

Corrie, S. L., and Kohn, M. J., 2011, Metamorphic history of the central Himalaya, Annapurna region, Nepal, and implications for tectonic models: Geological Society of America Bulletin, v. 123, n. 9–10, p. 1863–1879, https://doi.org/10.1130/B30376.1

Corrie, S. L., Kohn, M. J., and Vervoort, J. D., 2010, Young eclogite from the Greater Himalayan Sequence, Arun Valley, eastern Nepal: *P-T-t* path and tectonic implications: Earth and Planetary Science Letters, v. 289, n. 3–4, p. 406–416, https://doi.org/10.1016/j.epsl.2009.11.029

Cottle, J. M., Searle, M. P., Horstwood, M. S. A., and Waters, D. J., 2009, Timing of midcrustal metamorphism, melting, and deformation in the Mount Everest Region of southern Tibet revealed by U(-Th)-Pb geochronology: The Journal of Geology, v. 117, n. 6, p. 643–664, https://doi.org/10.1086/605994

Cottle, J. M., Waters, D. J., Riley, D., Beyssac, O., and Jessup, M. J., 2011, Metamorphic history of the South Tibetan Detachment System, Mt. Everest region, revealed by RSCM thermometry and phase equilibria modelling: Journal of Metamorphic Geology, v. 29, n. 5, p. 561–582, https://doi.org/10.1111/j.1525-1314.2011.00930.x

Coulon, C., Maluski, H., Bollinger, C., and Wang, S., 1986, Mesozoic and Cenozoic volcanic rocks from central and southern Tibet: ^{39}Ar-^{40}Ar dating, petrological characteristics and geodynamical significance: Earth and Planetary Science Letters, v. 79, n. 1–4, p. 281–302, https://doi.org/10.1016/0012-821X(86)90186-X

Coward, M. P., Kidd, W. S. F., Pan, Y., Shackleton, R. M., and Zhang, H., 1988, The structure of the 1985 Tibet Geotraverse, Lhasa to Golmud: Philosophical Transactions of the Royal Society of London, Series A, v. 327, p. 307–336, https://doi.org/10.1098/rsta.1988.0131

Cowgill, E., Yin, A., Harrison, T. M., and Wang, X.-F., 2003, Reconstruction of the Altyn Tagh fault based on U-Pb geochronology: Role of back thrusts, mantle sutures, and heterogeneous crustal strength in forming the Tibetan Plateau: Journal of Geophysical Research-Solid Earth, v. 108, n. B7, 2346, https://doi.org/10.1029/2002JB002080

Craddock, W. H., Kirby, E., Harkins, N. W., Zhang, H., Shi, X., and Liu, J., 2010, Rapid fluvial incision along the Yellow River during headward basin integration: Nature Geoscience, v. 3, p. 209–213, https://doi.org/10.1038/NGEO777

Currie, B. S., Rowley, D. B., and Tabor, N. J., 2005, Middle Miocene paleoaltimetry of southern Tibet: Implications for the role of mantle thickening and delamination in the Himalayan orogen: Geology, v. 33, p. 181–184, https://doi.org/10.1130/G21170.1

Currie, B. S., Polissar, P. J., Rowley, D. B., Ingalls, M., Li, S., Olack, G., and Freeman, K. H., 2016, Multiproxy paleoaltimetry of the Late Oligocene-Pliocene Oiyug Basin, southern Tibet: American Journal of Science, v. 316, n. 5, p. 401–436, https://doi.org/10.2475/05.2016.01

Dai, J., Wang, C., and Li, Y., 2012, Relicts of the Early Cretaceous seamounts in the central-western Yarlung Zangbo Suture Zone, southern Tibet: Journal of Asian Earth Sciences, v. 53, p. 25–37, https://doi.org/10.1016/j.jseaes.2011.12.024

Dai, J., Zhao, X., Wang, C., Zhu, L., Li, Y., and Finn, D., 2012, The vast proto-Tibetan Plateau: New constraints from Paleogene Hoh Xil Basin: Gondwana Research, v. 22, n. 2, p. 434–446, https://doi.org/10.1016/j.gr.2011.08.019

Dai, J., Wang, C., Hourigan, J. K., Li, Z., and Zhuang, G., 2013a, Exhumation history of the Gangdese Batholith, southern Tibetan Plateau: Evidence from apatite and zircon (U-Th)/He thermochronology: The Journal of Geology, v. 121, n. 2, p. 155–172, https://doi.org/10.1086/669250

Dai, J., Wang, C., Polat, A., Santosh, M., Li, Y., and Ge, Y., 2013b, Rapid forearc spreading between 130 and 120 Ma: Evidence from geochronology and geochemistry of the Xigaze ophiolite, southern Tibet: Lithos, v. 172–173, p. 1–16, https://doi.org/10.1016/j.lithos.2013.03.011

Daniel, C. G., Hollister, L. S., Parrish, R. R., and Grujic, D., 2003, Exhumation of the Main Central Thrust from lower crustal depths, eastern Bhutan Himalaya: Journal of Metamorphic Geology, v. 21, n. 4, p. 317–334, https://doi.org/10.1046/j.1525-1314.2003.00445.x

de Sigoyer, J., Chavagnac, V., Blichert-Toft, J., Villa, I. M., Luais, B., Guillot, S., Cosca, M., and Mascle, G., 2000, Dating the Indian continental subduction and collisional thickening in the northwest Himalaya:

Multichronology of the Tso Morari eclogites: Geology, v. 28, n. 6, p. 487–490, https://doi.org/10.1130/0091-7613(2000)28<487:DTICSA>2.0.CO;2

de Sigoyer, J., Vanderhaeghe, O., Duchêne, S., and Billerot, A., 2014, Generation and emplacement of Triassic granitoids within the Songpan Ganze accretionary-orogenic wedge in a context of slab retreat accommodated by tear faulting, Eastern Tibetan plateau, China: Journal of Asian Earth Sciences, v. 88, p. 192–216, https://doi.org/10.1016/j.jseaes.2014.01.010

Debon, F., Le Fort, P., Sheppard, S. M., and Sonet, J., 1986, The four plutonic belts of the Transhimalaya-Himalaya: A chemical, mineralogical, isotopic, and chronological synthesis along a Tibet-Nepal section: Journal of Petrology, v. 27, n. 1, p. 219–250, https://doi.org/10.1093/petrology/27.1.219

DeCelles, P. G., and Mitra, G., 1995, History of the Sevier orogenic wedge in terms of critical taper models, northeast Utah and southwest Wyoming: Geological Society of America Bulletin, v. 107, n. 4, p. 454–462, https://doi.org/10.1130/0016-7606(1995)107<0454:HOTSOW>2.3.CO;2

DeCelles, P. G., Gehrels, G. E., Quade, J., and Ojha, T. P., 1998, Eocene-early Miocene foreland basin development and the history of Himalayan thrusting, western and central Nepal: Tectonics, v. 17, n. 5, p. 741–765, https://doi.org/10.1029/98TC02598

DeCelles, P. G., Gehrels, G. E., Quade, J., LaReau, B., and Spurlin, M., 2000, Tectonic implications of U-Pb zircon ages of the Himalayan orogenic belt in Nepal: Science, v. 288, n. 5465, p. 497–499, https://doi.org/10.1126/science.288.5465.497

DeCelles, P. G., Robinson, D. M., Quade, J., Ojha, T. P., Garzione, C. N., Copeland, P., and Upreti, B. N., 2001, Stratigraphy, structure, and tectonic evolution of the Himalayan fold-thrust belt in western Nepal: Tectonics, v. 20, n. 4, p. 487–509, https://doi.org/10.1029/2000TC001226

DeCelles, P. G., Robinson, D. M., and Zandt, G., 2002, Implications of shortening in the Himalayan fold-thrust belt for uplift of the Tibetan Plateau: Tectonics, v. 21, n. 6, 1062, https://doi.org/10.1029/2001TC001322

DeCelles, P. G., Gehrels, G. E., Najman, Y., Martin, A. J., Carter, A., and Garzanti, E., 2004, Detrital geochronology and geochemistry of Cretaceous-Early Miocene strata of Nepal: implications for timing and diachroneity of initial Himalayan orogenesis: Earth and Planetary Science Letters, v. 227, n. 3–4, p. 313–330, https://doi.org/10.1016/j.epsl.2004.08.019

DeCelles, P. G., Kapp, P., Ding, L., and Gehrels, G. E., 2007a, Late Cretaceous to middle Tertiary basin evolution in the central Tibetan plateau: Changing environments in response to tectonic partitioning, aridification, and regional elevation gain: Geological Society of America Bulletin, v. 119, n. 5–6, p. 654–680, https://doi.org/10.1130/B26074.1

DeCelles, P. G., Quade, J., Kapp, P., Fan, M., Dettman, D. L., and Ding, L., 2007b, High and dry in central Tibet during the Late Oligocene: Earth and Planetary Science Letters, v. 253, n. 3–4, p. 389–401, https://doi.org/10.1016/j.epsl.2006.11.001

DeCelles, P. G., Ducea, M., Kapp, P., and Zandt, G., 2009, Cyclicity in Cordilleran Orogenic Systems: Nature Geoscience, v. 2, p. 251–257, https://doi.org/10.1038/NGEO469

DeCelles, P. G., Kapp, P., Quade, J., and Gehrels, G. E., 2011, Oligocene-Miocene Kailas Basin, southwestern Tibet: Record of postcollisional upper-plate extension in the Indus-Yarlung suture zone: Geological Society of America Bulletin, v. 123, n. 7–8, p. 1337–1362, https://doi.org/10.1130/B30258.1

DeCelles, P. G., Kapp, P., Gehrels, G. E., and Ding, L., 2014, Paleocene-Eocene foreland basin evolution in the Himalaya of southern Tibet and Nepal: Implications for the age of initial India-Asia collision: Tectonics, v. 33, n. 5, p. 824–849, https://doi.org/10.1002/2014TC003522

DeCelles, P. G., Carrapa, B., Horton, B. K., McNabb, J., Gehrels, G. E., and Boyd, J., 2015, The Miocene Arizaro Basin, central Andean hinterland: Response to partial lithosphere removal?, *in* DeCelles, P. G., Ducea, M. N., Carrapa, B., and Kapp, P. A., editors, Geodynamics of a Cordilleran Orogenic System: The Central Andes of Argentina and Northern Chile: Geological Society of America Memoir 212, https://doi.org/10.1130/2015.1212(18)

DeCelles, P. G., Carrapa, B., Gehrels, G. E., Chakraborty, T., and Ghosh, P., 2016a, Along-strike continuity of structure, stratigraphy, and kinematic history in the Himalayan thrust belt: The view from Northeastern India: Tectonics, v. 35, n. 12, https://doi.org/10.1002/2016TC004298

DeCelles, P. G., Castañeda, I. S., Carrapa, B., Liu, J., Quade, J., Leary, R., and Zhang, L., 2016b, Oligocene-Miocene Great Lakes in the India-Asia Collision Zone: Basin Research, v. 30, n. S1, p. 1–20, https://doi.org/10.1111/bre.12217

DeCelles, P. G., Leary, R. J., and Kapp, P., 2018, Cenozoic basin evolution in the Indus-Yarlung suture zone and High Himalaya, *in* Ingersoll, R. V., Lawton, T. F., and Graham, S. A., editors, Tectonics, Sedimentary Basins, and Provenance: A Celebration of William R. Dickinson's Career: Geological Society of America Special Papers, v. 540, p. 1–33, https://doi.org/10.1130/2018.2540(30)

Deng, W., 1991, Cenozoic volcanism and intraplate subduction at the northern margin of the Tibetan Plateau: Chinese Journal of Geochemistry, v. 10, n. 2, p. 140–152, https://doi.org/10.1007/BF02837714

Dewey, J. F., 1977, Suture zone complexities: A review: Tectonophysics, v. 40, n. 1–2, p. 53–67, https://doi.org/10.1016/0040-1951(77)90029-4

—— 1988, Extensional collapse of orogens: Tectonics, v. 7, n. 6, p. 1123–1139, https://doi.org/10.1029/TC007i006p01123

Dewey, J. F., Shackleton, R. M., Chang, C., and Yiyin, S., 1988, The tectonic evolution of the Tibetan Plateau: Philosophical Transactions of the Royal Society of London, Series A, v. 327, p. 379–413, https://doi.org/10.1098/rsta.1988.0135

Dewey, J. F., Cande, S., and Pitman III, W. C., 1989, Tectonic evolution of the India/Eurasia collision zone: Eclogae geologicae Helvetiae, v. 82, n. 3, p. 717–734.

Di Giuseppe, E., van Hunen, J., Funiciello, F., Faccenna, C., and Giardini, D., 2008, Slab stiffness control of trench motion: Insights from numerical models: Geochemistry, Geophysics, Geosystems, v. 9, n. 2, Q02014, https://doi.org/10.1029/2007GC001776

Dilek, Y., Imamverdiyev, N., and Altunkaynak, S., 2010, Geochemistry and tectonics of Cenozoic volcanism in the Lesser Caucasus (Azerbaijan) and the peri-Arabian region: Collision-induced mantle dynamics and its magmatic fingerprint: International Geology Review, v. 52, n. 4–6, p. 536–578, https://doi.org/10.1080/00206810903360422

Ding, H., Zhang, Z., Dong, X., Tian, Z., Xiang, H., Mu, H., Gou, Z., Shui, X., Li, W., and Mao, L., 2016a, Early Eocene (*c.* 50 Ma) collision of the Indian and Asian continents: Constraints from the North Himalayan metamorphic rocks, southeastern Tibet: Earth and Planetary Science Letters, v. 435, p. 64–73, https://doi.org/10.1016/j.epsl.2015.12.006

Ding, L., and Lai, Q., 2003, New geological evidence of crustal thickening in the Gangdese block prior to the Indo-Asian collision: Chinese Science Bulletin, v. 48, n. 15, p. 1604–1610, https://doi.org/10.1007/BF03183969

Ding, L., Kapp, P., Zhong, D., and Deng, W., 2003, Cenozoic volcanism in Tibet: Evidence for a transition from oceanic to continental subduction: Journal of Petrology, v. 44, n. 10, p. 1833–1865, https://doi.org/10.1093/petrology/egg061

Ding, L., Kapp, P., and Wan, X., 2005, Paleocene - Eocene record of ophiolite obduction and initial India-Asia collision, south-central Tibet: Tectonics, v. 24, n. 3, TC3001, https://doi.org/10.1029/2004TC001729

Ding, L., Kapp, P., Yue, Y., and Lai, Q., 2007, Postcollisional calc-alkaline lavas and xenoliths from the southern Qiangtang terrane, central Tibet: Earth and Planetary Science Letters, v. 254, n. 1–2, p. 28–38, https://doi.org/10.1016/j.epsl.2006.11.019

Ding, L., Yang, D., Cai, F. L., Pullen, A., Kapp, P., Gehrels, G. E., Zhang, L. Y., Zhang, Q. H., Lai, Q. Z., Yue, Y. H., and Shi, R. D., 2013, Provenance analysis of the Mesozoic Hoh-Xil-Songpan-Ganzi turbidites in northern Tibet: Implications for the tectonic evolution of the eastern Paleo-Tethys Ocean: Tectonics, v. 32, n. 1, p. 1–15, https://doi.org/10.1002/tect.20013

Ding, L., Xu, Q., Yue, Y., Wang, H., Cai, F., and Li, S., 2014, The Andean-type Gangdese Mountains: Paleoelevation record from the Paleocene-Eocene Linzhou Basin: Earth and Planetary Science Letters, v. 392, p. 250–264, https://doi.org/10.1016/j.epsl.2014.01.045

Ding, L., Qasim, M., Jadoon, I. A. K., Khan, M. A., Xu, Q., Cai, F., Wang, H., Baral, U., and Yue, Y., 2016b, The India-Asia collision in north Pakistan: Insight from the U-Pb detrital zircon provenance of Cenozoic foreland basin: Earth and Planetary Science Letters, v. 455, p. 49-61, https://doi.org/10.1016/j.epsl.2016.09.003

Ding, L., Maksatbek, S., Cai, F. L., Wang, H. Q., Song, P. P., Ji, W. Q., Xu, Q., Zhang, L. Y., Muhammad, Q., and Upendra, B., 2017a, Processes of initial collision and suturing between India and Asia: Science China Earth Sciences, v. 60, n. 4, p. 635–651, https://doi.org/10.1007/s11430-016-5244-x

Ding, L., Spicer, R. A., Yang, J., Xu, Q., Cai, F. L., Li, S., Lai, Q. Z., Wang, H., Spicer, T. E. V., Yue, Y., Shukla, A., Srivastava, G., Ali Khan, M., Bera, S., and Mehrotra, R., 2017b, Quantifying the rise of the Himalaya orogen and implications for the South Asian monsoon: Geology, v. 45, n. 3, p. 215–218, https://doi.org/10.1130/G38583.1

Donaldson, D. G., Webb, A. A. G., Menold, C. A., Kylander-Clark, A. R. C., and Hacker, B. R., 2013, Petrochronology of Himalayan ultrahigh-pressure eclogite: Geology, v. 41, n. 8, p. 835–838, https://doi.org/10.1130/G33699.1

Dong, X., Zhang, Z. H., and Santosh, M., 2010, Zircon U-Pb chronology of the Nyingtri Group, southern Lhasa terrane, Tibetan Plateau: Implications for Grenvillian and Pan-African provenance and Mesozoic-Cenozoic metamorphism: The Journal of Geology, v. 118, n. 6, p. 677–690, https://doi.org/10.1086/656355

Dong, X., Zhang, Z., Liu, F., Wang, W., Yu, F., and Shen, K., 2011a, Zircon U-Pb geochronology of the Nyainqentanglha Group from the Lhasa terrane: New constraints on the Triassic orogeny of the south Tibet: Journal of Asian Earth Sciences, v. 42, n. 4, p. 732–739, https://doi.org/10.1016/j.jseaes.2011.01.014

Dong, X., Zhang, Z., Santosh, M., Wang, W., Yu, F., and Liu, F., 2011b, Late Neoproterozoic thermal events in the northern Lhasa terrane, south Tibet: Zircon chronology and tectonic implications: Journal of Geodynamics, v. 52, n. 5, p. 389–405, https://doi.org/10.1016/j.jog.2011.05.002

Dong, Y.-L., Wang, B.-D., Zhao, W.-X., Yang, T.-N., and Xu, J.-F., 2016, Discovery of eclogite in the Bangong Co-Nujiang ophiolitic melange, central Tibet, and tectonic implications: Gondwana Research, v. 35, p. 115–123, https://doi.org/10.1016/j.gr.2016.03.010

Ducea, M., 2001, The California Arc: Thick granitic batholiths, eclogitic residues, lithospheric-scale thrusting, and magmatic flare-ups: GSA Today, v. 11, p. 4–10, https://doi.org/10.1130/1052-5173(2001)011<0004:TCATGB>2.0.CO;2

Ducea, M. N., Paterson, S. R., and DeCelles, P. G., 2015, High-volume magmatic events in subduction systems: Elements, v. 11, n. 2, p. 99–104, https://doi.org/10.2113/gselements.11.2.99

Dunkl, I., Antolín, B., Wemmer, K., Rantitsch, G., Kienast, M., Montomoli, C., Ding, L., Carosi, R., Appel, E., El Bay, R., Xu, Q., and von Eynatten, H., 2011, Metamorphic evolution of the Tethyan Himalayan flysch in SE Tibet, *in* Gloaguen, R., and Ratschbacher, L., editors, Growth and Collapse of the Tibetan Plateau, Geological Society, London, Special Publications, v. 353, p. 45–69, https://doi.org/10.1144/SP353.4

Dupuis, C., Hébert, R., Cubois-Côté, V., Wang, C. S., Li, Y. L., and Li, Z. J., 2005, Petrology and geochemistry of mafic rocks from mélange and flysch units adjacent to the Yarlung Zangbo Suture Zone, southern Tibet: Chemical Geology, v. 214, n. 3–4, p. 287–308, https://doi.org/10.1016/j.chemgeo.2004.10.005

Duputel, Z., Vergne, J., Rivera, L., Wittlinger, G., Farra, V., and Hetényi, G., 2016, The 2015 Gorkha earthquake: A large event illuminating the Main Himalayan Thrust fault: Geophysical Research Letters, v. 43, n. 6, p. 2517–2525, https://doi.org/10.1002/2016GL068083

Dürr, S. B., 1996, Provenance of Xigaze fore-arc basin clastic rocks (Cretaceous, south Tibet): Geological Society of America Bulletin, v. 108, n. 6, p. 669–684, https://doi.org/10.1130/0016-7606(1996)108<0669:POXFAB>2.3.CO;2

Duvall, A. R., Clark, M. K., van der Pluijm, B. A., and Li, C., 2011, Direct dating of Eocene reverse faulting in northeastern Tibet using Ar-dating of fault clays and low-temperature thermochronometry: Earth and Planetary Science Letters, v. 304, n. 3–4, p. 520–526, https://doi.org/10.1016/j.epsl.2011.02.028

Edwards, M. A., and Harrison, T. M., 1997, When did the roof collapse? Late Miocene north-south extension in the high Himalaya revealed by Th-Pb monazite dating of the Khula Kangri granite: Geology, v. 25, n. 6, p. 543–546, https://doi.org/10.1130/0091-7613(1997)025<0543:WDTRCL>2.3.CO;2

Einsele, G., Liu, B., Dürr, S., Frisch, W., Liu, G., Luterbacher, H. P., Ratschbacher, L., Ricken, W., Wendt, J., Wetzel, A., Yu, G., and Zheng, H., 1994, The Xigaze forearc basin: Evolution and facies architecture (Cretaceous, Tibet): Sedimentary Geology, v. 90, n. 1–2, p. 1–32, https://doi.org/10.1016/0037-0738(94)90014-0

Elliott, J. R., Jolivet, R., González, P. J., Avouac, J.-P., Hollingsworth, J., Searle, M. P., and Stevens, v. L., 2016, Himalayan megathrust geometry and relation to topography revealed by the Gorkha earthquake: Nature Geoscience, v. 9, p. 174–180, https://doi.org/10.1038/ngeo2623

England, P., and Houseman, G., 1989, Extension during continental convergence, with application to the Tibetan plateau: Journal of Geophysical Research-Solid Earth, v. 94, n. B12, p. 17561–17579, https://doi.org/10.1029/JB094iB12p17561

England, P., and Searle, M., 1986, The Cretaceous-Tertiary deformation of the Lhasa block and its implications for crustal thickening in Tibet: Tectonics, v. 5, n.1, p. 1–14, https://doi.org/10.1029/TC005i001p00001

Enkelmann, E., Weislogel, A., Ratschbacher, L., Eide, E., Renno, A., and Wooden, J., 2007, How was the Triassic Songpan-Ganzi basin filled? A provenance study: Tectonics, v. 26, n. 4, TC4007, https://doi.org/10.1029/2006TC002078

Faccenna, C., Becker, T. W., Conrad, C. P., and Husson, L., 2013, Mountain building and mantle dynamics: Tectonics, v. 32, n. 1, p. 80–93, https://doi.org/10.1029/2012TC003176

Fan, J.-J., Li, C., Xie, C.-M., Wang, M., and Chen, J.-W., 2015, The evolution of the Bangong-Nujiang Neo-Tethys ocean: Evidence from zircon U-Pb and Lu-Hf isotopic analyses of Early Cretaceous oceanic islands and ophiolites: Tectonophysics, v. 655, p. 27–40, https://doi.org/10.1016/j.tecto.2015.04.019

Fan, J.-J., Li, C., Wu, H., Zhang, Y.-Y., Wang, M., Chen, J.-W., and Xu, J.-X., 2016, Late Jurassic adakitic granodiorite in the Dong Co area, northern Tibet: Implications for subduction of the Bangong-Nujiang oceanic lithosphere and related accretion of the southern Qiangtang terrane: Tectonophysics, v. 691, Part B, p. 345–361, https://doi.org/10.1016/j.tecto.2016.10.026

Feng, M., Kumar, P., Mechie, J., Zhao, W., Kind, R., Su, H., Xue, G., Shi, D., and Qian, H., 2014, Structure of the crust and mantle down to 700 km depth beneath the East Qaidam basin and Qilian Shan from P and S receiver functions: Geophysical Journal International, v. 199, n. 3, p. 1416–1429, https://doi.org/10.1093/gji/ggu335

Fielding, E., Isacks, B., Barazangi, M., and Duncan, C., 1994, How flat is Tibet?: Geology, v. 22, n. 2, p. 163–167, https://doi.org/10.1130/0091-7613(1994)022<0163:HFIT>2.3.CO;2

Fu, B., and Awata, Y., 2007, Displacement and timing of left-lateral faulting in the Kunlun Fault Zone, northern Tibet, inferred from geologic and geomorphic features: Journal of Asian Earth Sciences, v. 29, n. 2–3, p. 253–265, https://doi.org/10.1016/j.jseaes.2006.03.004

Fuchs, G., 1975, Contributions to the geology of the north-western Himalayas: Abhandlungen der Geologischen Bundesanstalt, v. 32, p. 1–59.

——— 1987, The geology of southern Zanskar (Ladakh) - Evidence for the autochthony of the Tethys zone of the Himalaya: Abhandlungen der Geologischen Bundesanstalt, v. 130, p. 465–491.

Gansser, A., 1964, Geology of the Himalayas: London, Interscience, 289 p.

Gao, R., Lu, Z., Klemperer, S. L., Wang, H., Dong, S., Li, W., and Li, H., 2016, Crustal-scale duplexing beneath the Yarlung Zangbo suture in the western Himalaya: Nature Geoscience, v. 9, https://doi.org/10.1038/NGEO2730

Garzanti, E., and Hu, X., 2015, Latest Cretaceous Himalayan tectonics: Obduction, collision or Deccan-related uplift?: Gondwana Research, v. 28, n. 1, p. 165–178, https://doi.org/10.1016/j.gr.2014.03.010

Garzanti, E., Baud, A., and Mascle, G., 1987, Sedimentary record of the northward flight of India and its collision with Eurasia (Ladakh Himalaya, India): Geodinamica Acta, v. 1, n. 4–5, p. 297–312, https://doi.org/10.1080/09853111.1987.11105147

Garzanti, E., Radeff, G., and Malusà, M. G., 2018, Slab breakoff: A critical appraisal of a geological theory as applied in space and time: Earth-Science Reviews, v. 177, p. 303–319, https://doi.org/10.1016/j.earscirev.2017.11.012

Garzione, C. N., Dettman, D. L., Quade, J., DeCelles, P. G., and Butler, R. F., 2000, High times on the Tibetan plateau: Paleoelevation of the Thakkhola graben, Nepal: Geology, v. 28, n. 4, p. 339–342, https://doi.org/10.1130/0091-7613(2000)28<339:HTOTTP>2.0.CO;2

Garzione, C. N., DeCelles, P. G., Hodkinson, D. G., Ojha, T. P., and Upreti, B. N., 2003, East-west extension and Miocene environmental change in the southern Tibetan plateau: Thakkhola graben, central Nepal: Geological Society of America Bulletin, v. 115, n. 1, p. 3–20, https://doi.org/10.1130/0016-7606(2003)115<0003:EWEAME>2.0.CO;2

Ge, W.-P., Molnar, P., Shen, Z.-K., and Li, Q., 2015, Present-day crustal thinning in the southern and northern Tibetan Plateau revealed by GPS measurements: Geophysical Research Letters, v. 42, n. 13, p. 5227–5235, https://doi.org/10.1002/2015GL064347

Gébelin, A., Mulch, A., Teyssier, C., Jessup, M. J., Law, R. D., and Brunel, M., 2013, The Miocene elevation of Mount Everest: Geology, v. 41, n. 7, p. 799–802, https://doi.org/10.1130/G34331.1

Gébelin, A., Jessup, M. J., Teyssier, C., Cosca, M. A., Law, R. D., Brunel, M., and Mulch, A., 2017, Infiltration of meteoric water in the South Tibetan Detachment (Mount Everest, Himalaya): When and why?: Tectonics, v. 36, n. 4, p. 690–713, https://doi.org/10.1002/2016TC004399

Gehrels, G. E., DeCelles, P. G., Martin, A., Ojha, T. P., and Pinhassi, G., 2003, Initiation of the Himalayan Orogen as an Early Paleozoic thin-skinned thrust belt: GSA Today, v. 13, p. 4–9, https://doi.org/10.1130/1052-5173(2003)13<4:IOTHOA>2.0.CO;2

Gehrels, G. E., DeCelles, P. G., Ojha, T. P., and Upreti, B. N., 2006a, Geologic and U-Th-Pb geochronologic evidence for early Paleozoic tectonism in the Kathmandu thrust sheet, central Nepal Himalaya: Geological Society of America Bulletin, v. 118, n. 1–2, p. 185–198, https://doi.org/10.1130/B25753.1

Gehrels, G. E., DeCelles, P. G., Ojha, T. P., and Upreti, B. N., 2006b, Geologic and U-Pb geochronologic evidence for early Paleozoic tectonism in the Dadeldhura thrust sheet, far-west Nepal Himalaya: Journal of Asian Earth Sciences, v. 28, n. 4–6, p. 385–408, https://doi.org/10.1016/j.jseaes.2005.09.012

Gehrels, G., Kapp, P., DeCelles, P., Pullen, A., Blakey, R., Weislogel, A., Ding, L., Guynn, J., Martin, A., McQuarrie, N., and Yin, A., 2011, Detrital zircon geochronology of pre-Tertiary strata in the Tibetan-Himalayan orogen: Tectonics, v. 30, n. 5, TC5016, https://doi.org/10.1029/2011TC002868

Gibbons, A. D., Zahirovic, S., Müller, R. D., Whittaker, J. M., and Yatheesh, V., 2015, A tectonic model reconciling evidence for the collisions between India, Eurasia and intra-oceanic arcs of the central-eastern Tethys: Gondwana Research, v. 28, n. 2, p. 451–492, https://doi.org/10.1016/j.gr.2015.01.001

Gibson, R., Godin, L., Kellett, D. A., Cottle, J. M., and Archibald, D., 2016, Diachronous deformation along the base of the Himalayan metamorphic core, west-central Nepal: Geological Society of America Bulletin, v. 128, n. 5–6, p. 860–878, https://doi.org/10.1130/B31328.1

Gingerich, P. D., Abbas, S. G., and Arif, M., 1997, Early Eocene *Quettacyon parachai* (Condylarthra) from the Ghazij Formation of Baluchistan (Pakistan): Oldest Cenozoic land mammal from south Asia: Journal of Vertebrate Paleontology, v. 17, n. 4, p. 629–637, https://doi.org/10.1080/02724634.1997.10011012

Girardeau, J., Marcoux, J., Allègre, C. J., Bassoullet, J. P., Tang, Y., Xiao, X., Zao, Y., and Wang, X., 1984a, Tectonic environment and geodynamic significance of the Neo-Cimmerian Donqiao ophiolite, Bangong-Nujiang suture zone, Tibet: Nature, v. 307, p. 27–31, https://doi.org/10.1038/307027a0

Girardeau, J., Marcoux, J., and Zao, Y., 1984b, Lithologic and tectonic environment of the Xigaze ophiolite (Yarlung Zangbo suture zone, Southern Tibet, China), and kinematics of its emplacement: Eclogae geologicae Helvetiae, v. 77, p. 153–170.

Girardeau, J., Marcoux, J., Fourcade, E., Bassoullet, J. P., and Youking, T., 1985a, Xainxa ultramafic rocks, central Tibet, China: Tectonic environment and geodynamic significance: Geology, v. 13, n. 5, p. 330–333, https://doi.org/10.1130/0091-7613(1985)13<330:XURCTC>2.0.CO;2

Girardeau, J., Mercier, J.-C. C., and Yougong, Z., 1985b, Origin of the Xigaze ophiolite, Yarlung Zangbo suture zone, southern Tibet: Tectonophysics, v. 119, n. 1–4, p. 407–433, https://doi.org/10.1016/0040-1951(85)90048-4

Girardeau, J., Mercier, J. C. C., and Zao, Y., 1985c, Structure of the Xigaze ophiolite, Yarlung Zangbo suture zone, southern Tibet, China: Genetic implications: Tectonics, v. 4, n. 3, p. 267–288, https://doi.org/10.1029/TC004i003p00267

Gnos, E., Immenhauser, A., and Peters, T., 1997, Late Cretaceous/early Tertiary convergence between the Indian and Arabian plates recorded in ophiolites and related sediments: Tectonophysics, v. 271, n. 1–2, p. 1–19, https://doi.org/10.1016/S0040-1951(96)00249-1

Godin, L., 2003, Structural evolution of the Tethyan sedimentary sequence in the Annapurna area, central Nepal Himalaya: Journal of Asian Earth Sciences, v. 22, n. 4, p. 307–328, https://doi.org/10.1016/S1367-9120(03)00066-X

Godin, L., Parrish, R. R., Brown, R. L., and Hodges, K. V., 2001, Crustal thickening leading to exhumation of the Himalayan Metamorphic core of central Nepal: Insight from U-Pb geochronology and ^{40}Ar/^{39}Ar thermochronology: Tectonics, v. 20, n. 5, p. 729–747, https://doi.org/10.1029/2000TC001204

Godin, L., Grujic, D., Law, R. D., and Searle, M. P., 2006, Channel flow, ductile extrusion and exhumation in continental collision zones: An introduction, *in* Law, R. D., Searle, M. P., and Godin, L., editors, Channel Flow, Ductile Extrusion and Exhumation in Continental Collision Zones: Geological Society, London, Special Publicatios, v. 268, p. 1–23, https://doi.org/10.1144/GSL.SP.2006.268.01.01

Göğüş, O. H., and Pysklywec, R. N., 2008, Near-surface diagnostics of dripping or delaminating lithosphere: Journal of Geophysical Research-Solid Earth, v. 113, B11404, https://doi.org/10.1029/2007JB005123

Goscombe, B., Gray, D., and Hand, M., 2006, Crustal architecture of the Himalayan metamorphic front in eastern Nepal: Gondwana Research, v. 10, n. 3–4, p. 232–255, https://doi.org/10.1016/j.gr.2006.05.003

Goscombe, B., Gray, D., and Foster, D. A., 2018, Metamorphic response to collision in the Central Himalayan Orogen: Gondwana Research, v. 57, p. 191–265, https://doi.org/10.1016/j.gr.2018.02.002

Gourbet, L., Mahéo, G., Leloup, P. H., Paquette, J.-L., Sorrel, P., Henriquet, M., Liu, X., and Liu, X., 2017, Western Tibet relief evolution since the Oligo-Miocene: Gondwana Research, v. 41, p. 425–437, https://doi.org/10.1016/j.gr.2014.12.003

Griffin, W. L., Afonso, J. C., Belousova, E. A., Gain, S. E., Gong, X.-H., González-Jiménez, J. M., Howell, D., Huang, J.-X., McGowan, N., Pearson, N. J., Satsukawa, T., Shi, R., Williams, P., Xiong, Q., Yang, J.-S., Zhang, M., and O'Reilly, Y., 2016, Mantle recycling: Transition zone metamorphism of Tibetan ophiolitic peridotites and its tectonic implications: Journal of Petrology, v. 57, n. 4, p. 655–684, https://doi.org/10.1093/petrology/egw011

Grujic, D., Hollister, L. S., and Parrish, R. R., 2002, Himalayan metamorphic sequence as an orogenic channel: Insight from Bhutan: Earth and Planetary Science Letters, v. 198, n. 1–2, p. 177–191, https://doi.org/10.1016/S0012-821X(02)00482-X

Grujic, D., Warren, C. J., and Wooden, J. L., 2011, Rapid synconvergent exhumation of Miocene-aged lower orogenic crust in the eastern Himalaya: Lithosphere, v. 3, n. 5, p. 346–366, https://doi.org/10.1130/L154.1

Guillot, S., 1999, An overview of the metamorphic evolution in Central Nepal: Journal of Asian Earth Sciences, v. 17, n. 5–6, p. 713–725, https://doi.org/10.1016/S1367-9120(99)00045-0

Guillot, S., de Sigoyer, J., Lardeaux, J. M., and Mascle, G., 1997, Eclogitic metasediments from the Tso Morari area (Ladakh, Himalaya): Evidence for continental subduction during India-Asia convergence: Contributions to Mineralogy and Petrology, v. 128, n. 2–3, p. 197–212, https://doi.org/10.1007/s004100050303

Guillot, S., Cosca, M., Allemand, P., and Le Fort, P., 1999, Contrasting metamorphic and geochronologic evolution along the Himalayan belt, *in* Macfarlane, A., Sorkhabi, R. B., and Quade, J., editors, Himalaya and Tibet: Mountain Roots to Mountain Tops: Geological Society of America Special Papers, v. 328, p. 117–128, https://doi.org/10.1130/0-8137-2328-0.117

Guillot, S., Garzanti, E., Baratoux, D., Marquer, D., Mahéo, G., and de Sigoyer, J., 2003, Reconstructing the total shortening history of the NW Himalaya: Geochemistry, Geophysics, Geosystems, v. 4, n. 7, 1064, https://doi.org/10.1029/2002GC000484

Guillot, S., Mahéo, G., de Sigoyer, J., Hattori, K. H., and Pêcher, A., 2008, Tethyan and Indian subduction viewed from the Himalayan high- to ultrahigh-pressure metamorphic rocks: Tectonophysics, v. 451, n. 1–4, p. 225–241, https://doi.org/10.1016/j.tecto.2007.11.059

Guilmette, C., Hébert, R., Wang, C., and Villeneuve, M., 2009, Geochemistry and geochronology of the metamorphic sole underlying the Xigaze Ophiolite, Yarlung Zangbo Suture Zone, South Tibet: Lithos, v. 112, n. 1–2, p. 149–162, https://doi.org/10.1016/j.lithos.2009.05.027

Guilmette, C., Hébert, R., Dostal, J., Indares, A., Ullrich, T., Bédard, E., and Wang, C., 2012, Discovery of a dismembered metamorphic sole in the Saga ophiolitic melange, South Tibet: Assessing an Early Cretaceous disruption of the Neo-Tethyan supra-subduction zone and consequences on basin closing: Gondwana Research, v. 22, n. 2, p. 398–414, https://doi.org/10.1016/j.gr.2011.10.012

Guo, L., Zhang, H.-F., Harris, N., Parrish, R., Xu, W.-C., and Shi, Z.-L., 2012, Paleogene crustal anatexis and metamorphism in Lhasa terrane, eastern Himalayan syntaxis: Evidence from U-Pb zircon ages and Hf isotopic compositions of the Nyingchi Complex: Gondwana Research, v. 21, n. 1, p. 100–111, https://doi.org/10.1016/j.gr.2011.03.002

Guo, L., Zhang, H.-F., Harris, N., Pan, F.-B., and Xu, W.-C., 2013, Late Cretaceous (~81 Ma) high-temperature metamorphism in the southeastern Lhasa terrane: Implication for the Neo-Tethys ocean ridge subduction: Tectonophysics, v. 608, p. 112–126, https://doi.org/10.1016/j.tecto.2013.10.007

Gurnis, M., 1988, Large-scale mantle convection and the aggregation and dispersal of supercontinents: Nature, v. 332, p. 695–699, https://doi.org/10.1038/332695a0

Guynn, J. H., Kapp, P., Pullen, A., Heizler, M., Gehrels, G., and Ding, L., 2006, Tibetan basement rocks near Amdo reveal "missing" Mesozoic tectonism along the Bangong suture, central Tibet: Geology, v. 34, n. 6, p. 505–508, https://doi.org/10.1130/G22453.1

Guynn, J., Kapp, P., Gehrels, G. E., and Ding, L., 2012, U-Pb geochronology of basement rocks in central Tibet and paleogeographic implications: Journal of Asian Earth Sciences, v. 43, n. 1, p. 23–50, https://doi.org/10.1016/j.jseaes.2011.09.003

Hacker, B. R., and Gerya, T. V., 2013, Paradigms, new and old, for ultrahigh-pressure tectonism: Tectonophysics, v. 603, p. 79–88, https://doi.org/10.1016/j.tecto.2013.05.026

Hacker, B. R., Gnos, E., Ratschbacher, L., Grove, M., McWilliams, M., Sobolev, S. V., Wan, J., and Zhenhan, W., 2000, Hot and dry deep crustal xenoliths from Tibet: Science, v. 287, n. 5462, p. 2463–2466, https://doi.org/10.1126/science.287.5462.2463

Hafkenscheid, E., Wortle, M. J. R., and Spakman, W., 2006, Subduction history of the Tethyan region derived from seismic tomography and tectonic reconstructions: Journal of Geophysical Research-Solid Earth, v. 111, B08401, https://doi.org/10.1029/2005JB003791

Haider, v. L., Dunkl, I., von Eynatten, H., Ding, L., Frei, D., and Zhang, L., 2013, Cretaceous to Cenozoic evolution of the northern Lhasa Terrane and the Early Paleogene development of peneplains at Nam Co, Tibetan Plateau: Journal of Asian Earth Sciences, v. 70–71, p. 79–98, https://doi.org/10.1016/j.jseaes.2013.03.005

Hamilton, W. B., 1988, Plate tectonics and island arcs: Geological Society of America Bulletin, v. 100, n. 10, p. 1503–1527, https://doi.org/10.1130/0016-7606(1988)100<1503:PTAIA>2.3.CO;2

Harris, N. B. W., Xu, R., Lewis, C. L., Hawkesworth, C. J., and Zhang, Y., 1988, Isotope geochemistry of the 1985 Tibet Geotraverse, Lhasa to Golmud: Philosophical Transactions of the Royal Society of London, Series A, v. 327, n. 1594, p. 263–285, https://doi.org/10.1098/rsta.1988.0129

Harris, N. B. W., Caddick, M., Kosler, J., Goswami, S., Vance, D., and Tindle, A. G., 2004, The pressure-temperature-time path of migmatites from the Sikkim Himalaya: Journal of Metamorphic Geology, v. 22, n. 3, p. 249–264, https://doi.org 10.1111/j.1525-1314.2004.00511.x

Harrison, T. M., Copeland, P., Kidd, W. S. F., and Yin, A., 1992, Raising Tibet: Science, v. 255, n. 5052, p. 1663–1670, https://doi.org/10.1126/science.255.5052.1663

Harrison, T. M., Copeland, P., Hall, S. A., Quade, J., Burner, S., Ojha, T. P., and Kidd, W. S. F., 1993, Isotopic preservation of Himalayan/Tibetan uplift, denudation, and climatic histories of two molasse deposits: Journal of Geology, v. 101, n. 2, p. 157–175, https://doi.org/10.1086/648214

Haschke, M. R., Günther, A., Melnick, D., Echtler, H., Reutter, K.-J., Scheuber, E., and Oncken, O., 2006, Central and southern Andean tectonic evolution inferred from arc magmatism, *in* Oncken, O., Chong, G., Franz, G., Giese, P., Götze, H.-J., Ramos, v. A., Strecker, M. R., and Wigger, P., editors, The Andes - Active Subduction Orogeny: Berlin, Springer Verlag, p. 337–353, https://doi.org/10.1007/978-3-540-48684-8_16

Hauck, M. L., Nelson, K. D., Brown, L. D., Zhao, W., and Ross, A. R., 1998, Crustal structure of the Himalayan orogen at ~90° east longitude from Project INDEPTH deep reflection profiles: Tectonics, v. 17, n. 4, p. 481–500, https://doi.org/10.1029/98TC01314

He, D., Webb, A. A. G., Larson, K. P., Martin, A. J., and Schmitt, A. K., 2015, Extrusion vs. duplexing models of Himalayan mountain building 3: Duplexing dominates from the Oligocene to Present: International Geology Review, v. 57, n. 1, p. 1–27, https://doi.org/10.1080/00206814.2014.986669

He, D., Webb, A. A. G., Larson, K. P., and Schmitt, A. K., 2016, Extrusion vs. duplexing models of Himalayan mountain building 2: The South Tibet detachment at Dadeldhura klippe: Tectonophysics, v. 667, p. 87–107, https://doi.org/10.1016/j.tecto.2015.11.014

He, S., Kapp, P., DeCelles, P. G., Gehrels, G. E., and Heizler, M., 2007, Cretaceous-Tertiary geology of the Gangdese Arc in the Linzhou area, southern Tibet: Tectonophysics, v. 433, n. 1–4, p. 15–37, https://doi.org/10.1016/j.tecto.2007.01.005

Hébert, R., Bezard, R., Guilmette, C., Dostal, J., Wang, C. S., and Liu, Z. F., 2012, The Indus-Yarlung Zangbo ophiolites from Nanga Parbat to Namche Barwa syntaxes, southern Tibet: First synthesis of petrology, geochemistry, and geochronology with incidences on geodynamics reconstructions of Neo-Tethys: Gondwana Research, v. 22, n. 2, p. 377–397, https://doi.org/10.1016/j.gr.2011.10.013

Heim, A. A., and Gansser, A., 1939, Central Himalaya: Geological Observations of the Swiss Expedition, 1936: Delhi, Hindustan Publishing Corporation (India), 245 p.

Hennig, A., 1915, Zur Petrographie und Geologie von Sudwest Tibet, *in* Hedin, S., editor, Southern Tibet: Stockholm, Norstedt, p. 220.

Hetényi, G., Cattin, R., Brunet, F., Bollinger, L., Vergne, J., Nábělek, J. L., and Diament, M., 2007, Density distribution of the India plate beneath the Tibetan plateau: Geophysical and petrological constraints on the kinetics of lower-crustal eclogitization: Earth and Planetary Science Letters, v. 264, n. 1–2, p. 226–244, https://doi.org/10.1016/j.epsl.2007.09.036

Hetényi, G., Vergne, J., Bollinger, L., and Cattin, R., 2011, Discontinuous low-velocity zones in southern Tibet question the viability of the channel flow model, *in* Gloaguen, R., and Ratschbacher, L., editors, Growth and Collapse of the Tibetan Plateau: Geological Society, London, Special Publications, v. 353, p. 99–108, https://doi.org/10.1144/SP353.6

Hetzel, R., Dunkl, I., Haider, V., Strobl, M., von Eynatten, H., Ding, L., and Frei, D., 2011, Peneplain formation in southern Tibet predates the India-Asia collision and plateau uplift: Geology, v. 39, n. 10, p. 983–986, https://doi.org/10.1130/G32069.1

Hodges, K. V., 2000, Tectonics of the Himalaya and southern Tibet from two perspectives: Geological Society of America Bulletin, v. 112, n. 3, p. 324–350, https://doi.org/10.1130/0016-7606(2000)112<324:TOTHAS>2.0.CO;2

Hodges, K. V., Parrish, R. R., Housh, T. B., Lux, D. R., Burchfiel, B. C., Royden, L. H., and Chen, Z., 1992, Simultaneous Miocene extension and shortening in the Himalayan orogen: Science, v. 258, n. 5087, p. 1466–1470, https://doi.org/10.1126/science.258.5087.1466

Hodges, K. V., Parrish, R. R., and Searle, M. P., 1996, Tectonic evolution of the central Annapurna Range, Nepalese Himalayas: Tectonics, v. 15, n. 6, p. 1264-1291, https://doi.org/10.1029/96TC01791

Hodges, K. V., Hurtado, J. M., and Whipple, K. X., 2001, Southward extrusion of Tibetan crust and its effect on Himalayan tectonics: Tectonics, v. 20, n. 6, p. 799–809, https://doi.org/10.1029/2001TC001281

Horton, B. K., Yin, A., Spurlin, M. S., Zhou, J., and Wang, J., 2002, Paleocene-Eocene syncontractional sedimentation in narrow, lacustrine-dominated basins of east-central Tibet: Geological Society of America Bulletin, v. 114, n. 7, p. 771–786, https://doi.org/10.1130/0016-7606(2002)114<0771:PESSIN>2.0.CO;2

Horton, F., Lee, J., Hacker, B., Bowman-Kamaha'o, M., and Cosca, M., 2015, Himalayan gneiss dome formation in the middle crust and exhumation by normal faulting: New geochronology of Gianbul dome, northwestern India: Geological Society of America Bulletin, v. 127, n. 1–2, p. 162–180, https://doi.org/10.1130/B31005.1

Hossler, T., Bollinger, L., Sapkota, S. N., Lavé, J., Gupta, R. M., and Kandel, T. P., 2016, Surface ruptures of large Himalayan earthquakes in Western Nepal: Evidence along a reactivated strand of the Main Boundary Thrust: Earth and Planetary Science Letters, v. 434, p. 187–196, https://doi.org/10.1016/j.epsl.2015.11.042

Hou, Z.-Q., Zheng, Y.-C., Zeng, L.-S., Gao, L.-E., Huang, K.-X., Li, W., Li, Q.-Y., Fu, Q., Liang, W., and Sun, Q.-Z., 2012, Eocene-Oligocene granitoids in southern Tibet: Constraints on crustal anatexis and tectonic evolution of the Himalayan orogen: Earth and Planetary Science Letters, v. 349–350, p. 38–52, https://doi.org/10.1016/j.epsl.2012.06.030

Houseman, G. A., McKenzie, D. P., and Molnar, P., 1981, Convective instability of a thickened boundary layer and its relevance for the thermal evolution of continental convergent belts: Journal of Geophysical Research-Solid Earth, v. 86, n. B7, p. 6115–6132, https://doi.org/10.1029/JB086iB07p06115

Hsü, K. J., Guitang, P., and Şengör, A. M. C., 1995, Tectonic evolution of the Tibetan Plateau: A working hypothesis based on the archipelago model of orogenesis: International Geology Review, v. 37, n. 6, p. 473–508, https://doi.org/10.1080/00206819509465414

Hu, P.-y., Zhai, Q.-g., Wang, J., Tang, Y., Wang, H.-t., Zhu, Z.-c., and Wu, H., 2018, Middle Neoproterozoic (*ca.* 760 Ma) arc and back-arc system in the North Lhasa terrane, Tibet, inferred from coeval N-MORB- and arc-type gabbros: Precambrian Research, v. 316, p. 275–290, https://doi.org/10.1016/j.precamres.2018.08.022

Hu, X., Jansa, L., Chen, L., Griffin, W. L., O'Reilly, S. Y., and Wang, J., 2010, Provenance of Lower Cretaceous Wölong Volcaniclastics in the Tibetan Tethyan Himalaya: Implications for the final breakup of Eastern Gondwana: Sedimentary Geology, v. 223, n. 3–4, p. 193–205, https://doi.org/10.1016/j.sedgeo.2009.11.008

Hu, X., Sinclair, H. D., Wang, J., Jiang, H., and Wu, F., 2012, Late Cretaceous-Palaeogene stratigraphic and basin evolution in the Zhepure Mountain of southern Tibet: Implications for the timing of India-Asia initial collision: Basin Research, v. 24, n. 5, p. 520–543, https://doi.org/10.1111/j.1365-2117.2012.00543.x

Hu, X., Garzanti, E., Moore, T., and Raffi, I., 2015, Direct stratigraphic dating of India-Asia collision onset at the Selandian (middle Paleocene, 59 ± 1 Ma): Geology, v. 43, n. 10, p. 859–862, https://doi.org/10.1130/G36872.1

Hu, X., Garzanti, E., Wang, J., Huang, W., An, W., and Webb, A., 2016a, The timing of India-Asia collision onset – Facts, theories, controversies: Earth-Science Reviews, v. 160, p. 264–299, https://doi.org/10.1016/j.earscirev.2016.07.014

Hu, X., Wang, J., Boudagher-Fadel, M., Garzanti, E., and An, W., 2016b, New insights into the timing of the India-Asia collision from the Paleogene Quxia and Jialazi formations of the Xigaze forearc basin, South Tibet: Gondwana Research, v. 32, p. 76–92, , https://doi.org/10.1016/j.gr.2015.02.007

Huang, Q.-t., Liu, W.-l., Xia, B., Cai, Z.-r., Chen, W.-y., Li, J.-f., and Yin, Z.-x., 2017a, Petrogenesis of the Majiari ophiolite (western Tibet, China): Implications for intra-oceanic subduction in the Bangong-Nujiang Tethys: Journal of Asian Earth Sciences, v. 146, p. 337–351, https://doi.org/10.1016/j.jseaes.2017.06.008

Huang, W., van Hinsbergen, D. J. J., Maffione, M., Orme, D. A., Dupont-Nivet, G., Guilmette, C., Ding, L., Guo, Z., and Kapp, P., 2015, Lower Cretaceous Xigaze ophiolites formed in the Gangdese forearc: Evidence from paleomagnetism, sediment provenance, and stratigraphy: Earth and Planetary Science Letters, v. 415, p. 142–153, https://doi.org/10.1016/j.epsl.2015.01.032

Huang, W., Lippert, P. C., Jackson, M. J., Dekkers, M. J., Zhang, Y., Li, J., Guo, Z., Kapp, P., and van Hinsbergen, D. J. J., 2017b, Remagnetization of the Paleogene Tibetan Himalayan carbonate rocks in the Gamba area: Implications for reconstructing the lower plate in the India-Asia collision: Journal of Geophysical Research- Solid Earth, v. 122, n. 2, p. 808–825, https://doi.org/10.1002/2016JB013662

Huntington, K. W., Saylor, J., Quade, J., and Hudson, A. M., 2015, High late Miocene-Pliocene elevation of the Zhada Basin, southwestern Tibetan Plateau, from carbonate clumped isotope thermometry: Geological Society of America Bulletin, v. 127, n. 1–2, p. 181–199, https://doi.org/10.1130/B31000.1

Hurtado Jr., J. M., Hodges, K. V., and Whipple, K. X., 2001, Neotectonics of the Thakkhola graben and implications for recent activity on the South Tibetan fault system in the central Nepal Himalaya: Geological Society of America Bulletin, v. 113, n. 2, p. 222–240, https://doi.org/10.1130/0016-7606(2001)113<0222:NOTTGA>2.0.CO;2

Husson, L., Bernet, M., Guillot, S., Huyghe, P., Mugnier, J.-L., Replumaz, A., Robert, X., and Van der Beek, P., 2014, Dynamic ups and downs of the Himalaya: Geology, v.42, n. 10, p. 839–842, https://doi.org/10.1130/G36049.1

Iaccarino, S., Montomoli, C., Carosi, R., Massonne, H.-J., Langone, A., and Visonà, D., 2015, Pressure-temperature-time-deformation path of kyanite-bearing migmatitic paragneiss in the Kali Gandaki valley (Central Nepal): Investigation of Late Eocene-Early Oligocene melting processes: Lithos, v. 231, p. 103–121, https://doi.org/10.1016/j.lithos.2015.06.005

Imayama, T., Takeshita, T., Yi, K., Cho, D.-L., Kitajima, K., Tsutsumi, Y., Kayama, M., Nishido, H., Okumura, T., Yagi, K., Itaya, T., and Sano, Y., 2012, Two-stage partial melting and contrasting cooling history within the Higher Himalayan Crystalline Sequence in far-eastern Nepal Himalaya: Lithos, v. 134–135, p. 1–22, https://doi.org/10.1016/j.lithos.2011.12.004

Ingalls, M., Rowley, D. B., Currie, B. S., and Colman, A. S., 2016, Large-scale subduction of continental crust implied by India-Asia mass-balance calculation: Nature Geoscience, n. 9, p. 848–853, https://doi.org/10.1038/NGEO2806

Ingersoll, R. V., 2012, Tectonics of sedimentary basins, with revised nomenclature, *in* Busby, C., and Azor, A., editors, Tectonics of Sedimentary Basins, Recent Advances: Chichester, United Kingdom, Blackwell Publishing Ltd., p. 1–43, https://doi.org/10.1002/9781444347166.ch1

Isacks, B., and Molnar, P., 1971, Distribution of stresses in the descending lithosphere from a global survey of focal-mechanism solutions of mantle earthquakes: Reviews of Geophysics and Space Physics, v. 9, n. 1, p. 103–174, https://doi.org/10.1029/RG009i001p00103

Jackson, J., 2002, Strength of the continental lithosphere: Time to abandon the jelly sandwich?: GSA Today, v. 12, p. 4–10, https://doi.org/10.1130/1052-5173(2002)012<0004:SOTCLT>2.0.CO;2

Jacobson, C. E., Dawson, M. R., and Postlethwaite, C. E., 1988, Structure, metamorphism, and tectonic significance of the Pelona, Orocopia, and Rand schists, southern California, *in* Ernst, W. D., editor, Metamorphism and Crustal Evolution of the Western United States (Rubey Volume VII): New Jersey, Prentice-Hall, p. 976–997.

Jacobson, C. E., Hourigan, J. K., Haxel, G. B., and Grove, M., 2017, Extreme latest Cretaceous-Paleogene low-angle subduction: Zircon ages from Orocopia Schist at Cemetery Ridge, southwestern Arizona, USA: Geology, v. 45, n. 10, p. 951–954, https://doi.org/10.1130/G39278.1

Jadoul, F., Berra, F., and Garzanti, E., 1998, The Tethys Himalayan passive margin from Late Triassic to Early Cretaceous (South Tibet): Journal of Asian Earth Sciences, v. 16, n. 2–3, p. 173–194, https://doi.org/10.1016/S0743-9547(98)00013-0

Jagoutz, O., Royden, L., Holt, A. F., and Becker, T. W., 2015, Anomalously fast convergence of India and Eurasia caused by double subduction: Nature Geoscience, v. 8, p. 475–479, https://doi.org/10.1038/NGEO2418

Jagoutz, O., Macdonald, F. A., and Royden, L., 2016, Low-latitude arc-continent collision as a driver for global cooling: PNAS, v. 113, n. 18, p. 4935–4940, https://doi.org/10.1073/pnas.1523667113

Jain, A. K., Lal, N., Sulemani, B., Awasthi, A. K., Singh, S., Kumar, R., and Kumar, D., 2009, Detrital-zircon fission-track ages from the Lower Cenozoic sediments, NW Himalayan foreland basin: Clues for exhumation and denudation of the Himalaya during the India-Asia collision: Geological Society of America Bulletin, v. 121, n. 3–4, p. 519–535, https://doi.org/10.1130/B26304.1

Jessup, M. J., Cottle, J. M., Searle, M. P., Law, R. D., Newell, D. L., Tracy, R. J., and Waters, D. J., 2008a, *P-T-t-D* paths of Everest Series schist, Nepal: Journal of Metamorphic Geology, v. 26, n. 7, p. 717–739, https://doi.org/10.1111/j.1525-1314.2008.00784.x

Jessup, M. J., Newell, D. L., Cottle, J. M., Berger, A. L., and Spotila, J. A., 2008b, Orogen-parallel extension and exhumation enhanced by denudation in the trans-Himalayan Arun River gorge, Ama Drime Massif, Tibet-Nepal: Geology, v. 36, n. 7, p. 587–590, https://doi.org/10.1130/G24722A.1

Jessup, M. J., Langille, J. M., Cottle, J. M., and Ahmad, T., 2016, Crustal thickening, Barrovian metamorphism, and exhumation of midcrustal rocks during doming and extrusion: Insights from the Himalaya, NW India: Tectonics, v. 35, n. 1, p. 160–186; https://doi.org/10.1002/2015TC003962

Ji, W.-Q., Wu, F.-Y., Chung, S.-L., Li, J.-X., and Liu, C.-Z., 2009, Zircon U-Pb geochronology and Hf isotopic constraints on petrogenesis of the Gangdese batholith, southern Tibet: Chemical Geology, v. 262, n. 3–4, p. 229–245, https://doi.org/10.1016/j.chemgeo.2009.01.020

Ji, W.-Q., Wu, F.-Y., Liu, C.-Z., and Chung, S.-L., 2012, Early Eocene crustal thickening in southern Tibet: New age and geochemical constraints from the Gangdese batholith: Journal of Asian Earth Sciences, v. 53, p. 82–95, https://doi.org/10.1016/j.jseaes.2011.08.020

Ji, W.-Q., Wu, F.-Y., Chung, S.-L., Wang, X.-C., Liu, C.-Z., Li, Q.-L., Liu, Z.-C., Liu, X.-C., and Wang, J.-G., 2016, Eocene Neo-Tethyan slab breakoff constrained by 45 Ma oceanic island basalt-type magmatism in southern Tibet: Geology, v. 44, n. 4, p. 283–286, https://doi.org/10.1130/G37612.1

Jia, G., Bai, Y., Ma, Y., Sun, J., and Peng, P., 2015, Paleoelevation of Tibetan Lunpola basin in the Oligocene-Miocene transition estimated from leaf wax lipid dual isotopes: Global and Planetary Change, v. 126, p. 14–22, https://doi.org/10.1016/j.gloplacha.2014.12.007

Jiang, Z.-Q., Wang, Q., Li, Z.-X., Wyman, D. A., Tang, G.-J., Jia, X.-H., and Yang, Y.-H., 2012, Late Cretaceous (*ca.* 90 Ma) adakitic intrusive rocks in the Kelu area, Gangdese Belt (southern Tibet): Slab melting and implications for Cu-Au mineralization: Journal of Asian Earth Sciences, v. 53, p. 67–81, https://doi.org/10.1016/j.jseaes.2012.02.010

Jiang, Z.-Q., Wang, Q., Wyman, D. A., Li, Z.-X., Yang, J.-H., Shi, X.-B., Ma, L., Tang, G.-J., Gou, G.-N., Jia, X.-H., and Guo, H.-F., 2014, Transition from oceanic to continental lithosphere subduction in southern Tibet: Evidence from the Late Cretaceous-Early Oligocene ($\sim$91–30 Ma) intrusive rocks in the Chanang-Zedong area, southern Gangdese: Lithos, v. 196–197, p. 213–231, https://doi.org/10.1016/j.lithos.2014.03.001

Johnson, M. R. W., Oliver, G. J. H., Parrish, R. R., and Johnson, S. P., 2001, Synthrusting metamorphism, cooling, and erosion of the Himalayan Kathmandu Complex, Nepal: Tectonics, v. 20, n. 3, p. 394–415, https://doi.org/10.1029/2001TC900005

Jolivet, M., Brunel, M., Seward, D., Xu, Z., Yang, J., Roger, F., Tapponnier, P., Malavieille, J., Arnaud, N., and Wu, C., 2001, Mesozoic and Cenozoic tectonics of the northern edge of the Tibetan plateau: Fission-track constraints: Tectonophysics, v. 343, n. 1–2, p. 111–134, https://doi.org/10.1016/S0040-1951(01)00196-2

Jouanne, F., Mugnier, J. L., Gamond, J. F., Le Fort, P., Pandley, M. R., Bollinger, L., Flouzat, M., and Avouac, J. P., 2004, Current shortening across the Himalayas of Nepal: Geophysical Journal International, v. 157, n. 1, p. 1–14, https://doi.org/10.1111/j.1365-246X.2004.02180.x

Jouanne, F., Mugnier, J. L., Sapkota, S. N., Bascou, P., and Pecher, A., 2017, Estimation of coupling along the Main Himalayan Thrust in the central Himalaya: Journal of Asian Earth Sciences, v. 133, p. 62–71, https://doi.org/10.1016/j.jseaes.2016.05.028

Kakar, M. I., Collins, A. S., Mahmood, K., Foden, J. D., and Khan, M., 2012, U-Pb zircon crystallization age of the Muslim Bagh ophiolite: Enigmatic remains of an extensive pre-Himalayan arc: Geology, v. 40, n. 12, p. 1099–1102, https://doi.org/10.1130/G33270.1

Kali, E., Leloup, P. H., Arnaud, N., Mahéo, G., Liu, D., Boutonnet, E., Van der Woerd, J., Liu, X., Liu-Zeng, J., and Li, H., 2010, Exhumation history of the deepest central Himalayan rocks, Ama Drime range: Key pressure-temperature-deformation-time constraints on orogenic models: Tectonics, v. 29, n. 2, TC2014, https://doi.org/10.1029/2009TC002551

Kaneko, Y., Katayama, I., Yamamoto, H., Misawa, K., Ishikawa, M., Rehman, H. U., Kausar, A. B., and Shiraishi, K., 2003, Timing of Himalayan ultrahigh-pressure metamorphism: Sinking rate and subduction angle of the Indian continental crust beneath Asia: Journal of Metamorphic Geology, v. 21, n. 6, p. 589–599, https://doi.org/10.1046/j.1525-1314.2003.00466.x

Kang, Z.-Q., Xu, J.-F., Wilde, S. A., Feng, Z.-H., Chen, J.-L., Wang, B.-D., Fu, W.-C., and Pan, H.-B., 2014, Geochronology and geochemistry of the Sangri Group Volcanic Rocks, Southern Lhasa Terrane: Implications for the early subduction history of the Neo-Tethys and Gangdese Magmatic Arc: Lithos, v. 200–201, p. 157–168, https://doi.org/10.1016/j.lithos.2014.04.019

Kapp, P., and Guynn, J. H., 2004, Indian Punch Rifts Tibet: Geology, v. 32, n. 11, p. 993–996, https://doi.org/10.1130/G20689.1

Kapp, P., Yin, A., Manning, C. E., Murphy, M., Harrison, T. M., Spurlin, M., Ding, L., Deng, X.-G., and Wu, C.-M., 2000, Blueschist-bearing metamorphic core complexes in the Qiangtang block reveal deep crustal structure of northern Tibet: Geology, v. 28, n. 1, p. 19–22. https://doi.org/10.1130/0091-7613(2000)28<19:BMCCIT>2.0.CO;2

Kapp, P., Murphy, M. A., Yin, A., Harrison, T. M., Ding, L., and Guo, J., 2003a, Mesozoic and Cenozoic tectonic evolution of the Shiquanhe area of western Tibet: Tectonics, v. 22, n. 4, p. 1029, https://doi.org/10.1029/2001TC001332

Kapp, P., Yin, A., Manning, C. E., Harrison, T. M., Taylor, M. H., and Ding, L., 2003b, Tectonic evolution of the early Mesozoic blueschist-bearing Qiangtang metamorphic belt, central Tibet: Tectonics, v. 22, n. 4, 1043, https://doi.org/10.1029/2002TC001383

Kapp, P., Yin, A., Harrison, T. M., and Ding, L., 2005, Cretaceous-Tertiary shortening, basin development, and volcanism in central Tibet: Geological Society of America Bulletin, v. 117, n. 7–8, p. 865–878, https://doi.org/10.1130/B25595.1

Kapp, P., DeCelles, P. G., Gehrels, G. E., Heizler, M., and Ding, L., 2007a, Geological records of the Lhasa-Qiangtang and Indo-Asian collisions in the Nima basin area, central Tibet: Geological Society of America Bulletin, v. 119, n. 7–8, p. 917–932, https://doi.org/10.1130/B26033.1

Kapp, P., DeCelles, P. G., Leier, A. L., Fabijanic, J. M., He, S., Pullen, A., Gehrels, G. E., and Ding, L., 2007b, The Gangdese retroarc thrust belt revealed: GSA Today, v. 17, n. 7, p. 4–9, https://doi.org/10.1130/GSAT01707A.1

Karig, D. E., 1974, Evolution of arc systems in the western Pacific: Annual Review of Earth and Planetary Science, v. 2, p. 51–75, https://doi.org/10.1146/annurev.ea.02.050174.000411

Karplus, M. S., Zhao, W., Klemperer, S. L., Wu, Z., Mechie, J., Shi, D., Brown, L. D., and Chen, C., 2011, Injection of Tibetan crust beneath the south Qaidam Basin: Evidence from INDEPTH IV wide-angle seismic data: Journal of Geophysical Research-Solid Earth, v. 116, n. B7, B07301, https://doi.org/10.1029/2010JB007911

Kawakami, T., Aoya, M., Wallis, S. R., Lee, J., Terada, K., Wang, Y., and Heizler, M., 2007, Contact metamorphism in the Malashan dome, North Himalayan gneiss domes, southern Tibet: An example of shallow extensional tectonics in the Tethys Himalaya: Journal of Metamorphic Geology, v. 25, n. 8, p. 831–853, https://doi.org/10.1111/j.1525-1314.2007.00731.x

Kellett, D. A., and Godin, L., 2009, Pre-Miocene deformation of the Himalayan superstructure, Hidden valley, central Nepal: Journal of the Geological Society, London, v. 166, n. 2, p. 261–275, https://doi.org/10.1144/0016-76492008-097

Kellett, D. A., and Grujic, D., 2012, New insight into the South Tibetan detachment system: Not a single progressive deformation: Tectonics, v. 31, n. 2, TC2007 https://doi.org/10.1029/2011TC002957

Kellett, D. A., Grujic, D., Coutand, I., Cottle, J. M., and Mukul, M., 2013, The South Tibetan detachment system facilitates ultra rapid cooling of granulite-facies rocks in Sikkim Himalaya: Tectonics, v. 32, n. 2, p. 252–270, https://doi.org/10.1002/tect.20014

Kellett, D. A., Cottle, J. M., and Smit, M., 2014, Eocene deep crust at Ama Drime, Tibet: Early evolution of the Himalayan orogen: Lithosphere, v. 6, n. 4, p. 220–229, https://doi.org/10.1130/L350.1

Kellett, D. A., Cottle, J. M., and Larson, K. P., 2018, The South Tibetan Detachment System: History, advances, definition and future directions, *in* Treloar, P. J., and Searle, M. P., editors, Himalayan Tectonics: A Modern Synthesis: London, Geological Society, London, Special Publications, v. 483, https://doi.org/10.1144/SP483.2

Kelly, S., Butler, J. P., and Beaumont, C., 2016, Continental collision with a sandwiched accreted terrane: Insights into Himalayan-Tibetan lithospheric mantle tectonics?: Earth and Planetary Science Letters, v. 455, p. 176–195, https://doi.org/10.1016/j.epsl.2016.08.039

Kent, D. V., and Muttoni, G., 2008, Equatorial convergence of India and early Cenozoic climate trends: PNAS, v. 42, p. 16065–16070, https://doi.org/10.1073/pnas.0805382105

Khan, M. A., Jan, M. Q., and Weaver, B. L., 1993, Evolution of the lower arc crust in Kohistan, N. Pakistan: Temporal arc magmatism through early, mature and intra-arc rift stages, *in* Treloar, P. J., and Searle, M. P., editors, Himalayan Tectonics: Geological Society, London, Special Publications, v. 74, p. 123–138, https://doi.org/10.1144/GSL.SP.1993.074.01.10

Khan, M. A., Spicer, R. A., Bera, S., Ghosh, R., Yang, J., Spicer, T. E. V., Guo, S.-X., Su, T., Jacques, F., and Grote, P. J., 2014, Miocene to Pleistocene floras and climate of the Eastern Himalayan Siwaliks, and new palaeoelevation estimates for the Namling-Oiyug Basin, Tibet: Global and Planetary Change, v. 113, p. 1–10, https://doi.org/10.1016/j.gloplacha.2013.12.003

Kidd, W. S. F., Pan, Y., Chang, C., Coward, M. P., Dewey, J. F., Gansser, A., Molnar, P., Shackleton, R. M., and Sun, Y., 1988, Geological mapping of the 1985 Chinese-British Tibetan (Xizang-Qinghai) Plateau Geotraverse route: Philosophical Transactions of the Royal Society of London, Series A., v. 327, n. 1594, p. 287–305, https://doi.org/10.1098/rsta.1988.0130

Kind, R., Yuan, X., Saul, J., Nelson, D., Sobolev, S. V., Mechie, J., Zhao, W., Kosarev, G., Ni, J., Achauer, U., and Jiang, M., 2002, Seismic images of crust and upper mantle beneath Tibet: Evidence for Eurasian plate subduction: Science, v. 298, n. 5596, p. 1219–1221, https://doi.org/10.1126/science.1078115

King, J., Harris, N., Argles, T., Parrish, R., and Zhang, H., 2011, Contribution of crustal anatexis to the tectonic evolution of Indian crust beneath southern Tibet: Geological Society of America Bulletin, v. 123, n. 1–2, p. 218–239, https://doi.org/10.1130/B30085.1

Klemperer, S. L., 2006, Crustal flow in Tibet: Geophysical evidence for the physical state of Tibetan lithosphere, and inferred patterns of active flow, *in* Law, R. D., Searle, M. P., and Godin, L., editors, Channel Flow, Ductile Extrusion and Exhumation in Continental Collision Zones: Geological Society, London, Special Publications, v. 268, p. 39–70, https://doi.org/10.1144/GSL.SP.2006.268.01.03

Klootwijk, C. T., 1984, A review of Indian Phanerozoic palaeomagnetism: Implications for the India-Asia collision: Tectonophysics, v. 105, n. 1–4, p. 331–353, https://doi.org/10.1016/0040-1951(84)90212-9

Klootwijk, C. T., Conaghan, P. J., and Powell, C. M., 1985, The Himalayan Arc: Large-scale continental subduction, oroclinal bending and back-arc spreading: Earth and Planetary Science Letters, v. 75, n. 2–3, p. 167–183, https://doi.org/10.1016/0012-821X(85)90099-8

Kohn, M. J., 2008, P-T-t data from central Nepal support critical taper and repudiate large-scale channel flow of the Greater Himalayan Sequence: Geological Society of America Bulletin, v. 120, n. 3–4, p. 259–273, https://doi.org/10.1130/B26252.1

——— 2014, Himalayan metamorphism and its tectonic implications: Annual Review of Earth and Planetary Sciences, v. 42, p. 381–419, https://doi.org/10.1146/annurev-earth-060313-055005

Kohn, M. J., and Parkinson, C. D., 2002, Petrologic case for Eocene slab breakoff during the Indo-Asian collision: Geology, v. 30, n. 7, p. 591–594, https://doi.org/10.1130/0091-7613(2002)030<0591:PCFESB>2.0.CO;2

Kosarev, G., Kind, R., Sobolev, S. V., Yuan, X., Hanka, W., and Oreshin, S., 1999, Seismic evidence for detached Indian lithospheric mantle beneath Tibet: Science, v. 283, n. 5406, p. 1306–1309, https://doi.org/10.1126/science.283.5406.1306

Kufner, S.-K., Schurr, B., Sippl, C., Yuan, X., Ratschbacher, L., Akbar, A. s. M., Ischuk, A., Murodkulov, S., Schneider, F., Mechie, J., and Tilmann, F., 2016, Deep India meets deep Asia: Lithospheric indentation,

delamination and break-off under Pamir and Hindu Kush (Central Asia): Earth and Planetary Science Letters, v. 435, p. 171–184, https://doi.org/10.1016/j.epsl.2015.11.046
Kufner, S.-K., Schurr, B., Haberland, C., Zhang, Y., Saul, J., Ischuk, A., and Oimahmadov, I., 2017, Zooming into the Hindu Kush slab break-off: A rare glimpse on the terminal stage of subduction: Earth and Planetary Science Letters, v. 461, p. 127–140, https://doi.org/10.1016/j.epsl.2016.12.043
Kumar, P., Yuan, X., Kind, R., and Ni, J., 2006, Imaging the colliding Indian and Asian lithospheric plates beneath Tibet: Journal of Geophysical Research-Solid Earth, v. 111, n. B6, B06308, https://doi.org/10.1029/2005JB003930
Lai, S.-C., and Qin, J.-F., 2013, Adakitic rocks derived from partial melting of subducted continental crust: Evidence from the Eocene volcanic rocks in the northern Qiangtang block: Gondwana Research, v. 23, n. 2, p. 812–824, https://doi.org/10.1016/j.gr.2012.06.003
Lambiase, J. J., 1990, A model for the tectonic control of lacustrine stratigraphic sequences in continental rift basins, *in* Katez, B. J., editor, Lacustrine basin exploration: Case studies and modern analogues: American Association of Petroleum Geologists Memoir 50, p. 265–276.
Langille, J. M., Jessup, M. J., Cottle, J. M., Newell, D., and Seward, G., 2010, Kinematic evolution of the Ama Drime detachment: Insights into orogen-parallel extension and exhumation of the Ama Drime Massif, Tibet-Nepal: Journal of Structural Geology, v. 32, n. 7, p. 900–919, https://doi.org/10.1016/j.jsg.2010.04.005
Langille, J. M., Jessup, M. J., Cottle, J. M., Lederer, G., and Ahmad, T., 2012, Timing of metamorphism, melting and exhumation of the Leo Pargil dome, northwest India: Journal of Metamorphic Geology, v. 30, n. 8, p. 769–791, https://doi.org/10.1111/j.1525-1314.2012.00998.x
Larson, K. P., and Cottle, J. M., 2015, Initiation of crustal shortening in the Himalaya: Terra Nova, v. 27, n. 3, p. 169–174, https://doi.org/10.1111/ter.12145
Larson, K. P., Godin, L., Davis, W. J., and Davis, D. W., 2010, Out-of-sequence deformation and expansion of the Himalayan orogenic wedge: Insight from the Changgo culmination, south central Tibet: Tectonics, v. 29, n. 4, TC4013, https://doi.org/10.1029/2008TC002393
Larson, K. P., Ambrose, T. K., Webb, A. A. G., Cottle, J. M., and Shrestha, S., 2015, Reconciling Himalayan midcrustal discontinuities: The Main Central thrust system: Earth and Planetary Science Letters, v. 429, p. 139–146, https://doi.org/10.1016/j.epsl.2015.07.070
Laskowski, A. K., Kapp, P., Vervoort, J. D., and Ding, L., 2016, High-pressure Tethyan Himalaya rocks along the India-Asia suture zone in southern Tibet: Lithosphere, v. 8, n. 5, p. 574–582, https://doi.org/10.1130/L544.1
Laskowski, A. K., Kapp, P., Ding, L., Campbell, C., and Liu, X. H., 2017, Tectonic evolution of the Yarlung suture zone, Lopu Range region, southern Tibet: Tectonics, v. 36, n. 1, p. 108–136, https://doi.org/10.1002/2016TC004334
Lavé, J., and Avouac, J.-P., 2000, Active folding of fluvial terraces across the Siwaliks Hills, Himalayas of central Nepal: Journal of Geophysical Research-Solid Earth, v. 105, n. B3, p. 5735–5770, https://doi.org/10.1029/1999JB900292
——— 2001, Fluvial incision and tectonic uplift across the Himalayas of central Nepal: Journal of Geophysical Research, v. 106, n. B11, p. 26561–26591, https://doi.org/10.1029/2001JB000359
Leary, R., Orme, D. A., Laskowski, A. K., DeCelles, P. G., Kapp, P., Carrapa, B., and Dettinger, M., 2016a, Along-strike diachroneity in the deposition of the Kailas Formation in central southern Tibet: Implications for Indian slab dynamics: Geosphere, v. 12, n. 4, p. 1198–1223, https://doi.org/10.1130/GES01325.1
Leary, R. J., DeCelles, P. G., Quade, J., Gehrels, G. E., and Waanders, G., 2016b, The Liuqu Conglomerate, southern Tibet: Early Miocene basin development related to deformation within the Great Counter Thrust system: Lithosphere, v. 8, n. 5, p. 427–450, https://doi.org/10.1130/L542.1
Leary, R. J., Quade, J., DeCelles, P. G., and Reynolds, A., 2017, Evidence from paleosols for low to moderate elevation of the India-Asia suture zone during mid-Cenozoic time: Geology, v. 45, n. 5, p. 399–342, https://doi.org/10.1130/G38830.1
Lee, H.-Y., Chung, S.-L., Lo, C.-H., Ji, J., Lee, T.-Y., Qian, Q., and Zhang, Q., 2009, Eocene Neotethyan slab breakoff in southern Tibet inferred from the Linzizong volcanic record: Tectonophysics, v. 477, n. 1–2, p. 20–35, https://doi.org/10.1016/j.tecto.2009.02.031
Lee, J., and Whitehouse, M. J., 2007, Onset of mid-crustal extensional flow in southern Tibet: Evidence from U/Pb zircon ages: Geology, v. 35, n. 1, p. 45–48, https://doi.org/10.1130/G22842A.1
Lee, J., Hacker, B. R., Dinklage, W. S., Wang, Y., Gans, P., Calvert, A., Wan, J., Chen, W., Blythe, A. E., and McClelland, W., 2000, Evolution of the Kangmar Dome, southern Tibet: Structural, petrologic, and thermochronologic constraints: Tectonics, v. 19, n. 5, p. 872–895, https://doi.org/10.1029/1999TC001147
Lee, J., Hacker, B., and Wang, Y., 2004, Evolution of North Himalayan gneiss domes: Structural and metamorphic studies in Mabja Dome, southern Tibet: Journal of Structural Geology, v. 26, n. 12, p. 2297–2316, https://doi.org/10.1016/j.jsg.2004.02.013
Lee, J., McClelland, W., Wang, Y., Blythe, A., and McWilliams, M., 2006, Oligocene-Miocene middle crustal flow in southern Tibet: Geochronology of Mabja Dome, *in* Law, R. D., Searle, M. P., and Godin, L., editors, Channel Flow, Ductile Extrusion and Exhumation in Continental Collision Zones: Geological Society, London Special Publications, v. 268, p. 445–469, https://doi.org/10.1144/GSL.SP.2006.268.01.21
Lee, J., Hager, C., Wallis, S. R., Stockli, D. F., Whitehouse, M. J., Aoya, M., and Wang, Y., 2011, Middle to late Miocene extremely rapid exhumation and thermal reequilibration in the Kung Co rift, southern Tibet: Tectonics, v. 30, n. 2, TC2007, https://doi.org/10.1029/2010TC002745
Leech, M. L., Singh, S., Jain, A. K., Klemperer, S. L., and Manickavasagam, R. M., 2005, The onset of India-Asia continental collision: Early, steep subduction required by the timing of UHP metamorphism

in the western Himalaya: Earth and Planetary Science Letters, v. 234, n. 1–2, p. 83–97, https://doi.org/10.1016/j.epsl.2005.02.038

Leeder, M. R., Smith, A. B., and Yin, J., 1988, Sedimentology and palaeoenvironmental evolution of the 1985 Lhasa to Golmud geotraverse: Philosophical Transactions of the Royal Society of London, Series A, v. 327, n. 1594, p. 107–143, https://doi.org/10.1098/rsta.1988.0123

Leier, A. L., DeCelles, P. G., Kapp, P., and Ding, L., 2007a, The Takena Formation of the Lhasa terrane, southern Tibet: The record of a Late Cretaceous retroarc foreland basin: Geological Society of America Bulletin, v. 119, n. 1–2, p. 31–48, https://doi.org/10.1130/B25974.1

Leier, A. L., DeCelles, P. G., Kapp, P., and Gehrels, G. E., 2007b, Lower Cretaceous strata in the Lhasa terrane, Tibet, with implications for understanding the early tectonic history of the Tibetan Plateau: Journal of Sedimentary Research, v. 77, n. 10, p. 809–825, https://doi.org/10.2110/jsr.2007.078

Leloup, P. H., Liu, X., Mahéo, G., Paquette, J.-L., Arnaud, N., Aubray, A., and Liu, X., 2015, New constraints on the timing of partial melting and deformation along the Nyalam section (central Himalaya): Implications for extrusion models, *in* Mukherjee, S., Carosi, R., van der Beek, P. A., Mukherjee, B. K., and Robinson, D. M., editors, Tectonics of the Himalaya: Geological Society, London, Special Publications, v. 412, p. 131–175, https://doi.org/10.1144/SP412.11

Li, C., and Zheng, A., 1993, Paleozoic stratigraphy in the Qiangtang region of Tibet: Relations of the Gondwana and Yangtze continents and ocean closure near the end of the Carboniferous: International Geology Review, v. 35, n. 9, p. 797–804, https://doi.org/10.1080/00206819309465558

Li, C., Liren, C., Ke, H., Zengrong, Y., and Yurong, H., 1995, Study on the paleo-Tethys suture zone of Lungmu Co-Shuanghu, Tibet: Beijing, Geological Publishing House, 131 p.

Li, C., van der Hilst, R. D., Meltzer, A. S., and Engdahl, E. R., 2008, Subduction of the Indian lithosphere beneath the Tibetan Plateau and Burma: Earth and Planetary Science Letters, v. 274, n. 1–2, p. 157–168, https://doi.org/10.1016/j.epsl.2008.07.016

Li, G., Sandiford, M., Boger, S., Liu, X., and Wei, L., 2015a, Provenance of the Upper Cretaceous to Lower Tertiary sedimentary relicts in the Renbu mélange zone, within the Indus-Yarlung suture zone: Journal of Geology, v. 123, n. 1, p. 39–54, https://doi.org/10.1086/680207

Li, H. l., Van der Woerd, J., Tapponnier, P., Klinger, Y., Qi, X., Yang, J.-H., and Zhu, Y., 2005, Slip rate on the Kunlun fault at Hongshui Guo, and recurrence time of great events comparable to the 14/11/2001, Mw~7.9 Kokoxili earthquake: Earth and Planetary Science Letters, v. 237, n. 1–2, p. 285–299, https://doi.org/10.1016/j.epsl.2005.05.041

Li, H.-Q., Xu, Z.-Q., Webb, A. A. G., Li, T.-F., Ma, S.-W., and Huang, X.-M., 2017a, Early Jurassic tectonism occurred within the Basu metamorphic complex, eastern central Tibet: Implications for an archipelago-accretion orogenic model: Tectonophysics, v. 702, p. 29–41, https://doi.org/10.1016/j.tecto.2017.02.016

Li, J., and Batten, D. J., 2004, Early Cretaceous palynofloras from the Tanggula Mountains of the northern Qinghai-Xizang (Tibet) Plateau, China: Cretaceous Research, v. 25, n. 4, p. 531–542, https://doi.org/10.1016/j.cretres.2004.04.005

Li, J., Hu, X., Garzanti, E., An, W., and Wang, J., 2015b, Paleogene carbonate microfacies and sandstone provenance (Gamba area, South Tibet): Stratigraphic response to initial India-Asia continental collision: Journal of Asian Earth Sciences, v. 104, p. 39–54, https://doi.org/10.1016/j.jseaes.2014.10.027

Li, S.-M., Zhu, D.-C., Wang, Q., Zhao, Z., Zhang, L.-L., Liu, S.-A., Chang, Q.-S., Lu, Y.-H., Dai, J.-G., and Zheng, Y.-C., 2016a, Slab-derived adakites and subslab asthenosphere-derived OIB-type rocks at 156 ± 2 Ma from the north of Gerze, central Tibet: Records of the Bangong-Nujiang oceanic ridge subduction during the Late Jurassic: Lithos, v. 262, p. 456–469, https://doi.org/10.1016/j.lithos.2016.07.029

Li, S., Ding, L., Guilmette, C., Fu, J., Xu, Q., Yue, Y., and Henrique-Pinto, R., 2017b, The subduction-accretion history of the Bangong-Nujiang Ocean: Constraints from provenance and geochronology of the Mesozoic strata near Gaize, central Tibet: Tectonophysics, v. 702, p. 42–60, https://doi.org/10.1016/j.tecto.2017.02.023

Li, S., Ding, L., Xu, Q., Wang, H., Yue, Y., and Baral, U., 2017c, The evolution of Yarlung Tsangpo River: Constraints from the age and provenance of the Gangdese Conglomerates, southern Tibet: Gondwana Research, v. 41, p. 249–266, , https://doi.org/10.1016/j.gr.2015.05.010

Li, Y., Wang, C., Li, Y., Ma, C., Wang, L., and Peng, S., 2010, The Cretaceous tectonic event in the Qiangtang Basin and its implications for hydrocarbon accumulation: Petroleum Science, v. 7, n. 4, p. 466–471, https://doi.org/10.1007/s12182-010-0096-7

Li, Y., Wang, C., Zhao, X., Yin, A., and Ma, C., 2012, Cenozoic thrust system, basin evolution, and uplift of the Tanggula Range in the Tuotuohe region, central Tibet: Gondwana Research, v. 22, n. 2, p. 482–492, https://doi.org/10.1016/j.gr.2011.11.017

Li, Y., He, J., Han, Z., Wang, C., Ma, P., Zhou, A., Liu, S.-A., and Xu, M., 2016b, Late Jurassic sodium-rich adakitic intrusive rocks in the southern Qiangtang terrane, central Tibet, and their implications for the Bangong-Nujiang Ocean subduction: Lithos, v. 245, p. 34–46, https://doi.org/10.1016/j.lithos.2015.10.014

Li, Z.-H., Liu, M., and Gerya, T., 2016c, Lithosphere delamination in continental collisional orogens: A systematic numerical study: Journal of Geophysical Research-Solid Earth, v. 121, n. 7, p. 5186–5211, https://doi.org/10.1002/2016JB013106

Liang, X., Sandvol, E., Chen, Y. J., Hearn, T., Ni, J., Klemperer, S., Shen, Y., and Tilmann, F., 2012, A complex Tibetan upper mantle: A fragmented Indian slab and no south-verging subduction of Eurasian lithosphere: Earth and Planetary Science Letters, v. 333–334, p. 101–111, https://doi.org/10.1016/j.epsl.2012.03.036

Liang, X., Chen, Y., Tian, X., Chen, Y. J., Ni, J., Gallegos, A., Klemperer, S. L., Wang, M., Xu, T., Sun, C., Si, S., Lan, H., and Teng, J., 2016, 3D imaging of subducting and fragmenting Indian continental lithosphere beneath southern and central Tibet using body-wave fine-frequency tomography: Earth and Planetary Science Letters, v. 443, p. 162–175, https://doi.org/10.1016/j.epsl.2016.03.029

Liang, X., Wang, G., Yang, B., Ran, H., Zheng, Y., Du, J., and Li, L., 2017, Stepwise exhumation of the Triassic Lanling high-pressure metamorphic belt in Central Qiangtang, Tibet: Insights from a coupled study of metamorphism, deformation, and geochronology: Tectonics, v. 36, n. 4, p. 652–670, https://doi.org/10.1002/2016TC004455

Licht, A., van Cappelle, M., Abels, H. A., Ladant, J.-B., Trabucho-Alexandre, J., France-Lanord, C., Donnadieu, Y., Vandenberghe, J., Rigaudier, T., Lécuyer, C., Terry Jr., D., Adriaens, R., Boura, A., Guo, Z., Soe, A. N., Quade, J., Dupont-Nivet, G., and Jaeger, J.-J., 2014, Asian monsoons in a late Eocene greenhouse world: Nature, v. 513, p. 501–506, https://doi.org/10.1038/nature13704

Lippert, P. C., van Hinsbergen, D. J. J., and Dupont-Nivet, G., 2014, Early Cretaceous to present latitude of the central proto-Tibetan Plateau: A paleomagnetic synthesis with implications for Cenozoic tectonics, paleogeography, and climate of Asia, *in* Nie, J., Horton, B. K., and Hoke, G. D., editors, Toward an Improved Understanding of Uplift Mechanisms and the Elevation History of the Tibetan Plateau: Geological Society of America Special Paper 507, p. 1–21, https://doi.org/10.1130/2014.2507(01)

Liu, C.-Z., Chung, S.-L., Wu, F.-Y., Zhang, C., Xu, Y., Wang, J.-G., Chen, Y., and Guo, S., 2016a, Tethyan suturing in Southeast Asia: Zircon U-Pb and Hf-O isotopic constraints from Myanmar ophiolites: Geology, v. 44, n. 4, p. 311–314, https://doi.org/10.1130/G37342.1

Liu, D., Huang, Q., Fan, S., Zhang, L., Shi, R., and Ding, L., 2014a, Subduction of the Bangong-Nujiang Ocean: Constraints from granites in the Bangong Co area, Tibet: Geological Journal, v. 49, n. 2, p. 188–206, https://doi.org/10.1002/gj.2510

Liu, D., Shi, R., Ding, L., Huang, Q.-S., Zhang, X., Yue, Y., and Zhang, L., 2017, Zircon U-Pb age and Hf isotopic compositions of Mesozoic granitoids in southern Qiangtang, Tibet: Implications for the subduction of the Bangong-Nujiang Tethyan Ocean: Gondwana Research, v. 41, p. 157–172, https://doi.org/10.1016/j.gr.2015.04.007

Liu, G., and Einsele, G., 1996, Various types of olistostromes in a closing ocean basin, Tethyan Himalaya (Cretaceous, Tibet): Sedimentary Geology, v. 104, n. 1–4, p. 203–226, https://doi.org/10.1016/0037-0738(95)00129-8

Liu, J., and Aitchison, J. C., 2002, Upper Paleocene radiolarians from the Yamdrok mélange, south Xizang (Tibet), China: Micropaleontology, v. 48, Supplement 1, p. 145–154, https://www.jstor.org/stable/1486017

Liu, M., and Yang, Y., 2003, Extensional collapse of the Tibetan Plateau: Results of three-dimensional finite element modeling: Journal of Geophysical Research-Solid Earth, v. 108, n. B8, 2361, https://doi.org/10.1029/2002JB002248

Liu, S., Hu, R.-Z., Feng, C.-X., Zou, H.-B., Li, C., Chi, X.-G., Peng, J.-T., Zhong, H., Qi, L., Qi, Y.-Q., and Wang, T., 2008, Cenozoic high Sr/Y volcanic rocks in the Qiangtang terrane, northern Tibet: Geochemical and isotopic evidence for the origin of delaminated lower continental melts: Geological Magazine, v. 145, n. 4, p. 463–474, https://doi.org/10.1017/S0016756808004548

Liu, T., Zhai, Q.-g., Wang, J., Bao, P.-s., Qiangba, Z., Tang, S.-h., and Tang, Y., 2016b, Tectonic significance of the Dongqiao ophiolite in the north-central Tibetan plateau: Evidence from zircon dating, petrological, geochemical and Sr-Nd-Hf isotopic characterization: Journal of Asian Earth Sciences, v. 116, p. 139–154, https://doi.org/10.1016/j.jseaes.2015.11.014

Liu, W.-L., Xia, B., Zhong, Y., Cai, J.-X., Li, J.-F., Liu, H.-F., Cai, Z.-R., and Sun, Z.-L., 2014b, Age and composition of the Rebang Co and Julu ophiolites, central Tibet: Implications for the evolution of the Bangong Meso-Tethys: International Geology Review, v. 56, n. 4, p. 430–447, https://doi.org/10.1080/00206814.2013.873356

Liu, Z.-C., Wu, F.-Y., Ji, W.-Q., Wang, J.-G., and Liu, C.-Z., 2014c, Petrogenesis of the Ramba leucogranite in the Tethyan Himalaya and constraints on the channel flow model: Lithos, v. 208–209, p. 118–136, https://doi.org/10.1016/j.lithos.2014.08.022

Lombardo, B., and Rolfo, F., 2000, Two contrasting eclogite types in the Himalayas: Implications for the Himalayan orogeny: Journal of Geodynamics, v. 30, n. 1–2, p. 37–60, https://doi.org/10.1016/S0264-3707(99)00026-5

Long, S., McQuarrie, N., Tobgay, T., and Grujic, D., 2011, Geometry and crustal shortening of the Himalayan fold-thrust belt, eastern and central Bhutan: Geological Society of America Bulletin, v. 123, n. 7–8, p. 1427–1447, https://doi.org/10.1130/B30203.1

Long, S. P., McQuarrie, N., Tobgay, T., Coutand, I., Cooper, F. J., Reiners, P. W., Wartho, J.-A., and Hodges, K. V., 2012, Variable shortening rates in the eastern Himalayan thrust belt, Bhutan: Insights from multiple thermochronologic and geochronologic data sets tied to kinematic reconstructions: Tectonics, v. 31, n. 5, TC5004, https://doi.org/10.1029/2012TC003155

Luo, B., Dai, G., and Pan, Z., 1996, Oil and gas potential in Paleogene terrestrial Bangonghu-Dinging suture zone: Journal of China University of Geosciences, v. 21, p. 163–167.

Lyon-Caen, H., and Molnar, P., 1983, Constraints on the structure of the Himalaya from an analysis of gravity anomalies and a flexural model of the lithosphere: Journal of Geophysical Research-Solid Earth, v. 88, n. B10, p. 8171–8191, https://doi.org/10.1029/JB088iB10p08171

Ma, A., Hu, X., Kapp, P., Han, Z., Lai, W., and BouDagher-Fadel, M., 2018, The disappearance of a Late Jurassic remnant sea in the southern Qiangtang Block (Shamuluo Formation, Najiangco area): Implications for the tectonic uplift of central Tibet: Palaeogeography, Palaeoclimatology, Palaeoecology, v. 506, p. 30–47, https://doi.org/10.1016/j.palaeo.2018.06.005

Ma, L., Wang, Q., Li, Z.-X., Wyman, D. A., Jiang, Z.-Q., Yang, J.-H., Gou, G.-N., and Guo, H.-F., 2013, Early Late Cretaceous (*ca.* 93 Ma) norites and hornblendites in the Milin area, eastern Gangdese: Lithosphere-asthenosphere interaction during slab roll-back and an insight into early Late Cretaceous (*ca.* 100-80 Ma) magmatic "flare-up" in southern Lhasa (Tibet): Lithos, v. 172–173, p. 17–30, https://doi.org/10.1016/j.lithos.2013.03.007

Ma, L., Wang, B.-D., Jiang, Z.-Q., Wang, Q., Li, Z.-X., Wyman, D. A., Zhao, S.-R., Yang, J.-H., Guo, G.-N., and

Guo, H.-F., 2014, Petrogenesis of the Early Eocene adakitic rocks in the Napuri area, southern Lhasa: Partial melting of thickened lower crust during slab break-off and implications for crustal thickening in southern Tibet: Lithos, v. 196–197, p. 321–338, https://doi.org/10.1016/j.lithos.2014.02.011

Ma, L., Wang, Q., Wyman, D. A., Jiang, Z.-Q., Wu, F.-Y., Li, X.-H., Yang, J.-H., Gou, G.-N., and Guo, H.-F., 2015, Late Cretaceous back-arc extension and arc system evolution in the Gangdese area, southern Tibet: Geochronological, petrological, and Sr-Nd-Hf-O isotopic evidence from Dagze diabases: Journal of Geophysical Research-Solid Earth, v. 120, n. 9, p. 6159–6181, https://doi.org/10.1002/2015JB011966

Maffione, M., van Hinsbergen, D. J. J., Koornneef, L. M. T., Guilmette, C., Hodges, K., Borneman, N., Huang, W., Ding, L., and Kapp, P., 2015, Forearc hyperextension dismembered the south Tibetan ophiolites: Geology, v. 43, n. 6, p. 475–478, https://doi.org/10.1130/G36472.1

Magni, V., van Hunen, J., Funiciello, F., and Faccenna, C., 2012, Numerical models of slab migration in continental collision zones: Solid Earth, v. 3, n. 2, p. 293–306, https://doi.org/10.5194/se-3-293-2012

Makovsky, Y., and Klemperer, S. L., 1999, Measuring the seismic properties of Tibetan bright spots: Evidence for free aqueous fluids in the Tibetan middle crust: Journal of Geophysical Research-Solid Earth, v. 104, n. B5, p. 10795–10825, https://doi.org/10.1029/1998JB900074

Makovsky, Y., Klemperer, S. L., Ratschbacher, L., and Alsdorf, D., 1999, Midcrustal reflector on INDEPTH wide-angle profiles: An ophiolitic slab beneath the India-Asia suture in southern Tibet?: Tectonics, v. 18, n. 5, p. 793–808, https://doi.org/10.1029/1999TC900022

Malavieille, J., 2010, Impact of erosion, sedimentation, and structural heritage on the structure and kinematics of orogenic wedges: Analog models and case studies: GSA Today, v. 20, n. 1, p. 4–10, https://doi.org/10.1130/GSATG48A.1

Malpas, J., Zhou, M.-F., Robinson, P. T., and Reynolds, P. H., 2003, Geochemical and geochronological constraints on the origin and emplacement of the Yarlung Zangbo ophiolites, Southern Tibet, *in* Dilek, Y., and Robinson, P. T., editors, Ophiolites in Earth History: Geological Society, London, Special Publications, v. 218, p. 191–206, https://doi.org/10.1144/GSL.SP.2003.218.01.11

Maluski, H., Proust, F., and Xiao, X. C., 1982, $^{39}Ar/^{40}Ar$ dating of the trans-Himalayan calc-alkaline magmatism of southern Tibet: Nature, v. 298, p. 152–154, https://doi.org/10.1038/298152a0

Martin, A. J., 2017, A review of Himalayan stratigraphy, magmatism, and structure: Gondwana Research, v. 49, p. 42–80, https://doi.org/10.1016/j.gr.2017.04.031

Martin, A. J., Gehrels, G. E., and DeCelles, P. G., 2007, The tectonic significance of (U,Th)/Pb ages of monazite inclusions in garnet from the Himalaya of central Nepal: Chemical Geology, v. 244, n. 1–2, p. 1–24, https://doi.org/10.1016/j.chemgeo.2007.05.003

Matte, P., Tapponnier, P., Arnaud, N., Bourjot, L., Avouac, J. P., Vidal, P., Liu, Q., Pan, Y., and Wang, Y., 1996, Tectonics of Western Tibet, between the Tarim and the Indus: Earth and Planetary Science Letters, v. 142, n. 3–4, p. 311–330, https://doi.org/10.1016/0012-821X(96)00086-6

Mattern, F., Schneider, W., Li, Y., and Li, X., 1996, A traverse through the western Kunlun (Xinjiang, China): Tentative geodynamic implications for the Paleozoic and Mesozoic: Geologische Rundschau, v. 85, n. 4, p. 705–722, https://doi.org/10.1007/BF02440106

McCaffrey, R., and Nabelek, J., 1998, Role of oblique convergence in the active deformation of the Himalayas and southern Tibet plateau: Geology, v. 26, n. 8, p. 691–694, https://doi.org/10.1130/0091-7613(1998)026<0691:ROOCIT>2.3.CO;2

McCallister, A. T., Taylor, M. H., Murphy, M. A., Styron, R. H., and Stockli, D. F., 2014, Thermochronologic constraints on the late Cenozoic exhumation history of the Gurla Mandhata metamorphic core complex, Southwestern Tibet: Tectonics, v. 33, n. 2, p. 27–52, https://doi.org/10.1002/2013TC003302

McDermid, I. R. C., Aitchison, J. C., Davis, A. M., Harrison, T. M., and Grove, M., 2002, The Zedong terrane: A Late Jurassic intra-oceanic magmatic arc within the Yarlung-Tsangpo suture zone, southeastern Tibet: Chemical Geology, v. 187, n. 3–4, p. 267–277, https://doi.org/10.1016/S0009-2541(02)00040-2

McDermott, J. A., Whipple, K. X., Hodges, K. V., and van Soest, M. C., 2013, Evidence for Plio-Pleistocene north-south extension at the southern margin of the Tibetan Plateau, Nyalam region: Tectonics, v. 32, n. 3, p. 317–333, https://doi.org/10.1002/tect.20018

McQuarrie, N., Tobgay, T., Long, S. P., Reiners, P. W., and Cosca, M. A., 2014, Variable exhumation rates and variable displacement rates: Documenting recent slowing of Himalayan shortening in western Bhutan: Earth and Planetary Science Letters, v. 386, p. 161–174, https://doi.org/10.1016/j.epsl.2013.10.045

Meigs, A. J., Burbank, D. W., and Beck, R. A., 1995, Middle-late Miocene (>10 Ma) formation of the Main Boundary thrust in the western Himalaya: Geology, v. 23, n. 5, p. 423–426, https://doi.org/10.1130/0091-7613(1995)023<0423:MLMMFO>2.3.CO;2

Meng, F.-Y., Zhao, Z., Zhu, D.-C., Mo, X., Guan, Q., Huang, Y., Dong, G., Zhou, S., DePaolo, D. J., Harrison, T. M., Zhang, Z., Liu, J., Liu, Y., Hu, Z., and Yuan, H., 2014, Late Cretaceous magmatism in Mamba area, central Lhasa subterrane: Products of back-arc extension of Neo-Tethyan Ocean?: Gondwana Research, v. 26, n. 2, p. 505–520, https://doi.org/10.1016/j.gr.2013.07.017

Metcalf, K., and Kapp, P., 2017, The Yarlung suture mélange, Lopu Range, southern Tibet: Provenance of sandstone blocks and transition from oceanic subduction to continental collision: Gondwana Research, v. 48, p. 15–33, https://doi.org/10.1016/j.gr.2017.03.002

Metcalfe, I., 1988, Origin and assembly of Southeast Asian continental terranes, *in* Audley-Charles, M. G., and Hallam, A., editors, Gondwana and Tethys: Geological Society, London, Special Publications, v. 37, p. 101–118, https://doi.org/10.1144/GSL.SP.1988.037.01.08

Mitra, G., and Boyer, S. E., 1986, Energy balance and deformation mechanisms of duplexes: Journal of Structural Geology, v. 8, n. 3–4, p. 291–304, https://doi.org/10.1016/0191-8141(86)90050-7

Mitra, G., Bhattacharyya, K., and Mukul, M., 2010, The Lesser Himalayan Duplex in Sikkim: Implications for variations in Himalayan shortening: Journal Geological Society of India, v. 75, n. 1, p. 289–301, https://doi.org/10.1007/s12594-010-0016-x

Mo, X., Hou, Z., Niu, Y., Dong, G. C., Qu, X., Zhao, Z., and Yang, Z., 2007, Mantle contributions to crustal thickening during continental collision: Evidence from Cenozoic igneous rocks in southern Tibet: Lithos, v. 96, n. 1–2, p. 225–242, https://doi.org/10.1016/j.lithos.2006.10.005

Mo, X., Niu, Y., Dong, G., Zhao, Z., Hou, Z., Zhou, S., and Ke, S., 2008, Contribution of syncollisional felsic magmatism to continental crustal growth: A case study of the Paleogene Linzizong volcanic succession in southern Tibet: Chemical Geology, v. 250, n. 1–4, p. 49–67, https://doi.org/10.1016/j.chemgeo.2008.02.003

Molnar, P., and Atwater, T., 1978, Interarc spreading and Cordilleran tectonics as alternates related to the age of subducted oceanic lithosphere: Earth and Planetary Science Letters, v. 41, p. 330–340, https://doi.org/10.1016/0012-821X(78)90187-5

Molnar, P., and Lyon-Caen, H., 1989, Fault plane solutions of earthquakes and active tectonics of the Tibetan Plateau and its margins: Geophysical Journal International, v. 99, n. 1, p. 123–153, https://doi.org/10.1111/j.1365-246X.1989.tb02020.x

Molnar, P., and Stock, J. M., 2009, Slowing of India's convergence with Eurasia since 20 Ma and its implications for Tibetan mantle dynamics: Tectonics, v. 28, n. 3, TC3001, https://doi.org/10.1029/2008TC002271

Molnar, P., and Tapponnier, P., 1975, Cenozoic tectonics of Asia: Effects of a continental collision: Science, v. 189, n. 4201, p. 419–426, https://doi.org/10.1126/science.189.4201.419

——— 1978, Active tectonics of Tibet: Journal of Geophysical Research-Solid Earth, v. 83, n. B11, p. 5361–5375, https://doi.org/10.1029/JB083iB11p05361

——— 1981, A possible dependence of tectonic strength on the age of the crust in Asia: Earth and Planetary Science Letters, v. 52, n. 1, p. 107–114, https://doi.org/10.1016/0012-821X(81)90213-2

Molnar, P., England, P., and Martinod, J., 1993, Mantle dynamics, uplift of the Tibetan Plateau, and the India monsoon: Reviews of Geophysics, v. 31, n. 4, p. 357–396, https://doi.org/10.1029/93RG02030

Molnar, P., Boos, W. R., and Battisti, D. S., 2010, Orographic controls on climate and paleoclimate of Asia: Thermal and mechanical roles for the Tibetan Plateau: Annual Review of Earth and Planetary Science, v. 38, p. 77–102, https://doi.org/10.1146/annurev-earth-040809-152456

Montgomery, D. R., and Brandon, M. T., 2002, Topographic controls on erosion rates in tectonically active mountain ranges: Earth and Planetary Science Letters, v. 201, n. 3–4, p. 481–489, https://doi.org/10.1016/S0012-821X(02)00725-2

Montgomery, D. R., Balco, G., and Willett, S. D., 2001, Climate, tectonics, and the morphology of the Andes: Geology, v. 29, n. 7, p. 579–582, https://doi.org/10.1130/0091-7613(2001)029<0579:CTATMO>2.0.CO;2

Montomoli, C., Iaccarino, S., Carosi, R., Langone, A., and Visonà, D., 2013, Tectonometamorphic discontinuities within the Greater Himalayan Sequence in Western Nepal (Central Himalaya): Insights on the exhumation of crystalline rocks: Tectonophysics, v. 608, p. 1349–1370, https://doi.org/10.1016/j.tecto.2013.06.006

Moores, E. M., 1981, Ancient suture zones within continents: Science, v. 213, n. 4503, p. 41–46, https://doi.org/10.1126/science.213.4503.41

Morris, A., Meyer, M., Anderson, M. W., and MacLeod, C. J., 2016, Clockwise rotation of the entire Oman ophiolite occurred in a suprasubduction zone setting: Geology, v. 44, n. 12, p. 1055–1058, https://doi.org/10.1130/G38380.1

Mugnier, J. L., Huyghe, P., Chalaron, E., and Mascle, G., 1994, Recent movements along the Main Boundary Thrust of the Himalayas: Normal faulting in an overcritical thrust wedge?: Tectonophysics, v. 238, n. 1–4, p. 199–215, https://doi.org/10.1016/0040-1951(94)90056-6

Murphy, M. A., and Burgess, W. P., 2006, Geometry, kinematics, and landscape characteristics of an active transtension zone, Karakoram fault system, Southwest Tibet: Journal of Structural Geology, v. 28, n. 2, p. 268–283, https://doi.org/10.1016/j.jsg.2005.10.009

Murphy, M. A., and Copeland, P., 2005, Transtensional deformation in the central Himalaya and its role in accommodating growth of the Himalayan orogen: Tectonics, v. 24, n. 2, TC4012, https://doi.org/10.1029/2004TC001659

Murphy, M. A., and Yin, A., 2003, Structural evolution and sequence of thrusting in the Tethyan fold-thrust belt and Indus-Yalu suture zone, southwest Tibet: Geological Society of America Bulletin, v. 115, n. 1, p. 21–34, https://doi.org/10.1130/0016-7606(2003)115<0021:SEASOT>2.0.CO;2

Murphy, M. A., Yin, A., Harrison, T. M., Dürr, S. B., Chen, Z., Ryerson, F. J., Kidd, W. S. F., Wang, X., and Zhou, X., 1997, Did the Indo-Asian collision alone create the Tibetan plateau?: Geology, v. 25, n. 8, p. 719–722, https://doi.org/10.1130/0091-7613(1997)025<0719:DTIACA>2.3.CO;2

Murphy, M. A., Yin, A., Kapp, P., Harrison, T. M., Lin, D., and Jinghui, G., 2000, Southward propagation of the Karakoram fault system, southwest Tibet: Timing and magnitude of slip: Geology, v. 28, n. 5, p. 451–454, https://doi.org/10.1130/0091-7613(2000)28<451:SPOTKF>2.0.CO;2

Murphy, M. A., Yin, A., Kapp, P., Harrison, T. M., Manning, C. E., Ryerson, F. J., Ding, L., and Guo, J., 2002, Structural and thermal evolution of the Gurla Mandhata detachment system, southwest Tibet: Implications for the eastward extent of the Karakoram fault system: Geological Society of America Bulletin, v. 114, n. 4, p. 428–447, https://doi.org/10.1130/0016-7606(2002)114<0428:SEOTGM>2.0.CO;2

Murphy, M. A., Saylor, J. E., and Ding, L., 2009, Late Miocene topographic inversion in southwest Tibet based on integrated paleoelevation reconstructions and structural history: Earth and Planetary Science Letters, v. 282, n. 1–4, p. 1–9, https://doi.org/10.1016/j.epsl.2009.01.006

Murphy, M. A., Taylor, M. H., Gosse, J., Silver, C. R. P., Whipp, D. M., and Beaumont, C., 2014, Limit of strain partitioning in the Himalaya marked by large earthquakes in western Nepal: Nature Geoscience, v. 7, p. 38–42, https://doi.org/10.1038/NGEO2017

Myrow, P. M., Hughes, N. C., Goodge, J. W., Fanning, C. M., Williams, I. S., Peng, S., Bhargava, O. N., Parcha, S. K., and Pogue, K. R., 2010, Extraordinary transport and mixing of sediment across Himalayan central

Gondwana during the Cambro-Ordovician: Geological Society of America Bulletin, v. 122, n. 9–10, p. 1660–1670, https://doi.org/10.1130/B30123.1
Nábělek, J. L., Hetényi, G., Vergne, J., Sapkota, S., Kafle, B., Jiang, M., Su, H., Chen, J., Huang, B.-S., and the Hi-CLIMBTeam, 2009, Underplating in the Himalaya-Tibet collision zone revealed by the Hi-CLIMB experiment: Science, v. 325, n. 5946, p. 1371–1374, https://doi.org/10.1126/science.1167719
Nagy, C., Godin, L., Antolin, B., Cottle, J., and Archibald, D., 2015, Midi-Miocene initiation of orogen-parallel extension, NW Nepal Himalaya: Lithosphere, v. 7, n. 5, p. 483–502, https://doi.org/10.1130/L425.1
Najman, Y., Carter, A., Oliver, G., and Garzanti, E., 2005, Provenance of Eocene foreland basin sediments, Nepal: Constraints to the timing and diachroneity of early Himalayan orogenesis: Geology, v. 33, n. 4, p. 309–312, https://doi.org/10.1130/G21161.1
Najman, Y., Bickle, M., BouDagher-Fadel, M., Carter, A., Garzanti, E., Paul, M., Wijbrans, J., Willett, E., Oliver, G., Parrish, R., Akhter, S. H., Allen, R., Ando, S., Chisty, E., Reisberg, L., and Vezzoli, G., 2008, The Paleogene record of Himalayan erosion: Bengal Basin, Bangladesh: Earth and Planetary Science Letters, v. 273, n. 1–2, p. 1–14, https://doi.org/10.1016/j.epsl.2008.04.028
Najman, Y., Appel, E., Boudagher-Fadel, M., Bown, P., Carter, A., Garzanti, E., Godin, L., Han, J., Liebke, U., Oliver, G., Parrish, R., and Vezzoli, G., 2010, Timing of India-Asia collision: Geological, biostratigraphic, and palaeomagnetic constraints: Journal of Geophysical Research-Solid Earth, v. 115, B12416, https://doi.org/10.1029/2010JB007673
Nakata, T., 1989, Active faults of the Himalaya of India and Nepal, *in* Malinconica, L. L., Jr., and Lillie, R. J., editors, Tectonics of the western Himalayas: Geological Society of America Special Paper 232, p. 243–264, https://doi.org/10.1130/SPE232-p243
Negredo, A. M., Replumaz, A., Villaseñor, A., and Guillot, S., 2007, Modeling the evolution of continental subduction processes in the Pamir-Hindu Kush region: Earth and Planetary Science Letters, v. 259, n. 1–2, p. 212–225, https://doi.org/10.1016/j.epsl.2007.04.043
Nelson, K. D., Zhao, W., Brown, L. D., Kuo, J., Che, J., Liu, X., Klemperer, S. L., Makovsky, Y., Meissner, R., Mechie, J., Kind, R., Wenzel, F., Ni, J., Nabelek, J., Chen Leshou, Tan, H., Wei, W., Jones, A. G., Booker, J., Unsworth, M., Kidd, W. S. F., Hauck, M., Alsdorf, D., Ross, A., Cogan, M., Wu, C., Sandvol, E., and Edwards, M., 1996, Partially molten middle crust beneath southern Tibet: Synthesis of Project INDEPTH results: Nature, v. 274, n. 5293, p. 1684–1688, https://doi.org/10.1126/science.274.5293.1684
Ni, J., and Barazangi, M., 1983, High-frequency seismic wave propagation beneath the Indian Shield, Himalayan Arc, Tibetan Plateau and surrounding regions: High uppermost mantle velocities and efficient S_n propagation beneath Tibet: Geophysical Journal of the Royal Astronomical Society, v. 72, n. 3, p. 665–689, https://doi.org/10.1111/j.1365-246X.1983.tb02826.x
Nicolas, A., Girardeau, J., Marcoux, J., Dupre, B., Wang, X., Cao, Y., Zheng, H. B., and Xiao, X., 1981, The Xigaze ophiolite (Tibet): A peculiar oceanic lithosphere: Nature, v. 294, p. 414–417, https://doi.org/10.1038/294414a0
Nie, J., Ruetenik, G., Gallagher, K., Hoke, G., Garzione, C. N., Wang, W., Stockli, D., Hu, X., Wang, Z., Wang, Y., Stevens, T., Danišík, M., and Liu, S., 2018, Rapid incision of the Mekong River in the middle Miocene linked to monsoonal precipitation: Nature Geoscience, v. 11, p. 944–948, https://doi.org/10.1038/s41561-018-0244-z
Nie, S., Yin, A., Rowley, D. B., and Jin, Y., 1994, Exhumation of the Dabie Shan ultra-high pressure rocks and accumulation of the Songpan-Ganzi flysch sequence, central China: Geology, v. 22, n. 11, p. 999–1002, https://doi.org/10.1130/0091-7613(1994)022<0999:EOTDSU>2.3.CO;2
Nomade, S., Renne, P. R., Mo, X., Zhao, Z., and Zhou, S., 2004, Miocene volcanism in the Lhasa block, Tibet: Spatial trends and geodynamic implications: Earth and Planetary Science Letters, v. 221, n. 1–4, p. 227–243, https://doi.org/10.1016/S0012-821X(04)00072-X
O'Brien, P. J., Zotov, N., Law, R., Khan, M. A., and Jan, M. Q., 2001, Coesite in Himalayan eclogite and implications for models of India-Asia collision: Geology, v. 29, n. 5, p. 435–438, https://doi.org/10.1130/0091-7613(2001)029<0435:CIHEAI>2.0.CO;2
Orme, D. A., and Laskowski, A. K., 2016, Basin analysis of the Albian-Santonian Xigaze forearc, Lazi region, south-central Tibet: Journal of Sedimentary Research, v. 86, n. 8, p. 894–913, https://doi.org/10.2110/jsr.2016.59
Orme, D. A., Carrapa, B., and Kapp, P., 2015, Sedimentology, provenance and geochronology of the upper Cretaceous-lower Eocene western Xigaze forearc basin, southern Tibet: Basin Research, v. 27, n. 4, p. 387–411, https://doi.org/10.1111/bre.12080
Ou, Q., Wang, Q., Wyman, D. A., Zhang, H.-X., Yang, J.-H., Zeng, J.-P., Hao, L.-L., Chen, Y.-W., Liang, H., and Qi, Y., 2017, Eocene adakitic porphyries in the central-northern Qiangtang Block, central Tibet: Partial melting of thickened lower crust and implications of initial surface uplifting of the plateau: Journal of Geophysical Research-Solid Earth, v. 122, n. 2, p. 1025–1053, https://doi.org/10.1002/2016JB013259
Owens, T. J., and Zandt, G., 1997, Implications of crustal property variations for models of Tibetan plateau evolution: Nature, v. 387, p. 37–43, https://doi.org/10.1038/387037a0
Palin, R. M., Searle, M. P., St-Onge, M. R., Waters, D. J., Roberts, N. M. W., Horstwood, M. S. A., Parrish, R. R., Weller, O. M., Chen, S., and Yang, J., 2014, Monazite geochronology and petrology of kyanite- and sillimanite-grade migmatites from the northwestern flank of the eastern Himalayan syntaxis: Gondwana Research, v. 26, n. 1, p. 323–347, https://doi.org/10.1016/j.gr.2013.06.022
Pan, G., Ding, J., Yao, D., and Wang, L., 2004, Geological Map of the Qinghai-Xizang (Tibet) Plateau and Adjacent Areas with Guidebook: Chengdu, China, Chengdu Cartographic Publishing House, scale 1:1,500,000.
Pan, Y., ms, 1993, Unroofing history and structural evolution of the southern Lhasa terrane, Tibetan Plateau: Implications for the continental collision between India and Asia: Albany, New York, State University of New York, Albany, Ph. D. thesis, 287 p.

Pandey, M. R., Tandukar, R. P., Avouac, J. P., Vergne, J., and Héritier, T., 1999, Seismotectonics of the Nepal Himalaya from a local seismic network: Journal of Asian Earth Sciences, v. 17, n. 5–6, p. 703–712, https://doi.org/10.1016/S1367-9120(99)00034-6

Parrish, R. R., and Hodges, K. V., 1996, Isotopic constraints on the age and provenance of Lesser and Greater Himalayan sequences, Nepalese Himalaya: Geological Society of America Bulletin, v. 108, n. 7, p. 904–911, https://doi.org/10.1130/0016-7606(1996)108<0904:ICOTAA>2.3.CO;2

Parrish, R. R., Gough, S. J., Searle, M. P., and Waters, D. J., 2006, Plate velocity exhumation of ultrahigh-pressure eclogites in the Pakistan Himalaya: Geology, v. 34, n. 11, p. 989–992, https://doi.org/10.1130/G22796A.1

Patriat, P., and Achache, J., 1984, India-Eurasia collision chronology has implications for crustal shortening and driving mechanism of plates: Nature, v. 311, p. 615–620, https://doi.org/10.1038/311615a0

Pearce, J. A., and Deng, W., 1988, The ophiolites of the Tibetan Geotraverses, Lhasa to Golmud (1985) and Lhasa to Kathmandu (1986): Philosophical Transactions of the Royal Society of London, Series A, v. 327, p. 215–238, https://doi.org/10.1098/rsta.1988.0127

Pearce, J. A., and Mei, H., 1988, Volcanic rocks of the 1985 Tibet Geotraverse: Lhasa to Golmud: Philosophical Transactions of the Royal Society of London, Series A., v. 327, p. 169–201, https://doi.org/10.1098/rsta.1988.0125

Pêcher, A., 1989, The metamorphism in the Central Himalaya: Journal of Metamorphic Geology, v. 7, n. 1, p. 31–41, https://doi.org/10.1111/j.1525-1314.1989.tb00573.x

Pedersen, R. B., Searle, M. P., and Corfield, R. I., 2001, U-Pb zircon ages from the Spontang Ophiolite, Ladakh Himalaya: Journal of the Geological Society, London, v. 158, p. 513–520, https://doi.org/10.1144/jgs.158.3.513

Pepper, M., Gehrels, G., Pullen, A., Ibanez-Mejia, M., Ward, K. M., and Kapp, P., 2016, Magmatic history and crustal genesis of western South America: Constraints from U-Pb ages and Hf isotopes of detrital zircons in modern rivers: Geosphere, v. 12, n. 5, p. 1532–1555, https://doi.org/10.1130/GES01315.1

Phillips, R. J., Parrish, R. R., and Searle, M. P., 2004, Age constraints on ductile deformation and long-term slip rates along the Karakoram fault zone, Ladakh: Earth and Planetary Science Letters, v. 226, n. 3–4, p. 305–319, https://doi.org/10.1016/j.epsl.2004.07.037

Polissar, P. J., Freeman, K. H., Rowley, D. B., McInerney, F. A., and Currie, B. S., 2009, Paleoaltimetry of the Tibetan Plateau from *D/H* ratios of lipid biomarkers: Earth and Planetary Science Letters, v. 287, n. 1–2, p. 64–76, https://doi.org/10.1016/j.epsl.2009.07.037

Powers, P. M., Lillie, R. J., and Yeats, R. S., 1998, Structure and shortening of the Kangra and Dehra Dun reentrants, Sub-Himalaya, India: Geological Society of America Bulletin, v. 110, n. 8, p. 1010–1027, https://doi.org/10.1130/0016-7606(1998)110<1010:SASOTK>2.3.CO;2

Pozzi, J. P., Westphal, M., Girardeau, J., Besse, J., Zhou, Y. X., Chen, X. Y., and Xing, L. S., 1984, Paleomagnetism of the Xigaze ophiolite and flysch (Yarlung Zangbo suture zone, southern Tibet): Latitude and direction of spreading: Earth and Planetary Science Letters, v. 70, n. 2, p. 383–394, https://doi.org/10.1016/0012-821X(84)90022-0

Pullen, A., and Kapp, P., 2014, Mesozoic tectonic history and lithospheric structure of the Qiangtang terrane: Insights from the Qiangtang metamorphic belt, central Tibet, *in* Nie, J., Horton, B. K., and Hoke, G. D., editors, Towards an Improved Understanding of Uplift Mechanisms and the Elevation History of the Tibetan Plateau: Geological Society of America Special Paper 507, p. 71–87, https://doi.org/10.1130/2014.2507(04)

Pullen, A., Kapp, P., Gehrels, G. E., DeCelles, P. G., Brown, E. H., Fabijanic, J. M., and Ding, L., 2008a, Gangdese retroarc thrust belt and foreland basin deposits in the Damxung area, southern Tibet: Journal of Asian Earth Sciences, v. 33, n. 5–6, p. 323–336, https://doi.org/10.1016/j.jseaes.2008.01.005

Pullen, A., Kapp, P., Gehrels, G. E., Vervoort, J. D., and Ding, L., 2008b, Triassic continental subduction in central Tibet and Mediterranean-style closure of the Paleo-Tethys Ocean: Geology, v. 36, n. 5, p. 351–354, https://doi.org/10.1130/G24435A.1

Pullen, A., Kapp, P., DeCelles, P. G., Gehrels, G. E., and Ding, L., 2011a, Cenozoic anatexis and exhumation of Tethyan Sequence rocks in the Xiao Gurla Range, Southwest Tibet: Tectonophysics, v. 501, n. 1–4, p. 28–40, https://doi.org/10.1016/j.tecto.2011.01.008

Pullen, A., Kapp, P., Gehrels, G. E., Ding, L., and Zhang, Q., 2011b, Metamorphic rocks in central Tibet: Lateral variations and implications for crustal structure: Geological Society of America Bulletin, v. 123, n. 3–4, p. 585–600, https://doi.org/10.1130/B30154.1

Quade, J., Breecker, D. O., Daëron, M., and Eiler, J., 2011, The paleoaltimetry of Tibet: An isotopic perspective: American Journal of Science, v. 311, p. 77–115, https://doi.org/10.2475/02.2011.01

Quidelleur, X., Grove, M., Lovera, O. M., Harrison, T. M., and Yin, A., 1997, Thermal evolution and slip history of the Renbu-Zedong Thrust, southeastern Tibet: Journal of Geophysical Research, v. 102, n. B2, p. 2659–2679, https://doi.org/10.1029/96JB02483

Quigley, M., Liangjun, Y., Xiaohan, L., Wilson, C. J. L., Sandiford, M., and Phillips, D., 2006, ^{40}Ar/^{39}Ar thermochronology of the Kampa Dome, southern Tibet: Implications for tectonic evolution of the North Himalayan gneiss domes: Tectonophysics, v. 421, n. 3–4, p. 269–297, https://doi.org/10.1016/j.tecto.2006.05.002

Raiverman, V., Kunte, S. V., and Mukherjee, A., 1983, Basin geometry, Cenozoic sedimentation and hydrocarbon prospects in North-western Himalaya and Indo-Gangetic plains: Petroleum Asia Journal, v. 6, p. 67–92.

Raterman, N. S., Cowgill, E., and Ding, L., 2007, Variable structural style along the Karakoram fault explained using triple-junction analysis of intersecting faults: Geosphere, v. 3, n. 2, p. 71–85, https://doi.org/10.1130/GES00067.1

Ratschbacher, L., Frisch, W., Chen, C., and Pan, G., 1992, Deformation and motion along the southern

margin of the Lhasa Block (Tibet) prior to and during the India-Asia collision: Journal of Geodynamics, v. 16, n. 1–2, p. 21–54, https://doi.org/10.1016/0264-3707(92)90017-M
Ratschbacher, L., Frisch, W., Liu, G., and Chen, C. C., 1994, Distributed deformation in southern and western Tibet during and after the India-Asian collision: Journal of Geophysical Research-Solid Earth, v. 99, n. B10, p. 19917–19945, https://doi.org/10.1029/94JB00932
Ravikant, V., Wu, F.-Y., and Ji, W.-Q., 2011, U-Pb age and Hf isotopic constraints of detrital zircons from the Himalayan foreland Subathu sub-basin on the Tertiary palaeogeography of the Himalaya: Earth and Planetary Science Letters, v. 304, n. 3–4, p. 356–368, https://doi.org/10.1016/j.epsl.2011.02.009
Raymo, M. E., and Ruddiman, W. F., 1992, Tectonic forcing of late Cenozoic climate: Nature v. 359, p. 117–122, https://doi.org/10.1038/359117a0
Razi, A. S., Roecker, S. W., and Levin, V., 2016, The fate of the Indian lithosphere beneath western Tibet: Upper mantle elastic wave speed structure from a joint teleseismic and regional body wave tomographic study: Physics of the Earth and Planetary Interiors, v. 251, p. 11–23, https://doi.org/10.1016/j.pepi.2015.12.001
Regis, D., Warren, C. J., Young, D., and Roberts, N. M. W., 2014, Tectono-metamorphic evolution of the Jomolhari massif: Variations in timing of syn-collisional metamorphism across western Bhutan: Lithos, v. 190–191, p. 449–466, https://doi.org/10.1016/j.lithos.2014.01.001
Rehman, H. U., Kobayash, K., Tsujimori, T., Ota, T., Yamamoto, H., Nakamura, E., Kaneko, Y., Khan, T., Terbayashi, M., Yoshida, K., and Hirajima, T., 2013, Ion microprobe U-Th-Pb geochronology and study of micro-inclusions in zircon from the Himalayan high- and ultrahigh-pressure eclogites, Kaghan Valley of Pakistan: Journal of Asian Earth Sciences, v. 63, p. 179–196, https://doi.org/10.1016/j.jseaes.2012.04.025
Reid, A., Wilson, C. J. L., Shun, L., Pearson, N. J., and Belousova, E., 2007, Mesozoic plutons of the Yidun Arc, SW China: U/Pb geochronology and Hf isotopic signature: Ore Geology Reviews, v. 31, n. 1–4, p. 88–106, https://doi.org/10.1016/j.oregeorev.2004.11.003
Replumaz, A., and Tapponnier, P., 2003, Reconstruction of the deformed collision zone between India and Asia by backward motion of lithospheric blocks: Journal of Geophysical Research-Solid Earth, v. 108, n. B6, 2285, https://doi.org/10.1029/2001JB000661
Replumaz, A., Negredo, A. M., Guillot, S., van der Beek, P., and Villaseñor, A., 2010a, Crustal mass budget and recycling during the India/Asia collision: Tectonophysics, v. 492, n. 1–4, p. 99–107, https://doi.org/10.1016/j.tecto.2010.05.023
Replumaz, A., Negredo, A. M., Villaseñor, A., and Guillot, S., 2010b, Indian continental subduction and slab break-off during Tertiary collision: Terra Nova, v. 22, n. 4, p. 290–296; https://doi.org/10.1111/j.1365-3121.2010.00945.x
Robinson, A. C., 2015, Mesozoic tectonics of the Gondwanan terranes of the Pamir plateau: Journal of Asian Earth Sciences, v. 102, p. 170–179, https://doi.org/10.1016/j.jseaes.2014.09.012
Robinson, D. M., and Martin, A. J., 2014, Reconstructing the Greater Indian margin: A balanced cross section in central Nepal focusing on the Lesser Himalayan duplex: Tectonics, v. 33, n. 11, p. 2143–2168, https://doi.org/10.1002/2014TC003564
Robinson, D. M., and McQuarrie, N., 2012, Pulsed deformation and variable slip rates within the central Himalayan thrust belt: Lithosphere, v. 4, n. 5, p. 449–464, https://doi.org/10.1130/L204.1
Roecker, S. W., 1982, Velocity structure of the Pamir-Hindu Kush region: Possible evidence of subducted crust: Journal of Geophysical Research, v. 87, n. B2, p. 945–959, https://doi.org/10.1029/JB087iB02p00945
Roger, F., Arnaud, N., Gilder, S., Tapponnier, P., Jolivet, M., Brunel, M., Malavieille, J., Xu, Z., and Yang, J., 2003, Geochronological and geochemical constraints on Mesozoic suturing in east central Tibet: Tectonics, v. 22, n. 4, 1037, https://doi.org/10.1029/2002TC001466
Roger, F., Jolivet, M., and Malavieille, J., 2008, Tectonic evolution of the Triassic fold belts of Tibet: Comptes Rendus Geoscience, v. 340, n. 2–3, p. 180–189, https://doi.org/10.1016/j.crte.2007.10.014
——— 2010, The tectonic evolution of the Songpan-Garzê (North Tibet) and adjacent areas from Proterozoic to Present: A synthesis: Journal of Asian Earth Sciences, v. 39, n. 4, p. 254–269, https://doi.org/10.1016/j.jseaes.2010.03.008
Rohrmann, A., Kapp, P., Carrapa, B., Reiners, P. W., Guynn, J., Ding, L., and Heizler, M., 2012, Thermochronologic evidence for plateau formation in central Tibet by 45 Ma: Geology, v. 40, n. 2, p. 187–190, https://doi.org/10.1130/G32530.1
Rowley, D. B., and Currie, B. S., 2006, Palaeo-altimetry of the late Eocene to Miocene Lunpola basin, central Tibet: Nature, v. 439, p. 677-681, https://doi.org/10.1038/nature04506
Rowley, D. B., Pierrehumbert, R. T., and Currie, B. S., 2001, A new approach to stable isotope-based paleoaltimetry: Implications for paleoaltimetry and paleohypsometry of the High Himalaya since the Late Miocene: Earth and Planetary Science Letters, v. 188, n. 1–2, p. 253–268, https://doi.org/10.1016/S0012-821X(01)00324-7
Royden, L. H., Burchfiel, B. C., King, R. W., Wang, E., Chen, Z. J., Shen, F., and Liu, Y., 1997, Surface deformation and lower crustal flow in eastern Tibet: Science, v. 276, n. 5313, p. 788–790, https://doi.org/10.1126/science.276.5313.788
Royden, L. H., Burchfiel, B. C., and Van der Hilst, R. D., 2008, The geological evolution of the Tibetan Plateau: Science, v. 321, n. 5892, p. 1054–1058, https://doi.org/10.1126/science.1155371
Rust, J., Singh, H., Rana, R. S., McCann, T., Singh, L., Anderson, K., Sarkar, N., Nascimbene, P. C., Stebner, F., Thomas, J. C., Kraemer, M. S., Williams, C. J., Engel, M. S., Sahni, A., and Grimaldi, D., 2010, Biogeographic and evolutionary implications of a diverse paleobiota in amber from the early Eocene of India: PNAS, v. 107, n. 43, p. 18360–18365, https://doi.org/10.1073/pnas.1007407107
Rutte, D., Ratschbacher, L., Schneider, S., Stübner, K., Stearns, M. A., Gulzar, M. A., and Hacker, B. R., 2017a, Building the Pamir-Tibetan Plateau-Crustal stacking, extensional collapse, and lateral extrusion

in the Central Pamir: 1. Geometry and kinematics: Tectonics, v. 36, n. 3, p. 342–384, https://doi.org/10.1002/2016TC004293

Rutte, D., Ratschbacher, L., Khan, J., Stübner, K., Hacker, B. R., Stearns, M. A., Enkelmann, E., Jonckheere, R., Pfänder, J. A., Sperner, B., and Tichomirowa, M., 2017b, Building the Pamir-Tibetan Plateau-Crustal stacking, extensional collapse, and lateral extrusion in the Central Pamir: 2. Timing and rates: Tectonics, v. 36, n. 3, p. 385–419, https://doi.org/10.1002/2016TC004294

Sanchez, V. I., Murphy, M. A., Robinson, A. C., Lapen, T. J., and Heizler, M. T., 2013, Tectonic evolution of the India-Asia suture zone since Middle Eocene time, Lopukangri area, south-central Tibet: Journal of Asian Earth Sciences, v. 62, p. 205–220, https://doi.org/10.1016/j.jseaes.2012.09.004

Sapkota, S. N., Bollinger, L., Klinger, Y., Tapponnier, P., Gaudemer, Y., and Tiwari, D., 2013, Primary surface ruptures of the great Himalayan earthquakes in 1934 and 1255: Nature Geoscience, v. 6, p. 71–76, https://doi.org/10.1038/NGEO1669

Saylor, J. E., Quade, J., Dettman, D. L., DeCelles, P. G., Kapp, P. A., and Ding, L., 2009, The Late Miocene through present paleoelevation history of southwestern Tibet: American Journal of Science, v. 309, n. 1, p. 1–42, https://doi.org/10.2475/01.2009.01

Saylor, J., DeCelles, P. G., Gehrels, G., Murphy, M., Zhang, R., and Kapp, P., 2010, Basin formation in the High Himalaya by arc-parallel extension and tectonic damming: Zhada basin, southwestern Tibet: Tectonics, v. 29, n. 1, TC1004, https://doi.org/10.1029/2008TC002390

Schärer, U., Xu, R. H., and Allègre, C. J., 1984, U-Pb geochronology of Gangdese (Transhimalaya) plutonism in the Lhasa-Xigaze region, Tibet: Earth and Planetary Science Letters, v. 69, n. 2, p. 311–320, https://doi.org/10.1016/0012-821X(84)90190-0

Schellart, W. P., 2008, Kinematics and flow patterns in deep mantle and upper mantle subduction models: Influence of the mantle depth and slab to mantle viscosity ratio: Geochemistry, Geophysics, Geosystems, v. 9, n. 3, Q03014, https://doi.org/10.1029/2007GC001656

Schelling, D., 1992, The tectonostratigraphy and structure of the eastern Nepal Himalaya: Tectonics, v. 11, n. 5, p. 925–943, https://doi.org/10.1029/92TC00213

Schlische, R. W., 1992, Structural and stratigraphic development of the Newark extensional basin, eastern North America: Evidence for the growth of the basin and its bounding structures: Geological Society of America Bulletin, v. 104, n. 10, p. 1246–1263, https://doi.org/10.1130/0016-7606(1992)104<1246:SASDOT>2.3.CO;2

Schneider, W., Mattern, F., Wang, P., and Li, C., 2003, Tectonic and sedimentary basin evolution of the eastern Bangong-Nujiang zone (Tibet): A Reading cycle: Geologische Rundschau, v. 92, p. 228–254, https://doi.org/10.1007/s00531-003-0311-5

Schulte-Pelkum, V., Monsalve, G., Sheehan, A., Pandey, M. R., Sapkota, S., Bilham, R., and Wu, F., 2005, Imaging the Indian subcontinent beneath the Himalaya: Nature, v. 435, p. 1222–1225, https://doi.org/10.1038/nature03678

Schwab, M., Ratschbacher, L., Siebel, W., McWilliams, M., Minaev, V. T., Lutkov, V., Chen, F., Stanek, K., Nelson, B., Frisch, W., and Wooden, J. L., 2004, Assembly of the Pamirs: Age and origin of magmatic belts from the southern Tien Shan to the southern Pamirs and their relation to Tibet: Tectonics, v. 23, n. 4, TC4002, https://doi.org/10.1029/2003TC001583

Searle, M. P., 1986, Structural evolution and sequence of thrusting in the High Himalayan, Tibetan-Tethys and Indus suture zones of Zanskar and Ladakh, Western Himalaya: Journal of Structural Geology, v. 8, n. 8, p. 923–936, https://doi.org/10.1016/0191-8141(86)90037-4

Searle, M. P., and Treloar, P. J., 2010, Was Late Cretaceous-Paleocene obduction of ophiolite complexes the primary cause of crustal thickening and regional metamorphism in the Pakistan Himalaya?, *in* Kusky, T. M., Zhai, M.-G., and Xiao, W., editors, The Evolving Continents: Understanding Processes of Continental Growth: Geological Society, London, Special Publications, v. 338, p. 345–359, https://doi.org/10.1144/SP338.16

Searle, M. P., Windley, B. F., Coward, M. P., Cooper, D. J. W., Rex, A. J., Li, T., Xiao, X., Jan, M. Q., Thakur, V. C., and Kumar, S., 1987, The closing of the Tethys and the tectonics of the Himalaya: Geological Society of America Bulletin, v. 98, n. 6, p. 678–701, https://doi.org/10.1130/0016-7606(1987)98<678:TCOTAT>2.0.CO;2

Searle, M. P., Cooper, D. J. W., Rex, A. J., and Colchen, M., 1988, Collision tectonics of the Ladakh-Zanskar Himalaya: Philosophical Transactions of the Royal Society A, v. 326, n. 1589, p. 117–150, https://doi.org/10.1098/rsta.1988.0082

Searle, M. P., Parrish, R. R., Hodges, K. V., Hurford, A., Ayres, M. W., and Whitehouse, M. J., 1997, Shisha Pangma leucogranite, south Tibetan Himalaya: Field relations, geochemistry, age, origin, and emplacement: The Journal of Geology, v. 105, n. 3, p. 295–317, https://doi.org/10.1086/515924

Searle, M. P., Law, R. D., Godin, L., Larson, K. P., Streule, M. J., Cottle, J. M., and Jessup, M. J., 2008, Defining the Himalayan Main Central Thrust in Nepal: Journal of the Geological Society, London, v. 165, p. 523–534, https://doi.org/10.1144/0016-76492007-081

Searle, M. P., Elliott, J. R., Phillips, R. J., and Chung, S.-L., 2011, Crustal-lithospheric structure and continental extrusion of Tibet: Journal of the Geological Society, London, v. 168, p. 633–672, https://doi.org/10.1144/0016-76492010-139

Searle, M. P., Waters, D. J., Garber, J. M., Rioux, M., Cherry, A. G., and Ambrose, T. K., 2015, Structure and metamorphism beneath the obducting Oman ophiolite: Evidence from the Bani Hamid granulites, northern Oman mountains: Geosphere, v. 11, n. 6, p. , https://doi.org/10.1130/GES01199.1

Seeber, L., and Armbruster, J. G., 1984, Some elements of continental subduction along the Himalayan front: Tectonophysics, v. 105, n. 1–4, p. 263–278, https://doi.org/10.1016/0040-1951(84)90207-5

Seeber, L., and Pêcher, A., 1998, Strain partitioning along the Himalayan arc and the Nanga Parbat antiform: Geology, v. 26, n. 9, p. 791–794, https://doi.org/10.1130/0091-7613(1998)026<0791:SPATHA>2.3.CO;2

Seghedi, I., Downes, H., Szakács, A., Mason, P. R. D., Thirlwall, M. F., Roşu, E., Pécskay, Z., Márton, E., and Panaiotu, C., 2004, Neogene-Quaternary magmatism and geodynamics in the Carpathian-Pannonian region: A synthesis: Lithos, v. 72, v. 3–4, p. 117–146, https://doi.org/10.1016/j.lithos.2003.08.006
Şengör, A. M. C., 1984, The Cimmeride orogenic system and the tectonics of Eurasia: Geological Society of America Special Paper 195, p. 1–88, https://doi.org/10.1130/SPE195-p1
Şengör, A. M. C., and Natal'in, B. A., 1996, Paleotectonics of Asia: Fragments of a synthesis, *in* Yin, A., and Harrison, T. M., editors, The Tectonic Evolution of Asia: New York, Cambridge University Press, p. 486–640.
Shackleton, R. M., 1981, Structure of Southern Tibet: Report on a traverse from Lhasa to Khatmandu organised by Academia Sinica: Journal of Structural Geology, v. 3, n. 1, p. 97–105, https://doi.org/10.1016/0191-8141(81)90060-2
Shen, T., Wang, G., Leloup, P. H., van der Beek, P., Bernet, M., Cao, K., Wang, A., Liu, C. Y., and Zhang, K., 2016, Controls on Cenozoic exhumation of the Tethyan Himalaya from fission-track thermochronology and detrital zircon U-Pb geochronology in the Gyirong basin area, southern Tibet: Tectonics, v. 35, n. 7, p. 1713–1734, https://doi.org/10.1002/2016TC004149
Shen, Z.-k., Zhao, C., Yin, A., Li, Y., Jackson, D. D., Fang, P., and Dong, D., 2000, Contemporary crustal deformation in east Asia constrained by Global Positioning System measurements: Journal of Geophysical Research, v. 105, n. B3, p. 5721–5734, https://doi.org/10.1029/1999JB900391
Shi, R., Yang, J., Xu, Z., and Qi, X., 2004, Discovery of the boninite series volcanic rocks in the Bangong Lake ophiolite melange, western Tibet, and its tectonic implications: Chinese Science Bulletin, v. 49, n. 12, p. 1272–1278, https://doi.org/10.1360/04wd0006
Shi, R. D., 2007, SHRIMP dating of the Bangong Lake SSZ-type ophiolite: Constraints on the closure time of ocean in the Bangong Lake-Nujiang River, northwestern Tibet: Chinese Science Bulletin, v. 52, n. 7, p. 936–941, https://doi.org/10.1007/s11434-007-0134-z
Sippl, C., Schurr, B., Yuan, X., Mechie, J., Schneider, F. M., Gadoev, M., Orunbaev, S., Oimahmadov, I., Haberland, C., Abdybachaev, U., Minaev, V., Negmatullaev, S., and Radjabov, N., 2013, Geometry of the Pamir-Hindu Kush intermediate-depth earthquake zone from local seismic data: Journal of Geophysical Research-Solid Earth, v. 118, n. 4, p. 1438–1457, https://doi.org/110.1002/jgrb.50128
Smit, M. A., Hacker, B. R., and Lee, J., 2014, Tibetan garnet records early Eocene initiation of thickening in the Himalaya: Geology, v. 42, n. 7, p. 591–594, https://doi.org/10.1130/G35524.1
Smith, M. E., Cassel, E. J., Jicha, B. R., Singer, B. S., and Canada, A. S., 2017, Hinterland drainage closure and lake formation in response to middle Eocene Farallon slab removal, Nevada, U.S.A.: Earth and Planetary Science Letters, v. 479, p. 156–169, https://doi.org/10.1016/j.epsl.2017.09.023
Song, C., Wang, J., Fu, X., and He, L., 2013, Mesozoic and Cenozoic cooling history of the Qiangtang Block, northern Tibet, China: New constraints from apatite and zircon fission track data: Terrestrial, Atmospheric and Oceanic Sciences, v. 24, n. 6, p. 985–998, https://doi.org/10.3319/TAO.2013.07.05.02(TT)
Soucy La Roche, R., Godin, L., and Crowley, J. L., 2017, Reappraisal of emplacement models for Himalayan external crystalline nappes: The Jajarkot klippe, western Nepal: Geological Society of America Bulletin, v. 130, n. 5–6, p. 1041–1056, https://doi.org/10.1130/B31799.1
Spicer, R. A., Harris, N. B. W., Widdowson, M., Herman, A. B., Guo, S., Valdes, P. J., Wolfe, J. A., and Kelley, S. P., 2003, Constant elevation of southern Tibet over the past 15 million years: Nature, v. 421, p. 622–624, https://doi.org/10.1038/nature01356
Spurlin, M. S., Yin, A., Horton, B. K., Zhou, J., and Wang, J., 2005, Structural evolution of the Yushu-Nangqian region and its relationship to syncollisional igneous activity, east-central Tibet: Geological Society of America Bulletin, v. 117, n. 9–10, p. 1293–1317, https://doi.org/10.1130/B25572.1
St-Onge, M. R., Rayner, N., Palin, R. M., Searle, M. P., and Waters, D. J., 2013, Integrated pressure-temperature-time constraints for the Tso Morari dome (Northwest India): Implications for the burial and exhumation path of UHP units in the western Himalaya: Journal of Metamorphic Geology, v. 31, n. 5, p. 469–504, https://doi.org/10.1111/jmg.12030
Staisch, L. M., Niemi, N. A., Hong, C., Clark, M. K., Rowley, D. B., and Currie, B., 2014, A Cretaceous-Eocene depositional age for the Fenghuoshan Group, Hoh Xil Basin: Implications for the tectonic evolution of the northern Tibet Plateau: Tectonics, v. 33, n. 3, p. 281–301, https://doi.org/10.1002/2013TC003367
Staisch, L. M., Niemi, N. A., Clark, M. K., and Chang, H., 2016, Eocene to late Oligocene history of crustal shortening within the Hoh Xil Basin and implications for the uplift history of the northern Tibetan Plateau: Tectonics, v. 35, n. 4, p. 862–895, https://doi.org/10.1002/2015TC003972
Steck, A., 2003, Geology of the NW Indian Himalaya: Eclogae Geologicae Helvetiae, v. 96, p. 147–196.
Steck, A., Spring, L., Vannay, J.-C., Masson, H., Stutz, E., Bucher, H., Marchant, R., and Tieche, J.-C., 1993, Geological transect across the Northwestern Himalaya in eastern Ladakh and Lahul (A model for the continental collision of India and Asia): Eclogae Geologicae Helvetiae, v. 86, p. 219–263.
Stegman, D. R., Farrington, R., Capitanio, F. A., and Schellart, W. P., 2010, A regime diagram for subduction styles from 3-D numerical models of free subduction: Tectonophysics, v. 483, n. 1–2, p. 29–45, https://doi.org/10.1016/j.tecto.2009.08.041
Stern, R. J., 2004, Subduction initiation: Spontaneous and induced: Earth and Planetary Science Letters, v. 226, n. 3–4, p. 275–292, https://doi.org/10.1016/j.epsl.2004.08.007
Stevens, V. L., and Avouac, J. P., 2015, Interseismic coupling on the main Himalayan thrust: Geophysical Research Letters, v. 42, n. 14, p. 5828–5837, https://doi.org/10.1002/2015GL064845
Stübner, K., Ratschbacher, L., Rutte, D., Stanek, K., Minaev, V., Wiesinger, M., Gloaguen, R., and Project TIPAGE members, 2013a, The giant Shakhdara migmatitic gneiss dome, Pamir, India-Asia collision zone: 1. Geometry and kinematics: Tectonics, v. 32, n. 4, p. 948–979, https://doi.org/10.1002/tect.20057
Stübner, K., Ratschbacher, L., Weise, C., Chow, J., Hofmann, J., Khan, J., Rutte, D., Sperner, B., Pfänder, J. A., Hacker, B. R., Dunkl, I., Tichomirowa, M., Stearns, M. A., and Project TIPAGE members, 2013b,

The giant Shakhdara migmatitic gneiss dome, Pamir, India-Asia collision zone: 2. Timing of dome formation: Tectonics, v. 32, n. 5, p. 1404–1431, https://doi.org/10.1002/tect.20059

Stübner, K., Grujic, D., Parrish, R. R., Roberts, N. M. W., Kronz, A., Wooden, J., and Ahmad, T., 2014, Monazite geochronology unravels the timing of crustal thickening in NW Himalaya: Lithos, v. 210–211, p. 111–128, https://doi.org/10.1016/j.lithos.2014.09.024

Styron, R., Taylor, M. H., and Murphy, M. A., 2011, Oblique convergence, arc-parallel extension, and the role of strike-slip faulting in the High Himalaya: Geosphere, v. 7, n. 2, p. 582–596, https://doi.org/10.1130/GES00606.1

Styron, R., Taylor, M., and Sundell, K., 2015, Accelerated extension of Tibet linked to the northward underthrusting of Indian crust: Nature Geoscience, v. 8, p. 131–134, https://doi.org/10.1038/NGEO2336

Sun, B., Wang, Y.-F., Li, C.-S., Yang, J., Li, J.-F., Li, Y.-L., Deng, T., Wang, S.-Q., Zhao, M., Spicer, R. A., Ferguson, D. K., and Mehrotra, R. C., 2015a, Early Miocene elevation in northern Tibet estimated by palaeobotanical evidence: Scientific Reports, v. 5, article number 10379, https://doi.org/10.1038/srep10379

Sun, G., Hu, X., Sinclair, H. D., BouDagher-Fadel, M. K., and Wang, J., 2015b, Late Cretaceous evolution of the Coqen Basin (Lhasa terrane) and implications for early topographic growth on the Tibetan Plateau: Geological Society of America Bulletin, v. 127, n. 7–8, p. 1001–1020, https://doi.org/10.1130/B31137.1

Sun, G.-Y., Hu, X.-M., Zhu, D.-C., Hong, W.-T., Wang, J.-G., and Wang, Q., 2015c, Thickened juvenile lower crust-derived ~90 Ma adakitic rocks in the central Lhasa terrane, Tibet: Lithos, v. 224–225, p. 225-239, https://doi.org/10.1016/j.lithos.2015.03.010

Sun, J., and Jiang, M., 2013, Eocene seawater retreat from the southwest Tarim Basin and implications for early Cenozoic tectonic evolution in the Pamir Plateau: Tectonophysics, v. 588, p. 27–38, https://doi.org/10.1016/j.tecto.2012.11.031

Sun, J., Xu, Q., Liu, W., Zhang, Z., Xue, L., and Zhao, P., 2014, Palynological evidence for the latest Oligocene-early Miocene paleoelevation estimate in the Lunpola Basin, central Tibet: Palaeogeography, Palaeoclimatology, Palaeoecology, v. 399, p. 21–30, https://doi.org/10.1016/j.palaeo.2014.02.004

Sun, Z., Pei, J., Li, H., Xu, W., Jiang, W., Zhu, Z., Wang, X., and Yang, Z., 2012, Palaeomagnetism of late Cretaceous sediments from southern Tibet: Evidence for the consistent palaeolatitudes of the southern margin of Eurasia prior to the collision with India: Gondwana Research, v. 21, n. 1, p. 53–63, https://doi.org/10.1016/j.gr.2011.08.003

Sundell, K. E., Taylor, M. H., Styron, R. H., Stockli, D. F., Kapp, P., Hager, C., Liu, D., and Ding, L., 2013, Evidence for constriction and Pliocene acceleration of east-west extension in the North Lunggar rift region of west central Tibet: Tectonics, v. 32, n. 5, p. 1454–1479, https://doi.org/10.1002/tect.20086

Tang, X.-C., and Zhang, K.-J., 2014, Lawsonite- and glaucophane-bearing blueschists from NW Qiangtang, northern Tibet, China: Mineralogy, geochemistry, geochronology, and tectonic implications: International Geology Review, v. 56, n. 2, p. 150–166, https://doi.org/10.1080/00206814.2013.820866

Tapponnier, P., and Molnar, P., 1976, Slip-line field theory and large-scale continental tectonics: Nature, v. 264, p. 319–324, https://doi.org/10.1038/264319a0

Tapponnier, P., Mercier, J. L., Proust, F., Andrieux, J., Armijo, R., Bassoullet, J. P., Brunel, M., Burg, J. P., Colchen, M., Dupré, B., Girardeau, J., Marcoux, J., Mascle, G., Matte, P., Nicolas, A., Li, T., Xiao, X., Chang, C., Lin, P., Li, G., Wang, N., Chen, G., Han, T., Wang, X., Den, W., Zhen, H., Sheng, H., Cao, Y., Zhou, J., and Qiu, H., 1981, The Tibetan side of the India-Eurasia collision: Nature, v. 294, p. 405–410, https://doi.org/10.1038/294405a0

Tapponnier, P., Peltzer, G., Le Dain, A. Y., Armijo, R., and Cobbold, P., 1982, Propagating extrusion tectonics in Asia: New insights from simple experiments with plasticine: Geology, v. 10, n. 12, p. 611–616, https://doi.org/10.1130/0091-7613(1982)10<611:PETIAN>2.0.CO;2

Tapponnier, P., Xu, Z., Roger, F., Meyer, B., Arnaud, N., Wittlinger, G., and Yang, J., 2001, Oblique stepwise rise and growth of the Tibet Plateau: Science, v. 294, n. 5547, p. 1671–1677, https://doi.org/10.1126/science.105978

Tate, G. W., McQuarrie, N., van Hinsbergen, D. J. J., Bakker, R. R., Harris, R., and Jiang, H., 2015, Australia going down under: Quantifying continental subduction during arc-continent accretion in Timor-Leste: Geosphere, v. 11, n. 6, p. 1860–1883, https://doi.org/10.1130/GES01144.1

Taylor, M., and Yin, A., 2009, Active structures of the Himalayan-Tibetan orogen and their relationships to earthquake distribution, contemporary strain field, and Cenozoic volcanism: Geosphere, v. 5, n. 3, p. 199–214, https://doi.org/10.1130/GES00217.1

Taylor, M., Yin, A., Ryerson, F. J., Kapp, P., and Ding, L., 2003, Conjugate strike-slip faulting along the Bangong-Nujiang suture zone accommodates coeval east-west extension and north-south shortening in the interior of the Tibetan Plateau: Tectonics, v. 22, n. 4, 1044, https://doi.org/10.1029/2002TC001361

Tian, Y., Kohn, B. P., Phillips, D., Hu, S., Gleadow, A. J. W., and Carter, A., 2016, Late Cretaceous-earliest Paleogene deformation in the Longmen Shan fold-and-thrust belt, eastern Tibetan Plateau margin: Pre-Cenozoic thickened crust?: Tectonics, v. 35, n. 10, p. 2293–2312, https://doi.org/10.1002/2016TC004182

Thiede, R. C., Arrowsmith, J. R., Bookhagen, B., McWilliams, M., Sobel, E. R., and Strecker, M. R., 2006, Dome formation and extension in the Tethyan Himalaya, Leo Pargil, northwest India: Geological Society of America Bulletin, v. 118, n. 5–6, p. 635–650, https://doi.org/10.1130/B25872.1

Tiepolo, M., Tribuzio, R., and Vannucci, R., 2002, The compositions of mantle-derived melts developed during the Alpine continental collision: Contributions to Mineralogy and Petrology, v. 144, n. 1, p. 1–15, https://doi.org/10.1007/s00410-002-0387-0

Tiepolo, M., Tribuzio, R., Ji, W.-Q., Wu, F.-Y., and Lustrino, M., 2014, Alpine Tethys closure as revealed by amphibole-rich mafic and ultramafic rocks from the Adamello and the Bergell intrusions (Central

Alps): Journal of the Geological Society, London, v. 171, p. 793–799, https://doi.org/10.1144/jgs2013-139

Tilmann, F., Ni, J., and INDEPTH III Seismic Team, 2003, Seismic imaging of the downwelling Indian lithosphere beneath central Tibet: Science, v. 300, n. 5624, p. 1424–1427, https://doi.org/10.1126/science.1082777

Torsvik, T. H., Van der Voo, R., Preeden, U., Mac Niocaill, C., Steinberger, B., Doubrovine, P. V., van Hinsbergen, D. J. J., Domeier, M., Gaina, C., Tohver, E., Meert, J. G., McCausland, P. J. A., and Cocks, L. R., 2012, Phanerozoic polar wander, palaeogeography and dynamics: Earth-Science Reviews, v. 114, n. 3–4, p. 325–368, https://doi.org/10.1016/j.earscirev.2012.06.007

Treloar, P. J., Rex, D. C., and Williams, M. P., 1991, The role of erosion and extension in unroofing the Indian Plate thrust stack, Pakistan Himalaya: Geological Magazine, v. 128, n. 5, p. 465–478, https://doi.org/10.1017/S0016756800018628

Treloar, P. J., Petterson, M. G., Jan, M. Q., and Sullivan, M. A., 1996, A re-evaluation of the stratigraphy and evolution of the Kohistan arc sequence, Pakistan Himalaya: Implications for magmatic and tectonic arc-building processes: Journal of the Geological Society, London, v. 153, n. 5, p. 681–693, https://doi.org/10.1144/gsjgs.153.5.0681

Tseng, T.-L., Chen, W.-P., and Nowack, R. L., 2009, Northward thinning of Tibetan crust revealed by virtual seismic profiles: Geophysical Research Letters-Solid Earth, v. 36, n. 24, L24304, https://doi.org/10.1029/2009GL040457

Turner, S., Hawkesworth, C., Liu, J., Rogers, N., Kelley, S., and van Calsteren, P., 1993, Timing of Tibetan uplift constrained by analysis of volcanic rocks: Nature, v. 364, p. 50–54, https://doi.org/10.1038/364050a0

Turner, S., Arnaud, N., Liu, J., Rogers, N., Hawkesworth, C., Harris, N., Kelley, S., Van Calsteren, P., and Deng, W., 1996, Post-collision, shoshonitic volcanism on the Tibetan plateau: Implications for convective thinning of the lithosphere and the source of ocean island basalts: Journal of Petrology, v. 37, n. 1, p. 45–71, https://doi.org/10.1093/petrology/37.1.45

Van Buer, N. J., Jagoutz, O., Upadhyay, R., and Guillong, M., 2015, Mid-crustal detachment beneath western Tibet exhumed where conjugate Karakoram and Longmu-Gozha Co faults intersect: Earth and Planetary Science Letters, v. 413, p. 144–157, https://doi.org/10.1016/j.epsl.2014.12.053

Van der Voo, R., Spakman, W., and Bijwaard, H., 1999, Tethyan subducted slabs under India: Earth and Planetary Science Letters, v. 171, n. 1, p. 7–20, https://doi.org/10.1016/S0012-821X(99)00131-4

Van der Voo, R., van Hinsbergen, D. J. J., Domeier, M., Spakman, W., and Torsvik, T. H., 2015, Latest Jurassic-earliest Cretaceous closure of the Mongol-Okhotsk Ocean: A paleomagnetic and seismological-tomographic analysis, *in* Anderson, T. H., Didenko, A. N., Johnson, C. L., Khanchuk, A. I., and MacDonald, J. H., Jr., editors, Late Jurassic Margin of Laurasia-A Record of Faulting Accommodating Plate Rotation: Boulder, Geological Society of America Special Papers, v. 513, p. 589–606, https://doi.org/10.1130/2015.2513(19)

Van der Woerd, J., Ryerson, F. J., Tapponnier, P., Gaudemer, Y., Finkel, R., Meriaux, A. S., Caffee, M., Guoguang, Z., and Qunlu, H., 1998, Holocene left-slip rate determined by cosmogenic surface dating on the Xidatan segment of the Kunlun fault (Qinghai, China): Geology, v. 26, n. 8, p. 695–698, https://doi.org/10.1130/0091-7613(1998)026<0695:HLSRDB>2.3.CO;2

van Hinsbergen, D. J. J., Kapp, P., Dupont-Nivet, G., Lippert, P. C., DeCelles, P. G., and Torsvik, T. H., 2011a, Restoration of Cenozoic deformation in Asia and the size of Greater India: Tectonics, v. 30, n. 5, TC5003, https://doi.org/10.1029/2011TC002908

van Hinsbergen, D. J. J., Steinberger, B., Doubrovine, P. V., and Gassmöller, R., 2011b, Acceleration and deceleration of India-Asia convergence since the Cretaceous: Roles of mantle plumes and continental collision: Journal of Geophysical Research-Solid Earth, v. 116, n. B6, B06101, https://doi.org/10.1029/2010JB008051

van Hinsbergen, D. J. J., Lippert, P. C., Dupont-Nivet, G., McQuarrie, N., Doubrovine, P. V., Spakman, W., and Torsvik, T. H., 2012, Greater India Basin Hypothesis and a two-stage Cenozoic collision between India and Asia: Proceedings of the National Academy of Sciences of the United States of America, v. 109, n. 20, p. 7659–7664, https://doi.org/10.1073/pnas.1117262109

van Hinsbergen, D. J. J., Lippert, P. C., Li, S., Huang, W., Advokaat, E. L., and Spakman, W., 2019, Reconstructing Greater India: Paleogeographic, kinematic, and geodynamic perspectives: Tectonophysics, https://doi.org/10.1016/j.tecto.2018.04.006

Vannay, J.-C., and Hodges, K. V., 1996, Tectonometamorphic evolution of the Himalayan metamorphic core between the Annapurna and Dhaulagiri, central Nepal: Journal of Metamorphic Geology, v. 14, n. 5, p. 635–656, https://doi.org/10.1046/j.1525-1314.1996.00426.x

Vannay, J.-C., Grasemann, B., Rahn, M., Frank, W., Carter, A., Baudraz, V., and Cosca, M., 2004, Miocene to Holocene exhumation of metamorphic crustal wedges in the NW Himalaya: Evidence for tectonic extrusion coupled to fluvial erosion: Tectonics, v. 23, n. 1, p. TC1014, https://doi.org/10.1029/2002TC001429

Vergne, J., Wittlinger, G., Hui, Q., Tapponnier, P., Poupinet, G., Mei, J., Herquel, G., and Paul, A., 2002, Seismic evidence for stepwise thickening of the crust across the NE Tibetan plateau: Earth and Planetary Science Letters, v. 203, n. 1, p. 25–33, https://doi.org/10.1016/S0012-821X(02)00853-1

Vince, K. J., and Treloar, P. J., 1996, Miocene, north-vergent extensional displacement along the Main Mantle Thrust, NW Himalaya, Pakistan: Journal of the Geological Society, London, v. 153, n. 5, p. 677–680, https://doi.org/10.1144/gsjgs.153.5.0677

Volkmer, J. E., Kapp, P., Guynn, J. H., and Lai, Q., 2007, Cretaceous-Tertiary structural evolution of the north central Lhasa terrane, Tibet: Tectonics, v. 26, n. 6, TC6007, https://doi.org/10.1029/2005TC001832

Volkmer, J. E., Kapp, P., Horton, B. K., Gehrels, G. E., Minervini, J. M., and Ding, L., 2014, Northern Lhasa thrust belt of central Tibet: Evidence of Cretaceous - early Cenozoic shortening within a passive roof thrust system?, *in* Nie, J. S., Horton, B. K., and Hoke, G. D., editors, Towards an Improved Understanding of Uplift Mechanisms and the Elevation History of the Tibetan Plateau: Geological Society of America Special Papers, v. 507, p. 59–70, https://doi.org/10.1130/2014.2507(03)

Wagner, T., Lee, J., Hacker, B. R., and Seward, G., 2010, Kinematics and vorticity in Kangmar Dome, southern Tibet: Testing midcrustal channel flow models for the Himalaya: Tectonics, v. 29, n. 6, TC6011, https://doi.org/10.1029/2010TC002746

Wallis, S., Tsujimori, T., Aoya, M., Kawakami, T., Terada, K., Suzuki, K., and Hyodo, H., 2003, Cenozoic and Mesozoic metamorphism in the Longmenshan orogen: Implications for geodynamic models of eastern Tibet: Geology, v. 31, n. 9, p. 745–748, https://doi.org/10.1130/G19562.1

Wang, B.-D., Wang, L.-Q., Chung, S.-L., Chen, J.-L., Yin, F.-G., Liu, H., Li, X.-B., and Chen, L.-K., 2016a, Evolution of the Bangong-Nujiang Tethyan ocean: Insights from the geochronology and geochemistry of mafic rocks within ophiolites: Lithos, v. 245, p. 18–33, https://doi.org/10.1016/j.lithos.2015.07.016

Wang, C., Zhao, X., Liu, Z., Lippert, P. C., Graham, S. A., Coe, R. S., Yi, H., Zhu, L., Liu, S., and Li, Y., 2008a, Constraints on the early uplift history of the Tibetan Plateau: Proceedings of the National Academy of Sciences of the United States of America, v. 105, n. 13, p. 4987–4992, https://doi.org/10.1073/pnas.0703595105

Wang, C., Li, X., Liu, Z., Li, Y., Jansa, L., Dai, J., and Wei, Y., 2012, Revision of the Cretaceous-Paleogene stratigraphic framework, facies architecture and provenance of the Xigaze forearc basin along the Yarlung Zangbo suture zone: Gondwana Research, v. 22, n. 2, p. 415–433, https://doi.org/10.1016/j.gr.2011.09.014

Wang, C., Dai, J., Zhao, X., Li, Y., Graham, S. A., He, D., Ran, B., and Meng, J., 2014a, Outward-growth of the Tibetan Plateau during the Cenozoic: A review: Tectonophysics, v. 621, p. 1–43, https://doi.org/10.1016/j.tecto.2014.01.036

Wang, C., Ding, L., Zhang, L.-Y., Kapp, P., Pullen, A., and Yue, Y.-H., 2016b, Petrogenesis of Middle-Late Triassic volcanic rocks from the Gangdese belt, southern Lhasa terrane: Implications for early subduction of Neo-Tethyan oceanic lithosphere: Lithos, v. 262, p. 320–333, https://doi.org/10.1016/j.lithos.2016.07.021

Wang, E., Kamp, P. J. J., Xu, G., Hodges, K. V., Meng, K., Chen, L., Wang, G., and Luo, H., 2015b, Flexural bending of southern Tibet in a retro foreland setting: Scientific Reports, v. 5, article number 12076, https://doi.org/10.1038/srep12076

Wang, H., Currie, C. A., and DeCelles, P. G., 2015a, Hinterland basin formation and gravitational instabilities in the central Andes: Constraints from gravity data and geodynamic models, *in* DeCelles, P. G., Ducea, M. N., Carrapa, B., and Kapp, P. A., editors, Geodynamics of a Cordilleran Orogenic System: The Central Andes of Argentina and Northern Chile: Geological Society of America Memoirs, v. 212, p. 387–406, https://doi.org/10.1130/2015.1212(19)

Wang, J., Hu, X.-M., Jansa, L., and Huang, Z., 2011, Provenance of the Upper Cretaceous-Eocene deep-water sandstones in Sangdanlin, southern Tibet: Constraints on the timing of initial India-Asia collision: The Journal of Geology, v. 119, n. 3, p. 293–309, https://doi.org/10.1086/659145

Wang, J.-G., Hu, X.-M., Garzanti, E., and Wu, F.-Y., 2013, Upper Oligocene-Lower Miocene Gangrinboche Conglomerate in the Xigaze Area, Southern Tibet: Implications for Himalayan uplift and paleo-Yarlung-Zangbo initiation: The Journal of Geology, v. 121, n. 4, p. 425–444, https://doi.org/10.1086/670722

Wang, J.-M., Zhang, J.-J., Liu, K., Zhang, B., Wang, X.-X., Rai, S. M., and Scheltens, M., 2016c, Spatial and temporal evolution of tectonometamorphic discontinuities in the central Himalaya: Constraints from P-T paths and geochronology: Tectonophysics, v. 679, p. 41–60, https://doi.org/10.1016/j.tecto.2016.04.035

Wang, L. Q., Yao, D. S., Luo, J. N., Yan, Y. J., Liang, X. Z., Luo, J. M., and Ling, X. M., 2006, 1:500,000 geologic map of Gangdese-Himalaya, People's Republic of China. Unpublished (in Chinese).

Wang, Q., McDermott, F., Xu, J., Belloon, H., and Zhu, Y., 2005, Cenozoic K-rich adakitic volcanic rocks in the Hohxil area, northern Tibet: Lower-crustal melting in an intracontinental setting: Geology, v. 33, n. 6, p. 465–468, https://doi.org/10.1130/G21522.1

Wang, Q., Wyman, D. A., Li, Z.-X., Sun, W., Chung, S.-L., Vasconcelos, P. M., Zhang, Q., Dong, H., Yu, Y., Pearson, N., Qiu, H., Zhu, T., and Feng, X., 2010, Eocene north-south trending dikes in central Tibet: New constraints on the timing of east-west extension with implications for early plateau uplift?: Earth and Planetary Science Letters, v. 298, n. 1–2, p. 205–216, https://doi.org/10.1016/j.epsl.2010.07.046

Wang, Q., Zhu, D.-C., Zhao, Z.-D., Liu, S.-A., Chung, S.-L., Li, S.-M., Liu, D., Dai, J.-G., Wang, L.-Q., and Mo, X.-X., 2014b, Origin of the *ca.* 90 Ma magnesia-rich volcanic rocks in SE Nyima, central Tibet: Products of lithospheric delamination beneath the Lhasa-Qiangtang collision zone: Lithos, v. 198–199, p. 24–37, https://doi.org/10.1016/j.lithos.2014.03.019

Wang, W.-L., Aitchison, J. C., Lo, C.-H., and Zeng, Q.-G., 2008b, Geochemistry and geochronology of the amphibolite blocks in ophiolitic mélanges along Bangong-Nujiang suture, central Tibet: Journal of Asian Earth Sciences, v. 33, n. 1–2, p. 122–138, https://doi.org/10.1016/j.jseaes.2007.10.022

Wang, Y., Zheng, J., Zheng, Y., Liu, X., and Sun, G., 2015c, Paleocene-Early Eocene uplift of the Altyn Tagh Mountain: Evidence from detrital zircon fission track analysis and seismic sections in the northwestern Qaidam basin: Journal of Geophysical Research- Solid Earth, v. 120, n. 12, p. 8534–8550, https://doi.org/10.1002/2015JB011922

Wang, Y., Zhang, L., Zhang, J., and Wei, C., 2017, The youngest eclogite in central Himalaya: P-T path, U-Pb zircon age and its tectonic implication: Gondwana Research, v. 41, p. 188–206, https://doi.org/10.1016/j.gr.2015.10.013

Warren, C. J., Singh, A. K., Roberts, N. M. W., Regis, D., Halton, A. M., and Singh, R. B., 2014, Timing and conditions of peak metamorphism and cooling across the Zimithan Thrust, Arunachal Pradesh, India: Lithos, v. 200–201, p. 94–110, https://doi.org/10.1016/j.lithos.2014.04.005

Webb, A. A. G., 2013, Preliminary balanced palinspastic reconstruction of Cenozoic deformation across the

Himachal Himalaya (northwestern India): Geosphere, v. 9, n. 3, p. 572–587, https://doi.org/10.1130/GES00787.1
Webb, A. A. G., Yin, A., Harrison, T. M., Célérier, J., and Burgess, W. P., 2007, The leading edge of the Greater Himalayan Crystalline complex revealed in the NW Indian Himalaya: Implications for the evolution of the Himalayan orogen: Geology, v. 35, n. 10, p. 955–958, https://doi.org/10.1130/G23931A.1
Webb, A. A. G., Guo, H., Clift, P. D., Husson, L., Müller, T., Costantino, D., Yin, A., Xu, Z., Cao, H., and Wang, Q., 2017, The Himalaya in 3D: Slab dynamics controlled mountain building and monsoon intensification: Geosphere, v. 9, n. 4, p. 637–651, https://doi.org/10.1130/L636.1
Wei, Y., Zhang, K., Garzione, C. N., Xu, Y., Song, B., and Ji, J., 2016, Low palaeoelevation of the northern Lhasa terrane during late Eocene: Fossil foraminifera and stable isotope evidence from the Gerze Basin: Scientific Reports, v. 6, article number 27508, https://doi.org/10.1038/srep27508
Wei, Y., Zhao, Z., Niu, Y., Zhu, D.-C., Liu, D., Wang, Q., Hou, Z., Mo, X., and Wei, J., 2017, Geochronology and geochemistry of the Early Jurassic Yeba Formation volcanic rocks in southern Tibet: Initiation of back-arc rifting and crustal accretion in the southern Lhasa Terrane: Lithos, v. 278–281, p. 477–490, https://doi.org/10.1016/j.lithos.2017.02.013
Weislogel, A. L., 2008, Tectonostratigraphic and geochronologic constraints on evolution of the northeast Paleotethys from the Songpan-Ganzi complex, central China: Tectonophysics, v. 451, n. 1–4, p. 331–345, https://doi.org/10.1016/j.tecto.2007.11.053
Weislogel, A. L., Graham, S. A., Chang, E. Z., Wooden, J. L., Gehrels, G. E., and Yang, H., 2006, Detrital zircon provenance of the Late Triassic Songpan-Ganzi complex: Sedimentary record of collision of the North and South China blocks: Geology, v. 34, n. 2, p. 97–100, https://doi.org/10.1130/G21929.1
Weller, O. M., St-Onge, M. R., Searle, M. P., Waters, D. J., Rayner, N., Chen, S., Chung, S.-L., and Palin, R. M., 2015, Quantifying the *P-T-t* conditions of north-south Lhasa terrane accretion: New insight into the pre-Himalayan architecture of the Tibetan plateau: Journal of Metamorphic Geology, v. 33, n. 1, p. 91–113, https://doi.org/10.1111/jmg.12112
Weller, O. M., St-Onge, M. R., Rayner, N., Waters, D. J., Searle, M. P., and Palin, R. M., 2016, U-Pb zircon geochronology and phase equilibria modelling of a mafic eclogite from the Sumdo complex of south-east Tibet: Insights into prograde zircon growth and the assembly of the Tibetan plateau: Lithos, v. 262, p. 729–741, https://doi.org/10.1016/j.lithos.2016.06.005
Wen, D.-R., Liu, D., Chung, S.-L., Chu, M.-F., Ji, J., Zhang, Q., Song, B., Lee, T.-Y., Yeh, M.-W., and Lo, C.-H., 2008, Zircon SHRIMP U-Pb ages of the Gangdese Batholith and implications for Neotethyan subduction in southern Tibet: Chemical Geology, v. 252, n. 3–4, p. 191–201, https://doi.org/10.1016/j.chemgeo.2008.03.003
Wesnousky, S. G., Kumahara, Y., Chamlagain, D., Pierce, I. K., Karki, A., and Gautam, D., 2017, Geological observations on large earthquakes along the Himalayan frontal fault near Kathmandu, Nepal: Earth and Planetary Science Letters, v. 457, p. 366–375, https://doi.org/10.1016/j.epsl.2016.10.006
Whipple, K. X., Shirzaei, M., Hodges, K. V., and Arrowsmith, J. R., 2016, Active shortening within the Himalayan orogenic wedge implied by the 2015 Gorkha earthquake: Nature Geoscience, v. 9, p. 711–718, https://doi.org/10.1038/NGEO2797
White, L. T., and Lister, G. S., 2012, The collision of India with Asia: Journal of Geodynamics, v. 56–57, p. 7–17, https://doi.org/10.1016/j.jog.2011.06.006
Wiesmayr, G., and Grasemann, B., 2002, Eohimalayan fold and thrust belt: Implications for the geodynamic evolution of the NW-Himalaya (India): Tectonics, v. 21, n. 6, 1058, https://doi.org/10.1029/2002TC001363
Wilke, F. D. H., O'Brien, P. J., Gerdes, A., Timmerman, M. J., Sudo, M., and Khan, M. A., 2010, The multistage exhumation history of the Kaghan Valley UHP series, NW Himalaya, Pakistan from U-Pb and $^{40}Ar/^{39}Ar$ ages: European Journal of Mineralogy, v. 22, n. 5, p. 703–719, https://doi.org/10.1127/0935-1221/2010/0022-2051
Wittlinger, G., Farra, V., and Vergne, J., 2004, Lithospheric and upper mantle stratifications beneath Tibet: New insights from Sp conversions: Geophysical Research Letters, v. 31, n. 19, L19615, https://doi.org/10.1029/2004GL020955
Woodruff Jr., W. H., Horton, B. K., Kapp, P., and Stockli, D. F., 2013, Late Cenozoic evolution of the Lunggar extensional basin, Tibet: Implications for basin growth and exhumation in hinterland plateaus: Geological Society of America Bulletin, v. 125, n. 3–4, p. 343–358, https://doi.org/10.1130/B30664.1
Wu, F., Miao, D., Chang, M.-m., Shi, G., and Wang, N., 2017, Fossil climbing perch and associated plant megafossils indicate a warm and wet central Tibet during the late Oligocene: Scientific Reports, v. 7, article number 878, https://doi.org/10.1038/s41598-017-00928-9
Wu, F.-Y., Ji, W.-Q., Liu, C.-Z., and Chung, S.-L., 2010, Detrital zircon U-Pb and Hf isotopic data from the Xigaze fore-arc basin: Constraints on Transhimalayan magmatic evolution in southern Tibet: Chemical Geology, v. 271, n. 1–2, p. 13–25, https://doi.org/10.1016/j.chemgeo.2009.12.007
Wu, F.-Y., Ji, W.-Q., Wang, J.-G., Liu, C.-Z., Chung, S.-L., and Clift, P. D., 2014, Zircon U-Pb and Hf isotopic constraints on the onset time of India-Asia collision: American Journal of Science, v. 314, n. 2, p. 548–579, https://doi.org/10.2475/02.2014.04
Wu, H., Li, C., Chen, J., and Xie, C., 2015, Late Triassic tectonic framework and evolution of Central Qiangtang, Tibet, SW China: Lithosphere, v. 8, n. 2, p. 141–149, https://doi.org/10.1130/L468.1
Wu, H., Xie, C., Li, C., Wang, M., Fan, J., and Xu, W., 2016, Tectonic shortening and crustal thickening in subduction zones: Evidence from Middle-Late Jurassic magmatism in Southern Qiangtang, China: Gondwana Research, v. 39, p. 1–13, https://doi.org/10.1016/j.gr.2016.06.009
Wu, Z., Barosh, P. J., Wu, Z., Hu, D., Zhao, X., and Ye, P., 2008, Vast early Miocene lakes of the central Tibetan Plateau: Geological Society of America Bulletin, v. 120, n. 9–10, p. 1326–1337, https://doi.org/10.1130/B26043.1

Xiong, Q., Griffin, W. L., Zheng, J.-P., O'Reilly, S. Y., Pearson, N. J., Xu, B., and Belousova, E. A., 2016, Southward trench migration at ~130–120 Ma caused accretion of the Neo-Tethyan forearc lithosphere in Tibetan ophiolites: Earth and Planetary Science Letters, v. 438, p. 57–65, https://doi.org/10.1016/j.epsl.2016.01.014

Xiong, Q., Griffin, W. L., Zheng, J.-P., Pearson, N. J., and O'Reilly, S. Y., 2017a, Two-layered oceanic lithospheric mantle in a Tibetan ophiolite produced by episodic subduction of Tethyan slabs: Geochemistry, Geophysics, Geosystems, v. 18, n. 3, p. 1189–1213, https://doi.org/10.1002/2016GC006681

Xiong, Q., Henry, H., Griffin, W. L., Zheng, J.-P., Satsukawa, T., Pearson, N. J., and O'Reilly, S. Y., 2017b, High- and low-Cr chromitite and dunite in a Tibetan ophiolite: Evolution from mature subduction system to incipient forearc in the Neo-Tethyan Ocean: Contributions to Mineralogy and Petrology, v. 172, 45, https://doi.org/10.1007/s00410-017-1364-y

Xu, Q., Ding, L., Zhang, L., Cai, F., Lai, Q., Yang, D., and Liu-Zeng, J., 2013a, Paleogene high elevations in the Qiangtang Terrane, central Tibetan Plateau: Earth and Planetary Science Letters, v. 362, p. 31–42, https://doi.org/10.1016/j.epsl.2012.11.058

Xu, Q., Ding, L., Hetzel, R., Yue, Y., and Rades, E. F., 2015a, Low elevation of the northern Lhasa terrane in the Eocene: Implications for relief development in south Tibet: Terra Nova, v. 27, n. 6, p. 458–466, https://doi.org/10.1111/ter.12180

Xu, Q., Ding, L., Spicer, R. A., Liu, X., Li, S., and Wang, H., 2018, Stable isotopes reveal southward growth of the Himalayan-Tibetan Plateau since the Paleocene: Gondwana Research, v. 54, p. 50–61, https://doi.org/10.1016/j.gr.2017.10.005

Xu, R.-H., Schärer, U., and Allègre, C. J., 1985, Magmatism and metamorphism in the Lhasa block (Tibet): A geochronological study: The Journal of Geology, v. 93, n. 1, p. 41–57, https://doi.org/10.1086/628918

Xu, W.-C., Zhang, H.-F., Harris, N., Guo, L., and Pan, F.-B., 2013b, Rapid Eocene erosion, sedimentation and burial in the eastern Himalayan syntaxis and its geodynamic significance: Gondwana Research, v. 23, n. 2, p. 715–725, https://doi.org/10.1016/j.gr.2012.05.011

Xu, W.-C., Zhang, H.-F., Luo, B.-j., Guo, L., and Yang, H., 2015b, Adakite-like geochemical signature produced by amphibole-dominated fractionation of arc magmas: An example from the Late Cretaceous magmatism in Gangdese belt, south Tibet: Lithos, v. 232, p. 197–210, https://doi.org/10.1016/j.lithos.2015.07.001

Yan, D.-P., Zhou, M.-F., Li, S.-B., and Wei, G.-Q., 2011, Structural and geochronological constraints on the Mesozoic-Cenozoic tectonic evolution of the Longmen Shan thrust belt, eastern Tibetan Plateau: Tectonics, v. 30, n. 6, TC6005, https://doi.org/10.1029/2011TC002867

Yan, H., Long, X., Wang, X.-C., Li, J., Wang, Q., Yuan, C., and Sun, M., 2016, Middle Jurassic MORB-type gabbro, high-Mg diorite, calc-alkaline diorite and granodiorite in the Ando area, central Tibet: Evidence for a slab roll-back of the Bangong-Nujiang Ocean: Lithos, v. 264, p. 315–328, https://doi.org/10.1016/j.lithos.2016.09.002

Yang, J., Xu, Z., Li, Z., Xu, Z., Li, T., Ren, Y., Li, H. l., Chen, S., and Robinson, P. T., 2009, Discovery of an eclogite belt in the Lhasa block, Tibet: A new border for Paleo-Tethys?: Journal of Asian Earth Sciences, v. 34, n. 1, p. 76–89, https://doi.org/10.1016/j.jseaes.2008.04.001

Yang, T.-N., Hou, Z. Q., Wang, Y., Zhang, H.-R., and Wang, Z.-L., 2012, Late Paleozoic to Early Mesozoic tectonic evolution of northeast Tibet: Evidence from the Triassic composite western Jinsha-Garzê-Litang suture: Tectonics, v. 31, n. 4, TC4004, https://doi.org/10.1029/2011TC003044

Yin, A., 2000, Mode of Cenozoic east-west extension in Tibet suggesting a common origin of rifts in Asia during the Indo-Asian collision: Journal of Geophysical Research-Solid Earth, v. 105, n. B9, p. 21745–21759, https://doi.org/10.1029/2000JB900168

——— 2006, Cenozoic tectonic evolution of the Himalayan orogen as constrained by along-strike variation of structural geometry, exhumation history, and foreland sedimentation: Earth-Science Reviews, v. 76, n. 1–2, p. 1–131, https://doi.org/10.1016/j.earscirev.2005.05.004

Yin, A., and Harrison, T. M., 2000, Geologic Evolution of the Himalayan-Tibetan Orogen: Annual Review of Earth and Planetary Sciences, v. 28, p. 211–280, https://doi.org/10.1146/annurev.earth.28.1.211

Yin, A., and Taylor, M. H., 2011, Mechanics of V-shaped conjugate strike-slip faults and the corresponding continuum mode of continental deformation: Geological Society of America Bulletin, v. 123, 9–10, p. 1798–1821, https://doi.org/10.1130/B30159.1

Yin, A., Harrison, T. M., Ryerson, F. J., Chen, W. J., Kidd, W. S. F., and Copeland, P., 1994, Tertiary structural evolution of the Gangdese thrust system in southeastern Tibet: Journal of Geophysical Research-Solid Earth, v. 99, n. B9, p. 18175–18201, https://doi.org/10.1029/94JB00504

Yin, A., Harrison, T. M., Murphy, M. A., Grove, M., Nie, S., Ryerson, F. J., Wang, X. F., and Chen, Z. L., 1999, Tertiary deformation history of southeastern and southwestern Tibet during the Indo-Asian collision: Geological Society of America Bulletin, v. 111, n. 11, p. 1644–1664, https://doi.org/10.1130/0016-7606(1999)111<1644:TDHOSA>2.3.CO;2

Yin, A., Rumelhart, P. E., Butler, R., Cowgill, E., Harrison, T. M., Foster, D. A., Ingersoll, R. V., Zhang, Q., Zhou, X.-Q., Wang, X.-F., Hanson, A., and Raza, A., 2002, Tectonic history of the Altyn Tagh fault system in northern Tibet inferred from Cenozoic sedimentation: Geological Society of America Bulletin, v. 114, n. 10, p. 1257–1295, https://doi.org/10.1130/0016-7606(2002)114<1257:THOTAT>2.0.CO;2

Yin, A., Dang, Y.-Q., Wang, L.-C., Jiang, W.-M., Zhou, S.-P., Chen, X.-H., Gehrels, G. E., and McRivette, M. W., 2008, Cenozoic tectonic evolution of Qaidam basin and its surrounding regions (Part 1): The southern Qilian Shan-Nan Shan thrust belt and northern Qaidam basin: Geological Society of America Bulletin, v. 120, n. 7–8. p. 813–846, https://doi.org/10.1130/B26180.1

Yoshida, M., and Santosh, M., 2011, Supercontinents, mantle dynamics and plate tectonics: A perspective based on conceptual vs. numerical models: Earth-Science Reviews, v. 105, n. 1–2, p. 1–24, https://doi.org/10.1016/j.earscirev.2010.12.002

Zachos, J., Pagani, M., Sloan, L., Thomas, E., and Billups, K., 2001, Trends, rhythms, and aberrations in global climate 65 Ma to Present: Science, v. 292, p. 686–693, https://doi.org/10.1126/science.1059412
Zahirovic, S., Müller, R. D., Seton, M., Flament, N., Gurnis, M., and Whittaker, J., 2012, Insights on the kinematics of the India-Eurasia collision from global geodynamic models: Geochemistry, Geophysics, Geosystems, v. 13, n. 4, Q04W11, https://doi.org/10.1029/2011GC003883
Zahirovic, S., Matthews, K. J., Flament, N., Müller, R. D., Hill, K. C., Seton, M., and Gurnis, M., 2016, Tectonic evolution and deep mantle structure of the eastern Tethys since the latest Jurassic: Earth-Science Reviews, v. 162, p. 293–337, https://doi.org/10.1016/j.earscirev.2016.09.005
Zandt, G., Gilbert, H., Owens, T. J., Ducea, M., Saleeby, J., and Jones, C. H., 2004, Active foundering of a continental arc root beneath the southern Sierra Nevada in California: Nature, v. 431, p. 41–46, https://doi.org/10.1038/nature02847
Zeng, L., Gao, L.-E., Xie, K., and Liu-Zeng, J., 2011, Mid-Eocene high Sr/Y granites in the Northern Himalayan Gneiss Domes: Melting thickened lower continental crust: Earth and Planetary Science Letters, v. 303, n. 3–4, p. 251–266, https://doi.org/10.1016/j.epsl.2011.01.005
Zeng, L., Gao, L.-E., Tang, S., Hou, K., Guo, C., and Hu, G., 2014, Eocene magmatism in the Tethyan Himalaya, southern Tibet, *in* Mukherjee, S., Carosi, R., van der Beek, P. A., Mukherjee, B. K., and Robinson, D. M., editors, Tectonics of the Himalaya: London, Geological Society, London, Special Publications, v. 412, p. 287–316, https://doi.org/10.1144/SP412.8
Zeng, M., Zhang, X., Cao, H., Ettensohn, F. R., Cheng, W., and Lang, X., 2016, Late Triassic initial subduction of the Bangong-Nujiang Ocean beneath Qiangtang revealed: Stratigraphic and geochronological evidence from Gaize, Tibet: Basin Research, v. 28, n. 1, p. 147–157, https://doi.org/10.1111/bre.12105
Zhai, Q.-G., Zhang, R.-Y., Jahn, M.-M., Li, C., Song, S.-G., and Wang, J., 2011, Triassic eclogites from central Qiangtang, northern Tibet, China: Petrology, geochronology and metamorphic *P-T* path: Lithos, v. 125, n. 1–2, p. 173–189, https://doi.org/10.1016/j.lithos.2011.02.004
Zhang, C., Liu, C.-Z., Wu, F.-Y., Zhang, L.-L., and Ji, W.-Q., 2016a, Geochemistry and geochronology of mafic rocks from the Luobusa ophiolite, South Tibet: Lithos, v. 245, p. 93–108, https://doi.org/10.1016/j.lithos.2015.06.031
Zhang, H., Harris, N., Parrish, R., Kelley, S., Zhang, L., Rogers, N., Argles, T., and King, J., 2004a, Causes and consequences of protracted melting of the mid-crust exposed in the North Himalayan antiform: Earth and Planetary Science Letters, v. 228, n. 1–2, p. 195–212, https://doi.org/10.1016/j.epsl.2004.09.031
Zhang, K.-J., Xia, B.-D., Wang, G.-M., Li, Y.-T., and Ye, H.-F., 2004b, Early Cretaceous stratigraphy, depositional environments, sandstone provenance, and tectonic setting of central Tibet, western China: Geological Society of America Bulletin, v. 116, n. 9–10, p. 1202–1222, https://doi.org/10.1130/B25388.1
Zhang, K.-J., Cai, J.-X., Zhang, Y.-X., and Zhao, T.-P., 2006, Eclogites from central Qiangtang, northern Tibet (China) and tectonic implications: Earth and Planetary Science Letters, v. 245, n. 3–4, p. 722–729, https://doi.org/10.1016/j.epsl.2006.02.025
Zhang, K.-J., Zhang, Y.-X., Tang, X.-C., and Xia, B., 2012a, Late Mesozoic tectonic evolution and growth of the Tibetan plateau prior to the Indo-Asian collision: Earth-Science Reviews, v. 114, n. 3–4, p. 236–249, https://doi.org/10.1016/j.earscirev.2012.06.001
Zhang, L.-L., Liu, C.-Z., Wu, F.-Y., Ji, W.-Q., and Wang, J.-G., 2014a, Zedong terrane revisited: An intra-oceanic arc within Neo-Tethys or a part of the Asian active continental margin?: Journal of Asian Earth Sciences, v. 80, p. 34–55, https://doi.org/10.1016/j.jseaes.2013.10.029
Zhang, L.-Y., Ding, L., Pullen, A., Xu, Q., Liu, D.-L., Cai, F.-L., Yue, Y.-H., Lai, Q.-Z., Shi, R.-D., Ducea, M. N., Kapp, P., and Chapman, A., 2014b, Age and geochemistry of western Hoh-Xil-Songpan-Ganzi granitoids, northern Tibet: Implications for the Mesozoic closure of the Paleo-Tethys ocean: Lithos, v. 190–191, p. 328–348, https://doi.org/10.1016/j.lithos.2013.12.019
Zhang, L.-Y., Ducea, M. N., Ding, L., Pullen, A., Kapp, P., and Hoffman, D., 2014c, Southern Tibetan Oligocene-Miocene adakites: A record of Indian slab tearing: Lithos, v. 210–211, p. 209–223, https://doi.org/10.1016/j.lithos.2014.09.029
Zhang, P.-Z., Shen, Z., Wang, M., Gan, W., Bürgmann, R., Molnar, P., Wang, Q., Niu, Z., Sun, J., Wu, J., Hanrong, S., and Xinzhao, Y., 2004c, Continuous deformation of the Tibetan Plateau from global positioning system data: Geology, v. 32, n. 9, p. 809–812, https://doi.org/10.1130/G20554.1
Zhang, Q.-H., Ding, L., Cai, F.-L., Xu, X.-X., Zhang, L.-Y., Xu, Q., and Willems, H., 2011a, Early Cretaceous Gangdese retroarc foreland basin evolution in the Selin Co basin, central Tibet: Evidence from sedimentology and detrital zircon geochronology, *in* Gloaguen, R., and Ratschbacher, L., editors, Growth and Collapse of the Tibetan Plateau: Geological Society, London, Special Publications, v. 353, p. 27–44, https://doi.org/10.1144/SP353.3
Zhang, Q., Willems, H., Ding, L., Gräfe, K.-U., and Appel, E., 2012b, Initial India-Asia continental collision and foreland basin evolution in the Tethyan Himalaya of Tibet: Evidence from stratigraphy and paleontology: The Journal of Geology, v. 120, n. 2, p. 175–189, https://doi.org/10.1086/663876
Zhang, R., Murphy, M. A., Lapen, T. J., Sanchez, V., and Heizler, M., 2011b, Late Eocene crustal thickening followed by Early-Late Oligocene extension along the India-Asia suture zone: Evidence for cyclicity in the Himalayan orogen: Geosphere, v. 7, n. 5, p. 1249–1268, https://doi.org/10.1130/GES00643.1
Zhang, X., Shi, R., Huang, Q., Liu, D., Gong, X., Chen, S., Wu, K., Yi, G., Sun, Y., and Ding, L., 2014d, Early Jurassic high-pressure metamorphism of the Amdo terrane, Tibet: Constraints from zircon U-Pb geochronology of mafic granulites: Gondwana Research, v. 26, n. 3–4, p. 975–985, https://doi.org/10.1016/j.gr.2013.08.003
Zhang, Y.-X., Li, Z.-W., Zhu, L.-D., Zhang, K.-J., Yang, W.-G., and Jin, X., 2016b, Newly discovered eclogites from the Bangong Meso-Tethyan suture zone (Gaize, central Tibet, western China): Mineralogy,

geochemistry, geochronology, and tectonic implications: International Geology Review, v. 58, n. 5, p. 574–587, https://doi.org/10.1080/00206814.2015.1096215

Zhang, Z., Zhao, G., Santosh, M., Wang, J., Dong, X., and Shen, K., 2010a, Late Cretaceous charnockite with adakitic affinities from the Gangdese batholith, southeastern Tibet: Evidence for Neo-Tethyan mid-ocean ridge subduction?: Gondwana Research, v. 17, n. 4, p. 615–631, https://doi.org/10.1016/j.gr.2009.10.007

Zhang, Z., Dong, X., Xiang, H., Liou, J. G., and Santosh, M., 2013, Building of the deep Gangdese arc, south Tibet: Paleocene plutonism and granulite-facies metamorphism: Journal of Petrology, v. 54, n. 12, p. 2547–2580, https://doi.org/10.1093/petrology/egt056

Zhang, Z., Dong, X., Xiang, H., Ding, H., He, Z., and Liou, J. G., 2015, Reworking of the Gangdese magmatic arc, southeastern Tibet: Post-collisional metamorphism and anatexis: Journal of Metamorphic Geology, v. 33, n. 1, p. 1–21, https://doi.org/10.1111/jmg.12107

Zhang, Z. H., Deng, Y., Teng, J., Wang, C., Gao, R., Chen, Y., and Fan, W., 2011c, An overview of the crustal structure of the Tibetan plateau after 35 years of deep seismic soundings: Journal of Asian Earth Sciences, v. 40, n. 4, p. 977–989, https://doi.org/10.1016/j.jseaes.2010.03.010

Zhang, Z. M., Zhao, G. C., Santosh, M., Wang, J. L., Dong, X., and Liou, J. G., 2010b, Two stages of granulite facies metamorphism in the eastern Himalayan syntaxis, southern Tibet: Petrology, zircon geochronology and implications for the subduction of Neo-Tethys and the Indian continent beneath Asia: Journal of Metamorphic Geology, v. 28, n. 7, p. 719–733, https://doi.org/10.1111/j.1525-1314.2010.00885.x

Zhang, Z.-M., Dong, X., Liu, F., Lin, Y.-H., Yan, R., and Santosh, M., 2012c, Tectonic evolution of the Amdo terrane, central Tibet: Petrochemistry and zircon U-Pb geochronology: The Journal of Geology, v. 120, n. 4, p. 431–451, https://doi.org/10.1086/665799

Zhang, Z. M., Dong, X., Santosh, M., and Zhao, G. C., 2014d, Metamorphism and tectonic evolution of the Lhasa terrane, Central Tibet: Gondwana Research, v. 25, n. 1, p. 170–189, https://doi.org/10.1016/j.gr.2012.08.024

Zhao, J., Yuan, X., Liu, H., Kumar, P., Pei, S., Kind, R., Zhang, Z. H., Teng, J., Ding, L., Gao, X., Xu, Q., and Wang, W., 2010, The boundary between the Indian and Asian tectonic plates below Tibet: Proceedings of the National Academy of Science of the United States of America, v. 107, n. 25, p. 11229–11233, https://doi.org/10.1073/pnas.1001921107

Zhao, J., Jin, Z., Mooney, W. D., Okaya, N., Wang, S., Gao, X., Tang, L., Pei, S., Liu, H., and Xu, Q., 2013, Crustal structure of the central Qaidam basin imaged by seismic wide-angle reflection/refraction profiling: Tectonophysics, v. 584, p. 174–190, https://doi.org/10.1016/j.tecto.2012.09.005

Zhao, W.-L., and Morgan, W. J., 1985, Uplift of Tibetan plateau: Tectonics, v. 4, p. 359–369, https://doi.org/10.1029/TC004i004p00359

——— 1987, Injection of Indian crust into Tibetan lower crust: A two-dimensional finite element model study: Tectonics, v. 6, n. 4, p. 489–504, https://doi.org/10.1029/TC006i004p00489

Zhao, W., Mechie, J., Brown, L. D., Guo, J., Haines, S., Hearn, T., Klemperer, S. L., Ma, Y. S., Meissner, R., Nelson, K. D., Ni, J. F., Pananont, P., Rapine, R., Ross, A., and Saul, J., 2001, Crustal structure of central Tibet as derived from project INDEPTH wide-angle seismic data: Geophysical Journal International, v. 145, n. 2, p. 486–498, https://doi.org/10.1046/j.0956-540x.2001.01402.x

Zhao, Z., Bons, P. D., Wang, G., Liu, Y., and Zheng, Y., 2014, Origin and pre-Cenozoic evolution of the south Qiangtang basement, Central Tibet: Tectonophysics, v. 623, p. 52–66, https://doi.org/10.1016/j.tecto.2014.03.016

Zheng, Y.-C., Hou, Z.-Q., Gong, Y.-L., Liang, W., Sun, Q.-Z., Zhang, S., Fu, Q., Huang, K.-X., Li, Q.-Y., and Li, W., 2014, Petrogenesis of Cretaceous adakite-like intrusions of the Gangdese Plutonic Belt, southern Tibet: Implications for mid-oceanic ridge subduction and crustal growth: Lithos, v. 190–191, p. 240–263, https://doi.org/10.1016/j.lithos.2013.12.013

Zhong, S., Zhang, N., Li, Z.-X., and Roberts, J. H., 2007, Supercontinent cycles, true polar wander, and very long-wavelength mantle convection: Earth and Planetary Science Letters, v. 261, n. 3–4, p. 551–564, https://doi.org/10.1016/j.epsl.2007.07.049

Zhou, D., and Graham, S. A., 1996, The Songpan-Ganzi complex of the West Qinling Shan as a Triassic remnant ocean basin, *in* Yin, A., and Harrison, T. M., editors, The Tectonic Evolution of Asia: New York, Cambridge University Press, p. 281–299.

Zhou, H.-W., and Murphy, M. A., 2005, Tomographic evidence for wholesale underthrusting of India beneath the entire Tibetan plateau: Journal of Asian Earth Sciences, v. 25, n. 3, p. 445–457, https://doi.org/10.1016/j.jseaes.2004.04.007

Zhou, X., Zheng, J.-P., Xiong, Q., Yang, J.-S., Wu, Y.-B., Zhao, J.-H., Griffin, W. L., and Dai, H.-K., 2017, Early Mesozoic deep-crust reworking beneath the central Lhasa terrane (South Tibet): Evidence from intermediate gneiss xenoliths in granites: Lithos, v. 274–275, p. 225–239, https://doi.org/10.1016/j.lithos.2016.12.035

Zhu, B., Kidd, W. S. F., Rowley, D. B., Currie, B. S., and Shafique, N., 2005, Age of initiation of the India-Asia collision in the east-central Himalaya: The Journal of Geology, v. 113, n. 3, p. 265–285, https://doi.org/10.1086/428805

Zhu, D.-C., Pan, G.-T., Chung, S.-L., Liao, Z.-L., Wang, L.-Q., and Li, G.-M., 2008, SHRIMP zircon age and geochemical constraints on the origin of Lower Jurassic volcanic rocks from the Yeba Formation, southern Gangdese, south Tibet: International Geology Review, v. 50, n. 5, p. 442–471, https://doi.org/10.2747/0020-6814.50.5.442

Zhu, D.-C., Chung, S. L., Mo, X.-X., Zhao, Z.-D., Niu, Y., Song, B., and Yang, Y.-H., 2009a, The 132 Ma Comei-Bunbury large igneous province: Remnants identified in present-day southeastern Tibet and southwestern Australia: Geology, v. 37, n. 7, p. 583–586; https://doi.org/10.1130/G30001A.1

Zhu, D.-C., Mo, X.-X., Niu, Y., Zhao, Z.-D., Wang, L.-Q., Liu, Y.-S., and Wu, F.-Y., 2009b, Geochemical investigation of Early Cretaceous igneous rocks along an east-west traverse throughout the central Lhasa

Terrane, Tibet: Chemical Geology, v. 268, n. 3–4, p. 298–312, https://doi.org/10.1016/j.chemgeo.2009.09.008

Zhu, D.-C., Mo, X.-X., Niu, Y., Zhao, Z.-D., Wang, L.-Q., Pan, G.-T., and Wu, F.-Y., 2009c, Zircon U-Pb dating and *in-situ* Hf isotopic analysis of Permian peraluminous granite in the Lhasa terrane, southern Tibet: Implications for Permian collisional orogeny and paleogeography: Tectonophysics, v. 469, n. 1–4, p. 48–60, https://doi.org/10.1016/j.tecto.2009.01.017

Zhu, D.-C., Zhao, Z.-D., Pan, G.-T., Lee, H.-Y., Kang, Z.-Q., Liao, Z.-L., Wang, L.-Q., Li, G.-M., Dong, G.-C., and Liu, B., 2009d, Early Cretaceous subduction-related adakite-like rocks of the Gangdese Belt, southern Tibet: Products of slab melting and subsequent melt-peridotite interaction?: Journal of Asian Earth Sciences, v. 34, n. 3, p. 298–309, https://doi.org/10.1016/j.jseaes.2008.05.003

Zhu, D.-C., Mo, X.-X., Zhao, Z.-D., Niu, Y., Wang, L.-Q., Chu, Q.-H., Pan, G.-T., Xu, J.-F., and Zhou, C.-Y., 2010, Presence of Permian extension- and arc-type magmatism in southern Tibet: Paleogeographic implications: Geological Society of America Bulletin, v. 122, n. 7–8, p. 979–993, https://doi.org/10.1130/B30062.1

Zhu, D.-C., Zhao, Z.-D., Niu, Y., Dilek, Y., and Mo, X.-X., 2011a, Lhasa terrane in southern Tibet came from Australia: Geology, v. 39, n. 8, p. 727–730, https://doi.org/10.1130/G31895.1

Zhu, D.-C., Zhao, Z.-D., Niu, Y., Mo, X.-X., Chung, S.-L., Hou, Z.-Q., Wang, L.-Q., and Wu, F.-Y., 2011b, The Lhasa Terrane: Record of a microcontinent and its histories of drift and growth: Earth and Planetary Science Letters, v. 301, n. 1–2, p. 241–255, https://doi.org/10.1016/j.epsl.2010.11.005

Zhu, D.-C., Wang, Q., Zhao, Z.-D., Chung, S.-L., Cawood, P. A., Niu, Y., Liu, S.-A., Wu, F.-Y., and Mo, X.-X., 2015, Magmatic record of India-Asia collision: Scientific Reports, v. 5, article number 14289, https://doi.org/10.1038/srep14289

Zhu, D.-C., Li, S.-M., Cawood, P. A., Wang, Q., Zhao, Z.-D., Liu, S.-A., and Wang, L.-Q., 2016, Assembly of the Lhasa and Qiangtang terranes in central Tibet by divergent double subduction: Lithos, v. 245, p. 7–17, https://doi.org/10.1016/j.lithos.2015.06.023

Zhu, D. C., Wang, Q., and Zhao, Z. D., 2017, Constraining quantitatively the timing and process of continent-continent collision using magmatic record: Method and examples: Science China Earth Sciences, v. 60, n. 6, https://doi.org/10.1007/s11430-016-9041-x

Zhuang, G., Najman, Y., Guillot, S., Roddaz, M., Antoine, P.-O., Métais, G., Carter, A., Marivaux, L., and Solangi, S. H., 2015, Constraints on the collision and the pre-collision tectonic configuration between India and Asia from detrital geochronology, thermochronology, and geochemistry studies in the lower Indus basin, Pakistan: Earth and Planetary Science Letters, v. 432, p. 363–373, https://doi.org/10.1016/j.epsl.2015.10.026

Ziabrev, S. V., Aitchison, J. C., Abrajevitch, A. V., Badengzhu, Davis, A. M., and Luo, H., 2003, Precise radiolarian age constraints on the timing of ophiolite generation and sedimentation in the Dazhuqu terrane, Yarlung-Tsangpo suture zone, Tibet: Journal of the Geological Society, London, v. 160, p. 591–599, https://doi.org/10.1144/0016-764902-107

——— 2004, Bainang Terrane, Yarlung-Tsangpo suture, southern Tibet (Xizang, China): A record of intra-Neotethyan subduction-accretion processes preserved on the roof of the world: Journal of the Geological Society, London, v. 161, p. 523–538, https://doi.org/10.1144/0016-764903-099

Zuza, A. V., Cheng, X., and Yin, A., 2016, Testing models of Tibetan Plateau formation with Cenozoic shortening estimates across the Qilian Shan-Nan Shan thrust belt: Geosphere, v. 12, n. 2, p. 501–532, https://doi.org/10.1130/GES01254.1

Zyabrev, S. V., Kojima, S., and Ahmad, T., 2008, Radiolarian biostratigraphic constraints on the generation of the Nidar ophiolite and the onset of Dras arc volcanism: Tracing the evolution of the closing Tethys along the Indus - Yarlung-Tsangpo suture: Stratigraphy, v. 5, p. 99–112.